

**II YEAR**  
**PAPER - VI**  
**INORGANIC CHEMISTRY - II**

**UNIT I :**

**Coordination Chemistry - Stability and Reactions :**

Stability and instability of complexes - determination of stability constants by potentiometric and spectrophotometric methods, factors affecting stability: chelate and template effects, HSAB concept and symbiosis, theoretical basis of softness and hardness; stabilisation of unusual oxidation states.

Kinetic stability - lability and inertness, Ligand substitution reactions of square planar complexes - factors affecting reactivity of square planar complexes; the trans effect and its theories and utilisation in synthesis of complexes. Substitution reaction in Octahedral complexes - acid hydrolysis, base hydrolysis and anation reactions.

Electron transfer reactions - complementary and non-complementary reactions. Inner sphere and outer sphere processes outer sphere process in photochemical reactions.

**UNIT II :**

**Spectral Methods I :**

Electronic spectroscopy L-S coupling and j-j coupling schemes, microstates, Hund's rules and Term symbols; selection rules for electronic transition and hole formalism; Orgel and Tanabe - Sugano diagrams; evaluation of  $10Dq$  and  $B$  for Octahedral  $d2$  and  $d8$  systems

Charge transfer spectra; electronic spectra of lanthanide and actinide complexes.

Optical isomerism in octahedral chelate complexes, their absolute configuration determination from ORD and CD methods, information on stereochemistry and conformation of chelate complexes.

**UNIT III :**

**Spectral Methods II**

Mossbauer spectroscopy - Principles - isomer shift, quadrupole and magnetic interactions - MB spectroscopy of octahedral high and low spins Fe (II) and Fe (III) complexes. Information on oxidation state, pi-back coordination and structure in iron compounds. Studies on halides of tin (II) and tin (IV).

NMR : Application of Chemical shift and spin-spin coupling to structure determination using multiprobe NMR ( $^1H$ ,  $^{31}P$ ,  $^{19}F$ ,  $^{119}Sn$ ): effect of quadrupolar nuclei on NMR spectra. NMR Studies on Chemical exchange and dynamic processes in organic and organometallic compounds; NMR studies on fluxional molecules. Paramagnetic NMR and contact shifts; lanthanide shift reagents.

EPR : Application of hyperfine splitting and g-factor to structure determination zero-field splitting and kramer's degeneracy. Covalency of M-L bonding by EPR study. Application of EPR in the study of J.T. distortion in Cu (II) complexes

**UNIT IV :**

**Instrumental Analytical Techniques :**

(Instrumental aspects not required)

Spectroanalytical techniques : Principle and application of colourimetry, spectrophotometry and

fluorimetry, Flame photometry, colorimetry, atomic absorption, atomic emission and atomic fluorescence spectroscopy, light scattering, gravimetry, redox titrimetry and turbidimetry.

Thermogravimetry, thermogravimetric analysis (TGA), DTA and DSC methods. Electroanalytical techniques. Electrochemical cell and electrode potentials; electrochemical series and application of redox potential to inorganic reaction systems.

Classification and control of current and controlled potential techniques. Voltammetry, cyclic voltammetry and stripping voltammetry; amperometry and chronopotentiometry; Potentiometry and ion-selective electrodes (reference electrode).

Principle and operation of thin film, column and gas chromatographic methods. HPLC and HPTLC; application to inorganic substances. Ion exchange and application of ion-exchange and solvent extraction methods.

## Unit V

### Organometallic Chemistry

Introduction, EAN, stability of  $\pi$  and  $\sigma$  bond stability, Metal carbonyls - synthesis, properties, structure and bonding and IR of metal carbonyls, IR of  $\pi$  and  $\sigma$  bond carbonyls, M - PI acid complexes - preparation, properties and structural features of complexes with alkenes, alkyne, allyl and arene systems. Metallocenes - synthesis, properties, and bonding structure, ionic versus covalent versus ionic bonding in metallocene.

Substitution reactions and insertion, oxidative addition and reductive elimination insert in and elimination reactions; nucleophilic attack on  $\pi$  bond of coordinated ligands.

Homogeneous catalysis: hydroformylation, Fischer-Tropsch and synthesis gas; hydroformylation carboxylation of alcohols and oxygenation of alkenes.

Heterogeneous catalysis: Fischer-Tropsch process, Ziegler - Natta polymerisation.

### References :

1. D.F. Shriver, F.W. Atkins & C. E. Housecroft, Inorganic Chemistry, Oxford 1990.
2. W.L. Jolly, Modern Inorganic Chemistry, Prentice Hall company, 2nd Edn, 1991.
3. J.E. Huheey, E.A. Keay and R.L. Keay, Inorganic Chemistry, Harper and Row / Pearson Asia, 2,3 & 4th Edn, 1993.
4. F.A. Cotton and C. Wilkinson, Fundamentals of Inorganic Chemistry, John Wiley and Sons, 3,4 & 5 th edn, 1988.
5. B.E. Douglas, D.H. McDaniel and J.F. Alexander concepts and Models of Inorganic Chemistry, John Wiley & Sons, 2 Edn, 1980 and 3 (1991).
6. R.S. Drago, Physical Methods in Chemistry, W.E. Saunders, 1977.
7. E.A.V. Ebsworth et al, structural methods in Inorganic Chemistry, ELBS, 1987.
8. H.H. Willard, L.L. Mendir, J.A. Dean and F.A. Seftle, Instrumental methods of Analysis 6th edn. CBS publishers 1980.
9. Vogel's textbook of Quantitative chemical analysis. Revised by G.H. Jeffery, J. Bassett, J. Mendhan and R.C. Denney ELBS 5th edn, 1983.
10. D.A. Skoog and D.M. West, Principles of Instrumental Analysis, Holt - Saunders, 2 edn 1980.
11. D.A. Skoog and J.J. Leary, Instrumental analysis. Saunders college publishing 1992.

INDEX  
M.S. UNIVERSITY  
DIRECTORATE OF DISTANCE AND CONTINUING EDUCATION  
II YEAR M.SC. CHEMISTRY  
INORGANIC CHEMISTRY - II

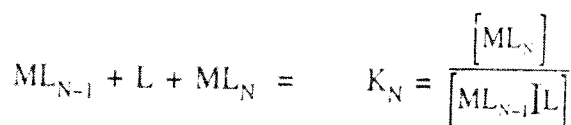
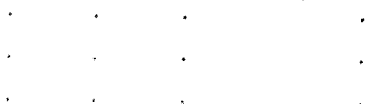
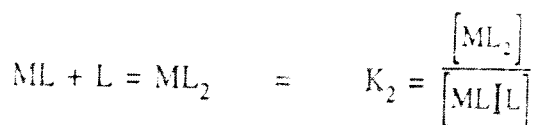
No.	Units	Page No.
1	UNIT - I STABILITY AND INSTABILITY OF COMPLEXES	1
2	UNIT - II SPECTRAL METHODS - I	26
3	UNIT - III SPECTRAL METHODS - II	51
4	UNIT - IV INSTRUMENTAL ANALYTICAL TECHNIQUES	87
5	UNIT - V ORGANOMETALLIC CHEMISTRY	148

UNIT - I

Stability and Instability of Complexes

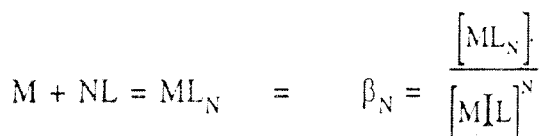
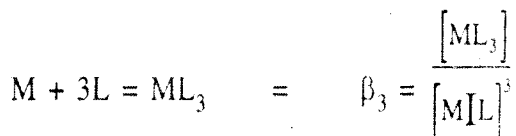
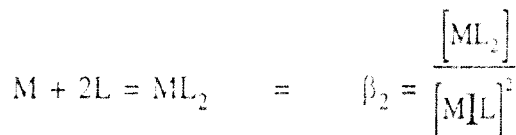
When we speak of the stability of a compound, we should be careful to specify what kind of stability we mean. In studying the formation of co-ordination complexes in solution, two kinds of stability come into question, namely, thermodynamic stability and kinetic stability. The thermo dynamic stability of a species is a measure of the extent to which this species will form from or be transformed into other species under certain conditions when the system has reached equilibrium. The kinetic stability of a species refers to the speed with which transformations leading to the attainment of equilibrium will occur. In this and the next several sections we will consider problems of thermodynamic stability, that is, the nature of equilibria once they are established.

Let us consider a metal ion, M and a monodentate ligand, L together in solution. Assuming that no insoluble products are formed, nor any species containing more than one metal ion, equilibrium expressions of the following sort will describe the system:



There will be N such equilibria, where N represents the maximum co-ordination number of the metal ion M for the ligand L. N may vary from one ligand to another. For instance,  $\text{Al}^{3+}$  forms  $\text{AlCl}_4$  and  $\text{AlF}_6^{3-}$ , and  $\text{Co}^{2+}$  forms  $\text{CoCl}_4$  and  $\text{Co}(\text{NH}_3)_6^{2+}$ , as the highest complexes with the ligands indicated.

Another way of expressing the equilibrium relations is :



since there can be only N independent equilibria in such a system, it is clear that the  $K_i$ 's and the  $\beta_i$ 's must be related. The relationship is indeed rather obvious. Consider, for example, the expression for  $\beta_3$ . Let us multiply both numerator and denominator by  $[\text{ML}][\text{ML}_2]$  and then rearrange slightly :

$$\beta_3 = \frac{[\text{ML}_3]}{[\text{M}][\text{L}]^3} \cdot \frac{[\text{ML}][\text{ML}_2]}{[\text{ML}][\text{ML}_2]}$$

$$\beta_3 = \frac{[\text{ML}]}{[\text{M}][\text{L}]} \cdot \frac{[\text{ML}_2]}{[\text{ML}][\text{L}]} \cdot \frac{[\text{ML}_3]}{[\text{ML}_2][\text{L}]} = K_1, K_2, K_3$$

It is not difficult to see that this kind of relationship is perfectly general, namely :

$$\beta_3 = K_1, K_2, K_3 \dots K_k = \prod_{i=1}^{i=k} K_i$$

The  $K_i$ 's are called the stepwise formation constants (or stepwise stability constants), and the  $\beta_i$ 's are called the over-all formation constants (or over-all stability constants); each type has its special convenience in certain cases.

With only a few exceptions the values of successive stability constants decrease regularly from  $K_1$  to  $K_n$  in any particular system. This is illustrated by the data for the Cd(II)- $\text{NH}_3$  system where the ligands are uncharged and by Cd(II)-CN system where the ligands are charged.

Cation	Ligand	$K_1$	$K_2$	$K_3$	$K_4$	$\beta_4$
$\text{Cd}^{2+}$	$\text{NH}_3$	$10^{2.65}$	$10^{2.10}$	$10^{1.44}$	$10^{0.93}$	$10^{7.12}$
$\text{Cd}^{2+}$	$\text{CN}^-$	$10^{5.48}$	$10^{5.12}$	$10^{4.63}$	$10^{3.55}$	$10^{18.8}$

It seems reasonable that positive metal ions should prefer anionic ligands to neutral ones. Formation of complexes occurs by replacement of molecules in the solvated shell of a metal cation in aqueous solution. A ligand is added to the solution of metal ion,  $\text{ML}$  first forms more rapidly than any other complex in the series as the substitution of water molecules from coordination sphere is facile. As addition of ligand is continued the  $\text{ML}_2$  concentration rises rapidly while the  $\text{ML}$  concentration drops. The progressive decrease in the successive stability constants may be ascribed to the fact that as more and more ligands move into the coordination sphere, Less and Less water molecules will be available to further ligands for replacement. With progressive intake of ligands the metal ion may also show less avidity for electrons. There are several reasons for a steady decrease in  $K_n$  values as the number of ligands increases : (i) statistical factor (ii) increase in sphere hindrance and (iii) Columbic factors in complexes with charged ligands.

#### DETERMINATION OF STABILITY CONSTANTS :

Spectrophotometric method (or) Job's continuous variation method.

This method is used for the determination of formula of a complex and dissociation constants of complexes of low solubility.

**Principle :** The method of continuous variation makes use of any measurable additive property, provided that this property has different values for the various species present in solution of a metal (M) and ligand (L). This method is mainly used for such solutions where only one complex is formed.

**Procedure :** Continuous variation method generally utilizes optical density as an additive property. Its various steps are :

(i) Make up a series of mixtures containing a total of 10 ml of metal ion and ligand in different proportions, e.g., 0 - 10, 1 - 9, .. 9 - 1, 10 - 0. It means that the sum of total analytical concentration  $C$  of complexing agent  $C_x$  and metal ion  $C_M$  is held constant and only that ratios are varied :

$$C_x + C_M = C \quad \dots (1)$$

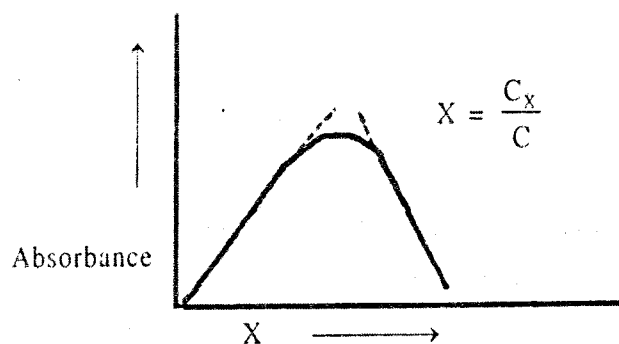


Fig 1.1

### Job's Method of Continuous Variation :

(i) Then, determine the optical densities of solutions prepared as in step (i) by means of a spectrophotometer at such a wave length of light that complex absorbs light strongly whereas the metal ion and ligand do not.

(ii) Draw a graph between mole fraction of ligand X ( $X = C_X/C$ ) and optical density. A curve of the type shown in Fig 1.1 is obtained. Extrapolate the legs of the curve until they cross. At the point of intersection the mole fraction gives the formula of a complex  $MX_n$ , i.e

$$n = \frac{C_X}{C_M} \quad \dots \quad (2)$$

Equation (I) may be written as :

$$\frac{C_X}{C} + \frac{C_M}{C} = \frac{C}{C}$$

But  $\frac{C_X}{C} = X \quad \dots \quad (3)$

or  $x + \frac{C_M}{C} = 1$  or  $\frac{C_M}{C} = 1 - X \quad \dots \quad (4)$

On dividing equation (3) by (4), we get

or  $\frac{C_X}{C_M} = \frac{X}{1 - X}$

or  $n = \frac{X}{1 - X} \quad [\because n = \frac{C_X}{C_M} \text{ from (2)}]$

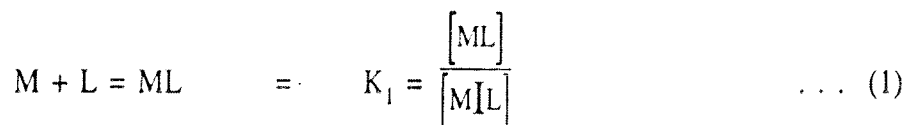
From the value of n, the formula of a complex  $MX_n$  can be determined.

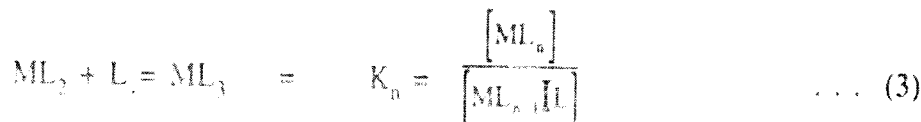
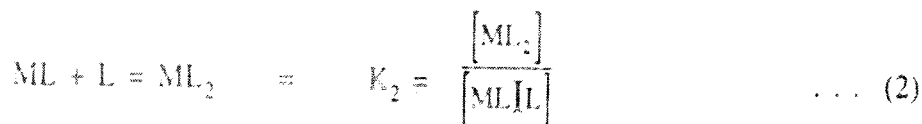
### Limitations of the Method :

- (i) The method of continuous variation applies provided that not more than one complex is formed under the given experimental conditions.
- (ii) This method is only applicable when there is no volume change on mixing the solutions of the metal ions and ligands.

### Bjerrum Method :

Bjerrum determined formation constants of metal complexes and chelate compounds in aqueous solutions. Bjerrum described the stepwise formation of series of metal complexes of the type  $ML, ML_2 \dots ML_n$  which are defined by equation (6) to (8).





Equation (1) can be written as

$$[ML] = K_1 (M) (L) \quad \dots (4)$$

Equation (2) can be written as

$$[ML_2] = K_1 (ML) (L) \quad \dots (5)$$

Substituting the value of (ML) from equation (4) in (5)

$$[ML_2] = K_1 K_2 (L)^2 (M)$$

Similarly, equation (3) can be written as

$$[ML_n] = K_1 \cdot K_2 \cdot K_3 \dots K_n (L)^n (M) \quad \dots (6)$$

Bjerrum introduced a function  $\bar{n}$ , which is defined as the average number of ligand molecules bound per mole of metal. It may be expressed mathematically as :

$$\bar{n} = \frac{(ML) + 2(ML_2) + 3(ML_3) + \dots + n(ML_n)}{(M) + (ML) + (ML_2) + (ML_3) + \dots + (ML_n)} \quad \dots (7)$$

Substituting eqs. (4), (6) and (7) in we get

$$\bar{n} = \frac{K_1 (M)(L) + 2K_1 K_2 (M)(L)^2 + nK_1 K_2 K_3 \dots + K_n (M)(L)^n}{(M) + K_1 (M)(L) + K_1 K_2 (M)(L)^2 + \dots + K_1 K_2 K_3 \dots K_n (M)(L)^n}$$

Cancelling 'M' throughout, we get

$$\bar{n} = \frac{K_1 (M)(L) + 2K_1 K_2 (L)^2 + \dots + K_1 K_2 \dots K_n (M)(L)^n}{1 + K_1 (L) + K_1 K_2 (L)^2 + \dots + K_1 K_2 K_3 \dots K_n (L)} \quad \dots (8)$$

Equation (8) is the so called Bjerrum formation function. If the concentration of unbound ligand (A) can be calculated experimentally,  $\bar{n}$  can be calculated from the equation:

$$\bar{n} = \frac{L_t - (L)}{M_t} \quad \dots (9)$$

where  $L_t$  and  $M_t$  denote the total concentration of ligand and metal, respectively.

Solution of equation (8) for the known values of  $\bar{n}$  and corresponding (L) values yields values of the formation constants, i.e.,  $K_1, K_2, K_3 \dots K_n$ .

Let us illustrate the Bjerrum method by calculating the formation constants for the complex between  $CuSO_4$  and 5-sulphosalicylic acid ( $H_2L$ ).

**Procedure :**

Titrate 100 ml of each solution i.e.,  $\text{CuSO}_4$  and 5-sulphosalicylic acid with standard NaOH solution at  $25^\circ \text{C}$ , noting the pH values after addition of the titrant base NaOH. Plot the pH versus ml of base curves and note the point of inflexion of the curve corresponding to the mixed solution (Fig.1.2). Read off the horizontal distance between the curves. Thus find values of  $\bar{n}$  and plot the formation curve of  $\bar{n}$  against  $-\log [L^{3-}]$ , the values of the latter having been found at various pH from the relation :

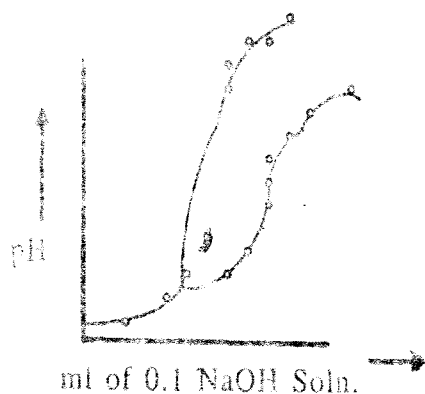


Fig. 1.2 Potentiometric titration of 5-sulphosalicylic acid ( $\text{HL}_3$ ) in the presence of  $\text{CuSO}_4$

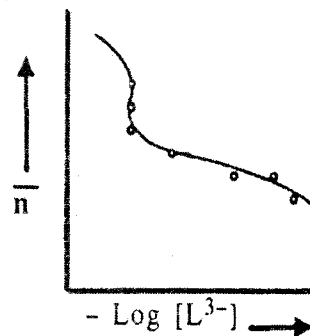


Fig 1.3 The formation curve

$$[L^{3-}] = \frac{[\text{HL}_3]_{\text{total}} - [\text{CuL}] - 2[\text{CuL}_2]}{\frac{[\text{H}^+]^2}{K_n K_m} + \frac{[\text{H}^+]}{K_m} + 1} \quad \dots (10)$$

where  $K_n$  and  $K_m$  are the second and third dissociation constants of  $\text{HL}_3$  which are  $3.03 \times 10^{-3}$  and  $1.31 \times 10^{-3}$  respectively.

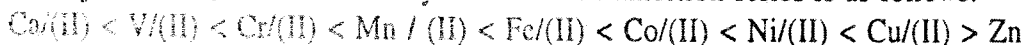
The values of  $K_1$  and  $K_2$  found from the formation curve (Fig. ) at  $\bar{n} = 0.5$  and  $\bar{n} = 1.5$  are  $K_1 = 2.2 \times 10^9$  and  $K_2 = 6.3 \times 10^6$ .

**Factors affecting stability :**

The stability constants of the metal complexes depend upon the metal ion, nature of the ligand, medium and the chelate effect.

**Nature of Metal Ion :**

1. Stability of complexes increases with decreasing size of the metal ion. The natural order of Irving-William, order of stability for the first transition series is as follows:



2. Stability constants for a complex increase with the charge of the central metal ion. Thus  $K$  for the Fe(II) complexes will be less than that for the corresponding Fe(III) complexes. A convenient criterion for the estimation of the complexing ability of the metal ion is the charge to radius ratio which is known as ionic potential. Thus, greater the ionic potential, greater is the stability.

3. Molecules containing heavy atoms and/or multiple bonds are more polarizable than those which do not give complexes with higher stability constants. Thus Cu(I) complexes have higher K values than the similar sized Na<sup>+</sup> complexes. Also between Ca<sup>2+</sup> and Cd (II) and Al (III) and Ga (III) the latter have larger K values for complex formation.

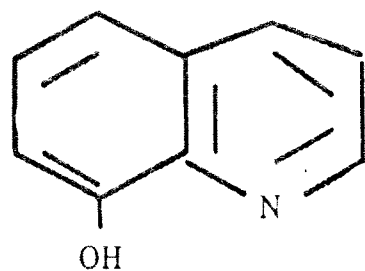
#### Nature of the Ligands :

1. In the case of neutral molecules like H<sub>2</sub>O, NH<sub>3</sub>, H<sub>2</sub>S etc., they are bound to metal ions through the attraction between the negative end of the ligand dipole and the metal ion. The more polar the ligand the greater will be the binding force to the metal ion and hence water would be expected to form metal complexes of greater stability than the other neutral ligands.

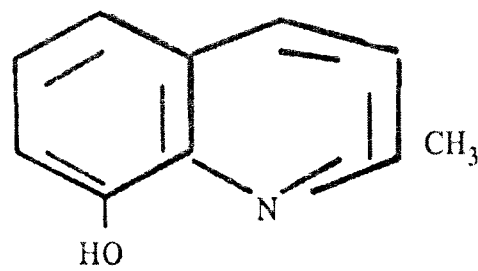
It has been observed that greater the base strength of the ligand greater is the tendency of the ligand to form stable metal complexes. The base strength of a molecule is a measure of the stability of the complex that the molecule forms with H<sup>+</sup>. From this point of view F<sup>-</sup> should form more stable complexes than Cl<sup>-</sup>, Br<sup>-</sup> or I<sup>-</sup> and NH<sub>3</sub> should be a better ligand than H<sub>2</sub>O. This predicted behaviour is observed for the metal ions.

The most stable complexes of the metals are formed with ligands that can accept electrons from the metal via pi bonding, i.e. ligands with vacant 'd' orbitals such as phosphines, sulphides or ligands with vacant pi molecular orbital such as CO, CN<sup>-</sup>.

Steric factor plays an important role in determining, the stability of the complexes. For example, 2-methyl-8-hydroxyquinoline given much less stable complexes than 8-hydroxyquinoline because of the steric hindrance caused by the methyl group adjacent to the site of coordination.



8 - Hydroxyquinoline



2- Methyl - 8 - Hydroxyquinoline

#### Nature of the Solvent :

As the complex formation involves covalent bonding solvent with low dielectric constants and low dipole moment are expected to increase the stability constant of the complexes and this had been observed to be the case.

## Chelate and Template Effects :

The extra stability conferred by the presence of a chelate ring in a metal complex is termed as the chelate effect and it depends upon (i) size and (ii) number of chelate rings.

When a bidentate or a polydentate ligand forms a ring structure including the metal ion, such complexes are called chelate complexes and the stability conferred by formation of a chelate complex is called chelate effect.

**1. Size of the ring :** Though a 4- membered chelate ring including metal ions exist in some nitrate, sulphate and carbonate complexes, the 5- and 6- membered rings are most stable ones. As the metal atom is larger than carbon and bond angles in octahedral complexes are near over  $90^\circ$  the 5-membered chelate rings become the stablest rings with saturated ligands. However, for resonance effects involving the d orbitals of the metal and the pi orbital electrons in the ligand molecule, the 6-membered rings attain maximum stability (Fig 1.4).

The chelate effect is best exemplified by the polydentate ligands which form several chelate rings with a metal atom giving such a high stability that EDTA (ethylenediaminetetraacetic acid) forms octahedral complexes with even the alkaline earth ions  $\text{Ca}^{2+}$  and  $\text{Mg}^{2+}$ .

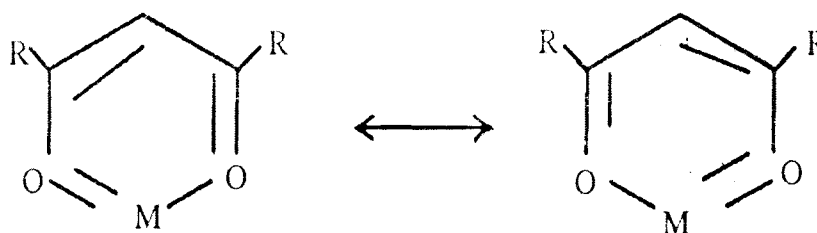


Fig 1.4 Reasonance stabilization of the chelate rings in metal acetylacetonate.

The higher membered rings are uncommon due to (i) strain set up in the heterocyclic ring and (ii) possibility of a long chain multidentate ligand bonding to more than one atom giving the formation of polynuclear complexes rather than chelated complexes.

(ii) Number of the Chelate Rings : Greater the number of chelate rings formed greater is the stability constant :

**Table 1 : Stability constants of some basic ligands with metal (II) ions**

No. of rings	Ligand	log $\beta$ for complexes with				
		Fe (II)	Co (II)	Ni (II)	Cu (II)	Zn (II)
0	$\text{NH}_3$	3.7	6.3	7.8	12.6	9.1
1	En	7.7	10.9	14.5	20.2	11.2
2	Trien	7.8	11.0	14.1	20.2	12.1
3	tren	8.8	12.8	14.0	18.3	14.6

Stability of chelate species depends upon the geometry. Thus  $[Ag(NH_3)_2]^+$  is more stable than  $[Ag(NH_3)_2]^+$ . This is because the linear structure of  $[Ag(NH_3)_2]^+$  gives rise to linear structure and the formation of a five membered chelate ring would involve strain and hence lesser stability.



### The concept of Hard and Soft Acids and Bases (HSAB)

Ligands and metal ions can be classified into two groups (a) and (b) according to their preferential bonding. Class (a) includes  $Li^+$ ,  $Na^+$ ,  $K^+$ ,  $Ca^{2+}$ ,  $Mg^{2+}$ ,  $Be^{2+}$ ,  $B^{3+}$ ,  $Al^{3+}$ ,  $Sc^{3+}$ ,  $Ti^{4+}$ ,  $Zr^{4+}$ ,  $Hf^{4+}$  and  $H^+$ . Class (b) metal ions include those of the heavier transition metals and those in lower oxidation states such as  $Cu^+$ ,  $Ag^+$ ,  $Hg^+$ ,  $Hg^{2+}$ ,  $Pd^{2+}$ ,  $Co^{2+}$ ,  $Ni^{2+}$ ,  $Fe^{2+}$ ,  $Cr^{2+}$  and  $Mn^{2+}$ . Both class (a) and class (b) metal ions have their own characteristic ligands (a) and (b) respectively.

Pearson has suggested the terms 'hard' and 'soft' acids and bases of class (a) and (b). Thus a hard acid is class (a) metal ion and a hard base is class (a) ligand like fluoride ion. Conversely, a soft acid is class (b) metal ion and a soft base is class (b) ligand such as phosphine or the thioether. Pearson has suggested a simple definition for soft base as 'one' in which the donor atom is of high polarizability, low electronegativity and is easily oxidized or associated with empty low lying orbitals. A hard base is defined as one with opposite properties. The donor atom of a hard base is of low polarizability, high electronegativity, is hard to reduce and is associated with empty orbitals of high energy. The definition of a soft acid is defined by Pearson as one which is highly polarizable, has a high positive charge, large size and several empty orbitals. A hard acid is defined as the other but it is distinguished by small size, high positive charge, low polarizability, empty orbitals which are easily excited to higher states. Some examples of hard and soft acids and bases are given below :

Hard acids	Soft acids
$H^+$ , $Li^+$ , $Na^+$ , $K^+$	$Ag^+$ , $Cu^+$ , $Hg^+$
$Ti^{4+}$ , $Zr^{4+}$ , $Hf^{4+}$	$Ag^+$ , $Cu^+$ , $Hg^+$
$BF_3$ , $BCl_3$	Metal ions of

Border line acids

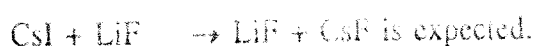


Hard bases	Border line	Soft bases
NH <sub>3</sub> , RNH <sub>2</sub> , N <sub>2</sub> H <sub>4</sub>	C <sub>6</sub> H <sub>5</sub> NH <sub>2</sub>	H <sup>-</sup> , R <sup>-</sup> , SO <sub>3</sub> <sup>-2</sup>
H <sub>2</sub> O, OH <sup>-</sup>	NO <sub>2</sub> <sup>-</sup>	R <sub>2</sub> S, RSH, R <sub>3</sub> P
CH <sub>3</sub> COO <sup>-</sup>	Br <sup>-</sup>	I <sup>-</sup> , CN <sup>-</sup>
F <sup>-</sup> , Cl <sup>-</sup>		

### Electronegativity and Hardness and softness :

In general, species having relatively high electro-negativities are hard and those having low electronegativities are soft. We are considering the ions and that although  $\text{I}_2$ , for example, has a low electronegativity,  $\text{Li}^+$  ion has a relatively high electronegativity resulting from the extremely high second ionization potential which make  $\text{Li}^+$  classified as hard acid. On the contrary transition metals in low oxidation states ( $\text{Cu}^+$ ,  $\text{Ag}^+$ , etc.) have relatively low ionization energies and low electro-negativity. These are soft acids. This relation between hardness and electro-negativity helps explain the fact that trifluoromethyl group is considerably harder than the methyl group and boron trifluoride is harder than boron.

Pearson has called attention to an interesting anomaly between the rule of hard and soft acids and bases and Pauling's original method of defining electronegativity. According to Pauling, the ionic resonance energy is proportional to the square of the difference in electronegativities of the constituent atoms. This implies that the most stable bonds are formed between elements farthest apart in electronegativity, such as cesium and fluorine. One might then predict the stable compound formation of  $\text{CsF}$  considering the ionic resonance energy of  $\text{Cs-F}$ . Then



But, the reverse is true.



Here the hard - soft acid base rule works. The two harder species ( $\text{Li}^+$ ,  $\text{F}^-$ ) prefer each other and the two softer species ( $\text{Cs}^+$ ,  $\text{I}^-$ ) also seem to prefer each other.

In general, with data available for bond energies and bond lengths, small atoms form strong covalent bonds and large atoms form weaker covalent bonds. Apparent exceptions to this trend are weak O-O, N-N, and F-F bonds. The data indicate that interpreting hard-hard interactions (bonds between small atoms) as purely electrostatic and those between larger atoms (soft-soft interactions) as strong covalent bonds is not accurate. Covalent bonding is strongest between small atoms that can achieve very good overlap. In the total bond energy of  $\text{LiF}$  bond ( $573 \text{ KJ mol}^{-1}$ ) roughly one-fourth comes from covalent bonding, one-half from a Madelung

(electrostatic) attraction between the partial charges on Li and F atoms and about one-fourth from the transfer of partial charge from the more electropositive lithium atom to the more electronegative fluorine atom (this latter corresponds roughly to Pauling's ionic resonance energy)

### **Theoretical Basis of HSAB concept :**

There is no complete unanimity among chemists concerning relative importance of the various possible factors that might affect the strength of hard-hard and soft-soft interactions.

A simple explanation for hard-hard interaction may be primarily electrostatic or ionic interaction. Most of the typical hard acids and bases are those that we might suppose to form ionic bonds such as  $\text{Li}^+$ ,  $\text{Na}^+$ ,  $\text{K}^+$ ,  $\text{F}^-$  and  $\text{OH}^-$ . Since the electrostatic or Madelung energy of an ion pair is inversely proportional to the interatomic distance, the smaller ions involved, the greater is the attraction between the hard acid and base. Since the electrostatic interaction does not account for the apparent stability of soft-soft interactions, it has been suggested that the predominant factor here is a covalent one. This correlation is well for the transition metals, Ag, Hg, etc., since it is usually assumed that bonds such as Ag-Cl are considerably more covalent than the corresponding ones of the alkali metals. In this regard the polarizing power and the polarizability of d-electrons becomes important. It has been pointed out that all really soft acids are transition metals with six or more d-electrons with  $d^{10}$  configuration ( $\text{Ag}^+$ ,  $\text{Hg}^{2+}$ ), being extremely good. From this point of view that polarization effects in soft-soft interactions resemble in some ways the ideas of Fajans although there are notable difference.

Pi bonding has been suggested as possibly contributing to soft-soft interactions. Pi bonding occurs most readily in those metal ions that have low oxidation states and large numbers of d electrons. Class (b) metal ions (soft Lewis acids) satisfy this criterion. Furthermore, the important  $\pi$  - bonding ligands such as carbon monoxide, phosphines, phosphates and heavier halogens are all soft bases. The presence of d - orbitals of the ligand in each case except carbon monoxide enhances  $\pi$  - bonding. Thus the second row elements N, O and F are precluded from entering into this type of interactions. Finally it should be pointed out that London dispersion energies increase with increasing size and polarisability and might thus stabilize a bond between two large polarizable (soft) atoms.

### **Symbiosis :**

The hardness and softness of an acidic or basic site is not an inherent property of the particular atom at that site but can be influenced by the substituent atoms. The addition of soft, polarizable substituents can soften and otherwise hard center and the presence of electron withdrawing substituents can reduce the softness of a site. The acidic boron atom ( $\text{B}^{3+}$ ) is borderline between hard and soft acids. Addition of three hard electronegative fluorine atoms hardens the boron and makes it a hard Lewis acid. Conversely, addition of three soft, electropositive hydrogens softens the boron and makes it a soft Lewis acid.

The hard  $\text{BF}_3$  molecule will prefer to bond another fluoride ion but the soft  $\text{BH}_3$  acid will prefer softer hydride ion.



In a competitive reaction, therefore the reaction proceeding to the right is



The fluorinated methanes isoelectronic with the above, behave in a similar manner.

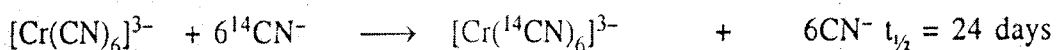
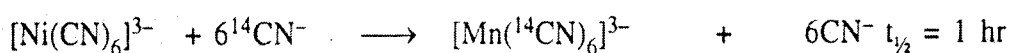
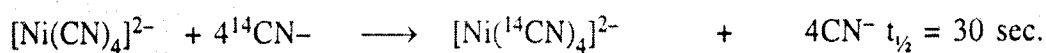


Jorgensen has referred to this tendency of fluoride ions to favour further co-ordination by a fourth fluoride ion (the same is true for hydride ions) as symbiosis. Although other factors can work to oppose the symbiotic tendency, it has widespread effect in inorganic chemistry and helps to explain the tendency for compounds to be symmetrically substituted rather than to have mixed substituents.

#### Kinetic stability, Lability and Inertness :

The terms 'stable' and 'unstable' are commonly reserved for thermodynamic reactivity, whereas kinetically reactive systems are said to be 'labile' and kinetically unreactive system inert (even though either may be thermodynamically unstable). The terms labile and inert are deviously relative, and two chemists might not use them in identical ways. Taube has suggested that those complexes which react completely within about one minute at  $25^\circ\text{C}$  should be considered as labile and those that take longer time be considered inert.

Consider the complexes  $[\text{Ni}(\text{CN})_4]^{2-}$ ,  $[\text{Mn}(\text{CN})_6]^{3-}$ ,  $[\text{Cr}(\text{CN})_6]^{3-}$ . All of these are extremely stable in the view of thermodynamics. Yet kinetically they are quite different. During the measurement of rate of exchange of radiocarbonlabelled cyanide the first is extremely labile the second is moderately so and only  $[\text{Cr}(\text{CN})_6]^{3-}$  is considered to be inert.



The tetracyanonickelate ion is a good example of a thermodynamically stable complex which is kinetically labile. The classic example of the opposite case (i.e) the kinetically inert complex which is thermodynamically unstable, is the hexamminecobalt (III) cation in acid solution. It is expected to decompose.



The tremendous thermodynamic driving force of six basic ammonia molecule attaching to six protons results in an equilibrium constant for the reaction  $\approx 10^{25}$ . Nevertheless acidification of a solution of hexaamminecobalt (III) results in no noticeable change and several days are required, at room temperature, for degradation of the complex despite the driving force of favourable thermodynamics. The inertness results from the absence of a suitable low-energy pathway for the acidolysis reaction. The difference between stable and inert can be expressed succinctly. Stable complexes have large positive free energies of reaction  $\Delta G$ ; inert complexes merely have large positive free energies of activation,  $\Delta G^*$ . The lability of  $\text{Ni}^{2+}$  complexes can be associated with the ready availability of  $\text{Ni}^{2+}$  to form 5- or 6- coordinated complexes. The additional bond energy of the fifth (or fifth and sixth) bond in part compensate for the loss of ligand field stabilization energy. In contrast, the reaction for  $[\text{Co}(\text{NH}_3)_6]^{3+}$  must involve either an extremely unstable 7-coordinate species or the formation of a 5-coordinate species with concomitant loss of bond energy and LFSE.

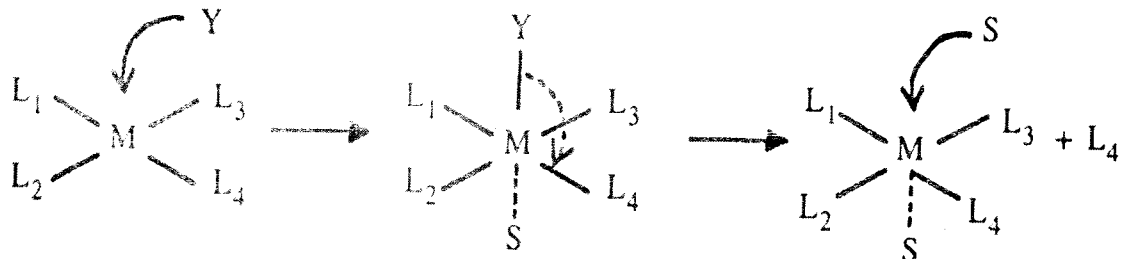
Kinetically labile complex has small (though) positive free energy of activation  $\Delta G^*$ . By contrast, a kinetically inert complex has a large positive  $\Delta G^*$ . Without fairly discussing the mechanistic aspects of the reactions, we can find the possible generalization. Since the electrostatic binding forces between the metal ion and ligand are larger for a higher cation charge, transition metal ions, however, have either non-zero CFSE or some Jahn-Teller distortion or both. Frequently geometric distortion can speed up the exchange of ligands because the rapid interconversion of axial and equatorial ligand, through molecular vibration stretches metal-ligand bonds. On the other hand, the extreme slowness of  $\text{Cr}^{3+}$ ,  $\text{Co}^{3+}$ ,  $\text{Ru}^{2+}$  and  $\text{Rh}^{3+}$  in octahedral complexes and  $\text{Pt}^{2+}$  in square-planar complexes can be attributed to crystal-field effects.

#### **Substitution in Planar Complexes :**

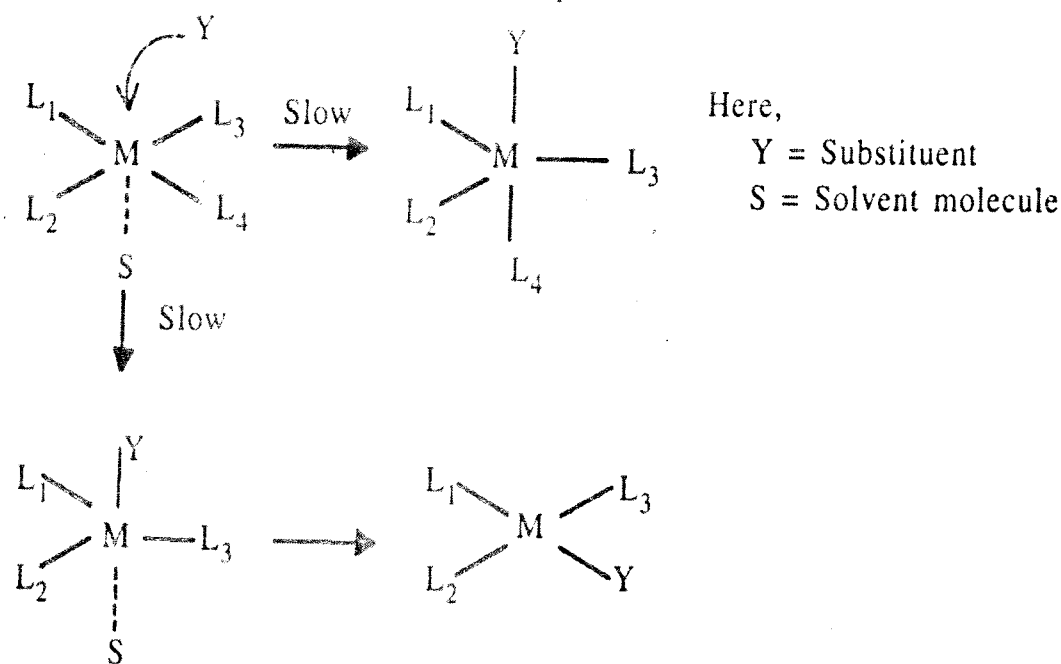
Nearly all kinetic works as square planar complexes which are almost all derivatives of  $d^8$  configuration, has been carried out on platinum (II) compounds the very limited data

for nickel (II), palladium (II) and gold (III) complexes show their reactions to be similar to those of platinum (II) complexes but much faster. Substitution in planar complexes is much less subject to steric factors than substitution in an octahedral complex.

There are two possible mechanisms for substitution in planar complexes. The first involves the formation of a square pyramidal, activated complex from which the most labile ligand ( $L_4$ ) is ejected.



The second mechanism by either pathway shown below, involves the formation of a 5-coordinate, trigonal bipyramid activated complex.



Kinetic studies of square planar  $Pt^{2+}$  complexes usually show a two-term rate law, suggesting two simultaneous mechanisms.

$$\text{Rate} = k [L_3PtL] = k_1 [L_3PtL] + k_2 [L_3PtL] [Y]$$

$$K = k_1 + k_2(Y)$$

The  $k_1$  (first order) mechanism presumably resembles the mechanism for octahedral substitution is being solvent controlled, though it may not be dissociative. We can get separate values for  $k_1$  and  $k_2$  by plotting  $k$  against  $(E)$  as in Fig.

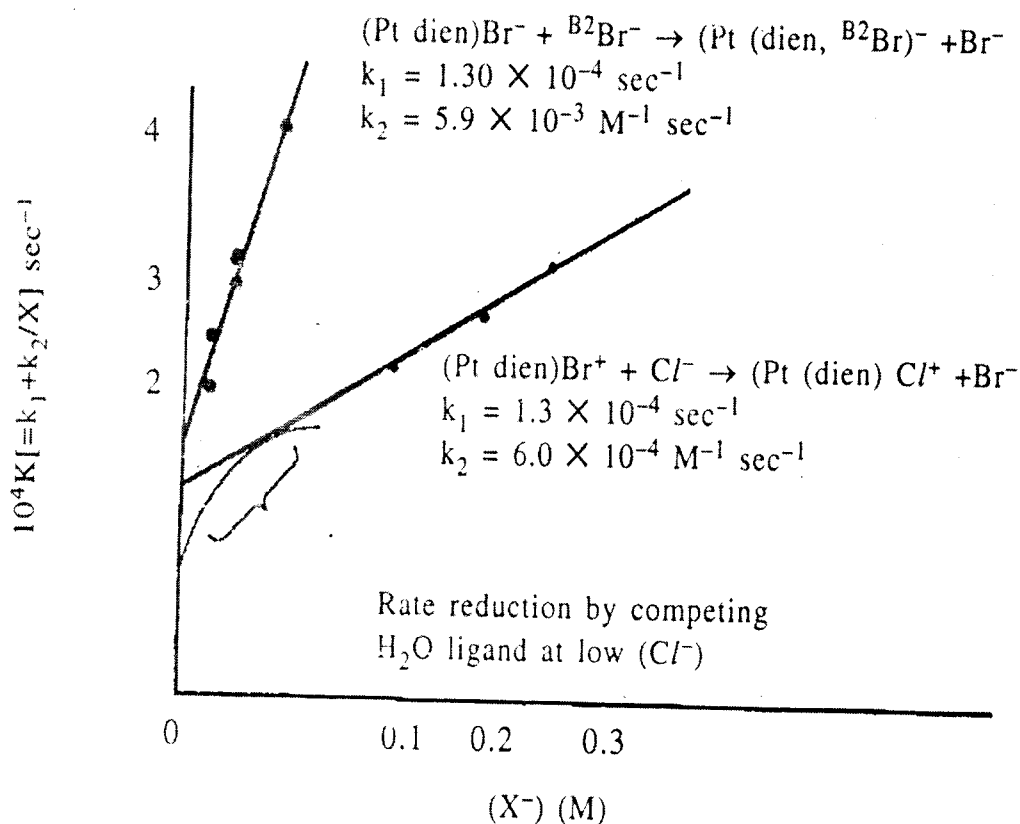
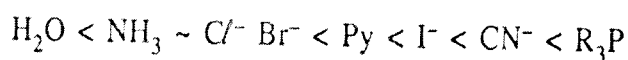


Fig. 1 : 5 : Rate data for first and second order substitution in  $(\text{Pt (dien) Br})^+$

The intercept ( $k_1$ ) is the same for both entering groups ( $\text{Y} = \text{Cl}^-$  and  $\text{Br}^-$ ), but the slope ( $k_2$ ) is quite different. This suggests that there is a strong bond-making or associative quality for the second-order mechanism. Further  $k_2$  is usually 10 - 100 times as large as  $k_1$ . There the experimental situation is that square-planar complexes undergo substitution predominantly by an associative mechanism. For most substitutions at Platinum (II),  $k_2$  is found to increase in the sequence,

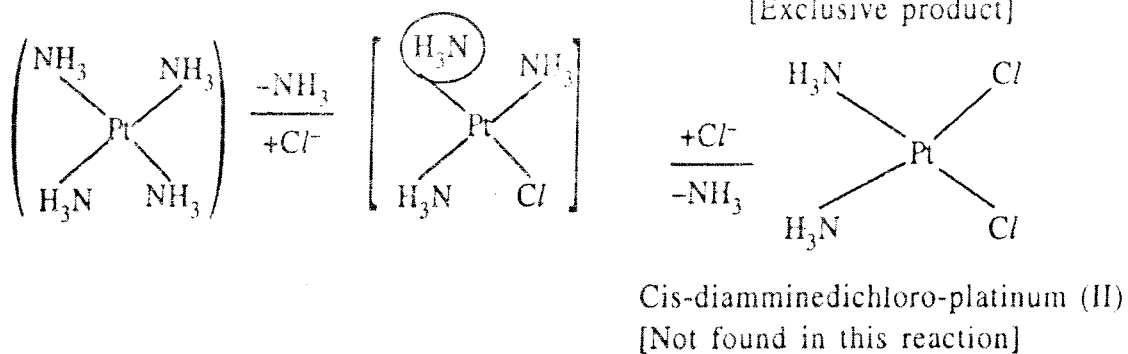
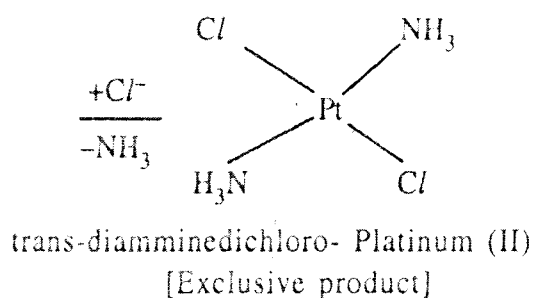
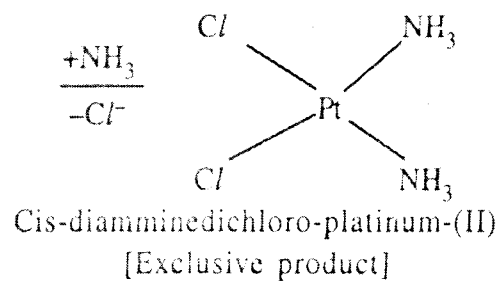
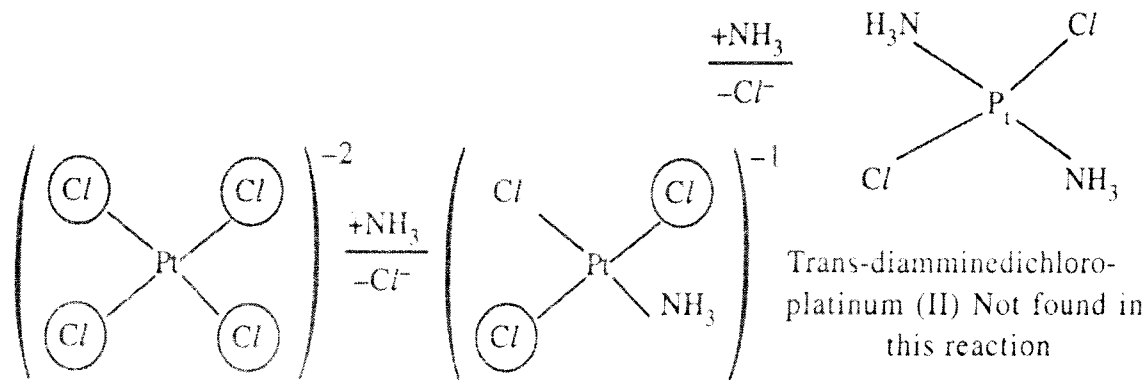


This sequence is sometimes referred to as the nucleophilicity sequence for substitution at Platinum (II).

### TRANS EFFECT :

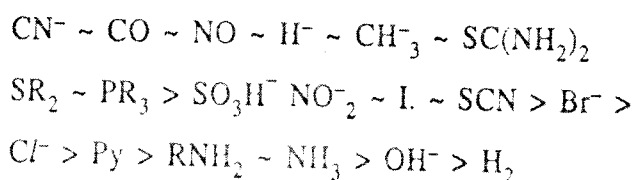
Ligand substitution reactions in square complexes such as those of  $\text{Pt}^{\text{II}}$  have some special features. A particular feature that attracts general interest is the so called transeffect.

Consider the two means of forming diamminedichloroplatinum (II). The first one is displacement of  $\text{Cl}^-$  ions from  $(\text{PtCl}_4)^{2-}$  by  $\text{NH}_3$  and the second one is displacement of ammonia by  $\text{Cl}^-$  in  $[\text{Pt}(\text{NH}_3)_4]^{2+}$ . It is found that two different isomers are formed.



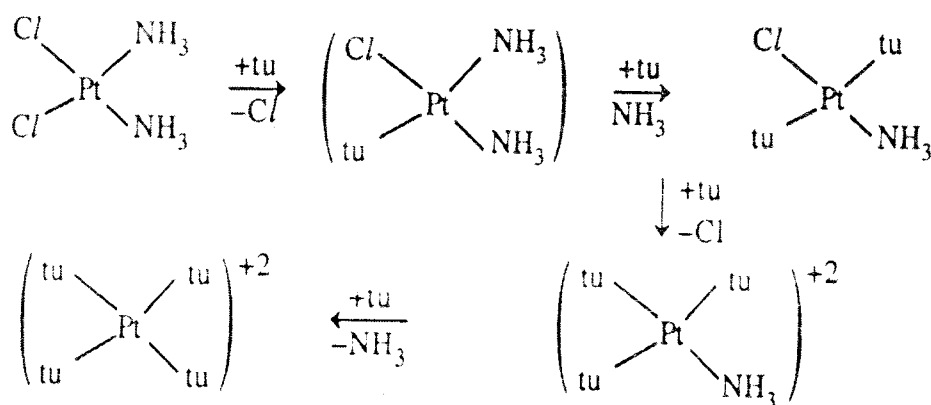
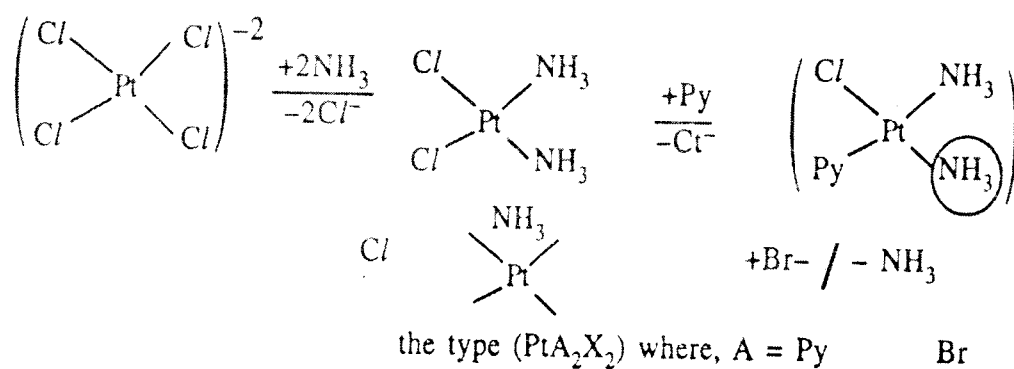
Reactions in the above equations can be rationalized as follows. Step one is a simple displacement and since all four groups present (either  $\text{NH}_3$  or  $\text{Cl}$ ) are identical, only one compound is formed. In second step, two products can potentially be formed in either reaction, but in particular only one is found and it differs between the two reactions. In both cases the isomer that is found is that which forms by substitution of a ligand trans to a chloride ion. The ligands trans to chloride ions have been circled, in the equations above to emphasize this

fact. The trans effect may be defined as the labilization of ligands trans to other, trans - directing ligands. By comparison of a large number of reactions, it is possible to set up a trans directing series. The order of ligands in this series is as follows :



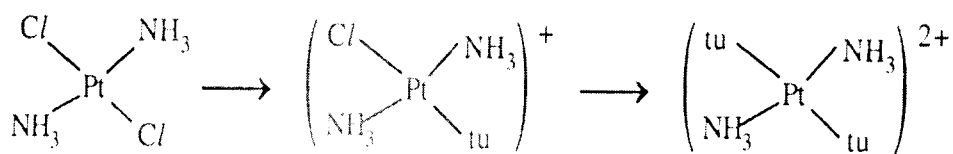
### Trans Effect in Synthesis :

It is possible to synthesise desired compounds by utilizing trans effect. For example, preparation of variedly substituted square planar complex the amminebromochloro(dine) platinum (II). By utilizing the trans effect, the reaction was carried out to get the product as in the following equation.

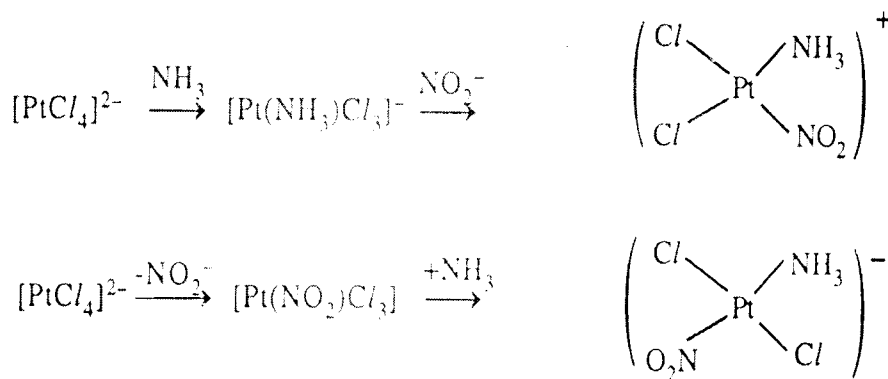


An interesting application of trans effect is in distinguishing cis and trans isomers of complexes of ammine and X = halide. Addition of thiourea (tu) to the cis isomer results in complete replacement of the former ligands.

But in the trans isomer the replacement stops after the two halide ions have been replaced, since the transammonia molecules do not labilize each other.

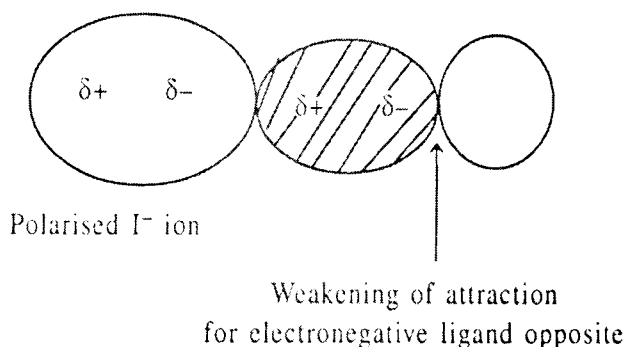


The trans effect is a useful aid in devising synthesis of platinum (II) complexes : thus for the preparation of cis and trans  $(\text{Pt NH}_3)(\text{NO}_2)\text{Cl}^-_2$  from  $(\text{PtCl}_4)^{2-}$ , we have to change the order of the two substitutions.



#### Mechanism of Trans Effect :

Two view points have been advanced with respect to the mechanism of trans effect. But these are not mutually exclusive. The first is a thermodynamic approach. A large, highly polarizable ligand like  $\text{I}^-$ , destored by the positive charge on the central atom, is imagined to polarize that atom itself to some extent thus weakens the bond between it and the opposite ligand Fig. (1.6). This theory was proposed by Grinberg.



#### 1.6 Representation of polarization of metal ion induced by highly polarizable ligand.

The second approach is a kinetic one and assumes an  $\text{S}_{\text{N}}2$  reaction. It uses the idea that a ligand which can accept electrons denoted back from the metal through  $d\pi - P\pi$  or  $d\pi - d\pi$  bonds will tend to reduce the electron density both above and below the bond situated

on the other side of the metal atom and thus open up the position for nucleophilic attack. This view is in better accord with the high position of ethylene in the trans-directing series, since this ligand cannot have a strong electrostatic effect.

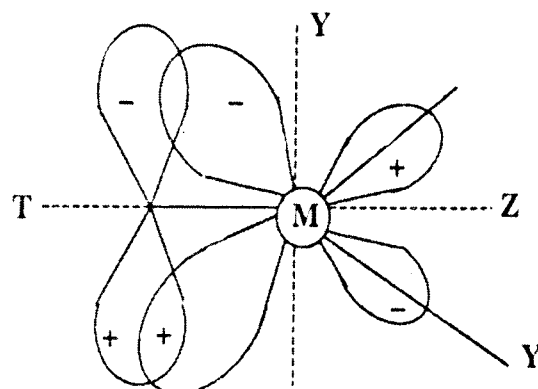
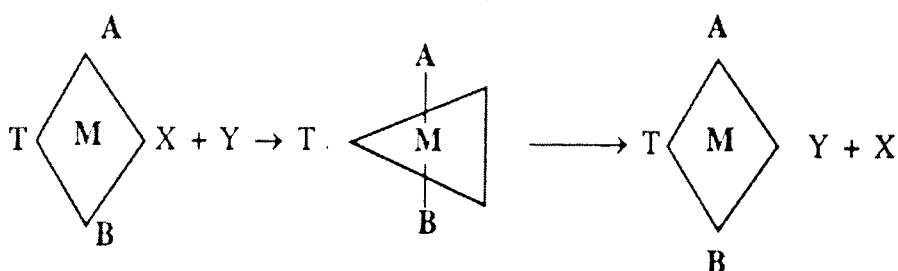


Fig. (1.7) The effect of  $\pi$  bonding on the electron density in the  $d_{xy}$  orbital and the consequent facilitation of substitution in the position trans to T.



### SUBSTITUTION IN OCTAHEDRAL COMPLEXES :

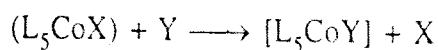
Most of the work in this field that has been earned out by classical methods involves complexes of chromium (III) ( $d^3$ ) or of low-spin cobalt (III) ( $d^6$ ), and it is with these that we study the mechanism of substitution in octahedral complexes. For most of the cations, the rate of substitution is nearly independent of the nature of incoming ligand, a fact which suggests exchange is predominantly dissociative ( $S_N1$ ) in character. The value of first order rate constant for the exchange of coordinated water for  $Cr^{3+}$  is about  $10^{-6} S^{-1}$ . We see that within a group of typical elements the rate constant increases with increasing cationic radius and further, the comparison of ions of similar radius (such as  $Li^+$ ,  $Mg^{2+}$  and  $Ga^{3+}$ ) show that increase in ionic charge retards substitution. Among dipositive cations of the first transition series, there is no correlation with ionic size and we deduce that electronic configuration must play a decisive part. The limited data for tripositive transition metal ions support a similar conclusion for these species too.

**Anation Reactions :** These are reactions in which an anion displaces  $H_2O$  from the coordination sphere. In general, attempt to distinguish between  $S_N1$  and  $S_N2$  mechanism have been unsuccessful because of complications such as ion pairing or the slow rate of anation compared to water exchange. In order to avoid the ion pairing problem, an anionic complex may be used and  $(Co(CN)_5H_2O)^{2-}$  has proved to be very suitable. The study proved that the reaction proceeds by an essential limiting  $S_N1$  mechanism with the intermediate  $(Co(C)_5)^{2-}$  having a long enough life time to discriminate between various ligands present in the solution.



#### Acid Hydrolysis of Cobalt (III) Complexes :

Whether hydrolysis of a complex  $[Co(NH_3)_5X]^{2+}$  yields  $[Co(NH_3)_5H_2O]^{3+}$  or  $[Co(NH_3)_5OH]^{2+}$  depends upon the hydrogenion concentration of the solution, the aquo complex being produced in acidic solution and hydroxo complex in basic solution. In acid hydrolysis the reaction rate is independent of the nature or the concentration of the entering group, which is further evidence for a dissociative mechanism. The rate of hydrolysis of Cobalt (III) ammine complexes are pH dependent and generally follow :



Here, in acid hydrolysis L is  $NH_3$  and Y is  $H_2O$ , and the general rate law is

$$V = k_A [L_5 CoX] + k_B [L_5 CoX] [OH^-]$$

In general,  $k_B$  (for base hydrolysis) is some  $10^5 - 10^6$  times  $k_A$  (for acid hydrolysis),

In low pH values the second term vanishes. The rate law is then compatible with either dissociation into  $[L_5Co]^{3+}$  and  $X^-$  or replacement of X by  $H_2O$  (present in effectively high concentration 55.5 M) Evidence for a dissociative mechanism in the case of  $X = H_2O$  is provided by the observation that the rate of exchange of water between  $[Co(NH_3)_5H_2O]^{2+}$  and  $H_2^{18}O$  decreases at high pressures. Further, a large increase in the rate when  $NH_3$  as ligand in  $[Co(NH_3)_5Cl]^{2+}$  is replaced by butylamine also indicates a dissociative mechanism and the same is true for another substantial increase on going from the doubly charged  $[Co(NH_3)_5Cl]^{2+}$  to the singly charged species  $trans - [Co(NH_3)_5Cl]^{2+}$ .

#### BASE HYDROLYSIS ( $S_N1$ ICB MECHANISM)

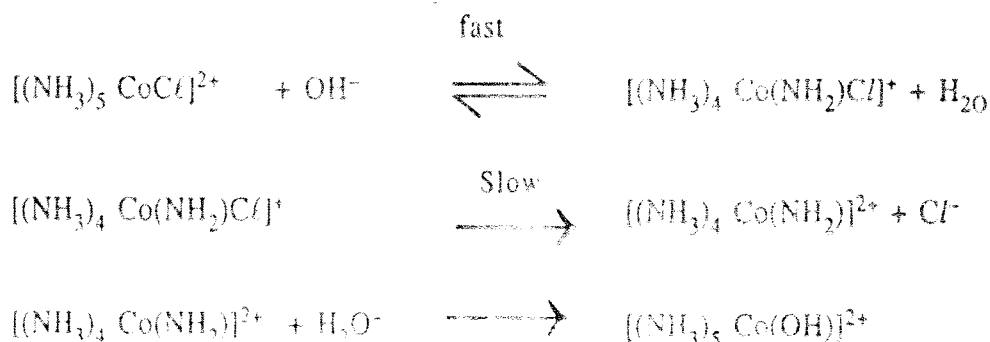
At pH values above 8, the first term of rate law disappears and the rate of the reaction is then given by

$$V = k_B [L_5 CoX] [OH^-]$$

The dependence upon hydroxide ion concentration can be taken as evidence of an associative ( $S_N2$ ) mechanism.



Although this adequately accounts for the kinetics of the reaction, the prevailing opinion is that the reaction takes place via an alternative mechanism. That is., the 7-coordinate complexes are not very stable compared to the relative stability of 5 - coordinate complexes. An alternative mechanism involving reaction through proton abstraction.



According to this view point the hydroxide ion would rapidly set up an equilibrium with the amidocobalt complex. The rate determining step would be the dissociation of this complex as in the acid hydrolysis discussed above. The concentration of the amido complex would be dependent, however on the hydroxide ion concentration through equilibrium hence the reaction rate would be proportional to the hydroxide ion concentration.

This mechanism assigned the symbolism  $S_N1\text{CB}$  for the first order reaction acting on the conjugate base of the complex (amido group is the conjugate base of ammine group), is supported by a number of observations. It rationalizes the fact that the hydroxide ion is unique in its million fold increase in rate over acid hydrolysis, other anions which are incapable of abstracting protons from the complex but which would otherwise be expected to be good nucleophiles in an  $S_N2$  reaction do not show this increase. Further more  $S_N1\text{CB}$  mechanism can apply only to complexes in which one or more ligands have ionizable hydrogen atoms. Thus complexes such as  $[\text{Co}(\text{Py})_4\text{Cl}_2]^+$  and  $[\text{Co}(\text{CN})_5\text{Cl}]^{2-}$  would not be expected to exhibit typical base hydrolysis and they, indeed, do not. The hydrolysis proceeds slowly and without dependence upon the hydroxide ion.

Further, interesting evidence for the conjugate base comes from the study of the activity of peroxide ion  $\text{OOH}^-$ , in base hydrolysis. Since  $\text{OOH}^-$  compared to  $\text{OH}^-$  should proceed slowly if its function is to form the conjugate base by removing a proton but faster if it attacks the metal in a genuine  $S_N2$  process. Experimental data are in agreement with the former.

## ELECTRON TRANSFER REACTIONS :

These can be divided into two main classes; (1) those in which the electron transfer effect has no net chemical change and (2) those in which there is a chemical change. The first types are called electron exchange processes and can be followed only by indirect methods like isotopic labeling or by nmr. The second type reactions are the usual oxidation – reduction reactions and can be followed by many chemical and physical methods. The electron exchange processes are of interest because of their particular suitability for the theoretical study.

There are two well-established general mechanisms for electron transfer processes. In one, each complex maintains its own complete coordination shell in the activated complex and the electron must tunnel through both of these shells. In the second mechanism there is at least one atom common to both coordination shells in the activated complex and usually the bridging atom (or atoms) is transferred along with the electron. These mechanisms are called, respectively the tunneling or outer sphere mechanism and the bridging or inner sphere mechanism.

### Outer sphere Mechanism :

This mechanism is certain to be the correct one when both species participating in the reaction undergo ligand exchange reactions more slowly than they undergo electron transfer. The simplest examples of oxidation-reduction reactions are those between species which differ only in charges such as  $[\text{Fe}(\text{CN})_6]^{4-}$  and  $[\text{Fe}(\text{CN})_6]^{3-}$  or  $[\text{IrCl}_6]^{3-}$  and  $[\text{IrCl}_6]^{2-}$ . Such reactions are commonly investigated by tracer methods, the broadening of e.s.r or n.m.r spectra can be sometimes utilized. In one novel method, the rate of loss of optical activity on mixing solution of a D-complex of one oxidation state and the L-complex of another oxidation state and (both complexes are kinetically inert) gives the rate of electron transfer by the reaction.

$$\text{D} - (\text{Os}(\text{dipy})_3]^{2+} + \text{L} [\text{Os}(\text{Dipy})_3]^{3+} \rightleftharpoons \text{L} - [\text{Os}(\text{dispy})_3]^{2+} + \text{D} - [\text{Os}(\text{dipy})_3]^{3+}$$

where both reactants are non-labile, e.g., in the case of  $[\text{Fe}(\text{CN})_6]^{4-}$  and  $[\text{Fe}(\text{CN})_6]^{3-}$ , a close approach of the metal atoms is impossible and the electron transfer must take place by a tunneling or outersphere mechanism.

In  $[\text{Fe}(\text{CN})_6]^{4-}$  and  $[\text{Fe}(\text{CN})_6]^{3-}$ , the Fe-C bond distances are nearly the same, since the iron atoms differ only in that the iron (II) ion has one more  $t_{2g}$  electron. On crystal field theory, this is in a non-bonding orbital, on ligand field theory it is at least partly dispersed over the ligands on account of  $\pi$ -bonding.

When electron transfer between the ions takes place, the products are at first in excited states, since according to Frank-Condon principle electron transfer is much faster than atomic

movement. If the geometries of the reacting complexes are only slightly different from what they would be in the transition state, the activation energy for the electron exchange is low and the reaction is rapid. For  $[\text{Co}(\text{NH}_3)_6]^{2+}$  and  $[\text{Co}(\text{NH}_3)_6]^{3+}$  on the other hand, the Co–C bond lengths (2.11 and 1.96 Å) are appreciably different and furthermore, the cobalt (II) complex is a high-spin one and the cobalt III complex a low spin one, the electronic configuration of the metal ions being  $(t_{2g})^5 (e_g)^2$  and  $(t_{2g})^6$ , respectively. After electron transfer these presumably become  $(t_{2g})^5 (e_g)^1$  and  $(t_{2g})^6 (e_g)^1$ , neither has a high 'activation' energy. Here, the electron exchange is slower than that in  $[\text{Fe}(\text{CN})_6]^{4-}$  and  $[\text{Fe}(\text{CN})_6]^{3-}$ .

In  $[\text{Fe}(\text{CN})_6]^{4-} - [\text{Fe}(\text{CN})_6]^{3-}$  exchange reaction is catalysed by alkali metal ions, the effect being greater for caesium and smaller for lithium. The very large cation  $\text{Ph}_4\text{As}^+$  has little effect. These results suggest that a partly desolvated cation accelerates exchange by helping to overcome electrostatic repulsion by formation of a transition state such as

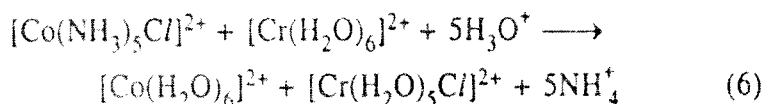


A small cation holds its hydration sheath too strongly, whilst a very large one does not bring the anions into close proximity. It is interesting to note that the  $\text{MnO}_4^{2-} \cdots \text{MnO}_4^-$  exchange reaction is also subject to alkali metal ion catalysis the order of effectiveness being same as for the  $[\text{Fe}(\text{CN})_6]^{4-} - [\text{Fe}(\text{CN})_6]^{3-}$  reaction.

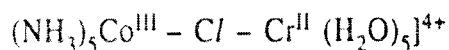
Outer-sphere reactions between complexes of different metals (e.g)  $[\text{Os}(\text{dipy})_3]^{2+} - [\text{Mo}(\text{CN})_8]^{3-}$  are usually faster than outer sphere exchange reactions between different oxidation states of the same element. Here the activation energy is lowered and rate is increased. It has been shown theoretically that there should be a relationship between the rates of such reactions and their standard free energies and there is considerable evidence in support of this theory.

### Inner Sphere Mechanism :

Many oxidation - reductions have been shown to occur by a ligand - bridging or inner sphere mechanism in which substitution of the coordination shell of one of the metal ions occurs. The classic example of such a reaction is that between  $[\text{Co}(\text{NH}_3)_5\text{Cl}]^{2+}$  and  $[\text{Cr}(\text{H}_2\text{O})_6]^{2+}$  in acidic solution, first investigated by Taube.



Both  $[\text{Co}(\text{NH}_3)_5\text{Cl}]^{2+}$  and  $[\text{Cr}(\text{H}_2\text{O})_5\text{Cl}]^{2+}$  are typical low spin and non-labile complexes (unlike the two aquoions in the equations). A reasonable explanation is that bridged intermediate is formed and breaks to give the chloro complex of chromium – (III).



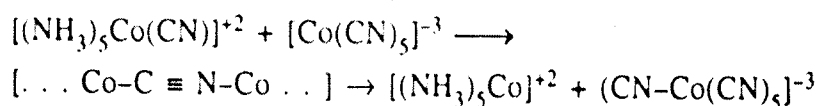
If the reaction is carried out in the presence of  $^{36}\text{Cl}^-$  in the solution none of the isotope appears in the chromium (III) complex, this fact provides further support for the bridging mechanism. Because the change in oxidation states of the metal ions is accompanied by transfer of a chlorine atom, the process is often referred to as an atom transfer reaction.

Among halide ions, the effectiveness for bridging purposes is  $\text{F}^- < \text{Cl}^- < \text{Br}^- < \text{I}^-$  in accordance with the expected order of ability to transmit an electron and undergo covalent bond-breakage. Bridging is taking place with halide ions, sulphate, phosphate, acetate, succinate, oxalate and maleate. Of the organic ions mentioned, oxalate and maleate (which contain conjugated systems) are considerably more effective than acetate and succinate.

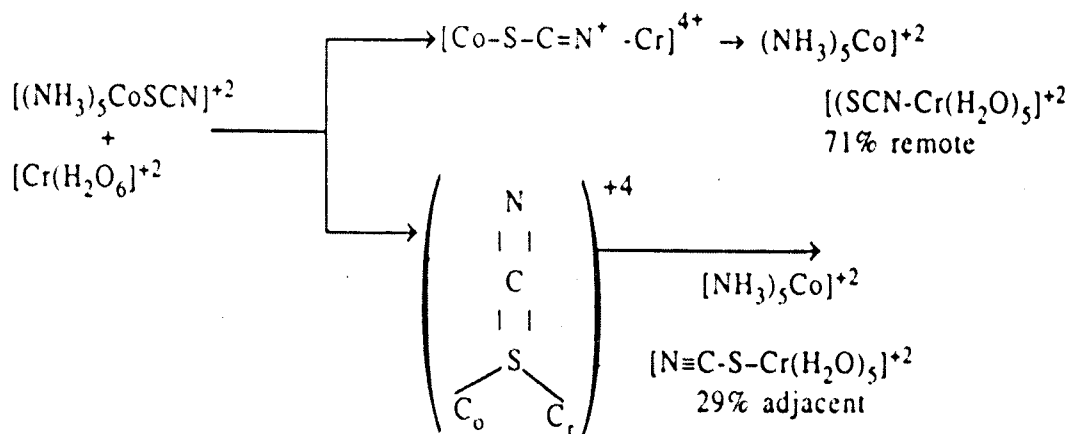
The same reductant may appear to react by both inner and outer sphere mechanism. We have examples like  $[\text{Co}(\text{CN})_5]^{3-}$  (obtained by addition of Cobalt (II) salt in excess of cyanide in the absence of air) reacts with  $[\text{Fe}(\text{CN})_6]^{3-}$  a binuclear complex  $[(\text{CN})_5\text{Co}(\text{CN})\text{Fe}(\text{CN})_5]^{6-}$  is produced and may be isolated as the barium salt, hydrolysis of the ion, which is very slow gives  $[(\text{Co}(\text{CN})_5\text{H}_2\text{O})]^{2-}$  and  $[\text{Fe}(\text{CN})_6]^{4-}$  showing that the bridging mechanism for electron transfer need not necessarily result in atom transfer.

Inner sphere mechanisms of this type have several consequences. The first one is the transfer of a ligand from one coordination sphere to another. A second is that for a such as the above, the rate will be less faster than the rate of exchange of the ligand in the absence of a redox reaction, since the exchange of ligand the ligand is an intimate part of the process. A third, less obvious consequence, is that the reaction is zero order in one important reactant, and the order changes to first order with change of site of attack the rate determining step.

If the bridging ligand contains more than one atom, the thermodynamically favoured isomer may not be the product obtained. The geometry of the bridge may result in a linkage isomer (remote attack) of the most product.



If thiocyanate ion is the ligand, the remote attack or adjacent attack leads to the formation of linkage isomers (eqn.8)



## Outersphere reactions in photochemical reactions :

The photochemistry of transition metal complexes is more varied than large organic molecules because of the possibility of different orbital types of excitation and of overall symmetry of the complex which may vary from  $O_h$  to  $C_3$ . A set of metal orbitals and a set of ligand orbitals are available. For  $\pi$  - bonding ligand a set of  $\pi$ ,  $\pi^*$  orbitals are also available. Basically four different types of low lying energy states can be described depending on whether the excitation is localized within the metal ion energy manifold or within the organic ligand energy manifold or delocalized. These are termed as follows :

- (i) d - d states or ligand - field states : They arise from promotion of an electron from  $t_{2g}$  (nonbonding) to  $e_g$  (antibonding orbital) for octahedral symmetry, an excitation confined essentially to the metal ion. The energy difference is determined by  $\Delta$ , the ligand field parameter. The  $\Delta$  is a function of ligand field strengths, the position of the metal ion in the periodic table and the oxidation state of the ion. Further splitting of the T states may arise due to interelectronic repulsion terms. These states are labeled according to group symmetry nomenclature. Because of the Laporte forbidden nature, molar extinction values are low,  $\epsilon \approx 1.150 \text{ l mol}^{-1} \text{ cm}^{-1}$ . The resulting increase in antibonding electron density decreases the net bonding in the complex and causes a lengthening of the metal ligand bonds.
- (ii) d- $\pi^*$  states : These arise from excitation of a metal electron of a  $\pi^*$  antibonding orbital located on the ligand system. This can be considered as transfer of an electron from the metal (M) to the ligand (L) and hence, is termed CTML type. Since such transfers leave the metal ion temporarily in an oxidized state such states are related to the redox potentials of the complex. The (d,  $\pi^*$ ) state should lie at relatively low energy for easily oxidizable complex. Thus, the change of central metal ion will considerably affect the position of the (d,  $\pi^*$ ) states. They have charge transfer character and high molar extinction,  $\epsilon = 10^4 \text{ l mol}^{-1} \text{ cm}^{-1}$ . The reverse process; the charge transfer from the ligand to the metal may also occur, i.e., CTLM type transitions.
- (iii)  $\pi - \pi^*$  states : These states arise from localized transition within the ligand energy levels. They lie at relatively high energies. The metal ions perturb them only slightly but can drastically affect the photophysical processes, originating from them.
- (iv)  $\pi - d$  states : Such states are expected to arise from a promotion of an electronic charge from ligand  $\pi$ - system to the higher orbitals of the metal (e-type for  $O_h$  symmetry).

These are not very well established.

Each of these promotional types of energy states can further be split by spin-orbital coupling interactions to give singlet and triplet states. For heavier elements the total angular momentum quantum number J becomes a 'good' quantum number. Spin-orbital coupling interaction energy can vary from  $500 \text{ cm}^{-1}$  ( $\text{Co}^{3+}$ ) to  $4000 \text{ cm}^{-1}$  ( $\text{Ir}^{3+}$ ). The relative ordering of energy levels can be altered by replacing metal ions, exchanging ligands, modifying the ligand or by varying the geometry. These levels can also be modified by solvent effects.

SPECTRAL METHODS - I

ELECTRONIC SPECTROSCOPY

L-S Coupling and Term Symbols :

In expressing the energy of an electron in terms of s, p, d, f states we are actually taking into account only two of the 4 quantum numbers necessary to completely describe the energy of an electron in an atom. In general, such a configuration will be highly degenerate because we are neglecting spin orbit interactions.

The term is an energy level of a system. The system may be specified by a configuration. Each configuration gives rise to a number of energy levels and hence to a number of terms. The term symbols are derived from Russell - Saunders or L-S coupling. We can assume that all the angular momenta of different electrons lie in an atom couple to give a resultant angular momentum L. Therefore

$$L = (l_1 + l_2), (l_1 + l_2 - 1), (l_1 + l_2 - 2) \dots ((l_1 - l_2))$$

Therefore, The total angular momentum will be =  $(2l + 1)$  values

For simple configuration of  $sp^2$  we have one 's' electron and 2 p electrons. For the 's' electron  $l = 0$ , therefore  $L_1 = 0$ . For the 2 p electrons  $l_1 = l_2 = 1$ .

$$L_2 = (1 + 1), (1 + 1 - 1), (1 + 1 - 2) = (l_1 - l_2) = 2, 1, 0.$$

In a similar manner, individual spin couple together to give a resultant spin S. The resultant spin S is obtained by the algebraic sum of the s values of separate electron  $S = \sum s_i$

The L and S values couple to give the total angular momentum quantum number J. The possible values for J are

$$J = L + S, L + S - 1, L + S - 2, \dots |L - S|$$

i.e.,  $|L + S| \dots |L - S|$

J may be positive or zero.

An atomic state with given L and S values thus consists of group of components having energies that are generally relatively close together. The number of components of the group is equal to the number of possible J values. The particular state is thus said to be a multiplet and to have a multiplicity equal to the number of J values.

If for instance  $S = 1/2$ , then  $J = L + 1/2$  i.e.,  $|L+S|$  and  $J = L + 1/2 - 1 = L - 1/2$  i.e.,  $|L-S|$

Therefore, the multiplicity is 2 and we have a doublet. If we consider a case with  $S = 1$  then

$J = L + 1 = L + 1$	$ L + S $
$J = L + 1 - 1 = L$	$ L + S - 1 $
$J = L + 1 - 2 = L - 1$	$ L - S $

Here the multiplicity is 3 and we have a triplet. In general, the multiplicity will be  $(2S + 1)$  provided that  $L$  is greater than  $S$ . If  $L < S$  there is only one possible value of  $J$ , although  $(2S + 1) > 1$ . For instance a line a electrons outside a closed shell could have  $l = 0 = L$  and  $S = 1/2 = S$  so that  $J = L + S = 0 + 1/2 = 1/2$  could have  $l = 0 = L$  and  $S = 1/2 = S$  so that  $2S + 1 = 2 \times 1/2 + 1 = 2$ .

In order to represent more completely the electronic state of an atom a scheme based on the use of spectral term symbols was introduced by H.N. Russell and F.A. Saunders. The term letters are derived as follows :

L	=	0	1	2	3	4	5	6
Term letter	=	S	P	D	F	G	H	I

The term letter is preceded by a superscript representing multiplicity of the term, that is  $2S + 1$ , and it is followed by a subscript giving the corresponding  $J$  value. Thus the term symbol is represented as  $^{2S+1}L_J$ .

For example : If  $L = 2$  and  $S = 1$ .

The term letter for  $L = 2$  is D

$$2S + 1 = 2 \times 1 + 1 = 3 \text{ and}$$

$$J = L + S = 2 + 1 = 3 = (L + S)$$

$$L + S - 1 = 2 + 1 - 1 = 2 = (L + S - 1)$$

$$L + S - 2 = 2 + 1 - 2 = 1 = (L - S)$$

The possible values of  $J$  are 3, 2 and 1. The three states of a triplet are  $^3D_3, ^3D_2, ^3D_1$ .

#### **j-j Coupling Scheme :**

Another possible relationship between electron repulsion and spin-orbit coupling perturbations is that in which the spin-orbit coupling is by much the more important. Then, instead of a configuration being split into terms as the first approximation, it is split into levels specified by spin-orbit coupling. The second step in this alternative relationship is to treat the electron repulsions as a perturbation on the spin-orbit coupling levels. Such an arrangement is known as the j,j coupling scheme; it is the direct reverse of the Russell-Saunders scheme. No ion of interest to ligand field theory comes anywhere near to conforming to the j,j coupling scheme. Amongst the heavier transition element ions many do not conform to either coupling scheme, and require something in between. To them an intermediate coupling scheme is said to apply. The only coupling scheme to be dealt with in detail here is the Russell - Saunders scheme, but occasional reference will be made to the intermediate coupling scheme.

In the Russell - Saunders coupling scheme each term is split up into a number of states which are specified by the total angular momentum quantum number,  $J$ . Each state is  $(2J + 1)$  - fold degenerate. The wave functions for the state are specified according to their  $Z$  component of total angular momentum,  $J_z$ , by the quantum number  $M_J$ .  $M_J$  course, runs in

integral steps from  $J$  to  $-J$ . For example if  $J = 2\frac{1}{2}, 1\frac{1}{2}, \frac{1}{2}, -\frac{1}{2}, -1\frac{1}{2}, -2\frac{1}{2}$ . The  $(2J - 1)$  fold degeneracy of a state is removed upon the application of a magnetic field.

Just as the total momentum of the state is specified by  $J$ , so it is possible to say that the orbital and spin angular momenta,  $l$  and  $s$ , of each individual electron are coupled together to give a total angular momentum for the electron,  $j$ , the  $Z$  component of the single electron total angular momentum, is specified by the quantum number,  $m_j$ , which proceeds in integral steps from  $j$  to  $-j$ . If, as outlined in the definition of the  $j$ - $j$  coupling scheme, spin-orbit coupling is the most important per-turbation action on a configuration, it is the coupling between the total angular momenta of the individual electrons which defines primary splitting of the energy of the configuration. This is the reason for the name  $j$ - $j$  coupling for the scheme.

### Term Symbols for $p^2$ Configuration :

If there are two or more electrons, it is usually necessary to proceed in a systematic fashion in generating these terms. The following is one method of doing so. The  $p^2$  configuration of carbon is used.

1. Determine the possible values of  $M_L$  and  $M_S$ , for the  $p^2$  configuration,  $L$  can have a maximum value of 2 and  $M_L$  can have values of  $-2, -1, 0, +1, +2$ . The electrons can be paired ( $M_S = 0$ ) or parallel ( $M_S = +1, -1$ ).

2. Determine the electron configurations that are allowed by the Pauli principle. The easiest way to do this is to draw up a number of sets of  $p$  orbitals as in Fig.2-1 each

$M_L =$	+2	0	-2	+1	0	-1	+1	0	-1	+1	0	-1	+1	0	-1
+1	↑↓			↑	↑	↓	↓			↑	↑		↓	↓	
0		↑↓		↑		↑	↓		↓	↓		↑	↑		↑
-1			↑↓		↑	↑		↓	↓		↓	↓		↑	↑

Fig. 2.1 Term splitting in the ground - state (vertical column represents a set of three  $p$  orbitals) and fill in electrons until all possible arrangements have been found. The  $M_L$  value for each arrangement can be found by summing  $m_l$  and  $M_S$  from the sum of  $m_s$  (spin-up electrons have arbitrarily been assigned  $m_s = +1/2$ ). Each microstate consists of one combination of  $M_L$  and  $M_S$ .

3. Set up a chart of microstates. For example, the microstate corresponding to the first vertical column in Fig. 2.1 has  $M_L = +2$  and  $M_S = 0$ . It is then entered into the table below under those values. Sometimes the  $m_l$  and  $m_s$  values are entered directly into the table,<sup>10</sup> but if the electron configurations have been carefully worked out, there is no need of this.

The fifteen microstates of  $p^2$  yield :

	$M_s$		
	+	0	-1
	-2		
	-1	x	x
$M_L$	0	x	x
	+1	x	x
	+2		

4. Resolve the chart of microstates into appropriate atomic states. An atomic state forms an array of microstates consisting  $2S + 1$  columns and  $2L + 1$  rows. For example, a  $^3p$  state requires a  $3 \times 3$  array of microstates. A  $^1D$  state requires a single column of 5 and a  $^5D$  requires a  $5 \times 5$  array, etc. Looking at the arrays of microstates, it is easy to spot the unique third microstate at  $M_L = 0$  and  $M_S = 0$ ; this must be a  $^1S$ . A central column of  $M_S = 0$  provides a  $^1D$ . Removing these two states from the table, one is left with an obvious  $3 \times 3$  array of a  $^3p$  state. The states of carbon are therefore  $^1S^1D$ , and  $^3P_{11}$ . The  $^3P$  is further split by differing J values to the terms  $^3P_1$  and  $^3P_2$ . The relative magnitude of these splittings can be seen in Fig. B.2. States for various electron configuration are shown in Table 2.1.

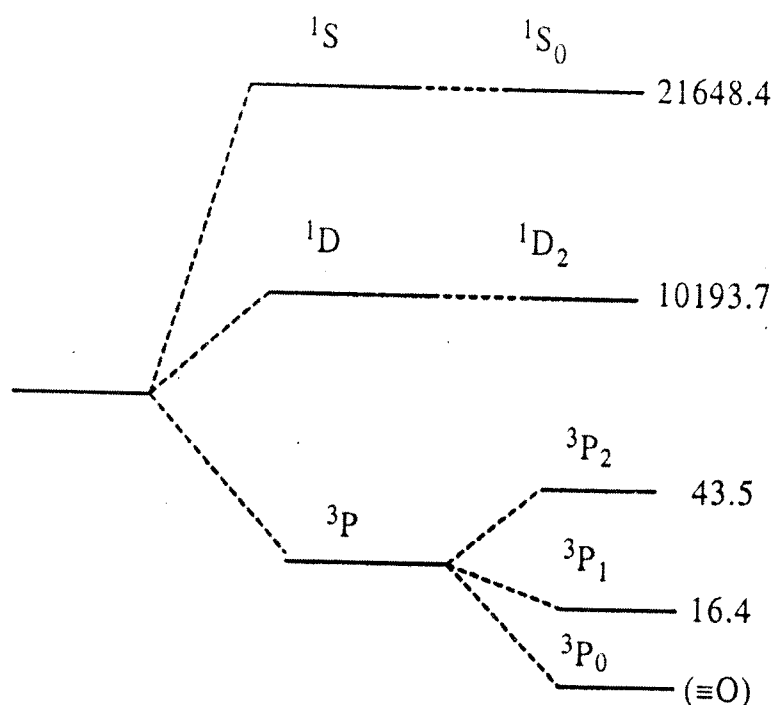


Fig.2.2 The fifteen microstates and resultant values of  $M_L$  and  $M_S$  for the  $1s^2 2s^2 2p^2$  electron configuration of carbon.

**Table 2.1 Multiple terms of various electron configurations**

Equivalent electrons	
$s^2, p^6, \text{ and } d^{10}$	$^1S$
$p \text{ and } p^5$	$^2P$
$p^2 \text{ and } p^4$	$^3P, ^1D, ^1S$
$p^3$	$^4S, ^2D, ^2P$
$d \text{ and } d^9$	$^2D$
$d^2 \text{ and } d^8$	$^3F, ^3P, ^1G, ^1D, ^1S$
$d^3 \text{ and } d^7$	$^4F, ^4P, ^2H, ^2G, ^2F, ^2D, ^2D, ^2P$
$d^4 \text{ and } d^6$	$^5D, ^3H, ^3G, ^3F, ^3F, ^3D, ^3P, ^3P, ^1I, ^1G, ^1G, ^1F, ^1D, ^1D, ^1S, ^1S$
$d^5$	$^6S, ^4G, ^4F, ^4D, ^4P, ^2I, ^2H, ^2G, ^2G, ^2F, ^2F, ^2D, ^2D, ^2P, ^2S$

Nonequivalent electrons	
$ss$	$^1S, ^3S$
$sp$	$^1P, ^3P$
$sd$	$^1D, ^3D$
$pp$	$^3D, ^1D, ^3P, ^1P, ^3S, ^1S$
$pd$	$^3F, ^1F, ^3D, ^1D, ^3P, ^1P$
$dd$	$^3G, ^1G, ^3F, ^1F, ^3D, ^1D, ^3P, ^1P, ^3S, ^1S$
$sss$	$^4S, ^2S, ^2S$
$ssp$	$^4P, ^2P, ^2P$
$ssp$	$^4D, ^2D, ^2D, ^4P, ^2P, ^2P, ^2P, ^2P, ^4S, ^2S, ^2S$
$spd$	$^4F, ^2F, ^2F, ^4D, ^2D, ^2D, ^4P, ^2P, ^2P$

Although the complexity of determining the appropriate terms increases with the number of electrons and with higher L values, the method outlined above (known as Russell-Saunders coupling) may be applied to atoms with more electrons than the carbon atom in the foregoing example. Russell-Saunders coupling (also called LS coupling because it assumes that the individual values of  $l$  and  $s$  couple to form L and S, respectively) is normally adequate, especially for lighter atoms. For heavier atoms with higher nuclear charges, coupling occurs between the spin and orbit for each electron ( $j = l + s$ ). The resultant coupling is known as jj coupling. In general, LS coupling is usually assumed and deviations are discussed in terms of the effects of spin-orbit interactions.

### Hund's rules :

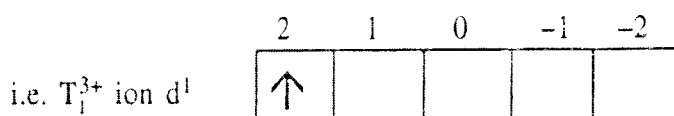
The ground state of an atom may be chosen by application of Hund's rules. Hund's first rule is that of maximum multiplicity. It states that the ground state will be that having the largest value of S, in the case of carbon the  $^3P$ . Such a system having a maximum number of parallel spins will be stabilized by the exchange energy resulting from their more favourable spatial distribution compared with that of paired electrons.

The second rule states that if two states have the same multiplicity, the one with the higher value of L will lie lower in energy. Thus the  $^1D$  lies lower in energy than the  $^1S$ . The greater stability of states in which the electrons are coupled to produce maximum angular momentum is also related to the spatial distribution and movement of the electrons.

The third rule states that for subshells that are less than half full, states with lower J are lower in energy; for subshells that are more than half full, states with higher J values are more stable. Applied to carbon, this rule predicts the ground state to be  $^3P_0$ .

### Term Symbols for $d^1$ and $d^2$ ions :

Suppose we calculate for  $d^1$



L

L = 2 Therefore term letter is D (one electron spin value =  $+\frac{1}{2}$ )

S =  $\frac{1}{2}$

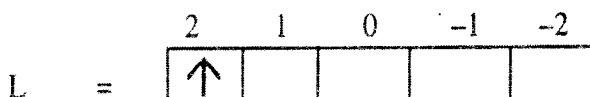
J = (L + S) to |L - S|  
 =  $2 + \frac{1}{2}$  and  $2 - \frac{1}{2} = \frac{5}{2}$  and  $\frac{3}{2}$

$2S + 1 = (2 \times \frac{1}{2} + 1) = 2$

The multiplicity is 2. The term symbol for  $d^1$  configuration is



$^2D_{5/2}$  This is spelt as doublet D five times half and  $^2D_{3/2}$  is doublet D three times half. For  $d^2$  ion.



L = 3

Term letter is F

$L_1 + L_2 = 2 + 1 + 3$  Multiplicity =  $2 + 1 + 3$ .

$l_1 - l_2 - 1 = 2 + 1 - 1 = 2$ . therefore term letter  $L = 3 = F$

$l_1 - l_2 = (2 - 1) = 1$ .  $2S + 1 = 2 \times 1 + 1 = 3$

(Since 2 electrons are unpaired  $2 \times 1/2 = 1$  for S)

$\therefore$  Ground term is  $^3F$  (triplet F)

L.S coupling is  $J = |L + S|$  to  $|L - S|$

$$L = \sum_i l_i \quad S = \sum_i s_i$$

$M_l$  is directly in the Z axis. Derivation of Ground terms of  $d^2$  ion. The 2 electrons are in d orbital (can be arranged in the following way of m).

	2	1	0	-1	-2
Triplet state	↑	↑			
	↑		↑		
	↑			↑	
	↑				↑
Singlet State	↑↓				
	↑	↓			
	↑		↓		
	↑			↓	
	↑				↓
				↓↑	
				↑↓	
	↑↑				
					↑↑

(The last \ is not different from the above / )

The first 'd' electron is arranged in 10 ways.

The second electron can combine with it in 9 ways only leading to the state called

'Microstates'.  $\frac{10 \times 9}{2} = 45$  microstates.

This arises in the following manner. This can be written as follows in a tabular form.

$M_{S1}$	4	3	2	1	0	-1	-2	-3	-4
0									
-1									

First we see that maximum  $m_l$  is possible in  $m_l = 4$  (in singlet state or paired state)

$$l_1 = l_2 = 2 \therefore l_1 + l_2 = 4 \quad m_l = 4$$

Now we have

**MULTIPLICITY**

$L = 4$	$S = 0$	$2S + 1 = 1$
$L = 3$	$S = 1$	$2S + 1 = 3$
$L = 2$	$S = 0$	$2S + 1 = 1$
$L = 1$	$S = 1$	$2S + 1 = 3$
$L = 0$	$S = 0$	$2S + 1 = 1$

For  $L = 4$  the term is G since the multiplicity is  $2S + 1 = 1$

It is  $^1G$  term (singlet G. For  $L = 3$ , the term is F

$2S + 1 = 3 \dots$  It is  $^3F$  (Triplet F).

For  $L = 2$ ,  $2S + 1 = 1$  and the term for  $L = 2$  is D.

Therefore it is  $^1D$  (singlet D)  $L = 1$ ,  $2S + 1 = 3$ .

The term for  $L = 1$  is P.  $\therefore$  The Term for  $L = 1$  is P.

Therefore it is  $^3P$  (Triplet P).

For  $L = 0$  and  $2S + 1 = 1$ . Term letter for  $L = 0$  is S.

$\therefore$  It is  $^1S$  (single S). Hence we find that for the  $d^2$  configuration the total energy term symbols in the ground state are

$$^1G, \quad ^3F, \quad ^1D, \quad ^3P, \quad ^1S$$

The ground term  $m_l$  for  $d^n$

$d_1^1$	2	$^2D$
$d^2$	3	$^3F$
$d^3$	3	$^4F$
$d^4$	2	$^5D$

$d^8$	3	$^3F$
$d^9$	2	$^2D$
$d^{10}$	0	$^1S$

### Orgel Diagrams :

Splitting of  $d^n$  terms in an octahedral field are as follows

$$S \rightarrow A_{1g}$$

$$P \rightarrow T_{1g}$$

$$D \rightarrow E_g + T_{2g}$$

$$F \rightarrow A_{2g} + T_{1g} + T_{2g}$$

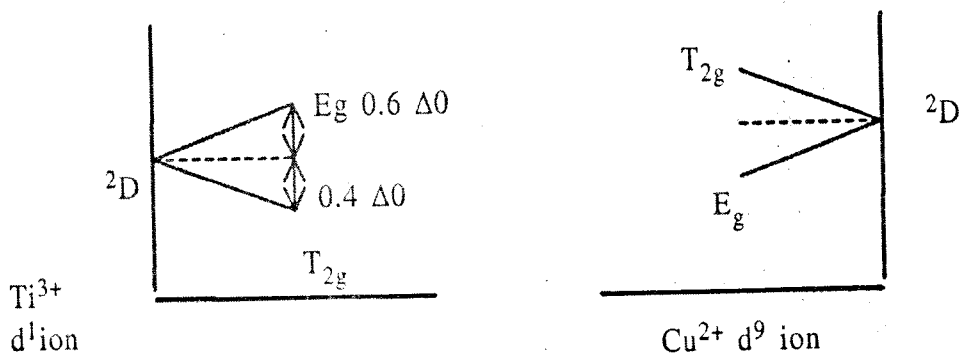
$$G \rightarrow A_{1g} + E_g + T_{1g} + T_{2g}$$

$$H \rightarrow E_g + T_{1g} + T_{1g} + T_{2g}$$

$$I \rightarrow A_{1g} + A_{2g} + E_g + T_{1g} + T_{2g} + T_{2g}$$

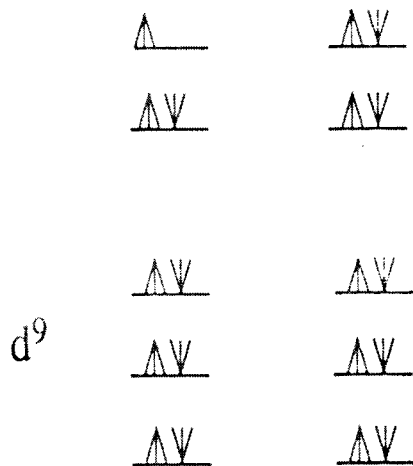
For  $[Ti(H_2O)_6]^{3+}$   $d$  configuration,  $m_l = 2$

$L = 2$  and  $S = \frac{1}{2}$  the grand term is  $^2D$  which is split into  $t_{2g}$  and  $e_g$  on the octahedral field and are written as  $^2T_{2g}$  and  $^2E_g$  (capital letters for states and small letters for  $e^-$ s).

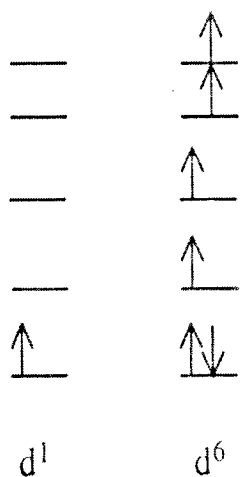


For  $d^9$  configuration of  $cu^{2+}$  in an octahedral field (actually a rare occurrence of Jahn Teller effect) the ground state is  $^2D$  and again split into  $t_{2g}$  and  $e_g$  corresponding to production of an electron from  $t_{2g}$  and  $e_g$ . But in this case, the state of lower energy is  $^2E_g$  and that of the higher energy is  $^2T_{2g}$ .

This is because the ground state is  $T_{2g}^6 e_g^3$  and is doubly degenerate. It can be  $T_{2g}^6(dx^2 - y^2)^2 (dz^2)$  (or)  $T_{2g}^6(dx^2 - y^2) (d_z^2)^2$  Whilst the excited state is triply degenerate. It can be  $(d_{xy})^2 (d_{yz})^2 (d_{xz})^1 e_g^1$ , (or)  $(d_{xy})^1 (d_{yz})^2 (d_{xz})^2 e_g^1$  (or)  $(d_{xy})^2 (d_{yz})^1 (d_{xz})^2 e_g^1$ . Thus for the  $d^9$  in octahedral field, the diagram for a  $d^1$  ion is inverted. (or we can say a hole is present in the  $e_g$  level in ground state and a hole in  $t_{2g}$  level in the excited state)



The diagram for  $d^1$  and  $d^9$  ions is also inverted by a change from grand state excited state from octahedral to tetrahedral field although for a given metal and distance  $\Delta t$  is only  $4/9 \Delta O$  further since high spin  $d^6$  differs from  $d^1$  only in that an  $e^-$  has been added to each orbital.



The diagram for this configuration is the same as for  $d^1$  by analogy ( $t_{2g}^1$  and  $t_{2g}^4 e_g^2$ ). By analogy high spin  $d^4$  has the same diagram as  $d^9$ . These relations are shown by Orgel diagram. Analogous reasoning for  $d^2$  and  $d^7$  and  $d^3$  and  $d^8$  also have the same diagrams.

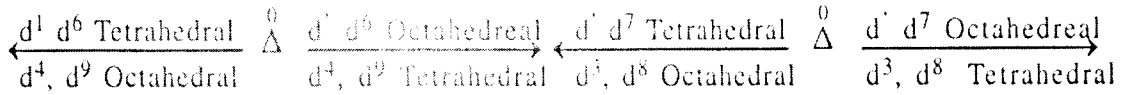
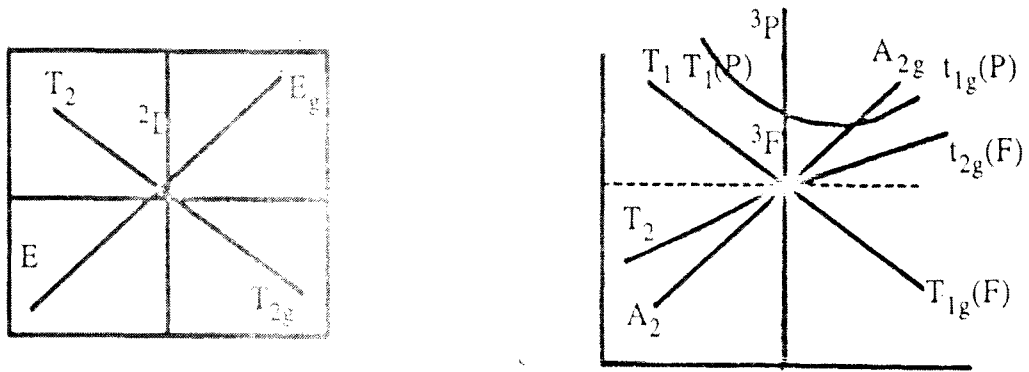


Fig. 2.3 : Orgel Diagrams for  $d^2 - d^8$  ions

Orgel Diagram for  $d^2$  ion ( $V^{3+}$  ion) :

In the absence of an external field  $d^2$  ion produces 2 states. The low energy  $^3F$  and high energy  $^3P$  states. In an octahedral field  $F$  splits into  $T_1$ ,  $T_2$  and  $A_2$  states. The ground state for  $d^2$  ion is  $dxy^1 dyz^1 dxz^0$ .

Orgel Diagrams for  $d^2 - d^8$  ions

In the absence of an external field  $d^2$  ion produces 2 states. The low energy  $^3F$  and high energy  $^3P$  states. In an octahedral field  $F$  splits into  $T_1$ ,  $T_2$  and  $A_2$  states. The ground

$dxy^1 dyz^0 dxz^1$ ,  $dxy^0 dyz^1 dxz^1$  and this is  $^3T_{1g}(F)$  state. If we excite one of these electrons to the higher energy  $e_g$  orbital there are two possibilities for the excited state configuration  $t_{2g}^1 e_g^1$ . If the  $dxz$  or  $dyz$  electrons is promoted it goes to the  $dz^2$  orbital which will experience less repulsion from  $dxy$  orbital similarly if the electron is excited from the  $dxy$  will be more stable than  $dyz$ . The arrangements  $(dxy)^1 (dyz)^1$ ;  $(dxz)^1 (dx^2-y^2)^1$ ,  $(dyz)^1 (dx^2-y^2)^1$ , produces  $^3T_{1g}(F)$  state. The other arrangement  $(dxy)^1 (dx^2-y^2)^1$ ,  $(dyz)^1 (dz^2)^1$   $(dxz)^1 (dz^2)^1$  produces  $^3T_{1g}(P)$  state. Lastly if the two electrons are promoted they give rise to  $t_{2g}^0 e_g^2$ ;  $(dx^2-y^2)^1 (dz^2)^1$  which is singly degenerate  $^3A_{2g}(F)$ ,  $^3A_{2g}(F)$  states and  $3p$  state is unsplit. The Orgel diagrams are applicable to weak field, high spin case only.



is greatly stabilized by the ligand field and drops rapidly becoming the ground state  $10Dq/B=20$ . At this point spin pairing takes place and hence there is a discontinuity in the diagram shown by the vertical line. Beyond this point the low spin  $^1A_{1g}$  term is the ground state. The  $^5E_g$  and  $^5T_{2g}$  continue to diverge with increasing field strength as might with respect be supposed from the Orgel diagram but quickly rise in energy to  $^1A_{1g}$  state and becomes unimportant. The arrows represent transitions in  $[CoF_6]^{3-}$  and  $[Co(en)_3]^{3+}$ . For high spin  $[CoF_6]^{3-}$  complex quintet state is important and one transition  $^5T_{2g} \rightarrow ^5E_g$  should be observed. Indeed the blue colour of this complex results from a single peak at  $1300\text{ cm}^{-1}$ . For low spin Co(III) complexes we would expect transition  $^1A_{1g} \rightarrow ^1T_{1g}$  and  $^1A_{1g} \rightarrow ^1T_{2g}$ . Further more although we should expect both of these transitions to increase in energy as the field increases, we might expect the latter to increase more rapidly than the former (compare slopes of  $T_{1g}$  &  $T_{2g}$ ). Thus the spectra of Co(III) complexes are therefore expected to show two absorption peaks and these peaks should appear more widely spaced at large values of  $D_q$ . The spectra of the yellow  $[Co(en)_3]^{3+}$  and the green  $[Co(ox)_3]^{3-}$  shown below confirms the expectations.

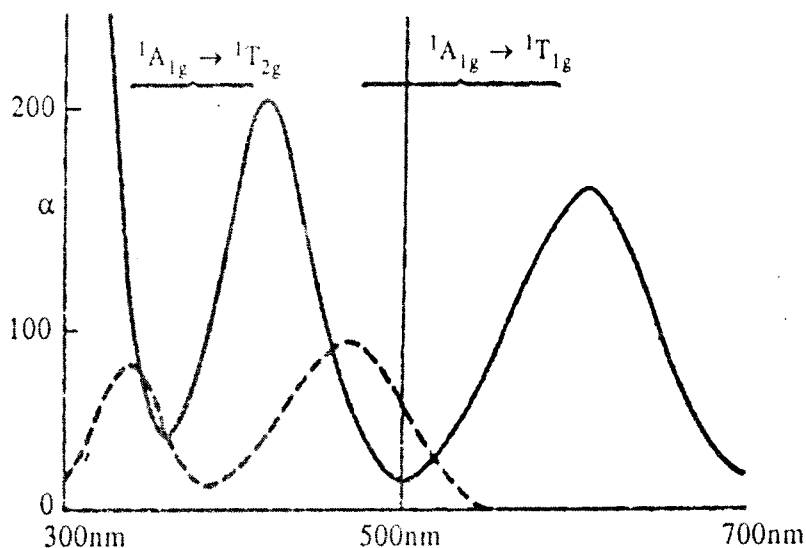


Fig 2.5.

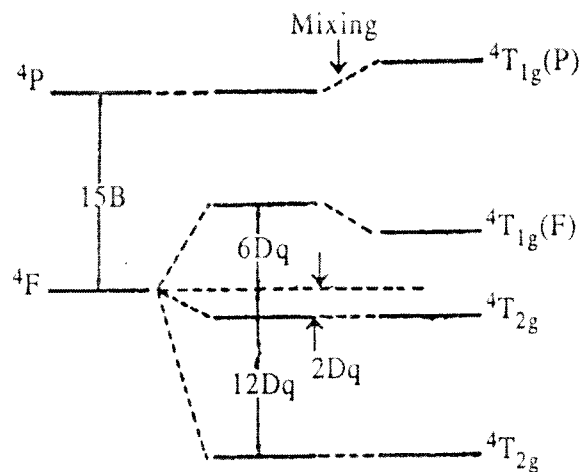


Fig. 2.6

We can compare the experimental results from spectra with those expected from theory. In general, the observed transitions will be  ${}^4A_{2g} \rightarrow {}^4T_{2g}$ ,  ${}^4A_{2g} \rightarrow {}^4T_{1g}(F)$ , and  ${}^4A_{2g} \rightarrow {}^4T_{1g}(P)$ . The transitions arising from the  ${}^2G$  state are either not observed or are very weak since they are spin forbidden. When we compare the experimental results for  $[\text{CrF}_6]^{-3}$ ,  $[\text{Cr}(\text{ox})_3]^{-3}$  and  $[\text{Cr}(\text{en})_3]^{+3}$  with the theoretical expectations, we obtain some interesting results. The  ${}^4A_{2g} \rightarrow {}^4T_{2g}$  transition [Band I, equal to 10 Dq] increases in progressing from  $L = \text{F}^-$  to  $L = \text{en}$ , as expected on the basis of the spectrochemical series. The  ${}^4A_{2g} \rightarrow {}^4T_{1g}(F)$  transition is expected to be 18Dq, or 80% greater than the  ${}^4A_{2g} \rightarrow {}^4T_{2g}$ . The transition  ${}^4A_{2g} \rightarrow {}^4T_{1g}(P)$  is expected, on the basis of the free ion, to be 15B, or  $15 \times 918 \text{ cm}^{-1} = 13770 \text{ cm}^{-1}$ . It can be seen that these expectations are not realized very closely by the experimental results. Two corrections must be made in order to improve the interpretation and correlation of the spectra. First, the extent of the mixing of the F and P terms was not included in approximation I. This will be discussed presently, but we must first note that even if this is known exactly, the experimental results cannot be duplicated using the free-ion value of B, even if it, too, is known exactly. The apparent value of B in complexes is always smaller than that of the free ion. This phenomenon is known as the nephelauxetic effect and is attributed to delocalization of the metal electrons over molecular orbitals that encompass not only the metal but the ligands

as electrons over molecular orbitals that encompass not only the metal but the ligands as electrons over molecular orbitals that encompass not only the metal but the ligands as well.

As a result of this delocalization or "cloud expanding" the

**Table 2.2 : Values of B for transition metal ions (cm<sup>-1</sup>)**

Metal	M <sup>+2</sup>	M <sup>+3</sup>
Ti	695	-
V	755	861
Cr	810	918
Mn	860	965
Fe	917	1015
Co	971	1065
Ni	1030	1115

average interelectronic repulsion is reduced and B' (representing B in the complex) is smaller. The nephelauxetic ratio  $\beta$ , is given by :

$$\beta = \frac{B'}{B}$$

It is always less than one and decrease with increasing delocalization. Estimates of  $\beta$  may be obtained from the nephelauxetic parameters  $h_x$  for the ligand and  $k_M$  for the metal :

$$(1 - \beta) = h_x \cdot k_M$$

If all three transitions are observed, it is a simple matter to assign a value to B' since the following equation must hold :

$$15B' = \gamma_3 + \gamma_2 - 3\gamma_1$$

where  $\gamma$  is the absorption occurring at the lowest frequency. For example, the value of B' in the fluoro complex is

$$= \frac{34400 + 22700 - 3(14900)}{15} = 827 \text{ cm}^{-1}$$

If only two transitions are observed (for example,  $\gamma_3$  may be obscured by a charge transfer band) it is still possible to calculate B' but the methods are beyond the scope of this book. However, sufficient spectra have been analyzed for the more common ligands and metal ions that  $\beta$  may be estimated and in turn used to estimate B from the free - ion value B.

If  $10 Dq$  can be measured directly as in the case of Cr(III) spectra ( $10 Dq = \gamma_1$ ) and

B', it is quite simple to estimate all of the transitions. For high - spin octahedral  $d^3$  and  $d^8$  and tetrahedral  $d^2$  and  $d^7$  species the appropriate equations are :

$$\gamma_1 = A_{2g} \rightarrow T_{2g} = 10 Dq$$

$$\gamma_2 = A_{2g} \rightarrow T_{1g}(F) = 7.5 B' + 15Dq - \frac{1}{2} (225B'^2 + 100 Dq^2 - 180B'Dq)^{1/2}$$

$$\gamma_3 = A_{2g} \rightarrow T_{1g}(P) = 7.5 B' + 15Dq - \frac{1}{2} (225B'^2 + 100 Dq^2 - 180B'Dq)^{1/2}$$

Using these equations, more accurate estimates can be made of the transitions and the spectrum fitted quite suitably.

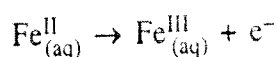
### Charge Transfer spectra :

Most transition metal complexes are coloured if the d-electron configuration is any thing other than  $d^0$  or  $d^{10}$ . The absorptions are transitions between terms that represent rearrangements of the d-electrons and most peaks appearing in the near infrared and visible ranges of the spectrum and even out into the ultraviolet represent d - d transitions. In the UV (high energy) range and sometimes down into the visible are peaks that represent the transfer of an electron from a ligand - based orbital to a metal based orbital (charge - transfer transition) charge - transfer peaks are usually quite intense but they are difficult to predict quantitatively. Charge - transfer bands usually occur in the near ultraviolet, often there is overlap between the end of a charge-transfer band and d-d absorption and when this happens it is impossible to obtain the full d - d spectrum of the complex.

In the series of complexes of formula  $[\text{Co}(\text{NH}_3)_5\text{X}]^{2+}$  where X is a halogens strong absorption in the ultraviolet takes place at progressively higher frequency for X = I, Br, Cl, F for X = F the spectrum is, infact, nearly the same as for X =  $\text{NH}_3$ . this suggests that the shift to higher frequencies is associated with increasing difficulty of transferring an electron from the ligand to metal (L  $\rightarrow$  M). The same process is believed to occur in the highly coloured compounds formed by interactions of iron (III) and thiocyanate or phenols. If the frequency of transition is low enough reduction of the metal occurs. Thus solutions of copper (II) in the presence of high concentration of  $\text{F}^-$  remains blue; in the present of high concentration of  $\text{Cl}^-$  and  $\text{Br}^-$  dark solutions are produced and iodide effects reduction to copper (I) iodide.

A majority of C - T complexes of transition metals involves ligand to metal electron transfers as is to be expected from the availability of non-bonding or antibonding orbitals of the metal, the reverse process also takes place. Metal to ligand (M  $\rightarrow$  L) CT occurs in the red complexes of iron (II) with dipyriddy and o-phenonthroline; it is obviously favoured if the metal is in a low oxidation state and the ligand has a low lying antibonding orbital. In pression

blue  $KFe^{III} [Fe^{II}(CN)_6]$  high spin Fe (III) is octahedrally coordinated by the nitrogen atoms of six cyanide ions and low spin iron (II) by six carbon atoms. In the excited state the former is reduced to high spin iron (II) and the latter oxidized to low - spin iron (III).



### Optical isomerism in octahedral chelate complexes :

The optical activity of complex compounds may result from either asymmetry of the molecule itself or from the ligand present in the molecule. For e.g.  $[Co(en)_3]^{3+}$  lacks a plane of symmetry. As a result such complexes can exist in either of the two optically active forms.

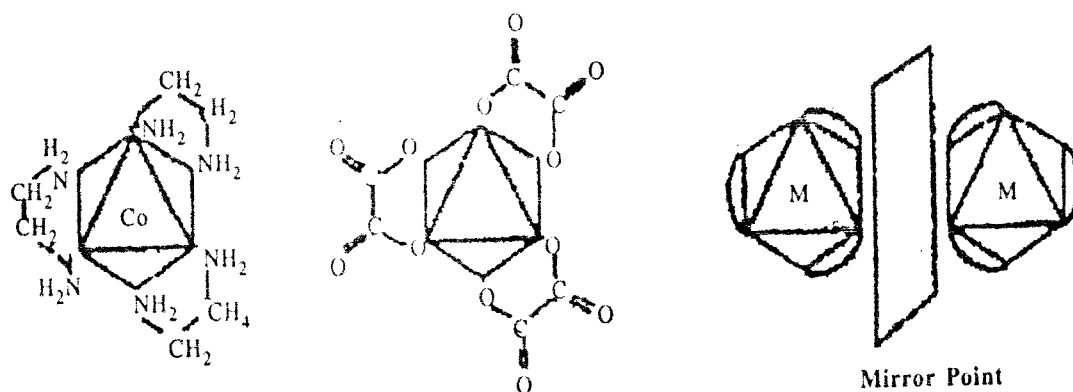


Fig. 2.7 Optical isomers of  $[Co(en)_3]^{3+}$

$[Co(en)_3]^{3+}$  exhibits optical isomerism. An operation criterion for lack of a plane of symmetry (and hence for optical isomerism) is the non-super imposability of the optical isomers. In 4-coordinated complexes, tetrahedral complexes with tris chelates with unsymmetrical ligands form optical isomers.

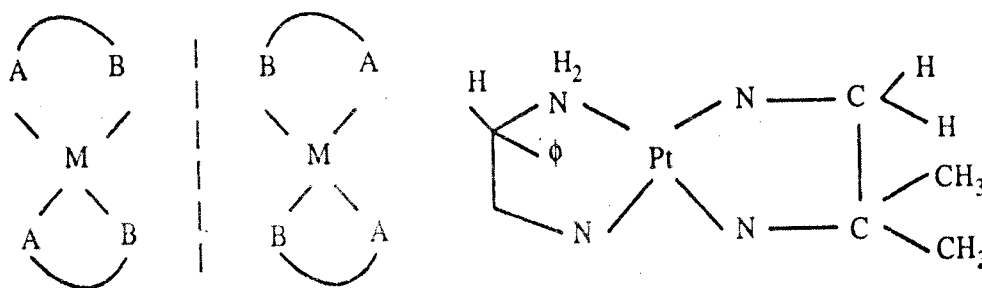


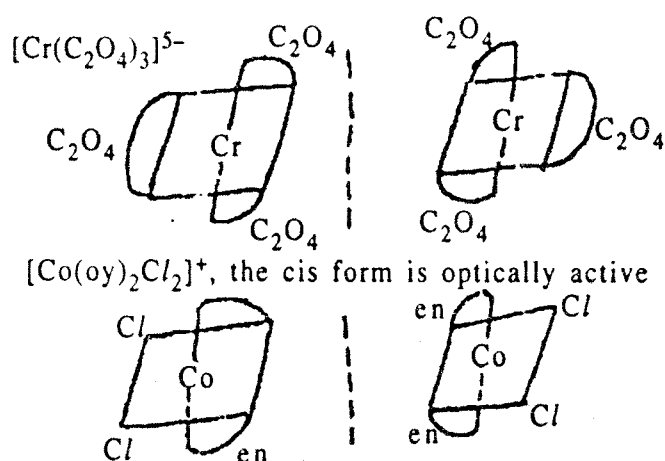
Fig 2.8 Tetrahedral isomers showing optical activity

Optical isomers can occur in nonchelate complexes with three or more different kinds of ligands and no more than two of any one kind, namely, in the cases of  $[Ma_2b_2c_2]$ ,  $[Ma_2b_2cd]$ ,  $[Ma_2bcde]$  and  $[Mabcdef]$ . For  $[Ma_2b_2c_2]$  case there are five geometrical isomers. Eg;  $[Cr(NH_3)_2(H_2O)_2Br_2]$ .

Fig. 2.9 Optical Isomers of  $[Ma_2b_2c_2]$

Both (a) and (B) are optical isomers. No resolution of a complex containing only monodentate ligands has a yet been reported.

A great deal of work on optical isomerism has been done with octahedral containing chelate ligands. The most common types are those containing three bidentate ligands or two bidentate and two monodentate ligands. The enantiomorphs in these cases are



Isomers of  $[M(C_2O_4)(NH_3)_2(Py)_2]$  shows the following structures as in

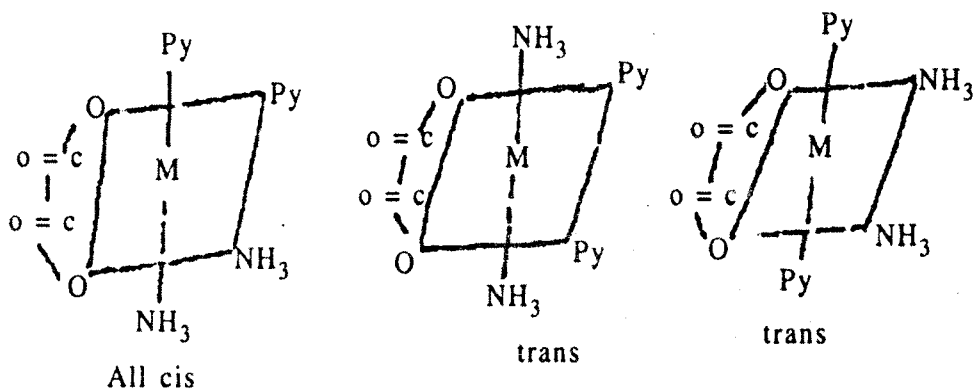


Fig 2.11 All cistrans trans

There are three isomers possible for this complex. These show geometrical isomerism. The mirror images of these isomers are all non-super imposable and hence are optically active.

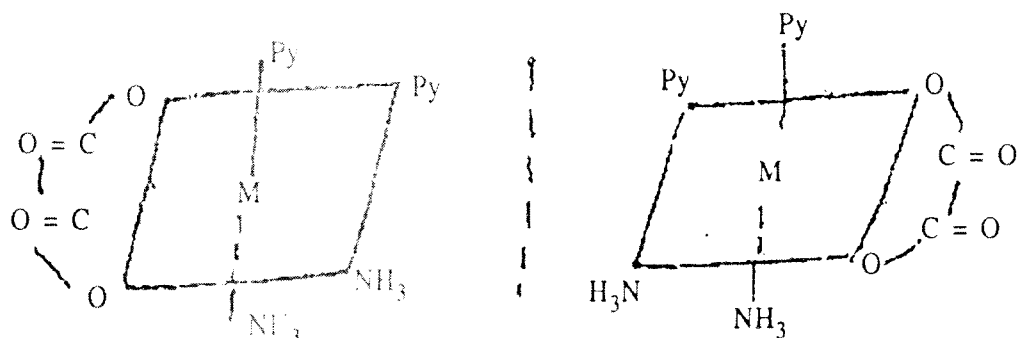


Fig. 2.12 Optically active

### Optical Rotatory Dispersion and Circular Dichroism

Two related methods of optical analysis, optical rotatory dispersion (ORD) and circular dichroism (CD), have been used extensively in assigning absolute configurations. In order to discuss these two methods it is necessary to say a word or two about the interaction between electromagnetic radiation and matter. The refraction of light (as measured by the refractive index,  $\eta$ ) results from the induction of dipoles in the medium (from the interaction between the electric vector of the light and the electrons of matter). If all of the molecules are symmetric and nonabsorbing, the only effect will be that the light is slowed (relative to a vacuum) when passing through the medium.

In that part of the spectrum over which a particular compound is transparent, the index of refraction is relatively constant. In the neighborhood of an absorption band, however, dramatic changes take place. The absorption bands result from excitation of electrons from lower to higher levels, and under these conditions the interaction between electromagnetic radiation and the electrons is at a maximum.

If plane-polarized light is passed through a solution containing optically active molecules of one of the two enantiomeric configurations, it will be rotated either right (+ or dextrorotatory) or left (– or levorotatory) as seen by the observer. The specific rotation at wavelength  $\lambda$  is defined as

$$[\alpha]_{\lambda} = \frac{\alpha}{lc}$$

Where  $\alpha$  is the rotation measured in degrees,  $l$  is the length of the light path (in decimeters) through the optically active medium, and  $c$  is the concentration in grams per cubic centimeter of the solution. The molecular rotation  $[\phi]$ , may be defined as

$$[\phi] = \frac{M[\alpha]}{100}$$

Where M is the molecular weight of the optically active compound.

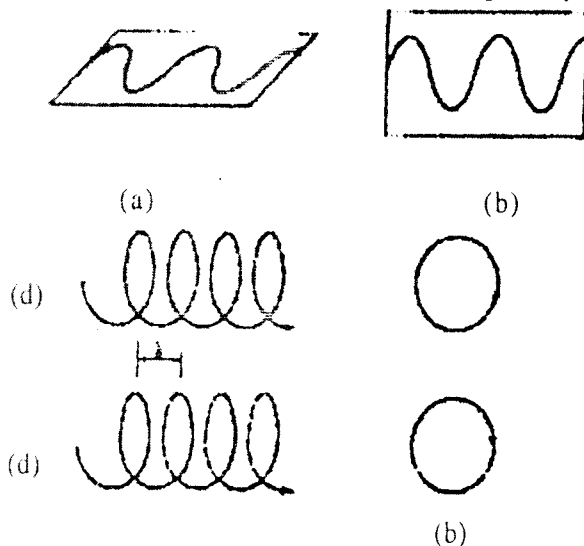
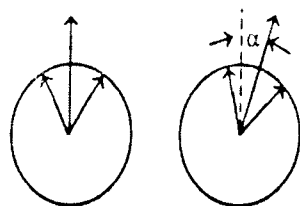


Fig. 2.13

The optical rotation arises from unequal refraction of left and right circularly polarized light. Plane-polarized light may be considered to be light in which the electric vector vibrates only in one plane. It may be decomposed into two circularly polarized components of equal intensities, rotating in opposite directions with the electric vector passing through one revolution for each wavelength.

The rotation of plane-polarized light arises from the fact that asymmetric molecules have different refractive indices,  $\eta_l$  and  $\eta_d$  for left and right circularly polarized light. The two components interact differently with the medium and emerge out of phase. If recombined, the plane of polarization has been rotated.



(Fig 2.14)

If the rotation is measured in a region far from absorption bands, the difference in refractive index is the only factor involved. Nevertheless, the specific rotation depends upon the wavelength of the light used and this should always be stated. Thus if the sodium D line ( $\lambda = 589 \text{ nm}$ ) is used, as is common, the rotation can be reported as  $[\alpha]_D$  or  $[\alpha]_{589}$ .

The variation in specific rotation increases as an absorption band is approached. The reason is that the refractive indices  $n_l$  and  $n_d$  change rapid with change in wavelength just as for nonpolarized light. As a result, the specific rotation drops to a minimum, passes through zero at maximum absorption, and rises quickly to a maximum. The measurement of the variation of rotation with wavelength is called optical rotatory dispersion (ORD) and the abrupt reversal of rotation in the vicinity of an absorption band is called the cotton effect Fig. 2.15a. If the complex was initially dextrorotatory, the effect is reversed with the ORD curve rising to a maximum, falling sharply to a minimum, and then slowly rising Fig. 2.15b. As a result of the change in sign of the rotation as a function of wavelength, confusion has arisen in the literature when the wavelength was not specified.

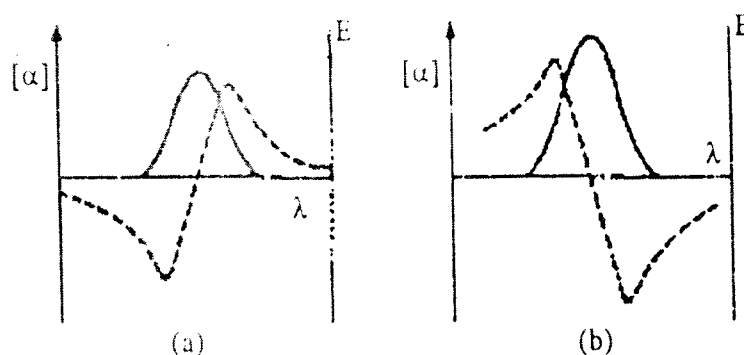


Fig. 2.15 a and b

ORD curves such as shown in fig. 2.15 are useful in the assignment of absolute configurations. For example, the configurations of the enantiomers of tris (ethylenediamine) cobalt (III), tris (alaninato) cobalt (III), and bis (ethylenediamine) glutamatocobalt (III) are known from X-ray investigations and it is found that the there D - enantiomers of these complexes have similar ORD spectra.

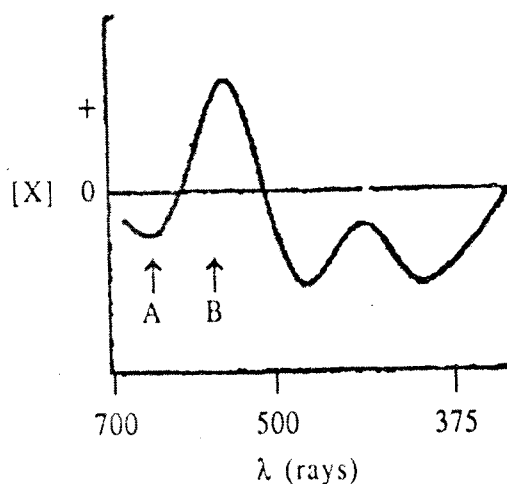


Fig. 2.16

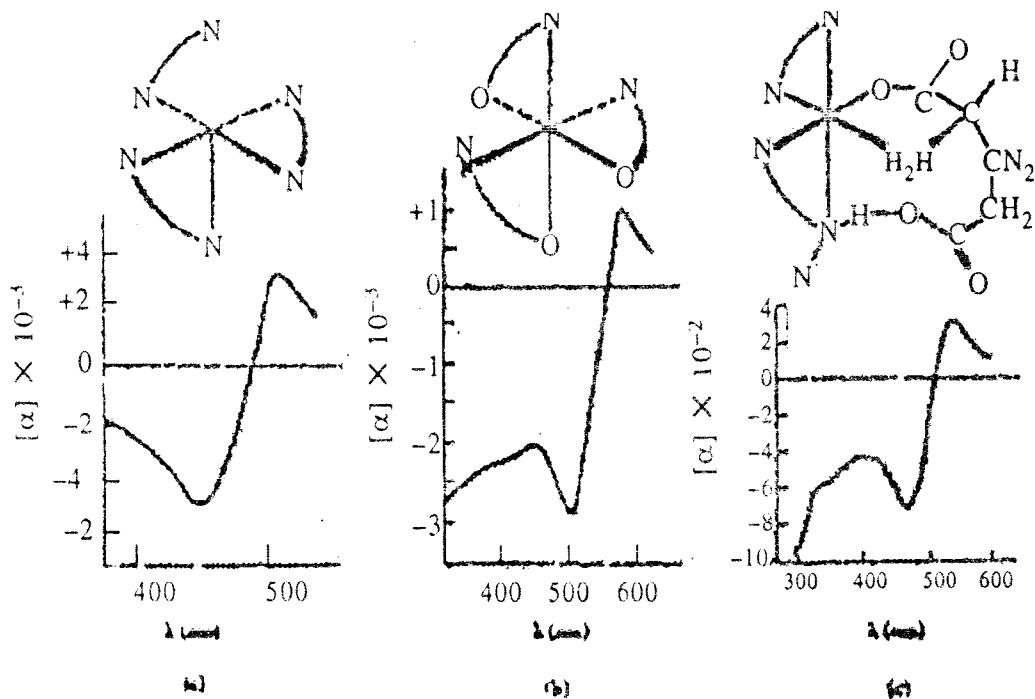
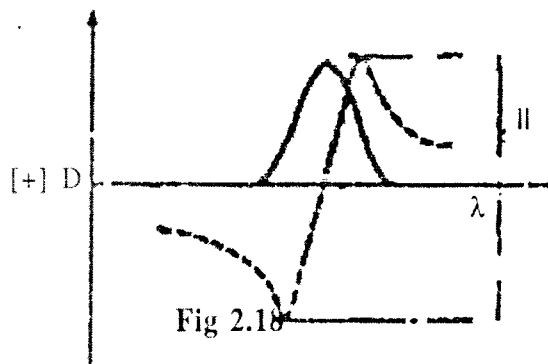


Fig. 2.17

A general rule may be stated: "If in analogous compounds, corresponding electronic transitions show cotton effects of the same sign, the compounds have the same optical configuration". On this basis the D-configuration could have been assigned to any of these in the absence of X-ray data simply on the basis of the similarity of the ORD spectra to one of known configuration. The chief difficulty is the requirement of "corresponding electronic transitions". Often it is difficult or impossible to resolve spectra with overlapping cotton effects.

In addition to the rapid change in refractive indices in the neighborhood of absorption peaks, there will be differential absorption of the two circularly polarized components. The difference between the extinction coefficients of left and right polarized light ( $\epsilon_l - \epsilon_d$ ) is called the circular dichroism (CD). It is intimately related to the ORD and the absorption spectrum of the complex. In the past ORD has often been of more value than CD, but this has been a result of instrumentation since usually CD can give at least as much information as ORD. Since CD occurs only within an absorption band it is somewhat simpler to interpret than ORD, which may be complicated by the overlapping of effects from several bands, some far removed from the area of the spectrum being studied. Complete reviews and comparisons of the two methods are available.



Information on stereochemistry and conformation of chelate complexes.

In addition to the asymmetry generated by the tris (chelate) structure of octahedral complexes, it is possible to have asymmetry in the ligand as well. For example, the gauche configuration that ethylenediamine assumes when bonding to a metal is inherently asymmetrical.

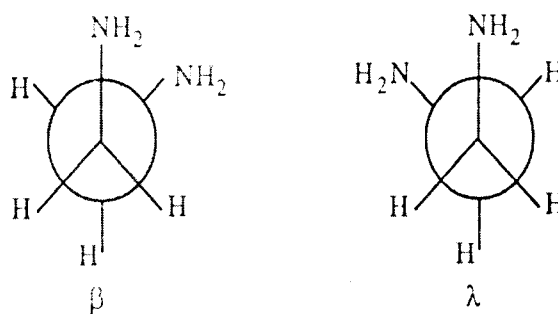


Fig. 2.19

and could in principle be resolved were it not for the almost complete absence of an energy barrier preventing racemization. Attachment of the chelate to the metal retains the asymmetry of the gauche form, but the two enantiomers can still inter-convert through a planar conformation at a very low energy, similar to the i

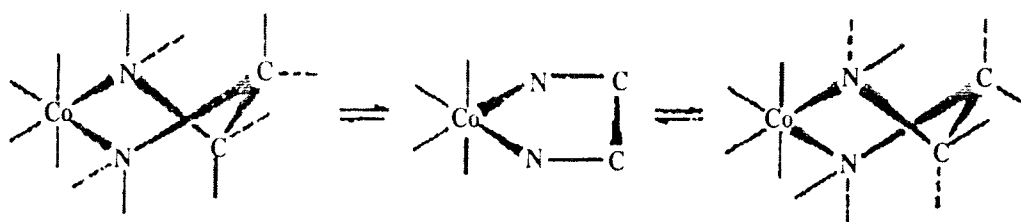


Fig 2.20

Thus, although it is possible in principle to describe two optical isomers of a complex such as  $[\text{Co}(\text{NH}_3)_4(\text{en})]^{+3}$ , in practice it proves to be impossible to isolate them.

If two or more rings are present in one complex, they can interact with each other and certain conformations might be expected to be stabilized as a result of possible reductions in interatomic repulsions. For example, consider a square planar complex containing two chelated

rings of ethylenediamine. From a purely statistical point of view we might expect to find three structures, which may be formulated  $M\delta\delta$ ,  $M\lambda\lambda$ ,  $M\delta\lambda$  (which is identical to  $M\lambda\delta$ ). The first two molecules lack a plane of symmetry, but  $M\delta\lambda$  is a meso form. Corey and Bailar were the first to show that the  $M\delta\delta$  and  $M\lambda\lambda$  forms should predominate over the meso form since the latter has unfavourable H-H interactions of the axial-axial and equatorial-equatorial type between the two rings Fig. 2.21. The enantiomeric  $M\delta\delta$  and  $M\lambda\lambda$  forms are expected to be about  $4\text{kJ mol}^{-1}$  more stable, other factors being equal.

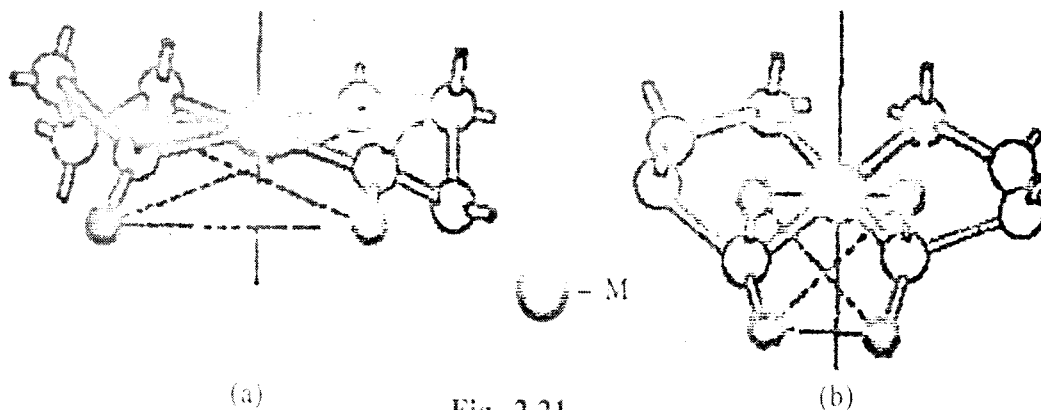


Fig. 2.21

More important consequences result for octahedral tris (chelate) complexes. Again from purely statistical arguments, we might expect to find  $M\delta\delta\delta$ ,  $M\delta\delta\lambda$ ,  $M\delta\lambda\lambda$  and  $M\lambda\lambda\lambda$  forms. In addition, these will be optically active from the tris (chelate) structure as well, so there are expected to be eight distinct isomers formed. In general, a much smaller number is found, usually only two. This stereoselectivity is most easily followed by using an optically active ligand such as propylenediamine,  $\text{CH}_3\text{CH}(\text{NH}_2)\text{CH}_2\text{NH}_2$ . The five membered chelate ring will give rise to two types of substituent positions, those that are essentially axial and those that are essentially equatorial. All substituents larger than hydrogen will cause the ring to adopt a conformation in which the substituents larger than hydrogen will cause the ring to adopt a conformation in which the substituent is in an equatorial position.

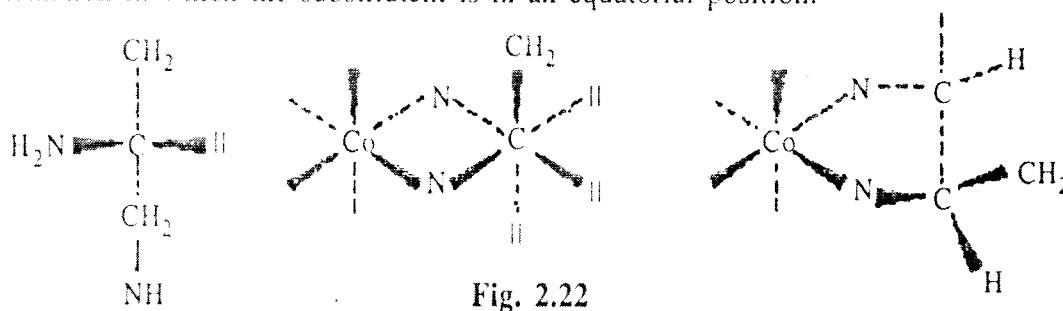
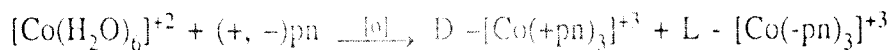


Fig. 2.22

As a result of this strong conformational propensity, (-) propylenediamine bonds preferentially as a  $\lambda$  chelate and (+) propylenediamine bonds as a  $\delta$  chelate. This reduces the number of expected isomers to four:  $\Lambda - M\delta\delta\delta$  (=D- $M\delta\delta\delta$ ),  $\Lambda - M\lambda\lambda\lambda$  (=D- $M\lambda\lambda\lambda$ ),  $\Delta - M\delta\delta\delta$  (=L- $M\delta\delta\delta$ ), and  $\Delta - M\lambda\lambda\lambda$  (=L- $M\lambda\lambda\lambda$ ) where  $\Lambda$ ,  $\Delta$ , D and L refer to the absolute configuration about the metal related  $\Lambda-(+)_589^- [\text{Co}(\text{en})_3]^{3+}$  (= the D enantiomer) (see

Fig. 2.17). In a typical reaction such as a oxidation of cobalt (II) chloride in the presence of racemic propylenediamine. Only two isomers were isolated.



The difference in stability between the various isomers has been related to preferred packing arrangements of chelate rings about the central metal atom. Thus, for (+) - propylenediamine (which forms a  $\delta$  chelate) the most efficient method of fitting around a metal will be in the form of left-handed helix. This arrangement minimizes the various repulsions. It has been termed the lel isomer since the C-C bonds are parallel to the three-fold axis of the complex (Fig. 2.23)

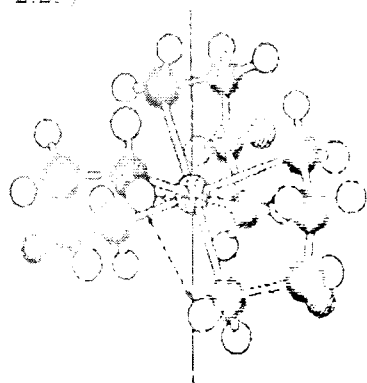


Fig 2.23

The alternative isomer, in which the ligands form a right-handed helix about the metal, is known as the ob isomer since the C-C bonds are oblique to the threefold axis (Fig.2.24)

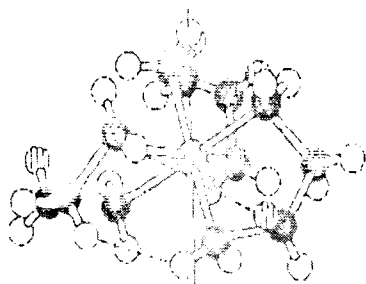
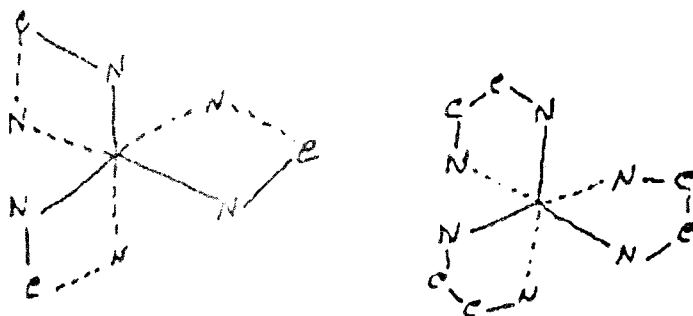


Fig. 2.24

The interactions between the hydrogen atoms of the various rings stabilize the lel isomer by a few kilojoules per mole (Fig. 2.25).



## UNIT - III

### SPECTRAL METHODS - II

#### Mossbauer Spectroscopy :

Mossbauer spectroscopy, abbreviated as MB spectroscopy, involves nuclear transitions that result from the absorption of  $\gamma$ -rays by the sample. This transition is characterized by a change in the nuclear spin quantum number,  $I$ . The conditions for absorption depend upon the electron density about the nucleus, and the number of peaks obtained is related to the symmetry of the compound. As a result, structural information can be obtained.

To understand the principles of this method, first consider a gaseous system consisting of a radioactive source of  $\gamma$ -rays and the sample, which can absorb  $\gamma$ - rays. When a gamma ray is emitted by the source nucleus, it decays to the ground state. The energies of the emitted  $\gamma$ -rays,  $E_\gamma$ , have a range of 10 to 100 keV and are given by equation :

$$E_\gamma = E_\gamma + D - R \quad \dots (1)$$

Where  $E_\gamma$  is the difference in energy between the excited state and ground state of the source nucleus;  $D$ , the Doppler shift, is due to the translational motion of the nucleus, and  $R$  is the recoil energy of the nucleus. The recoil energy, similar to that occurring when a bullet leaves a gun, is generally  $10^{-2}$  to  $10^{-3}$  eV and is given by the equation :

$$R = E_\gamma^2/2mc^2 \quad \dots (2)$$

where  $m$  is the mass of the nucleus and  $c$  is the velocity of light. The Doppler shift accounts for the fact that the energy of  $\gamma$ -rays emitted from a nucleus in a gas molecule moving in the same direction as the emitted ray is different from the energy of a  $\gamma$ -ray from a nucleus in a gas molecule moving in the opposite direction. The distribution of energies resulting from the translational motion of the source nuclei in many directions is referred to as Doppler broadening. The left-hand curve of Fig. 3.1 is taken as  $E_\gamma$ , the energy difference between the nuclear ground and excited states of the source. The energy difference  $R$ , between the dotted line and the average energy of the left-hand curve is the recoil energy transmitted to the source nucleus when a  $\gamma$ -ray is emitted.

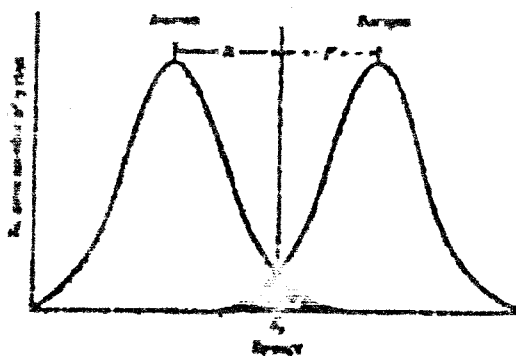


Fig. 3.1 Distribution of energies of emitted and absorbed  $\gamma$  - rays

In MB spectroscopy the energy of the  $\gamma$ -ray absorbed for a transition in the sample is given by :

$$E_{\gamma} = E_{\gamma} + D + R \quad \dots (3)$$

In this case, R is added because the exciting  $\gamma$ -ray must have energy necessary to bring about the transition and effect recoil of the absorbing nucleus. The quantity D has the same significance as before, and the value of  $E_{\gamma}$ , is assumed to be the same for the source and the sample. The curve in the right half of Fig. 3.1 shows the distribution of  $\gamma$ -ray energies necessary for absorption. The relationship of the sample and source energies can be seen from the entire figure. As indicated by the shaded region, there is only a very slight probability that the  $\gamma$ -ray energy from the source will match that required for absorption by the sample. Since the nuclear energy levels are quantized, there is accordingly a very low probability that the  $\gamma$ -ray from the source will be absorbed to give a nuclear transition in the sample. The main cause for nonmatching of  $\gamma$ -ray energies is the recoil energy, with the distribution for emission centered about  $E_{\gamma} - R$ , whereas that for absorption is centered about  $E_{\gamma} + R$ . The quantity R for a gaseous molecule ( $\sim 10^{-1}$  eV) is very much larger than the typical Doppler energy. The source would have to move with a velocity of  $2 \times 10^4$  cm sec $^{-1}$  to obtain a Doppler effect large enough to make the source and sample peaks overlap, and these velocities are not readily obtainable. However, if the quantity R could be reduced, or if conditions for a recoilless transition could be found, the sample would have a higher probability of absorbing  $\gamma$ -rays from the source. As indicated by equation (2), R can be decreased by increasing m, the mass. By placing the nucleus of the sample and source in a solid, the mass is effectively that of the solid and the recoil energy will be small as indicated by equation. For this reason, MB spectra are almost always obtained on solid samples employing solid sources.

By going to the solid state we have very much reduced the widths of the resonance lines over that shown in Fig.1. The Doppler broadening is now negligible, and R becomes  $\sim 10^{-1}$  eV for a 100 keV gamma ray and an emitting mass number of 100. The full width of a resonance line at half height is given by the Heisenberg uncertainty principle as  $\Delta E = \hbar/t = 4.56 \times 10^{-16} / 0.977 \times 10^{-7} = 4.67 \times 10^{-9}$  eV or 0.097 mm sec $^{-1}$  (for  $^{57}\text{Fe}$ ). The line widths are infinitesimal compared to the source energy of  $1.4 \times 10^4$  eV. The range of excited state lifetimes for Mossbauer nuclei is  $\sim 10^{-5}$  sec, and this leads to line widths of  $10^{-11}$  eV to  $10^{-6}$  eV for most nuclei.

Our main concern will be with the factors affecting the energy required for  $\gamma$ -ray absorption by the sample. There are three main types of interaction of the nuclei with the chemical environment that result in small changes in the energy required for absorption : (1) resonance line shifts from changes in electron environment, (2) quadrupole interactions,

and (3) magnetic interactions. These effects give us information of chemical significance and will be our prime concern.

The electron environment about the nucleus influences the energy of the  $\gamma$ -ray necessary to cause the nuclear transition from the ground to excited state, i.e.,  $E_\gamma$  in the sample. The energy of  $\gamma$ -rays from the source can be varied over the range of the energy differences arising from electron environments in different samples by moving the source relative to the sample. The higher the velocity at which the source is moved towards the sample, the higher the average energy of the emitted  $\gamma$ -ray (by the Doppler effect) and vice versa. The energy change  $\Delta E_S$  of a photon associated with the source moving relative to the sample is given by :

$$\Delta E_S = \frac{\gamma_0}{C} E_\gamma \cos\theta \quad \dots (4)$$

Where  $E_\gamma$  is the stationary energy of the photon,  $\gamma_0$  is the velocity of the source and  $\theta$  is the angle between the velocity of the source and the line connecting the source and the sample. When the source is moving directly toward the sample,  $\cos \theta = 1$ . In order to obtain an MB spectrum, the source is moved relative to the sample, and the source velocity at which maximum absorption of  $\gamma$ -rays occurs is determined.

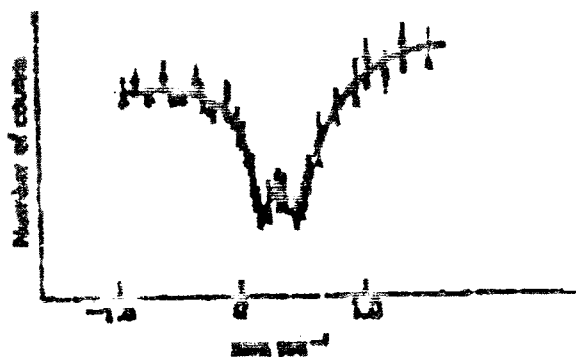


Fig. 3.2 MB Spectrum of  $\text{FeFe}(\text{CN})_6$

Consider, as a simple example, the MB spectrum of  $\text{Fe}^{3+} [\text{Fe}^{\text{III}}(\text{CN})_6]$ . [Where  $\text{Fe}^{3+}$  and  $\text{Fe}^{\text{III}}$  designate weak and strong field in iron (III), respectively. This substance contains iron in two different chemical environments, and  $\gamma$ -rays of two different energies are required to cause transitions in the different nuclei. To obtain the MB spectrum, the source is moved relative to the fixed sample, and the absorption of  $\gamma$ -rays is plotted as a function of source velocity as shown in fig. 3.2. The peaks correspond to source velocities at which maximum  $\gamma$ -ray absorption by the sample occurs. Negative relative velocities correspond to moving the source away from the sample, and positive relative velocity at which the source is being moved is plotted along the abscissa of Fig 3.2, and this quantity is related to the energy of the  $\gamma$ -rays. For a  $^{57}\text{Fe}$  source emitting a 14.4 keV  $\gamma$ -rays, the energy is changed by 4.8 to

$10^{-8}$  eV or  $0.0011$  cal mole $^{-1}$  for every mm sec $^{-1}$  of velocity imposed upon the source. This result can be calculated from equation (4) :

$$\Delta E_S = \frac{1 \text{ mm sec}^{-1}}{3.00 \times 10^{11} \text{ mm sec}^{-1}} \times 14.4 \times 10^3 \text{ eV} = 4.80 \times 10^{-8} \text{ eV}$$

This energy is equivalent to a frequency of 11.6 MHz ( $\gamma = E/h$ , where  $h = 4.14 \times 10^{-15}$  eV sec). For other nuclei having a  $\gamma$ -ray energy of  $E_\gamma$  (in keV),

$$1 \text{ mm sec}^{-1} = 11.6 \times \frac{E_\gamma}{14.4} \text{ MHz}$$

Referring again to the abscissa of Fig. 3.2, one sees that the energy difference between the nuclear transitions for Fe $^{3+}$  and Fe $^{III}$  in Fe[Fe(CN) $_6$ ] is very small, corresponding to about  $2 \times 10^{-8}$  eV. The peak in the spectrum in Fig 3.2 at 0.03 mm sec $^{-1}$  is assigned to Fe $^{III}$  and that at 0.53 to the cation Fe $^{3+}$  by comparison of this spectrum with those for a large number of cyanide complexes of iron. Different line positions that result from different chemical environments are indicated by the values for the source velocity in units of cm $^{-1}$  or mm sec $^{-1}$ , and are referred to as isomer shifts, center shifts, or chemical shifts.

#### Isomer Shift :

The two different peaks in Fig. 3.2 arise from the isomer shift differences of the two different iron atoms in octahedral sites. The isomer shift results from the electrostatic interaction of the charge distribution in the nucleus with the electron density that has a finite probability of existing at the nucleus. Only s electrons have a finite probability of overlapping the nuclear density, so the isomer shift can be evaluated by considering this interaction. It should be remembered that p, d and other electron densities can influence s electron density by screening the s density from the nuclear charge. Assuming the nucleus to be a uniformly charged sphere of radius R and the s electron density over the nucleus to be a constant given by  $\Psi_s^2(o)$ , the difference between the electrostatic interaction of a spherical distribution of electron density with a point nucleus and that for a nucleus with radius R is given by

$$\delta E = K[\Psi_s^2(o)] R^2 \quad \dots (5)$$

where K is a nuclear constant. Since R will have different values for the ground state and the excited state, the electron density at the nucleus will interact differently with the two states and thus will influence the energy of the transition; i.e.,

$$\delta E_e = \delta E_g K [\Psi_s^2(o),(o)] R_e^2 - R_g^2 \quad \dots (6a)$$

Where the subscript e refers to the excited state and g to the ground state. The influence of  $\Psi_s^2(o)$  on the energy of the transition is illustrated in Fig. 3.3 for  $^{57}\text{Fe}$ , which has  $I = \frac{1}{2}$  for

the ground state and  $I = 3/2$  for the excited state. The energies of these two states are affected differently by  $\Psi_S^2(o)$ , and the transition energy is changed.

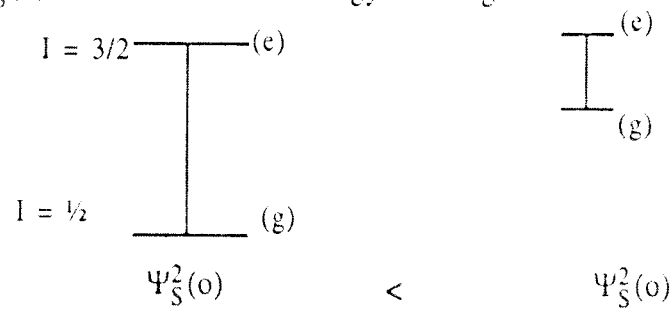


Fig. 3.3 Changes in the energy of the Mossbauer transition for different values of  $\Psi_S^2(o)$ .

This is a graphical illustration of equation (5 - 6a) with two different values of  $\psi_S^2(o)$  for an  $^{57}\text{Fe}$  nucleus. The differences in  $^{57}\text{Fe}$ , must result from a cubic or spherical distribution of bonded atoms in order for this diagram to apply.

The R values are constant for a given nucleus, but  $\psi_S^2(o)$  varies from compound to compound. The center shift in the Mossbauer spectrum is the difference between the energy of this transition in sample (or absorber) and the energy of the same transition in the source. This difference is given by the difference in equations of the form of (6a) for the source and sample, or :

$$\text{C.S} = K (R_e^2 - R_g^2) \{ [\Psi_S^2(o)]_a - [\Psi_S^2(o)]_b \} \quad \dots (6b)$$

Where the subscripts a and b refer to absorber and source, respectively. Standard sources are usually employed (e.g.,  $^{57}\text{Co}$  in Pd for iron Mossbauer spectra, or  $\text{BaSnO}_3$  for tin spectra). The  $^{57}\text{Co}$  decays to  $^{57}\text{Fe}$  in an excited state via electron capture. The excited  $^{57}\text{Fe}$  decays to stable  $^{57}\text{Fe}$  by  $\gamma$ -ray emission. When standard sources are employed  $[\Psi_S^2(o)]_b$  is replaced by a constant, C. Furthermore, the employed expression for the center shift :

$$\text{C. S} = K' \frac{\delta R}{R} = [\psi_S^2(o)_a - C] \quad \dots (6c)$$

where  $\delta R = R_e - R_g$ , C is a constant characteristic of the source; and  $K'$  is  $2KR^2$ . Both  $K'$  and  $\delta R/R$  are constants for a given nucleus, so the center shift is directly proportional to the s electron density at the sample nucleus. The term center shift is used for the experimentally determined center of the peak; the term isomer shift is now used when the center shift has been corrected for the small Doppler contribution from the thermal motion of the Mossbauer atom. The sign of  $\delta R$  depends upon the differences between the effective nuclear charge radius, R, of the excited and ground states ( $R_e^2 - R_g^2$ ). For the  $^{57}\text{Fe}$  nucleus, the excited state is smaller than the ground state, and an increase in s-electron density produces a negative shift. In tin, the sign of  $\delta R$  is positive, so the opposite trend of shift with s electron density is observed.

As mentioned above, electron density in p or d orbitals can screen the electron density from the nuclear charge by virtue of the fact that the electron density in d and p orbitals penetrates the s orbital. Hartree-Fock calculations show (6, 7) that a decrease in the number of d electrons causes a marked increase in the total s electron density at the iron nucleus. Accordingly, with comparable ligands and with negative  $\delta R/R$ ,  $\text{Fe}^{2+}$  has an appreciably larger center shift than  $\text{Fe}^{3+}$ . When these ions are examined in a series of molecules, the interpretation becomes more difficult for the d, s and p electron densities are modified by covalent bonding. For  $^{57}\text{Fe}$ , for example, an increase in 4s density decreases the center shift, while an increase in 3d density increases the center shift. A series of high spin iron complexes have been interpreted on this basis. In the case of  $^{119}\text{Sn}$ , the center shift increases with an increased s electron density and decreases with an increase in p electron density.

#### Quadrupole Interactions :

The discussion of the center shift in the previous section applies to systems with a spherical or cubic distribution of electron density. As discussed in the degeneracy of nuclear energy levels for nuclei with  $I > 1/2$  is removed by a non-cubic electron or ligand distribution. For non-integral spins, the splitting does not remove the + or - degeneracy of the  $m_I$  levels, but we obtain a different level for each  $\pm m_I$  set. Thus, the electric field gradient can lead to  $I + 1/2$  different levels for half-integer values of I (e.g., two for  $I = 3/2$  corresponding to  $\pm 1/2$  and  $\pm 3/2$ ). For integer values of I we obtain  $2I + 1$  levels (e.g., five for  $I = 2$  corresponding to 2, 1, 0, -1, -2). The influence of this splitting on the nuclear energy levels and the spectral appearance is illustrated in Fig. 3.4 for  $^{57}\text{Fe}$ . The ground state is not split but the excited state is split, leading to two peaks in the spectrum. The center shift is determined from the center of the two resulting peaks. When both the ground and excited states have large values for I, complex Mossbauer spectra result.

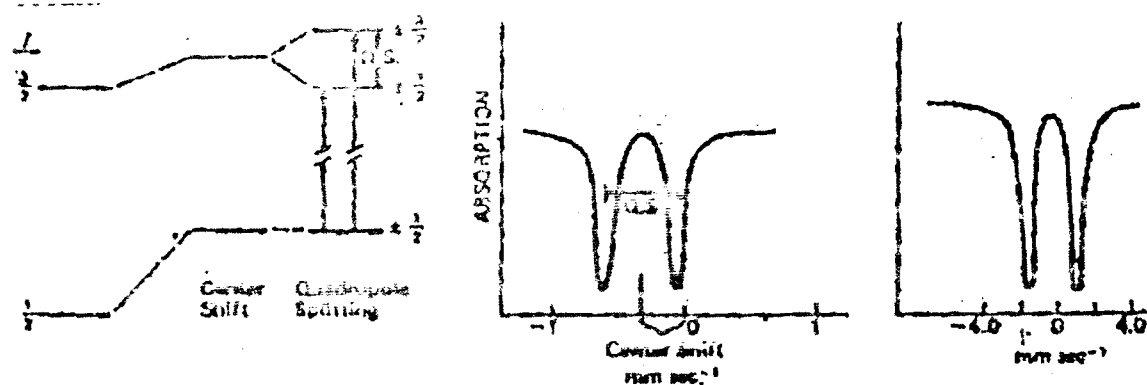


Fig. 3.4 The influence of a non-cubic electronic environment on (A) on nuclear energy states of  $^{57}\text{Fe}$  and (B) the Mossbauer spectrum (C) the iron MB spectrum of  $\text{Fe}(\text{CO})_5$  at liquid  $\text{N}_2$  temperature (9)

The Hamiltonian for the quadrupole coupling is the same as that discussed for nqr.

$$H_Q = \frac{e^2 Qq}{4I(2I-1)} [(3I^2 - I(I+1) + (n/2)(I_+^2 + I_-^2)]$$

For the  $I = 3/2$  case ( $^{57}\text{Fe}$  and  $^{119}\text{Sn}$ ), the quadrupole splitting (Q.S) is given by

$$\text{Q.S} = \frac{1}{2} e^2 Qq (1 + n^2/3)^{1/2} \dots (7)$$

For  $^{57}\text{Fe}$ ,  $q$  and  $n$  cannot be determined from the quadrupole splitting. The sign of the quadrupole coupling constant is another quantity of interest. If  $m_I = \pm 3/2$  is at high energy, the sign is positive; the sign is negative if  $\pm 1/2$  from  $I = 3/2$  is highest. From powder spectra, the intensities of the transitions to  $\pm 1/2$  and  $\pm 3/2$  are similar, and it becomes difficult to determine the sign. The sign can be obtained from spectra of ordered systems or from measurement of a polycrystalline sample in a magnetic field (vide infra) for systems in which the  $I$  values of the ground and excited states are larger than those for iron, the spectra are more complex and contain more information. The splitting of the excited state will not occur in a spherically symmetric or cubic field but will occur only when there is a field gradient at the nucleus caused by asymmetric  $p$  or  $d$  electron distribution in the compound. A field gradient exists in the trigonal bipyramidal molecule iron pentacarbonyl, so a splitting of the nuclear excited state is expected, giving rise to a doublet in the spectrum as indicated in fig. 3.4.

If the  $t_{2g}$  set and the  $e_g$  set of orbitals in octahedral transition metal ion complexes have equal populations in the component orbitals, the quadrupole splitting will be zero. Low spin iron (II) complexes ( $t_{2g}^6$ ) will not give rise to quadrupole splitting unless the degeneracy is removed, and these orbitals can interact differently with the ligand molecular orbitals. On the other hand, high spin iron (II) ( $t_{2g}^4 e_g^2$ ) has an imbalance in the  $t_{2g}$  set, and a large quadrupole splitting is often seen. If the ligand environment about iron (II) were perfectly octahedral,  $d_{xy}$ ,  $d_{yz}$  and  $d_{xz}$  would be degenerate and no splitting would be detected. "However, this system is subject to Jahn - Teller distortion, which can lead to a large field gradient. When the energy separation of  $t_{2g}$  orbitals from Jahn-Teller effects is of the order of magnitude of  $kT$ , a very temperature - dependent quadrupole splitting is observed. The ground state in the distorted complex can be obtained if the sign of  $q$  is known. The sign can be obtained from oriented systems or from studies in a large magnetic field. Similar consideration apply to high spin and low spin iron (III) compounds.

#### Magnetic Interactions :

As shown in Fig. 3.4 non-cubic electronic environment in an iron complex splits the degenerate  $I = 3/2$  excited state of  $^{57}\text{Fe}$  into  $m_I$  states  $\pm 1/2$  and  $\pm 3/2$ . The Mossbauer spectrum consists of a doublet corresponding to the two transitions shown in Fig.4. When an effective magnetic field  $H_{\text{eff}}$  acts on this system, the degeneracies of the  $\pm 1/2$  ground state as well as the  $\pm 3/2$  excited states are removed<sup>(10)</sup> as shown in Fig. 3.5. The ordering of the levels reflects

the fact that the ground-state moment is positive and the excited state moment is negative. The resulting six-line spectrum is shown in Fig. 5(B). Since the transitions are magnetic dipole in character, the selection rule is  $\Delta m = 0$ ,

$$H_m = -g_N \mu_N I \cdot H_{\text{eff}} \quad \dots (8)$$

Where  $g_N = 0.18$  and  $I = 1/2$  for the nuclear ground state and  $g = -0.10$  and  $I = 3/2$  for the excited state. The intensity of the lines changes with  $\theta$ , the orientation of the  $H_{\text{eff}}$  relative to the direction of the Mossbauer radiation. For an ordered sample, the  $\Delta m = 0$  transition has zero intensity for a field parallel to the radiation. When  $\theta = 90^\circ$ , the  $\Delta m = 0$  transitions are the most intense of the six.

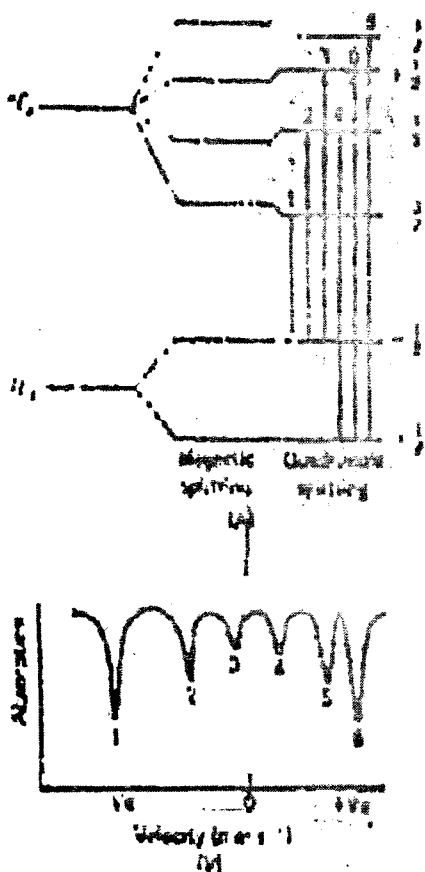
The effective field of equation (8) consists of the internal field and the applied field:

$$H_{\text{eff}} = H + H_{\text{int}} \quad \dots (9)$$

and is given by

$$H_{\text{int}} = - \langle S \rangle \cdot A / g_N \mu_N \quad \dots (10)$$

where  $\langle S \rangle$  is the expectation value of the spin and  $A$  the hyperfine coupling tensor. The internal magnetic field controls the magnetic hyperfine and it depends in a complex way on the zero field splitting parameters  $D$  and  $E$ , on the electronic  $g$  tensors and  $A$  tensors, and on the orientation of the molecule relative to the applied field.



3.5 Magnetic and quadrupole splitting in a ferromagnetic  $^{57}\text{Fe}$  compound (a) Energy level diagram. (B) Expected Mossbauer spectrum [Copyright c 1973 Mc Graw-Hill Book Co. (UK) Limited. From G.M. Bancroft, "Mossbauer Spectroscopy" Reproduced by permission)

Internal fields exist in some systems in the absence of an applied magnetic field. The  $\langle S \rangle$  of equation (10) is zero for diamagnetic systems and for systems with integer values of  $S$  in the absence of an applied field. These spectra consist of quadrupole doublets. For compounds with half-integer spin (Kramers' doublets), two cases need be considered. With fast electron relaxation, the  $\langle S \rangle$  averaged over all thermally accessible states is zero in zero magnetic field, leading to quadrupole doublets. In the slow relaxation limit, magnetic Mossbauer spectra can be obtained, generally at liquid helium temperatures. These spectra generally are studied at weak applied field to simplify them by decoupling hyperfine interactions with ligand nuclei.

#### Applications :

Facsimiles of spectra obtained on some iron complexes are given in Fig.3.6. As mentioned previously, for high spin iron complexes in which all six ligands are equivalent, a virtually spherical electric field at the nucleus is expected for  $\text{Fe}^{3+}$  ( $d^5$ ) ( $t_{2g}^3 e_g^2$ ) but not  $\text{Fe}^{2+}$  ( $d^6$ ) ( $t_{2g}^4 e_g^2$ ). As a result of the field gradients at the nucleus, quadrupole splitting should be detected in the spectra of high spin iron (II) complexes but not for high spin iron (III) complexes. This is borne out in spectra A and B of the complexes illustrated in Fig. 3.6 for low spin complexes, iron (II) has configuration  $t_{2g}^6$  and iron (III) has  $t_{2g}^5$ .

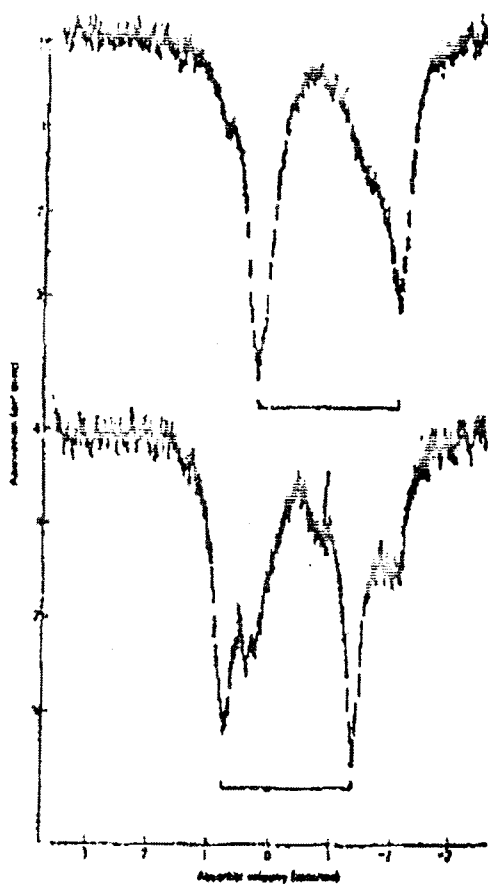


Fig 3.6 Emission Mossbauer Spectra of (A) the dimethyl imidazole adduct of cobalt protoporphyrin IX dimethyl ester and (B) its  $\text{O}_2$  adduct

As a result, quadrupole splitting is now expected for iron (III) but not iron (II) in the strong field complexes. This conclusion is confirmed experimentally by the spectra of ferrocyanide and ferricyanide ions. When the ligand arrangement in a strong field iron (II) complex does not consist of six equivalent ligands, e.g.,  $[(\text{Fe}(\text{CN})_5\text{NH}_3)]^{3-}$ , quadrupole splitting of the strong field iron (II) will result. The quadrupole splitting is roughly related to the differences in the d orbital populations by

$$Q_{\text{valence}} = K_d \left[ -N_{d_{z^2}} + N_{d_{x^2-y^2}} + N_{d_{xy}} - \frac{1}{2} (N_{d_{xy}} + N_{d_{xy}}) \right] \dots (11)$$

Table - 3.1 Quadrupole Splitting  $\Delta E_Q$ , and Isomer Shift,  $\delta$  for some Iron Compounds ( $\delta E_Q$  in  $\text{mm sec}^{-1}$ )

Compounds	$\Delta E_Q$	$\delta$	Compound	$\Delta E_Q$	$\delta$
High Spin Fe(II)			Low Spin Fe(II)		
$\text{FeSO}_4 \cdot 7\text{H}_2\text{O}$	3.2	1.19	$\text{K}_4[\text{Fe}(\text{CN})_6] \cdot 3\text{H}_2\text{O}$		-0.13
	3.15	1.3			-0.16
$\text{FeSO}_4(\text{anhydrous})$	2.7	1.2		<0.1	+0.05
$\text{Fe}(\text{NH}_4)_2(\text{SO}_4)_2 \cdot 6\text{H}_2\text{O}$	1.75	1.19	$\text{Na}_4[\text{Fe}(\text{CN})_6] \cdot 10\text{H}_2\text{O}$	<0.2	-1.01
	1.75	1.3	$\text{Na}_3[\text{Fe}(\text{CN})_5\text{NH}_3]$	0.6	-0.05
$\text{FeCl}_2 \cdot 4\text{H}_2\text{O}$	3.00	1.35	$\text{K}_2[\text{Fe}(\text{CN})_5\text{NO}]$	1.85	-0.27
$\text{FeC}_4\text{H}_4\text{O}_6$	2.6	1.25		1.76	-0.28
$\text{FeF}_2$	2.68		$\text{Zn}[\text{Fe}(\text{CN})_5\text{NO}]$	1.90	-0.27
$\text{FeC}_2\text{O}_4 \cdot 2\text{H}_2\text{O}$	1.7	1.25			
High Spin Fe(II)			Low Spin Fe(III)		
$\text{FeCl}_3 \cdot 6\text{H}_2\text{O}$	0.2	0.85	$\text{K}_3[\text{Fe}(\text{CN})_6]$		-0.12
$\text{FeCl}_3(\text{anhydrous})$	0.2	0.5			0.17
$\text{FeCl}_3 \cdot 2\text{NH}_4\text{Cl} \cdot \text{H}_2\text{O}$	0.3	0.45	$\text{Na}_3[\text{Fe}(\text{CN})_6]$	0.60	-0.17
$\text{Fe}(\text{NO}_3)_3 \cdot 9\text{H}_2\text{O}$	0.4	0.4			
$\text{Fe}_2(\text{C}_2\text{O}_4)_3$	0.5	0.45			
$\text{Fe}_2(\text{C}_4\text{H}_4\text{O}_6)_3$	0.77	0.43			
$\text{Fe}_2\text{O}_3$	0.12	0.47			

Values measured at room temperature for  $\Delta E_Q$  and the isomer shift,  $\delta$ , for a number of iron complexes have been collected and are listed in Table - 3.1 for iron complexes, isomer shifts in a positive direction correspond to a decrease in electron density in the region of the

nucleus. For high spin complexes, a correlation exists between isomer shift and s electron density. An increase in  $\delta$  of  $0.2 \text{ mm sec}^{-1}$  is equivalent to a decrease in charge density of 8% at the nucleus. The negative values obtained for the low spin ferricyanides compared to high spin iron (III) complexes indicate more electron density at the nucleus in the ferricyanide ions. This has been explained as being due to extensive  $\pi$  bonding in the ferricyanides, which removes d electron density from the metal ion, which in turn decreases the shielding of the s electrons. This effect increases s electron density at the nucleus and decreases  $\delta$ .

The MB spectrum of the material prepared from iron (III) sulfate and  $\text{K}_4\text{Fe}(\text{CN})_6$  is identical to the spectra for the compounds prepared either from iron (II) sulfate and  $\text{K}_3\text{Fe}(\text{CN})_6$  or by atmospheric oxidation of the compound from iron (II) sulfate and  $\text{K}_4\text{Fe}(\text{CN})_6$ . The spectra of these materials indicate that the cation is high spin iron (III), while the anion is low spin iron (II).

## Nuclear Magnetic Resonance Spectroscopy

### Basic Principles

We know that a spinning electron has a magnetic moment which interacts with an applied magnetic field. The same is true of a proton, through the magnetic moment associated with it is only about  $\frac{1}{2000}$  of that associated with an electron. The neutron also, however, has spin and gives rise to a magnetic moment, presumably because, although it has no net charge, there is an uneven charge distribution within it. The magnetic moments of nuclei containing both protons and neutrons may be finite or zero according to how the spins of the constituent nucleons are aligned, the resultant amount of spin being expressed by a nuclear spin quantum number,  $I$ . In this book we shall be concerned mainly with nuclei having  $I = \frac{1}{2}$  (e.g.  $^1_1\text{H}$ ,  $^{13}_6\text{C}$ ,  $^{19}_9\text{F}$ , and  $^{31}_{15}\text{P}$ ). If we place such a nucleus in a magnetic field, the nuclear magnetic moment can have only two allowed orientations, parallel and antiparallel to the field. The former is of lower energy, but the difference between them is very small indeed ( $0.025 \text{ J mol}^{-1}$  for a hydrogen nucleus in a field of 1.409 tesla (14090 gauss)) and so the two orientations, are almost equally common. Nevertheless, transitions between them may be observed in the radiofrequency region by the use of a resonance effect. In the case of the proton the resonance frequency at a field of 1.409 tesla is  $60 \times 10^6 \text{ S}^{-1}$  (or 60 MHz, the unit of frequency being the hertz, Hz or 1 cycle per second).

The resonance condition specified in the previous paragraph holds only for nuclei with no associated electrons. In an atom, the applied field  $B_0$  induces a circulation of electrons round the nucleus which sets up a field proportional to and opposing the field  $B_0$ , so that the nucleus feels the effect of a diminished field  $B_0(1 - \sigma)$ , where  $\sigma$  is called the shielding constant. For an actual atom the resonance condition is given by

$$\gamma = \frac{\gamma_N B_0(1 - \sigma)}{2\pi} \quad \dots \quad (12)$$

where  $\gamma_N$  is a constant called the magnetogyric ratio for the nucleus under discussion;  $\gamma$  is slightly different for atoms of a given element in different chemical environments since these have different values of  $\sigma$ . The range in values for  $\sigma$  increases as the number of electrons in the atom increases, being a minimum for  $^1\text{H}$ . Since resonance frequencies observed depend upon field strength, we need to specify both  $\gamma$  and  $B_0$  in order to describe an absorption precisely. But it is very difficult to measure  $B_0$  accurately, and it is therefore universal practice to measure the difference in  $\gamma$  for energy absorption from that for a reference compound; this is tetramethylsilane (TMS),  $(\text{CH}_3)_4\text{Si}$ , for both  $^1\text{H}$  and  $^{13}\text{C}$ , well away from those for these nuclei in other compounds; it is also volatile, soluble in nearly all organic solvents, and very unreactive. In water the salt  $(\text{CH}_3)_3\text{SiCD}_2\text{CD}_2\text{SO}_3^-\text{Na}^+$  is used.

### Chemical Shift

$$\text{Chemical shift is defined by } \delta = \frac{\gamma(\text{Sample}) - \gamma(\text{TMS})}{\gamma(\text{TMS})} \times 10^6 \text{ ppm}$$

Tetramethylsilane is a convenient standard because it gives a single sharp absorption for both  $^1\text{H}$  and  $^{13}\text{C}$ , well away from those for these nuclei in other compounds; it is also volatile, soluble in nearly all organic solvents, and very unreactive. In water the salt  $(\text{CH}_3)_3\text{SiCD}_2\text{CD}_2\text{SO}_3^-\text{Na}^+$  is used.

Under the normal conditions of measurement of  $^1\text{H}$ ,  $^{19}\text{F}$  and  $^{31}\text{P}$  magnetic resonance spectra (i.e. spectra of nuclei of high relative abundance), the intensity ratio of the absorptions is proportional to the number of nuclei giving rise to the absorptions. Thus for ethanol,  $\text{CH}_3\text{CH}_2\text{OH}$ , the proton magnetic resonance spectrum measured under low resolution contains three peaks at  $\delta = 5.2, 3.7$  and  $1.2$  ppm of relative intensity 1:2:3 assigned to the OH,  $\text{CH}_2$  and  $\text{CH}_3$  protons respectively. They are well-established rules correlating the values of proton chemical shifts and environments in organic compounds; but such rules are less useful in inorganic chemistry (few inorganic molecules contain protons in several different environments), and we shall not discuss them here beyond remarking that whilst the chemical shifts of the  $\text{CH}_3$  and  $\text{CH}_2$  protons are constant, that of the OH proton is affected by the extent of hydrogen bonding in which it is involved.

## Spin-Spin Coupling

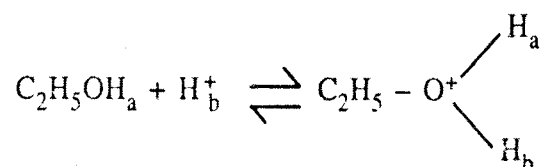
The proton magnetic resonance spectrum of ethanol is a highly instructive example which we shall now consider further. For very carefully purified ethanol under high resolution the spectrum (fig. 1.3a) contains  $\text{CH}_3$  and OH proton peaks each consisting of a triplet in which the relative intensities of the fine structure peaks are 1:2:1 and a  $\text{CH}_2$  proton peak which is an octet whose components have relative intensities 1:1:3:3:3:3:1:1. The origin of these splitting patterns may be explained by considering the methyl group triplet. The protons of the methyl group are under the influence not only of the applied field, but also of the spins of the two protons of the  $\text{CH}_2$  group, each of which may have its magnetic moment lined up with or against the applied field. Denoting these possibilities by arrows pointing up and down respectively, there are four possible combinations :

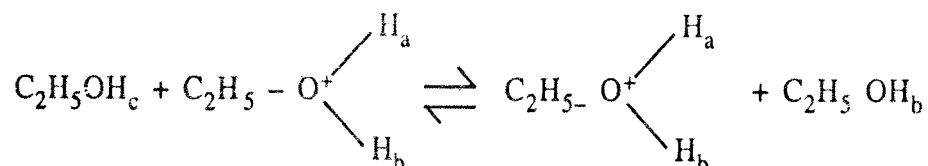


Of these, (ii) and (iii) have the same effect on the  $\text{CH}_3$  group protons, so that the combined effects of the  $\text{CH}_2$  group protons are in the ratio 1 : 2 : 1. Another triplet arises from the effect of the  $\text{CH}_2$  group protons on that of the OH group. In general, spin coupling, as the phenomenon is called, to one proton leads to a doublet, to two protons to a 1 : 2 : 1 triplet to three protons to a 1 : 3 : 3 : 1 quartet, and so, on. The octet associated with the  $\text{CH}_2$  Protons arises from the splitting of the  $\text{CH}_2$  Proton resonance into a doublet by the OH proton, followed by the splitting of each peak of the doublet into a quarter by the  $\text{CH}_3$  protons.

The magnitude of the frequency difference between fine structural peaks in a particular multiplet (the spin-spin coupling constant,  $J$ ) is independent of the strength of the external field or the input frequency used, a fact which makes it possible to distinguish spin-spin splittings from the effects of non-equivalent protons having different chemical shifts. Coupling constants are expressed in  $\text{H}_z$ . Both of the split signals, when two are split show that same splitting. Splitting of equivalent proton signals, and splitting by protons other than those on adjacent carbon atoms, are generally not observed.

If a trace of acid is added to pure ethanol, the resulting high-resolution spectrum is that normally observed and is shown in fig. 3.7(b); a singlet (OH), a quartet ( $\text{CH}_2$ ) and a triplet ( $\text{CH}_3$ ). The singlet structure of the OH proton resonance under these conditions can be used to illustrate an aspect of nuclear magnetic resonance spectroscopy that we have not yet mentioned. In order for a proton resonance signal to be observed, the proton must be in a single state for not less than about  $10^{-2}$  s; this is much longer than the time required for proton exchange between different molecules in the presence of a trace of acid, which may be represented by the scheme :





Because of this proton exchange the average spin state of the OH proton is zero, and it then neither affects, nor is affected by, the CH<sub>2</sub> protons. Such exchange reactions are general for protons bonded to oxygen or nitrogen. Since they are accelerated by a rise in temperature, the observance of spin-spin coupling is sometimes possible only at low temperatures. Conversely, the temperature dependence of a spectrum tells us something about the activation energy and mechanism of the exchange process.

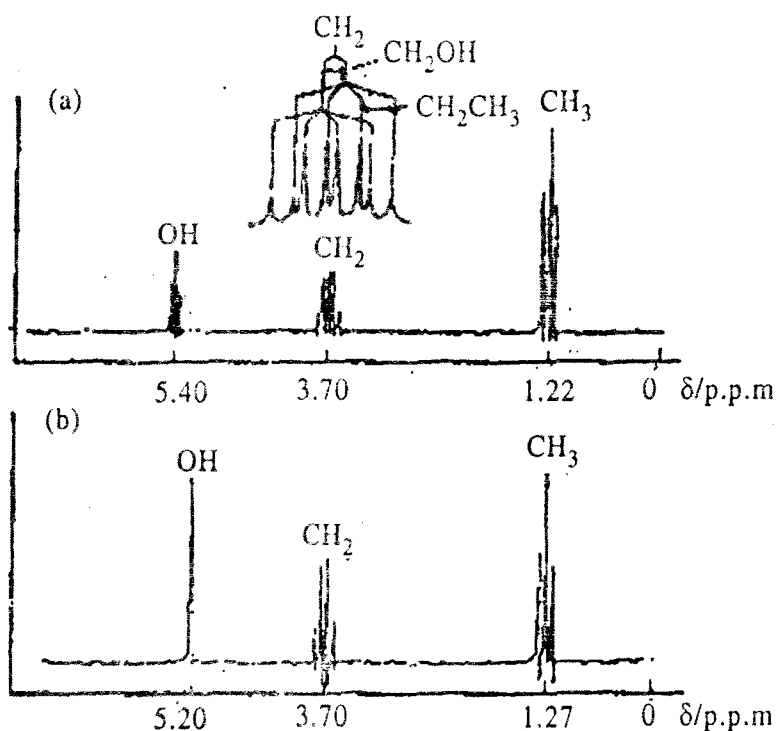


Fig. 3.7 High resolution proton magnetic resonance spectrum of (a) pure ethanol; and (b) ethanol containing a trace acid.

### Structure Determination using Multiprobe

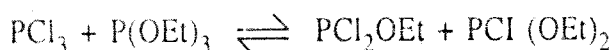
The nucleus <sup>12</sup>C has  $I = 0$  and hence can give no nuclear magnetic resonance spectrum. The low natural abundance of <sup>13</sup>C (1.1 per cent) leads to special difficulties in the observation of <sup>13</sup>C spectra, which are overcome by the technique of Pulsed Fourier Transform (PFT) spectroscopy. In this, all <sup>13</sup>C nuclei present are excited by a short pulse, and the frequencies of transitions to lower energy levels are sorted out from the complex spectrum by the mathematical method of Fourier analysis, performed by computer. For spectra measured by

this method relative intensities of signals are not proportional to numbers of nuclei present in different environments, only qualitative information about the kinds of different  $^{13}\text{C}$  atoms being obtainable. Further, because of the low natural abundance of the isotope (so that any molecule is unlikely to contain more than one  $^{13}\text{C}$  atom),  $^{13}\text{C}$  spin-spin coupling is normally observed only for compounds made from  $^{13}\text{C}$  enriched materials.

The following examples illustrate some of the applications of nuclear resonance spectroscopy in inorganic chemistry.

A number of hydrated cations in aqueous solution undergo exchange with solvent water at rates slow enough for coordinated and solvent water containing the isotope  $^{17}\text{O}$  (which has a nuclear magnetic moment) to be distinguished, and from intensity ratios hydration numbers can be obtained.  $\text{Be}^{2+}$  and  $\text{Al}^{3+}$ , for example, are found to be present as  $[\text{Be}(\text{H}_2\text{O})_4]^{2+}$  and  $[\text{Al}(\text{H}_2\text{O})_6]^{3+}$  respectively.

A reaction such as



in which the types and numbers of each type of bond remain constant is known as a redistribution reaction. This can be followed by  $^{31}\text{P}$  chemical shifts which are different in the four compounds. Rate data may be obtained by following the variation in relative intensities with time, equilibrium constants (and hence standard free energy changes) by determining the relative intensities when no further change takes place, and standard enthalpy and entropy changes by determining the equilibrium constants at different temperatures. As would be expected  $\Delta H^\circ$  for reactions of this kind is almost zero, the redistribution of the groups attached to the phosphorous atoms being caused by an increase in the entropy of the system.

In investigating inorganic structures by high resolution nuclear magnetic resonance spectroscopy, the relatively long time-scale of the method ( $10^{-1}$ – $10^{-5}$  s, depending on the nucleus being studied) must always be borne in mind. Especially at higher temperatures (where the activation energy for intramolecular rearrangement is very much more easily acquired), nuclear magnetic resonance diffraction methods. In these circumstances, however, the information obtained about the energetics of rearrangement (from which something concerning the mechanism can be inferred) may be of major significance, since few methods for the study of such processes are available. The  $^{19}\text{F}$  resonance in bromine pentafluoride at ordinary temperatures, for example, consists of two peaks of relative intensities 1:4, the intense line being a doublet, and the weak line a quintet with the relative intensities 1:4:6:4:1. This indicates that the molecule is a square pyramid. At  $180^\circ\text{C}$  the spectrum collapses to a single line, the fluorine atoms then being, for nuclear magnetic resonance purposes, identical. A similar state of affairs holds in the case of sulphur tetrafluoride. The spectrum at  $-98^\circ\text{C}$  consists of two triplets each of relative intensities 1:2:1; this shows that there are two non-equivalent pairs of fluorine atoms, and is in agreement with the structure established by the methods as a trigonal bipyramid with one of the equatorial positions occupied by an unshared pair of electrons. At  $-58^\circ\text{C}$  only two broad peaks are seen, and

at room temperature there is only a single absorption. For  $\text{Fe}(\text{CO})_5$  (containing  $^{13}\text{C}$ ) and  $\text{PF}_5$ , intramolecular exchange is found to occur even down to  $-100^\circ\text{C}$ . Showing that the activation energies for exchange must be extremely small. This suggests that exchange involves only a simple molecular vibration of the type shown for  $\text{PF}_5$  in Fig. 3.8. In recent years extensive studies by means of  $^1\text{H}$  and  $^{13}\text{C}$  nuclear magnetic resonance spectroscopy have been made of intramolecular rearrangements of organic ligands coordinated to metal atoms.

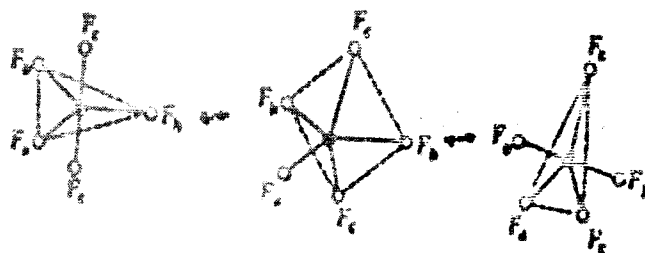


Fig 3.8 Intra molecular exchange of fluorine atoms in  $\text{PF}_5$  via a square pyramidal intermediate

#### Effect of Quadrupolar nuclei on NMR spectra :

Quadrupolar nuclei are often very efficiently relaxed by the fluctuating electric fields that arise from the dipolar solvent and solute molecules. The mechanism of quadrupole relaxation depends upon the interaction of the quadrupolar nucleus with the electric field gradient at the nucleus. This gradient arises when the quadrupolar nucleus is in a molecule in which it is surrounded by a non-spherical distribution of electron density.

The field gradient,  $q$ , is used to describe the deviation of the electronic charge cloud about the nucleus from spherical symmetry. If the groups about the nucleus in question have cubic symmetry (e.g  $T_d$  or  $O_h$  point groups), the charge cloud is spherical and the value of  $q$  is zero. If the molecule has cylindrical symmetry (a threefold or higher symmetry axis), the deviation from spherical symmetry is expressed by the magnitude of  $q$ . If the molecule has less than cylindrical symmetry, two parameters are usually needed,  $q$  and  $n$ . The quantity  $n$  is referred to as the asymmetry parameter. The word "usually" is inserted because certain combinations of angles and charges can cause fortuitous cancellations of effects leading to  $n = 0$ . The axis of largest  $q$  is labeled  $z$  and is described by  $q_{zz}$ . The other axes described by field gradients  $q_{xx}$  and  $q_{yy}$ , are described by the asymmetry parameter, which is defined as :

$$n = (q_{xx} - q_{yy}) / q_{zz}$$

#### Chemical Exchange and Dynamic process in Inorganic and Organometallic compounds:

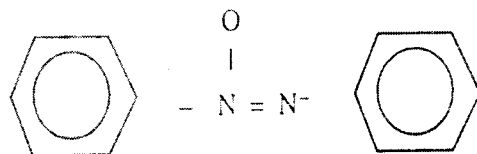
The effectiveness of the relaxation depends upon the magnitude of the field gradient. Rapid nuclear quadrupole relaxation has a pronounced effect on the linewidth obtained in the nmr spectrum of the quadrupolar nucleus, and it also influences the nmr spectra of protons or other nuclei attached to this quadrupolar nucleus. In the latter case, splittings of a proton

from the quadrupolar nucleus may not be observed or the proton signal may be so extensively broadened that the signal itself is not observed. This can be understood by analogy to the effect of chemical exchange on the proton nmr spectra. Either rapid chemical exchange or rapid nuclear quadrupole relaxation in effect places the proton on a nucleus (or nuclei, for chemical exchange) whose spin state is rapidly changing. Nuclear quadrupole relaxation rates often correspond to an intermediate rate of chemical exchange, so extensive broadening is usually observed. As a result of quadrupole relaxation, the proton nmr spectrum of  $^{14}\text{NH}_3$  ( $^{14}\text{N}$ ,  $I = 1$ ) consists of three very broad signals; while in the absence of this effect, the spectrum of  $^{15}\text{NH}_3$  ( $^{15}\text{N}$ ,  $I = \frac{1}{2}$ ) consists of a sharp doublet. On the other hand, in  $^{14}\text{NH}_4^+$ , where a spherical distribution of electron density gives rise to a zero field gradient, a sharp three-line spectrum results. In a molecule with a very large field gradient, a broad signal with no fine structure is commonly obtained.

When one attempts to obtain an nmr spectrum of a nucleus with a quadrupole moment (e.g.  $^{35}\text{Cl}$  and  $^{14}\text{N}$ ) that undergoes relaxation readily, the signals are sometimes broadened so extensively that no spectrum is obtained. This is the case for most halogen (except fluorine) compounds. Sharp signals have been obtained for the halide ions and symmetrical compounds of the halogens (e.g.,  $\text{ClO}_4^-$ ), where the spherical charge distribution gives rise to only small field gradients at the nucleus, leading to larger values for  $T_1$ .

Solutions of  $\text{I}^-$  ( $^{127}\text{I}$ ,  $I = 5/2$ ) give rise to an nmr signal. When iodine is added, the triiodide ion,  $\text{I}_3^-$ , is formed, destroying the cubic symmetry of the iodide ion so that quadrupole broadening becomes effective and the signal disappears. Small amounts of iodine result in a broadening of the iodide resonance, and the rate constant for the reaction  $\text{I}^- + \text{I}^2 \rightarrow \text{I}_3^-$  can be calculated from the broadening. It is interesting to note that chlorine chemical shifts have been observed for the compounds:  $\text{SiCl}_4$ ,  $\text{CrO}_2\text{Cl}_2$ ,  $\text{VOCl}_3$ , and  $\text{TiCl}_4$ , where the chlorine is in an environment of lower than cubic symmetry.

An interesting effect has been reported for the fluorine nmr spectrum of  $\text{NF}_3$ . The changes in a series of spectra obtained as a function of temperature are opposite to those normally obtained for exchange processes. At  $-205^\circ\text{C}$  a sharp single peak is obtained for  $\text{NF}_3$ ; as the temperature is raised the line broadens and a spectrum consisting of a sharp triplet ( $I = 1$  for  $^{14}\text{N}$ ) results at  $20^\circ\text{C}$ . It is proposed that at low temperature the slow molecular motions are most effective for quadrupole relaxation of  $^{14}\text{N}$ ; as a result, a single line is obtained. At higher temperatures, relaxation is not as effective and the lifetime of a given state for the  $^{14}\text{N}$  nucleus is sufficient to cause spin-spin splitting. A similar effect is observed for pyrrole. The  $^{14}\text{N}$  spectrum of azoxybenzene exhibits only a singlet. The nitrogens are not equivalent, and it is proposed that the field gradient at the N-O nitrogens is so large as to make this resonance unobservable.



The double resonance technique has been successfully used on the proton nmr spectrum of  $\text{Al}(\text{BH}_4)_3$ . This molecule contains six Al-H-B bridge bonds. Both B and  $^{27}\text{Al}$  ( $I = 5/2$ ) have quadrupole moments. The proton nmr at 30 MHz consists of a single broad line (Fig. 3.9 (A)). When the  $^{11}\text{B}$  nucleus is saturated ( $^1\text{H} \rightarrow \{^{11}\text{B}\}$ ), the proton resonance spectrum in Fig. 3.9 (B) results. Fig. 3.9 (C) represents the proton nmr spectrum when the sample is irradiated with frequency corresponding to that of  $^{27}\text{Al}$  ( $^1\text{H} \rightarrow ^{27}\text{Al}$ ). The four large peaks in (C) arise from  $^{11}\text{B}$  splitting of the proton and the smaller peaks from  $^{10}\text{B}$  splitting. The bridging and terminal hydrogens are not distinguished because of a rapid proton exchange reaction that makes all hydrogen magnetically equivalent;

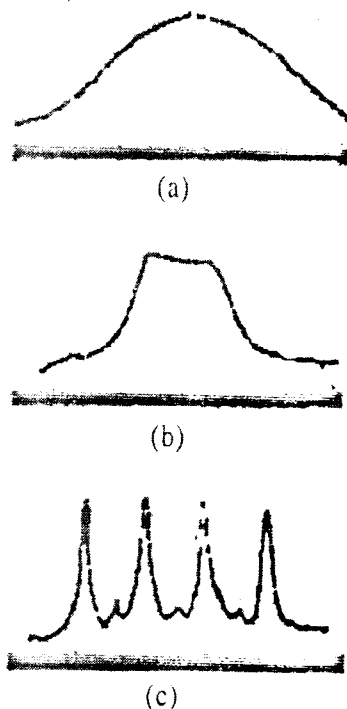


Fig. 3.9 Proton nmr of  $\text{Al}(\text{BH}_4)_3$  (A) proton resonance. (B) Proton resonance,  $^{11}\text{B}$  saturated. (C) Proton resonance,  $^{27}\text{Al}$  saturated. (From R.A. Ogg, Jr. and J.D. Ray, Disc. Faraday Soc., 19, 239 (1955).

#### Fluxional Molecules and NMR studies :

For some coordination numbers two possible geometries are almost equal in stabilities for atleast a few compounds. These polytopal systems can be crystallized in both geometries under the right circumstances to observe a dynamic between the two forms. Molecules that interconvert geometries are said to be stereochemically nonrigid or fluxional. Fluxional molecules differ from others in possessing more than a single configuration representing an energy minimum.

Nuclear magnetic resonance techniques have proved invaluable in the study of fluxional molecules. There are two limiting cases depending upon the rate of interconversion. Consider a molecule in which there are two environments for the protons and no interconversion takes place. There will be two resonance lines separated by a difference ( $\Delta$ ), that reflects the

difference in the environment of the two sites. At the other extreme, if interconversion takes place with a frequency which is larger with respect to separation  $\Delta$ , the spin of the proton hardly loses phase from the time it is in a particular site until it is at that site again. As far as the response on the proton is concerned it behaves as though it were in an average environment and a single line found at the average frequency.

For e.g. consider the trihapto - allyl complex. At low temperatures it would yield a spectrum as given below with two large doublets for the hydrogen atoms  $H_s$  in syn cis position relative to the fifth hydrogen and the two hydrogen atoms  $H_a$  in anti or trans positions relative to the fifth hydrogen atom. The molecule is rigid, so each of the three types of hydrogen produces a distinctive chemical shift depending upon its environment.



Fig. 3.10 a Typical spectrum of trihaptoallyl system

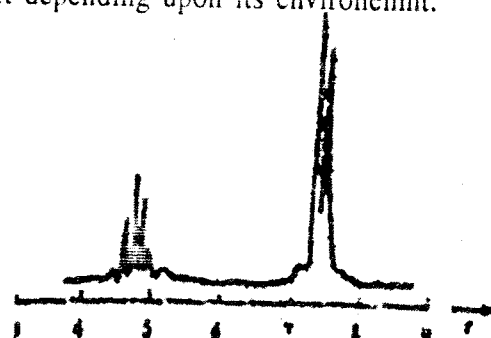


Fig. 3.10b Spectrum of Fluxional allyl system showing time Averaging of the four terminal hydrogen.

Upon warming the spectrum often changes with collapse of the two doublets into one. This spectrum indicates that on a time average there are two types of hydrogens: four terminal hydrogens and one non-terminal hydrogen atom. The four terminal hydrogens and one non-terminal hydrogen atom. The four terminal hydrogen atoms are equivalent. This could result from the molecule rapidly interconverting.

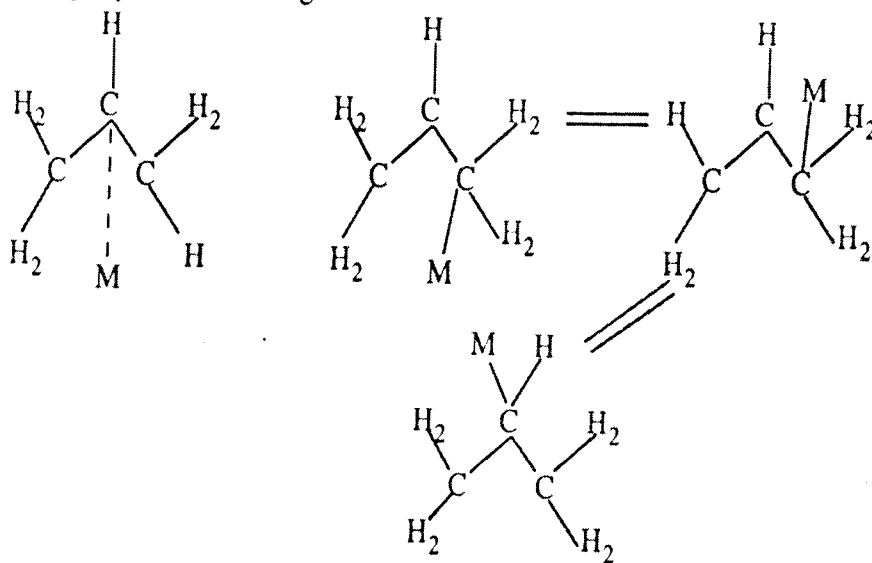


Fig. 3.11

In such a rapidly interconverting system the distinction between H<sub>s</sub> and H<sub>a</sub> is lost. A somewhat similar system has been found for the complex between tetramethylallene and ironcarbonyl.

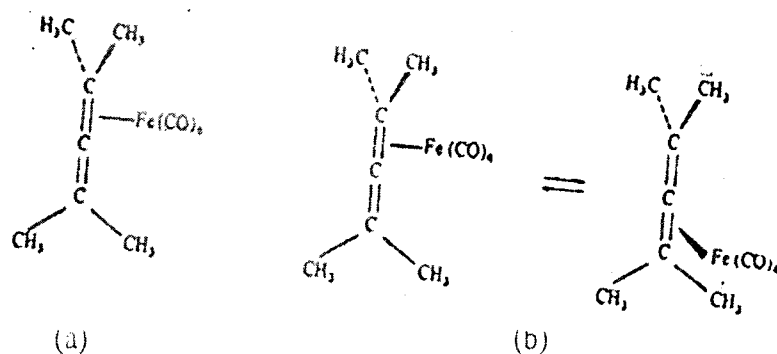


Fig. 3.12 Tetramethylalleneiron tetracarbonyl

Below  $-60^\circ$  the pmr spectrum shows three peaks in the ratio 1 : 1 : 2 representing the three cis hydrogen atoms, three trans hydrogen atoms and six hydrogen atoms in a plane perpendicular to the carbon - iron bond. As the temperature is raised, the spectrum collapses to a single resonance for the average environment of the 12 hydrogens as the iron presumably migrates around the allene  $\pi$  system.

Cyclic systems like ferrocenophane show fluxional behaviour, we know that the rings in ferrocene are free to rotate. Ordinarily this is not observable as all the protons are equivalent whether the molecule is static or fluxional. Mueller - Westerhoff and Co- workers described a ferrocenophane (two ferrocene molecules linked by methylene bridges) that undergoes unusual fluxional behaviour. The methylene bridges 'flip' over to the opposite conformation faster than can be followed on the NMR time scale. Thus the NMR spectrum is unexpectedly simple; a sharp singlet for the methylenic protons and two narrow multiplets for the  $\alpha$ - and  $\beta$  - protons of the rings.

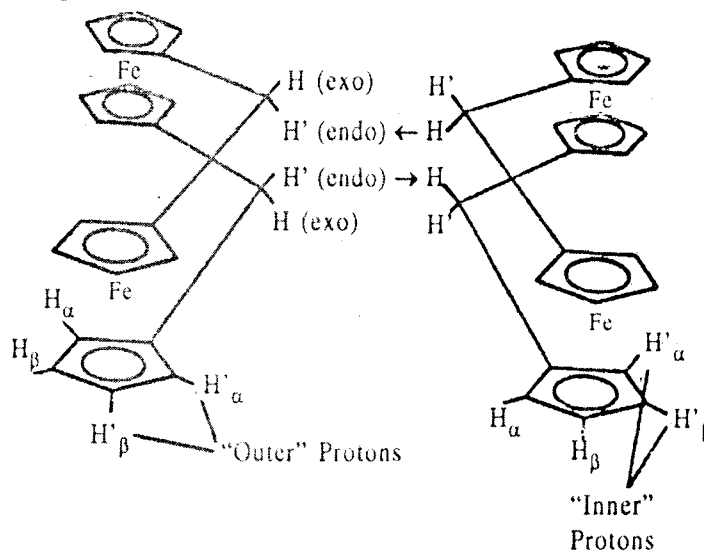


Fig. 3.13 The fluxional, "inside-out" behaviour of the ferrocenophane molecule. Note the inter-conversion of the methylenic hydrogen atoms :  $\text{exo} \rightleftharpoons \text{endo}$ . Note also that the "outer" protons become "inner" protons. As a result of this averaging, there are only three magnetically distinct kinds of protons :  $\alpha$ ,  $\beta$  and bridge.

Another example of fluxional behaviour in cyclopentadienyl compounds is found in  $\text{Cp}_2\text{Hg}$ , which shows the following two structures.

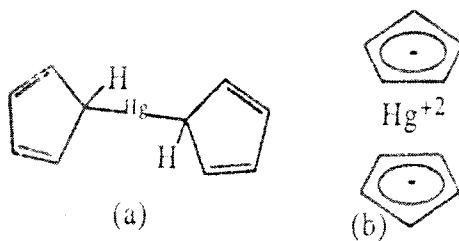


Fig. 3.14 Possible structures for bis(cyclopentadienyl) mercury : (a) monohapto complex; (b) penta - hapto complex

The first corresponds to divalent mercury bonded to two  $\text{C}_5\text{H}_5$  groups (Monohapto complex) the second to an ion structure analogous to the magnesium compound (pentahapto complex). Structure (a) might be expected to exhibit three types of hydrogen resonances in the ratio 1:2:2, whereas all of the hydrogen atoms are equivalent in (b). The NMR spectrum of the compound below  $-70^\circ\text{C}$  contains of a single peak indicating equivalence of all the protons. On the other hand the IR spectrum is much more complex. It was thus proposed that the mercury ring bonds are undergoing a constant precession and this point is supported by more recent works.

### Contact Shift

Magnetic moments aligned along the external magnetic field from spin density at every point all over the molecule (except that at the resonating nucleus) can also couple with the nuclear magnetic moment. The coupling is dipolar in origin. The relevant Hamiltonian for the general case of coupled magnetic moment vectors  $\mu_1 = g_N\mu_N I$  and  $\mu_2 = g\mu_B S$  was given in equation

$$\hat{H}_{\text{dip}} = -g\mu_B g_N \mu_N \left( \frac{S \cdot I}{r^3} - \frac{3(S \cdot r)(I \cdot r)}{r^5} \right) \dots (13)$$

When both I and S are aligned along the external magnetic field (as is the case when g is isotropic) the energy of interaction is :

$$E_{\text{dip}} = \frac{\mu_1 \mu_2}{r^3} (3\cos^2 \gamma - 1) \dots (14)$$

where  $\mu_1$  is the nuclear magnetic moment,  $\mu_2$  is the electron magnetic moment, and r is the distance between the origins of the two vectors. The meaning of the angle  $\gamma$  is illustrated in Fig. 3.15.

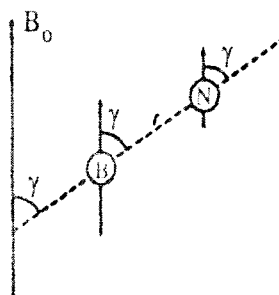


Fig. 3.15. The dipolar interaction energy between the electron and nuclear magnetic dipoles in an isotropic situation is a function of the angle  $\gamma$  between the electron-nucleus vector,  $r$ , and the external magnetic field,  $B_0$ .

The electron magnetic moment arises from the excess population of the Zeeman levels times the spin density at a given point and  $r$  is the distance between the nucleus and the given point. In order to evaluate the interaction energy over all space, integration is needed. This dipolar contribution to the electron-nucleus hyperfine coupling can be measured in the solid state or a frozen solution, with epr and ENDOR. In solution, where random and isotropic rotation occurs, the energy described above averages to zero for an isotropic  $g$  because the integral for  $\cos \gamma$  ranging from 1 to  $-1$  of equation (14) is zero. For this averaging to occur, the rotation rate in radians/sec $^{-1}$ , has to be faster than  $E_{\text{dip}}/h$ . This condition is easily satisfied in solution even for macromolecules.

Now, let us suppose that  $\mu_2$  is not isotropic but changes its magnitude as the orientation of the molecule changes with respect to the external magnetic field. Under these circumstances,  $\mu_2$  is anisotropic and the integration of equation (14) over  $\cos \gamma$  is not zero. Thus, an added contribution to the hyperfine coupling results, that is, an additional magnetic field is sensed by the nucleus giving rise to a contribution to the chemical magnetic field is sensed by the nucleus giving rise to a contribution to the chemical shift. The value of  $\mu_2$  will be anisotropic when there is an orbital contribution to the magnetic moment which, by its nature, changes in different directions of the molecular frame. In this case  $g$  also becomes anisotropic and therefore orientation dependent. Thus, the same effects that give rise to anisotropy in  $g$  also give rise to a shift contribution. This shift contribution is isotropic because the dipolar effect is averaged by rotation in solution. Because it is isotropic, like the contact contribution, it is called a pseudocontact shift and is also referred to in the literature as an isotropic dipolar shift. The through space nature of the pseudocontact effect is comparable to the neighbour anisotropic contribution, which was seen to be dependent upon differences in  $\chi_{\text{DIA}}$  for different orientations. In a similar fashion, anisotropy for  $\chi_{\text{para}}$  to the pseudocontact shift.

The complete evaluation of the pseudocontact shift requires knowledge of the spin density distribution over the entire molecule. This information is usually not available. If the

unpaired electrons are assumed to be localized only on the metal ion, a point model leads to equations for evaluating the pseudocontact contribution to the isotropic shift. The general equation in SI units' is

$$\frac{\Delta\gamma_{i(\text{pc})}}{\gamma} = -\frac{1}{4\pi} (1/3N_A) (\chi_{zz} - \frac{1}{2}(\chi_{xx} + \chi_{yy})) \frac{3\cos^2\theta_1 - 1}{r_i^3} - \frac{1}{4\pi} (1/2N_A) (\chi_{xx} + \chi_{yy}) \frac{\sin^2\theta_1 \cos 2\phi}{r_i^3} \dots (15)$$

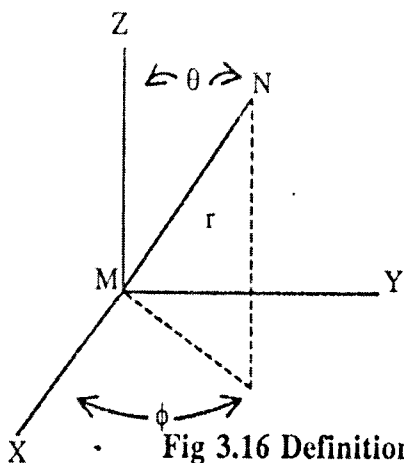


Fig 3.16 Definition of the quantities in equation

Here,  $N_A$  is Avogadro's constant  $\chi_{xx} + \chi_{yy}$  and  $\chi_{zz}$  are the susceptibility components, and the angles  $\theta$  and  $\phi$  are defined in Fig. 3.16. The coordinates  $x$ ,  $y$  and  $z$  are defined by the principal directions of the magnetic susceptibility tensor.

**Shift reagents :**

The solvent may affect the screening of particular protons by several possible mechanisms such as van der Waals interaction, anisotropy of the susceptibilities of the surrounding molecules, and the reaction field of the medium and specific solutesolvent interactions. Polyhalogenated hydrocarbon solvents tend to cause the largest shifts, up to 0.5 ppm downfield. This is thought to be due to van der Waals interactions leading to a decrease in the diamagnetic shielding of the nucleus. In 3.16a the complex pattern has been resolved (see the upper trace) by the addition of 50% benzene to the  $\text{CCl}_4$  solution in which the NMR spectrum was initially taken. Benzene solvent molecules associate with electron deficient sites in solute molecules. Because benzene is highly anisotropic, different protons in the solute experience shielding or deshielding depending on their orientations to the benzene ring. In this particular example, the ring protons are shielded (located above the benzene ring) and appear at higher field.

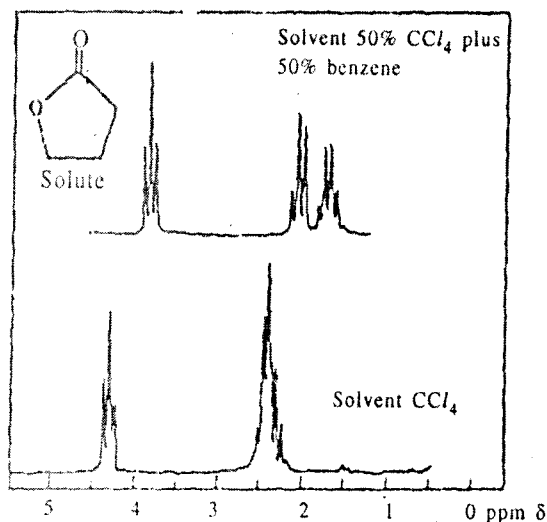


Fig. 3.16a Solvent effect on an NMR spectrum

An isolated carbonyl group induces a solvent effect that changes sign near a plane drawn through the carbonyl carbon atom and perpendicular to the carbonyl group. The corresponding shift relative to pyridine changes sign near a plane drawn through the  $\alpha$ -carbon atoms. Thus, in the case of an equatorial proton adjacent to the carbonyl group in a cyclohexanone ring, the shift is small or zero in benzene and negative in pyridine, whereas for axial protons or methyl groups, the shift is positive in benzene and small or zero in pyridine.

Proton resonance peaks are spread across a broader range of magnetic field strength by the addition of a paramagnetic compound to the solution being studied. The most commonly used shift reagents are lanthanide fluorinated  $\beta$ -diketones. They function by acting as Lewis acids, forming a complex with the substance under investigation that acts as a nucleophile. Induced shifts are attributed to a pseudocontact, or dipolar interaction, between the shift reagent and the nucleophile. The most commonly used metal chelates are those of Eu(III) and Yb(III), which normally induce downfield shifts, and Pr(III), which induces upfield shifts. Shift reagents give a resolution of peaks comparable to the resolution achievable with 100- or even 220 MHz spectrometers (figure 3.17). The faster and easiest technique for obtaining induced shifts is to add a few milligrams of shift reagent directly to the nucleophile dissolved in solvent. Increments of shift reagent are added until sufficient resolution is attained. There is essentially a linear dependence of the chemical shifts upon added shift reagent. The most frequently used solvents are chloroform and carbon tetrachloride. Once shift reagents have been used to resolve the NMR peaks of a compound, spin-decoupling experiments become possible.

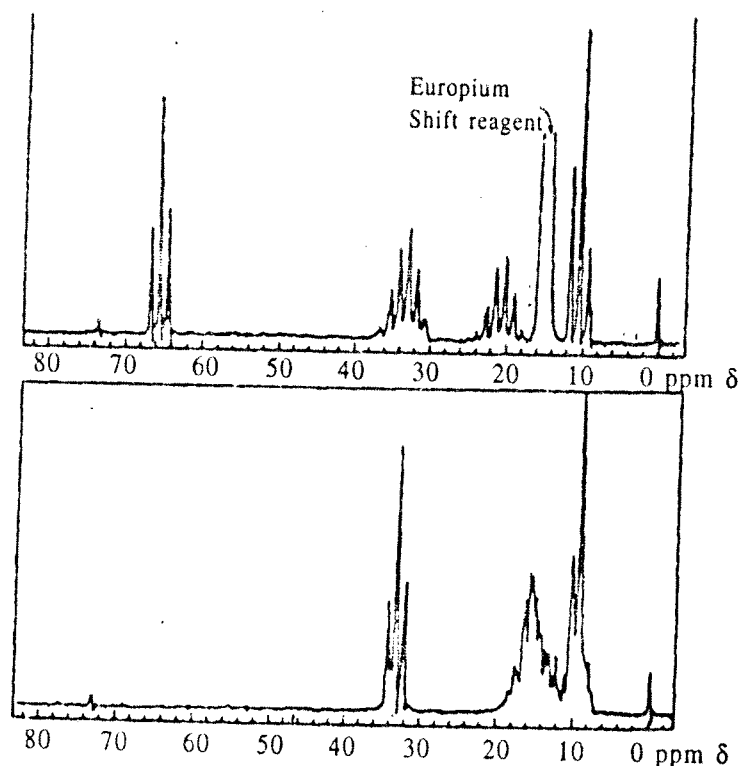


Fig 3.17 NMR spectra of di-n-butyl ether ( $1.0 \times 10^{-4}$ ) moles in 0.5 mL  $\text{CCl}_4$  alone (lower trace) and with  $5.0 \times 10^{-5}$  moles of tris (1, 1, 1, 2, 2, 3, 3-hepta-fluoro-7, 7-dimethyl-4, 6-octanedione) europium (III) added (upper trace).

### EPR

Electron spin resonance (esr) or electron paramagnetic resonance (epr) is very similar to nuclear magnetic resonance in many ways. It is also an absorption spectroscopic technique, which is possible only for molecules with unpaired electrons.

### Principle

A single unpaired electron possesses a spin number of  $\frac{1}{2}$  and may exist in either of the two degenerate energy states, namely  $+\frac{1}{2}$  or  $-\frac{1}{2}$  when a magnetic field is applied, the degeneracy is lifted and the transition from the low energy state  $\left(m_s = -\frac{1}{2}\right)$  to the high energy state  $\left(m_s = +\frac{1}{2}\right)$  can be achieved by absorption or radiation in the microwave region. The energy,  $\Delta E$ , of the transition is given by

$$\Delta E = h\nu = g \beta H_0, \text{ where}$$

$h$  = Planck's constant

$\gamma$  = Frequency of microwave radiation

$\beta$  = the Bohr magneton =  $\frac{eh}{4\pi mc}$

e = electron charge

m = mass of an electron

c = velocity of light

g = Lande's spectroscopic splitting factor, it has a value of 2.0023 for a free electron

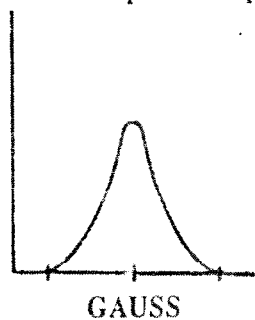


Fig. 3.18 (a) Gauss

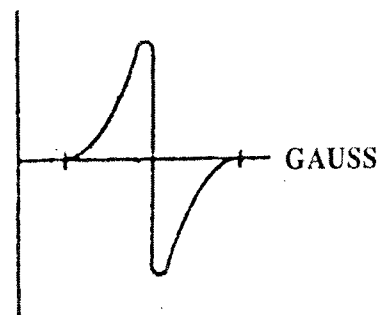


Fig. 3.19 (b)

As in nmr, the energy requirement for a transition is dependent upon the strength of the applied magnetic field. If a 3.4 kilo gauss field is applied, the frequency of the radiation used for excitation is 9.5 GHz = (1GHz =  $10^9$  Hz). The Bohr magneton is about 1000 times larger than the nuclear magneton. Hence the spin magnetic moment of the electron is about 1000 times larger than nuclear magnetic moment. Therefore, the energy difference between the upper state and the lower state is greater in the case of electrons than in the case of protons exposed to the same magnetic field.

The esr spectrum of a free electron consists of a single absorption peak as shown in fig. 3.18a. But the resonance lines are always recorded as a first derivative spectrum fig. 3.18 b. An electron spin resonance spectrum provides two kinds of information :

1. The position of absorption, and
2. The magnetic interaction of the unpaired electron with its neighbouring nuclei with  $I \neq 0$

The position of the signal is indicated by the g value. For a free electron the g value is 2.0023. Departure from this value is attributed to interactions with the orbital angular momentum by neighbouring groups. Hence the value is dependent upon the chemical environment. For example, if an electron in a molecule is free to move about due to complete delocalization, then the g value is very close to the value of the free electron. On the other hand, if its movement is restricted and completely localized, then the value of g differs considerably from 2.0023. Liquids, because of molecular collisions, generally possess a single g value (isotropic) indicating randomization of the interactions with neighbouring molecules. But in paramagnetic solids, the g may have different values along the coordinate axes x, y and z.

To measure the  $g$  value of a free radical, the sample and a reference compound with a known  $g$  value (DPPH - diphenylpicrylhydrazyl radical) are taken in two separate sample tubes and placed in a dual sample cavity of the esr instrument. The esr spectrum is then recorded. The spectrum will show two signals with a field separation of  $\Delta H$ . The  $g$  value for the unknown substance is given by

$$G = g_{\text{ref}} \left( 1 - \frac{\Delta H}{H} \right), \text{ where } H \text{ is the resonance frequency.}$$

### Hyperfine Splitting :

The esr signal is due to the transition of the electron from the spin state  $m_s = -\frac{1}{2}$  to the spin state  $m_s = +\frac{1}{2}$ . These spin states interact with the magnetic moments of nuclei, with which the unpaired electron may be partially or wholly associated. This interaction may lead to further splitting of resonance signals into several lines. For example, in hydrogen atom the electron is associated with a nucleus with  $I = \frac{1}{2}$ . In the presence of an external magnetic field, the lower energy state  $\left( m_s = -\frac{1}{2} \right)$  is either associated with the nucleus,  $m_I = +\frac{1}{2}$  or with the nucleus  $m_I$ . Thus the lower energy state is split into two sub-energy states. The sub-energy state with  $m_s = \frac{1}{2}$  and  $m_I = \frac{1}{2}$  has a lower energy than the sub-energy state with  $m_s = -\frac{1}{2}$ . In the same manner, the higher energy state with  $\left( m_s = +\frac{1}{2} \right)$  is also split into two sub-energy states; one with  $m_s = +\frac{1}{2}$ ,  $m_I = +\frac{1}{2}$  (lower sub-energy state) and other with  $m_s = +\frac{1}{2}$ ,  $m_I = -\frac{1}{2}$  (higher sub-energy state). In general, if the nuclear spin is  $I$ , there will be  $2I + 1$  energy levels for each value of  $m_s$ . The selection rule for the allowed esr transition is  $\Delta m_I = 0$  and  $\Delta M_s = \pm 1$ .

The transition from the state  $m_s = -\frac{1}{2}$ ,  $m_I = +\frac{1}{2}$  to  $m_s = +\frac{1}{2}$ ,  $m_I = +\frac{1}{2}$  and from the state  $m_s = -\frac{1}{2}$ ,  $m_I = -\frac{1}{2}$  to the state  $m_s = +\frac{1}{2}$ ,  $m_I = -\frac{1}{2}$  are allowed (fig. 3.19b). Thus the esr signal is split into a doublet (b). The distance between the two adjacent split signals is known as hyperfine splitting constant  $a$  (measured in Hz).

For a system of one unpaired electron, interacting with three equivalent protons (e.g., methyl radical) the repetitive splitting procedure as shown (3.19a) would lead to a quartet signal. The inner levels are three-fold degenerate and hence their intensities are three times stronger than the outer lines in the spectrum 3.19(b)

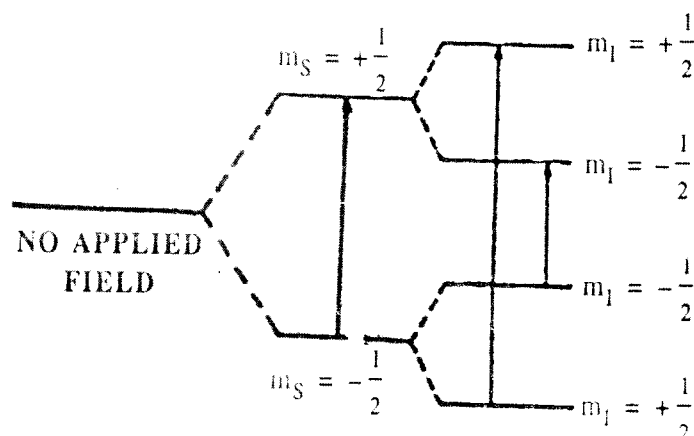


Fig 3.19 a

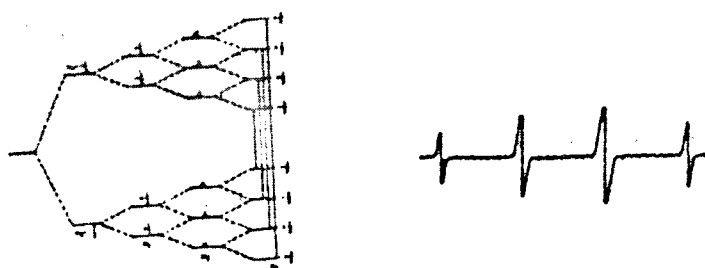


Fig. 3.19 b

The coordination x, y and z are defined by the principal directions of the magnetic susceptibility tensor. (Note that  $x$  (SI) =  $4\pi \times 10^{-6} \chi$  (egs emu))

#### Application of EPR in Transition Metal Ion Complexes : Kramers' Degeneracy

The epr spectra of transition metal ion complexes contain a wealth of information about their electronic structures. The additional information and accompanying complications that are characteristic of transition metal ion systems arise because of the approximate degeneracy of the d-orbitals and because many of the molecules contain more than one unpaired electron. These properties give rise to orbital contributions and zero-field effects. As a result of appreciable orbital angular moments, the g-values for many metal complexes are very anisotropic. Spin-orbit coupling also gives rise to large zero-field splittings (of  $10 \text{ cm}^{-1}$  or more) by mixing ground and excited states.

An important theorem that summarizes the properties of multielectron systems is Kramers' rule. This rule states that if an ion has an odd number of electrons, the degeneracy of every level must remain at least twofold in the absence of a magnetic field. With an odd number of electrons,  $m_j$  quantum numbers will be given by  $\pm 1/2$  to  $\pm J$ . Therefore, any ion with an odd number of electrons must always have as its lowest level at least a doublet, called a Kramer's doublet. This degeneracy can then be removed by a magnetic field, and an epr spectrum should be observed. On the other hand, for a system with an even number of electrons,  $m_j = 0, \pm 1, \dots, \pm J$ . The degeneracy may be completely removed by a low symmetry crystal field, so only singlet levels remain that could be separated by energies so large that an epr transition would not be observed in the microwave region. This discussion is illustrated by the energy level splittings in Fig. 3.20. For the even electron system, the ground state is non-degenerate and the  $J = 0$  to 1 transition energy is quite frequently outside the microwave region.

A number of factors, other than those that are instrumental, affect the epr line width. As in nmr, spin-lattice, spin-spin, and exchange interactions are important,

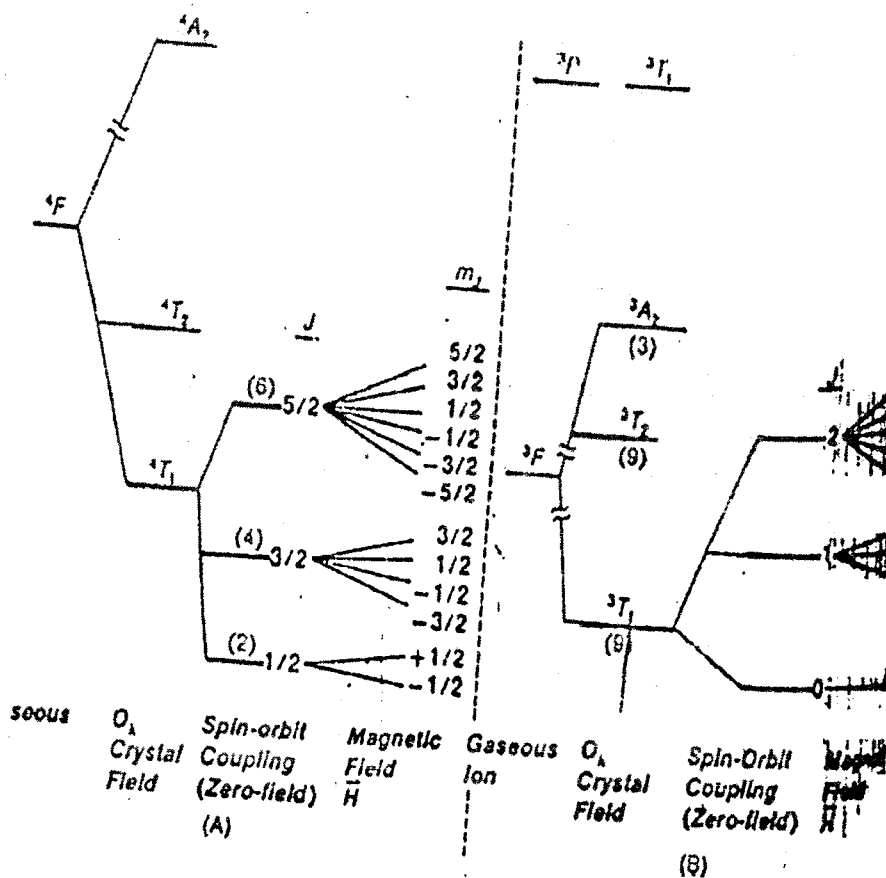


Fig. 3.20 The splitting of the gaseous ion degeneracy of (A)  $\text{Co}^{2+}$  and (B) by the crystalfield, spin-orbit coupling, and a magnetic field. The T state is regarded as having an effective L, called  $L'$  equal to 1; for an A state,  $L' = 0$ . Then  $V = L' + S, \dots, L' - S$ . Only the zero-field and magnetic field splittings of the ground state are shown.

Broadening due to spin-lattice relaxation results from the interaction of the paramagnetic ions with the thermal vibrations of the lattice. The variation in spin-lattice relaxation times in different systems is quite large. For some compounds, the life time is sufficiently long to allow the observation of spectra at room temperature, while in others this is not possible. Since these relaxation times generally increase as the temperature decreases, many of the transition metal compounds need to be cooled to liquid N<sub>2</sub> or liquid He temperatures before well-resolved spectra are observed.

Spin-spin interaction results from the magnetic fields that originate in neighbouring paramagnetic ions. As a result of these fields, the total field at each ion is slightly altered and the energy levels are shifted. A distribution of energies results, producing a broad signal. This effect varies as  $(1/r^3) \cdot (1 - 3 \cos^2 \theta)$ , where  $r$  is the distance between ions and  $\theta$  is the angle between the field and the symmetry axis. Since this effect is reduced by increasing the distance between paramagnetic ions, it is often convenient to examine transition metal ion systems by diluting them in an isomorphous diamagnetic host. For example, a copper complex could be studied as a powder or single crystal by diluting it in a host lattice of an analogous zinc complex or by examining it in a frozen solution. Dilution of the solid isolates the electron spin of given complex from that of another paramagnetic molecule, and the spin lifetime is lengthened. If a frozen solution is used, it must form a good glass; otherwise, paramagnetic aggregates form, which lead to a spectrum with broadened lines, it is often necessary to remove O<sub>2</sub> from the solvent because this can lead to a broadening of the resonance. Even in a well-formed glass, one cannot usually detect hyperfine splittings smaller than 3 or 4 gauss.

Line widths are altered considerably by chemical exchange processes. This effect can also be reduced by dilution. If the exchange occurs between equivalent paramagnetic species, the lines broaden at the base and become narrower at the center. When exchange involves dissimilar ions, the resonances of the separate lines merge to produce a single line, which may be broad or narrow depending upon the exchange rate. Such an effect is observed for CuSO<sub>4</sub> · 5H<sub>2</sub>O which has two distinct copper sites per unit cell.

#### **Zerofield Splitting :**

Transition metal systems are rich in information arising from metal hyperfine coupling and zero-field splitting. Fig.3.21 illustrates the rich cobalt hyperfine interaction in Co<sub>3</sub>(CO)<sub>9</sub>Se. The spin hamiltonian for a single nucleus with spin  $I$  and a single effective electronic spin  $S$  can be written to include these extra effects as

$$\hat{H} = \beta \bar{H} \cdot \hat{g} \cdot \hat{S} + \hat{D} \cdot \hat{S} + h_S \cdot \hat{A} \cdot \hat{I} - g_N \beta_N \bar{H} \cdot \hat{I}$$

In the previous section, we discussed the  $\beta \bar{H} \cdot \hat{g} \cdot \hat{S}$  term and the complications introduced by orbital contributions. The next term incorporates the zero-field effects previously described by the dipolar tensor, D, which has a zero trace. The last two terms arise when  $I \neq 0$ .

In transition metal ion systems, this term is employed to describe any effect that removes the spin degeneracy, including dipolar interactions and spin-orbital splitting. A low symmetry crystal field often gives rise to a large zero-field effect.

In an axially symmetric field (i.e. tetragonal or trigonal), the epr spin Hamiltonian that can be used to fit the observed spectra for effective spin systems lower than quartet takes the form.

$$\hat{H}_{spin} = D \left[ \hat{S}_z^2 - \frac{1}{3} S(S+1) \right] + g_1 \beta \hat{H}_z \hat{S}_z + g_1 \beta (\hat{H}_x \hat{S}_x + \hat{H}_y \hat{S}_y) + A \hat{S}_z \hat{I}_z + A_1 (\hat{S}_x \hat{I}_x + \hat{S}_y \hat{I}_y) + Q \left[ \hat{I}_z^2 - \frac{1}{3} I(I+1) \right] - \gamma \beta_N \hat{H}_0 \cdot \hat{I}$$

The first term describes the zero-field splitting, the next two terms describe the effect of the magnetic field on the spin multiplicity remaining after zero-field splitting, the terms in A and  $A_1$  measure the hyperfine splitting parallel and perpendicular to the main axis, and Q measures the small changes in the spectrum produced by the nuclear quadrupole interaction. All of these effects have been discussed previously. The final term takes into account the fact that the nuclear magnetic moment  $\mu_N$  can interact directly with the external field  $\mu_N H_0 = \gamma \beta_N H_0 \cdot \hat{I}$ , where  $\gamma$  is the nuclear magnetogyric ratio and  $\beta_N$  is the nuclear Bohr magneton. This is the nuclear Zeeman effect, which gave rise to transitions in nmr. This interaction can affect the paramagnetic resonance spectrum only when the unpaired electrons are coupled to the nucleus by nuclear hyperfine or quadrupole interactions. Even when such coupling occurs, the effect is usually negligible in comparison with the other terms.

In the case of distortion of lower symmetry, there are three different components  $g_x$ ,  $g_y$  and  $g_z$  and three different hyperfine interaction constants  $A_x$ ,  $A_y$ , and  $A_z$ . Two additional terms need to be included:  $E (\hat{S}_x^2 - \hat{S}_y^2)$  as an additional zero - field splitting and

$Q(I_x^2 - I_y^2)$  as a further quadrupole interaction. The symbols P and P' are often used in place of Q' and Q'', respectively.

The importance of the spin Hamiltonian is that it provides a standard phenomenological way in which the epr spectrum can be described in terms of a small number of constants. Once values for the constants have been determined from experiment, calculations relating these parameters to the electronic configurations and the energy states of the ion are often possible.

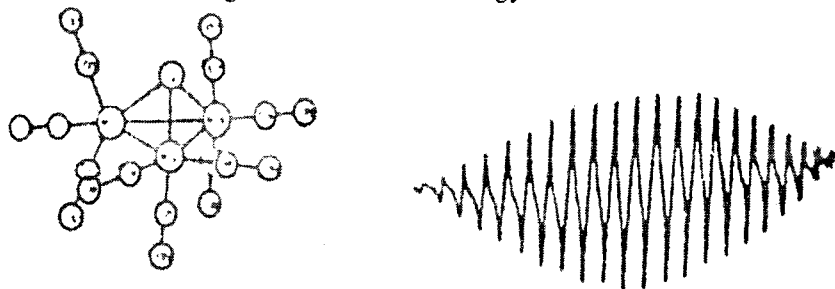


Figure 3.21 (A) Basic molecular geometry of the  $\text{Co}_3(\text{CO})_9\text{Se}$  Complex. (B) The epr spectrum of a single crystal of  $\text{Fe Co}_2(\text{CO})_9 \text{Se}$  doped with about 0.5% of paramagnetic  $\text{Co}_3(\text{CO})_9\text{Se}$ . This spectrum containing 22 hyperfine components was recorded at 77K with the molecular threefold axis parallel to the magnetic field direction.

The splitting of the  $^6\text{S}$  state of an octahedral manganese (II) complex is illustrated in Fig-13-10(A). Here we have the interesting Fig. 3.22 case in which  $\text{O}_h \text{Mn}^{2+}$  has a  $6\text{A}_{1g}$  ground state, which is split by zero-field effects.

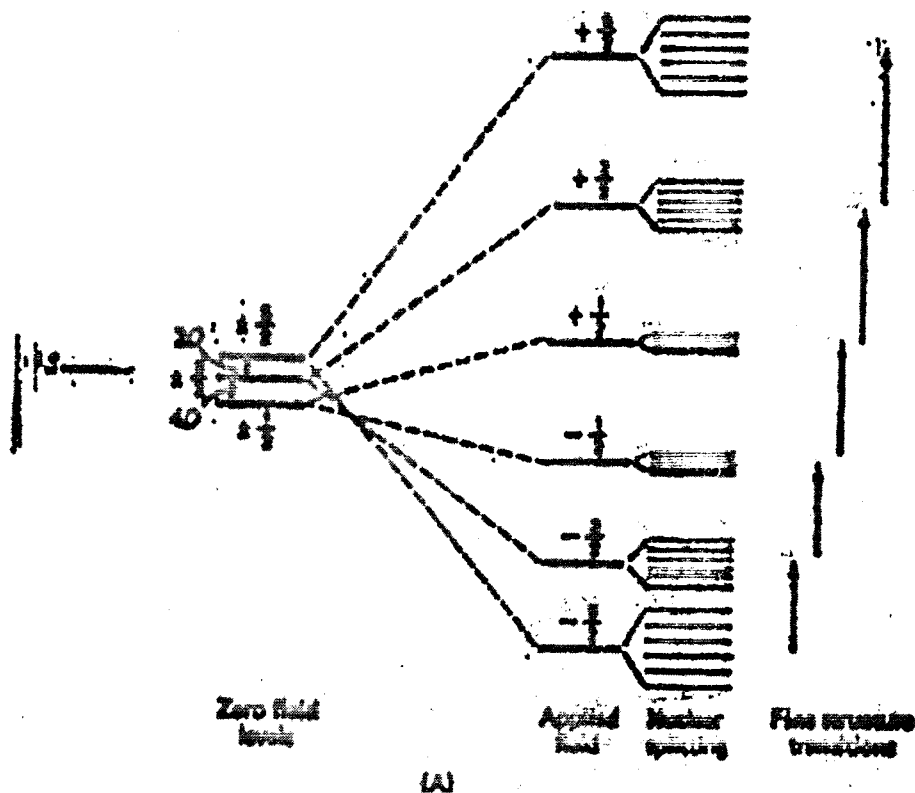


Fig 3.22 (A) Splitting of the levels in an octahedral Mn(II) spectrum

Spin-orbit coupling mixes into the ground state excited  ${}^4T_2$  states that are split by the crystal field, and this mixing gives rise to a small zero-field splitting in  $Mn^{2+}$ . The dipolar interaction of the electron spins is small in comparison to the higher state mixing in this complex. The orbital effects are very interesting in this example because the ground state is  ${}^6S$ , and thus the excited  ${}^4T_2$  state can only be mixed in by second order spin-orbit effects. Thus, the zero-field splitting is relatively small, for example, of the order of  $0.5\text{ cm}^{-1}$  in certain manganese (II) porphyrins. As indicated in Fig. 3.22A, the zero-field splitting produces three doubly degenerate spin states,  $M_S = \pm 5/2, \pm 3/2, \pm 1/2$ , (Kramers' degeneracy). Each of these is split into two singlets by the applied field, producing six levels. As a result of this splitting, five transitions ( $-5/2 \rightarrow -3/2, -3/2 \rightarrow -1/2, -1/2 \rightarrow 1/2, 1/2 \rightarrow 3/2, 3/2 \rightarrow 5/2$ ) are expected. The spectrum is further split by the nuclear hyperfine interaction with the manganese nucleus ( $I = 5/2$ ). This would give rise to thirty peaks in the spectrum.

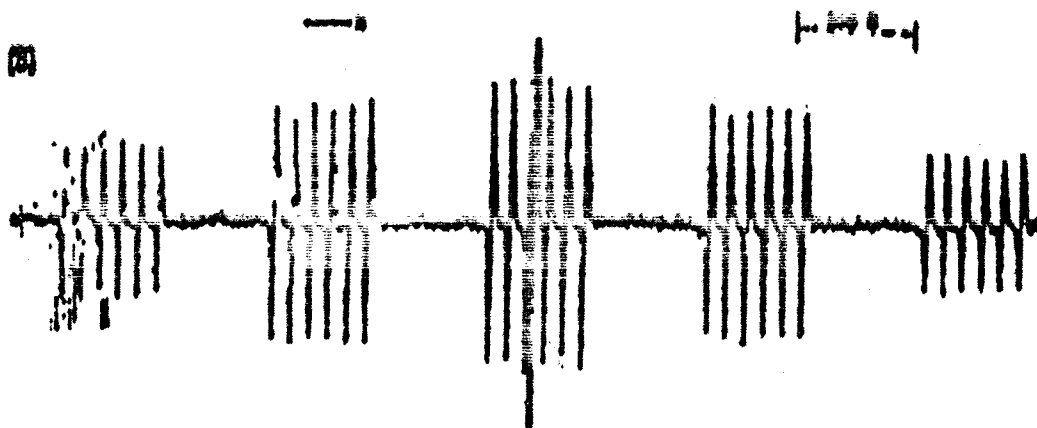


Fig. 3.22B (B) Spectrum of a single crystal of  $Mn^{2+}$  doped into  $MgV_2O_6$ , showing the five allowed transitions (fine structure), each split by the manganese nucleus

( $I = 5/2$ ) (hyperfine structure). At 300K,  $g_x = 2.0042 \pm 0.0005$ ,

$$g_y = 2.0092 \pm 0.001, \text{ and } g_z = 2.0005 \pm 0.0005,$$

$$A_x = A_y = A_z = -78 \pm 5G; \text{ and } D_x = 218 \pm 5G, D_y = -87 \pm 5G \text{ and } D_z = -306 \pm 20G.$$

[Modified from H.N Ng and C. Calvo, *Can. J. Chem.*, 50, 3619 (1972). Reproduced by permission of the National Research Council of Canada]

In contrast to hyperfine splitting, the term fine splitting is used when an absorption band is split because of non-degeneracy arising from zero-field splitting. Components of fine splitting have varying intensities: the intensity is greatest for the central lines and smallest for the outermost lines. In simple cases, the separation between lines varies as  $3 \cos^2 \theta$

- 1, where  $\theta$  is again the angle between the direction of the field and the molecular z-axis.

In Fig. 3.23, the influence of zero-field splitting on an  $S = 1$  system is indicated for a fixed molecular orientation. In the absence of zero-field effects, the two  $[\Delta m_s] = 1$  transitions are degenerate and only one peak would result.

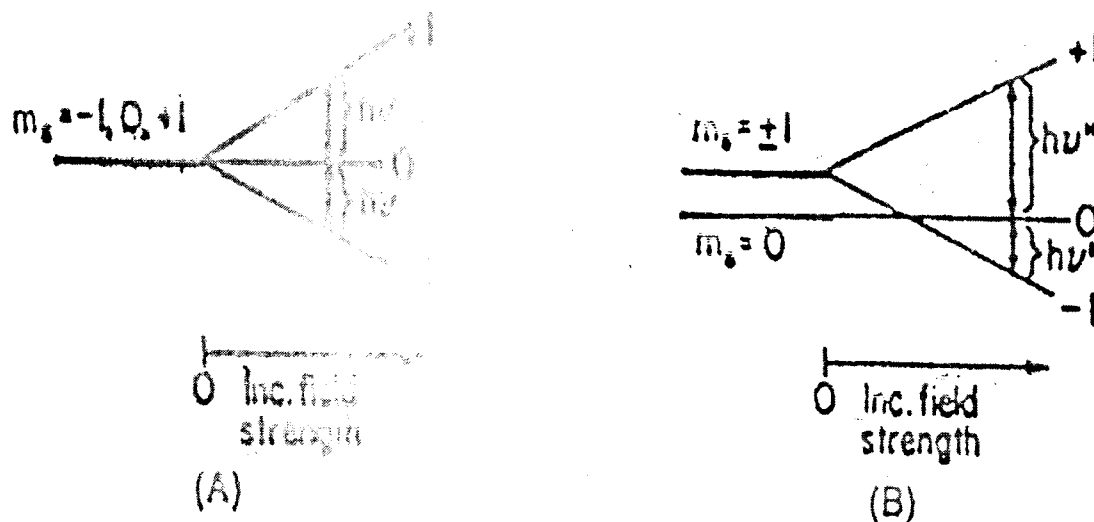


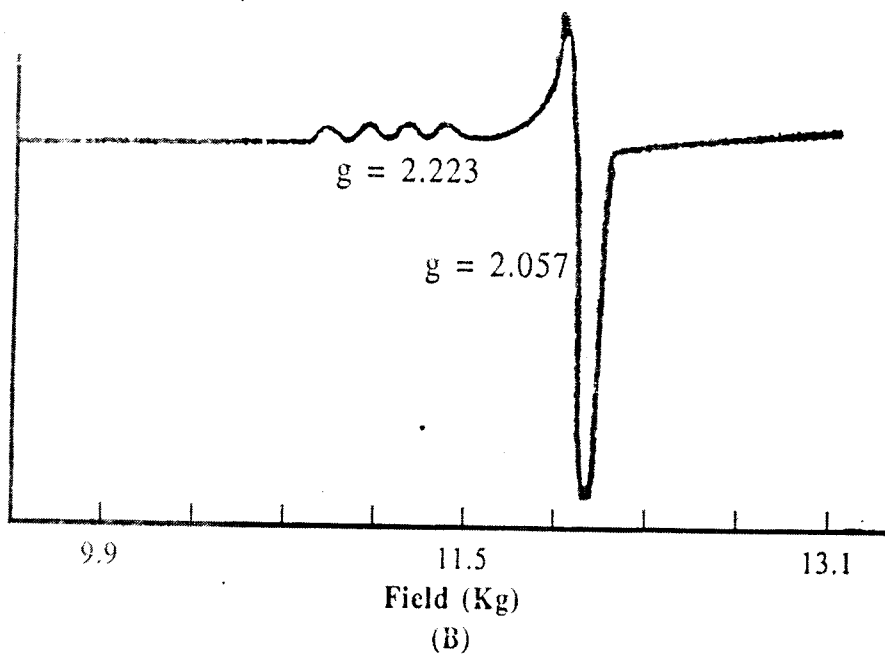
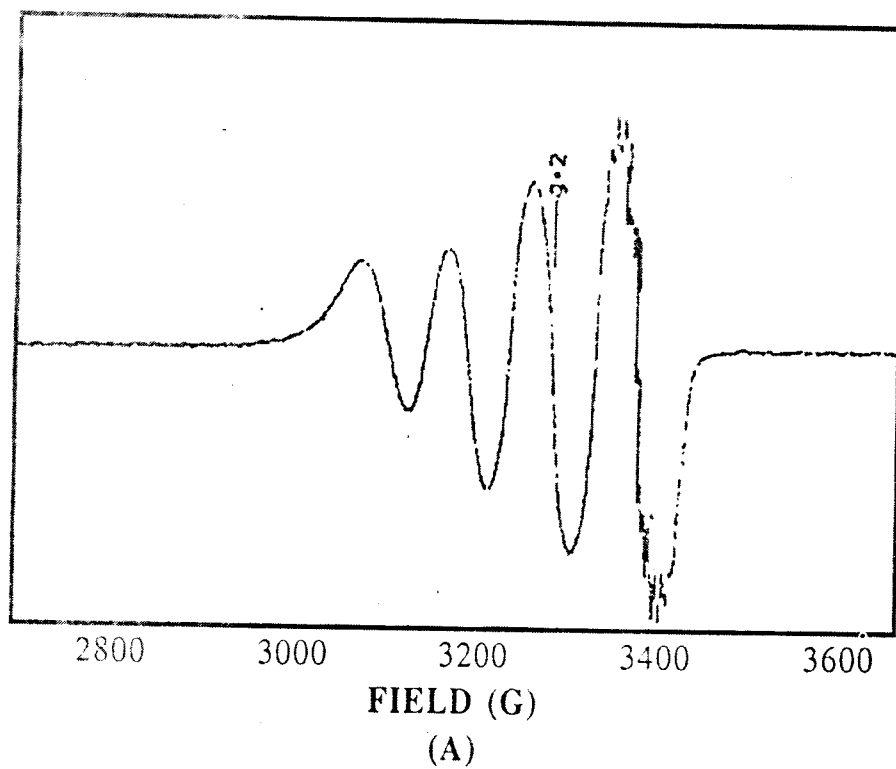
Fig. 3.23 The energy level diagram and transitions for a molecule or ion with  $S = 1$ , (A) in the absence of and (B) in the presence of zero-field splitting. The system in (B) is aligned with the z-axis, for the effect is very anisotropic.

For the splitting shown in Fig. 13-11(B), two transitions would be observed in the spectrum. A specific example of this type of system is the  ${}^3A_{2g}$  ground state of nickel (II) in an  $O_h$  field. Spin-orbit coupling mixes in excited states, which split the  ${}^3A_{2g}$  configuration. Recall that zero-field splitting is very anisotropic, providing a relaxation mechanism for the electron spin state. Accordingly, epr spectra of Ni (II)  $O_h$  complexes are difficult to detect, and when they are studied liquid nitrogen or helium temperature must generally be employed. At room temperature, nmr spectra can be measured. In some systems, sharp double quantum transitions ( $|\Delta m_s| = 2$ ) can be seen in the epr spectrum.

#### Application of EPR in the study of J.T. Distortion in Cu(II) complexes.

The  $d^9$  configuration has been very extensively studied. In an octahedral field, the ground state is  ${}^2E_g$ . A large Jahn-Teller effect is expected, making observation of the epr spectrum at room temperature possible. In tetragonal complexes, the ground state is  $d_{x^2-y^2}$  (x- and y-axes point at the ligands) and sharp lines result. Note that the quadrupolar

interaction of the copper nucleus can be determined from this experiment. The epr results fit the spin Hamiltonian.



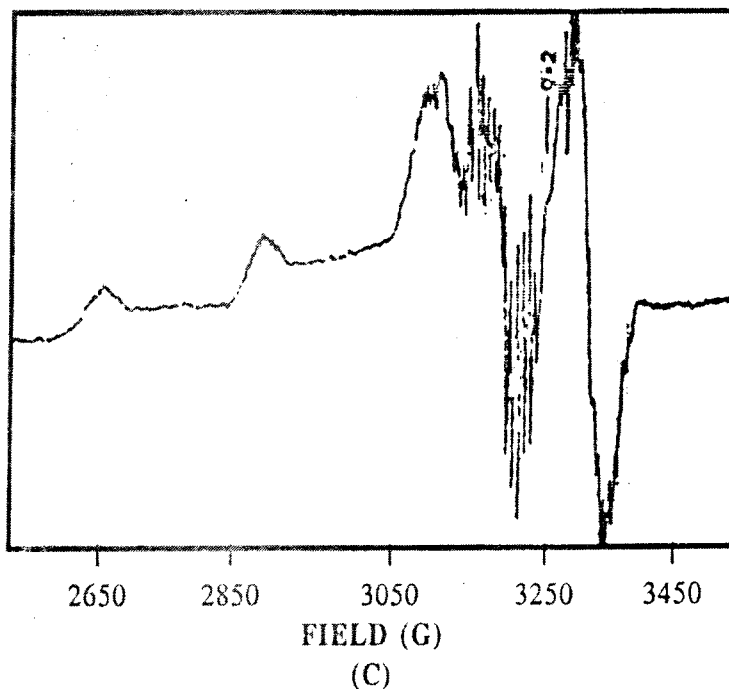


Fig.3.24 "Typical" epr spectra for copper (II) complexes. (A) A typical solution spectrum for a square planar Schiff base ligand. [From E.Hasty, T.J. Colburn, and D.N.Hendrickson, *Inorg. Chem.* 12, 2414 (1973). (B) Glass or powder sample run at Q-band frequencies on an axial complex (C) Glass or doped powder spectrum of the complex in (A) run at at X-band frequencies.

Some typical copper (II) spectra are shown in Fig. 13.24. In (A), an isotropic solution spectrum is shown. Both nitrogen and proton ligand hyperfine structures are seen on the high field peak, but not on the low field peaks. This is attributed to differences in the relaxation times for the transition, which depend upon the  $m_l$  value associated with the transition. The solvent employed influences the molecular correlation time, which in turn also influences the spectral appearance.

In (B), an anisotropic spectrum is shown at Q-band frequencies. Such spectra are observed in glass or powder samples of copper complexes diluted in hosts. The low field  $g_1$  and high field  $g_1$  peaks are well separated. With the higher microwave energy, the individual peaks are broader so the super-hyperfine splitting is not detected on the  $g_1$  peak. In the spectrum in (C), at X - band frequencies, the  $g_1$  and  $g_1$  transitions overlap, but much more ligand hyperfine structure is detected. As mentioned earlier, the temperature dependence of the spectra of many copper (II) systems has been interpreted in terms of Jahn-Teller effects.

## UNIT - IV

### INSTRUMENTAL ANALYTICAL TECHNIQUES

#### Beer-Lambert's Law :

The radiant power of a beam of radiation is proportional to the number of photons per unit time. Absorption occurs when a photon collides with a molecule and raises that molecule to some excited state. Each molecule can be thought of as having a cross-sectional area for photon capture, and photons must pass within this area to interact with the molecule. The cross-sectional area varies with wavelength and represents, in effect, a probability that photons will be captured by any given molecule. The rate of absorption as a beam of photons passes through a medium depends on the number of photon collisions with absorbing atoms or molecules per unit time. If the number of absorbing molecules is doubled, by doubling either the length of the path of radiation through the medium or the concentration of absorbing species, the rate of absorption of photons doubles. Likewise, doubling the beam power doubles the number of photons that pass through the medium in unit time and doubles the number of collisions with absorbing molecules in unit time when the number of absorbing molecules remains constant.

If a parallel beam of monochromatic radiation of radiant power,  $P_0$ , traverses an infinitesimally small distance,  $dx$ , of an absorber, the decrease in power,  $-dp$ , is given by equation 1, since the number of absorbing species is proportional to the thickness but is independent of  $P$  :

$$-dp = k'P dx \quad \dots (1)$$

The proportionality constant  $k$ , depends on the wavelength of the radiation. The concentration,  $C$ , is assumed constant. Separating the variables in equation (1) gives which is a mathematical statement of the fact that the radiant

$$\frac{-dp}{P} = -d(\ln P) = k'dx \quad \dots (2)$$

power absorbed is proportional to the thickness traversed. Now if it is stipulated that  $P_0$  is the radiant power of the transmitted (unabsorbed) radiation that emerges from the absorbing medium at  $x = b$ , Equation 2 can be integrated along the entire path :

$$-\int_{P_0}^P d \ln P = k' \int_0^b dx \quad \dots (3)$$

obtaining

$$\ln P_0 - \ln P = \ln \left( \frac{P_0}{P} \right) = k'b \quad \dots (4)$$

Equation 4 is known as Lambert's law (or Bouguer's law, since Bouguer really established this relationship several years before Lambert, but Bouguer's publication was not generally known) and states simply that, for parallel, monochromatic radiation that passes through an absorber of constant concentration, the radiant power decreases logarithmically as the path length increases arithmetically.

The dependence of radiant power on the concentration of absorbing species can be developed in a parallel manner if the wavelength and the distance traversed by the beam in the sample remain constant. In this case the number of absorbing molecules that collide with photons is proportional to the concentration,  $C$ . Thus,

$$-dp = k''P dC \quad \dots \quad (5)$$

and separation of variables followed by integration from  $C = 0$  to  $C = C$  yields

$$\ln \frac{P_0}{P} = k'' C \quad \dots \quad (6)$$

This relationship is known as Beer's law. If both concentration and thickness are variable, the combined Lambert-Beer law (often known simply as Beer's law) becomes

$$\ln \frac{P_0}{P} = kbC \quad (7)$$

Replacing natural logarithms by base -10 logarithms and calling the new constant  $a$  in accordance with accepted practice give

$$\log \frac{P_0}{P} = abC \quad \dots \quad (8)$$

Absorbance,  $A$ , is defined as

$$A = \log \frac{P_0}{P} = abC \quad \dots \quad (9)$$

Transmittance  $T$ , is defined as.

$$T = \frac{P}{P_0} \quad \dots \quad (10)$$

So that

$$A = \log \frac{1}{T} = -\log T \quad (11)$$

Percent transmittance is merely  $100T$

The proportionality constant  $a$  in Equations 8 and 9 is known as the absorptivity if  $C$  is given in grams of absorbing material per liter and 'b' is in centimeters; therefore, 'a' has the

units liter g<sup>-1</sup> cm<sup>-1</sup>. If concentration is expressed in molar concentration and 'b' is in centimeters, the proportionality constant is called the molar absorptivity and is designated as ε. Thus the Lambert-Beer law can also be written as

$$A = \log \frac{P_0}{P} = \epsilon bC \quad \dots \dots (12)$$

where ε is in units of liter mole<sup>-1</sup> cm<sup>-1</sup>.

As radiation passes through a cell (reference of sample), some radiation is reflected at each surface where there is a change in the refractive index. Instead of measuring P<sub>0</sub> as the radiant power that impinges on the cell, reflection losses can be almost entirely compensated by taking P<sub>0</sub> as the radiant power transmitted through a cell that contains only pure solvent. The sample to be measured should be placed in a cell as nearly identical as possible. Cells should be free of scratches, dirt, and fingerprints, all of which scatter radiation. Turbidities in the solvent or the sample also scatter radiation.

A plot of absorbance versus concentration should be a straight line passing through the origin, as shown as in Fig 1 Readout scales and meter scales on spectrophotometers are usually calibrated to read absorbance as well as transmittance.

Absorption of radiation by molecules at specific wavelengths is frequently used for quantitative analyses owing to the direct relationship between absorbance and concentration described earlier. The sensitivity of spectrometric analysis is dictated by the magnitude of the absorptivity and the minimum absorbance that can be measured with required degree of certainty.

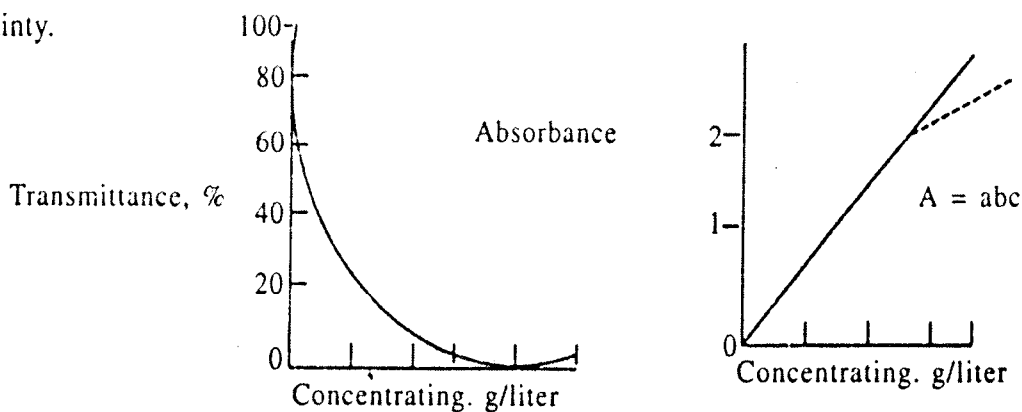


Fig. 4.1 Representation of Beer's law and Comparison between scales in Absorbance and Transmittance

### Principle and Applications of colourimetry

The basic principle of colourimetric measurements consists of comparing the colour intensity produced by the unknown amount of the substance with the colour intensity produced by a known amount of the same substance under the same conditions. For this several experimental methods are available.

**Standard Series Method :** In this method special tubes called Nessler tubes are used. These are colourless glass tubes of uniform cross-section with flat bottoms. These are available in different capacities (50 ml, 100 ml, etc). The solution of the substance being determined is taken in a Nessler tube. The colour is developed by the addition of a suitable reagent, if the substance is not coloured. The solution is made up to a definite volume and mixed thoroughly. The colour is compared with those of a series of standards prepared in the same way from known amounts of the substances being determined. For the comparison of colours, the Nessler tubes are arranged adjacent to one another in a wooden rack provided with an inclined reflector which reflects light up through the tubes. The colours are compared by looking vertically down through the Nessler tubes. The concentration of the unknown is equal to that of the known solution whose colour it matches exactly. Nessler tube is shown in Fig. 4.2

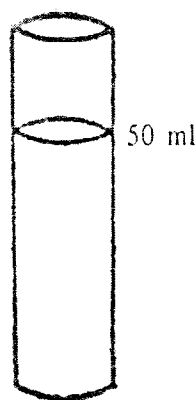


Fig. 4.2 Nessler Tube

**Colorimetric Titration :** In this method a known volume of the test solution is taken in a Nessler tube, the colour is developed by the addition of the reagent and the solution is made up to a definite volume, say 50 ml. In another tube almost an equivalent quantity of water (slightly less) is taken together with the reagent. A solution containing the known amount of the substance being determined is run into this Nessler tube from a burette till the colours produced in the two tubes match. Since the volumes of the solution in the two Nessler tubes will be different, several determinations should be carried out by adjusting the volume of water taken initially in the blank. This method cannot be used where the substance to be determined requires a preliminary treatment before the colour nickel solution has to be pre-treated with bromine water and therefore the titrimetric method cannot be used.

**Duboscq Colorimeter :**

This method is also based on visual colour comparisons. Light from a source in the base of the instrument passes through the windows in the base through the solutions whose colours are to be compared. The solutions are taken in two cups provided for them. On looking

through the eyepiece, a circular field is visible, light from one cup illuminating one half and light the second cup illuminating the other half of the field. The pathlength for the two cups can be changed by adjusting the positions of what are called plungers or the cups. This is done till the two halves of the field are identical in their intensity. The Dubosecq colorimeter is shown in Fig. 4.3, Applying the fundamental principle of colorimetry, we get

$$c_1 l_1 = c_2 l_2$$

$$c_2 = c_1 l_1 / l_2$$

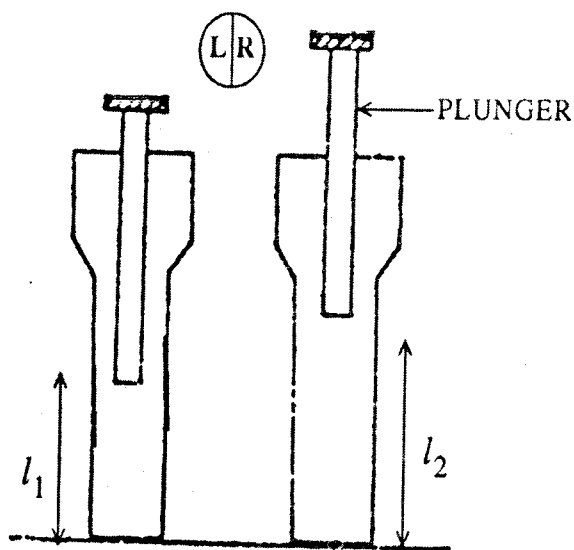


Fig. 4.3 The Duboscq Colorimeter

#### Photoelectric colorimeter :

Progress in the development of colorimetric methods has resulted largely from application of the photoelectric cell to the problem of colour measurement. This improvement has eliminated the difficulties which generally complicate visual comparisons. A photoelectric colorimeter makes use of a light-sensitive device like photomissive cell. A photoemissive cell (also called phototube) makes use of a cathode which emits electrons when illuminated. The emission of electrons causes a current to flow through an outside circuit. This current may be amplified and taken as a measure of the intensity of light striking the photosensitive substance.

A number of commercial photoelectric colorimeters are available. These essentially consist of a light source, a light filter, a container for the solution, a photocell to receive the transmitted light and a device to measure the current produced in the photocell. A schematic diagram of the set up is given in Fig. 4.4

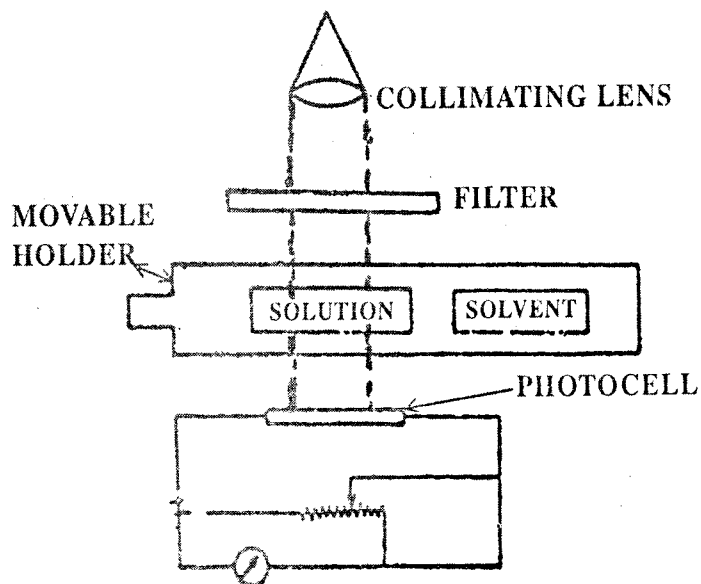


Fig. 4.4 Photoelectric colorimeter

Filters consist of coloured glass or glass coated with coloured gellatin. These transmit light from a narrow region of the spectrum, absorbing at the same time other components. Use of an appropriate filter increases the sensitivity of measurements.

Using a sliding sample carriage either the reference solution or the pure solvent taken in small cells can be brought into position, i.e., across the path of the light. The current measurements are made using a sensitive microammeter calibrated in percentage transmission and optical density. After adjusting the percentage transmittance of pure solvent to a value of 100 using a rheostat, readings are taken on the scale for the solution

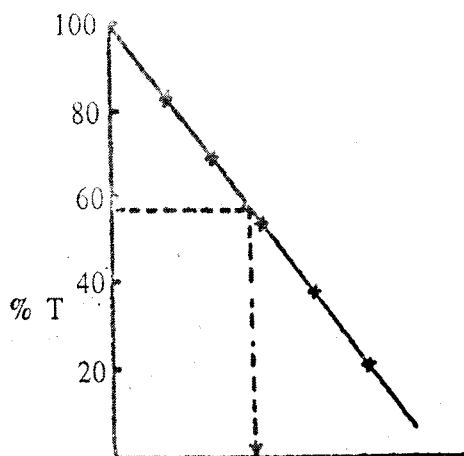


Fig. 4.5 Transmittance versus concentration plot.

Standard solutions of different concentrations, preferably in the range of the unknown, are prepared and for each one of these solutions the transmittance is measured. A plot of transmittance versus concentration is drawn. From the graph, the concentration of the unknown solution can be found, using the value of transmittance.

### **Spectrophotometers :**

With spectrophotometers, it is possible to measure optical density or transmittance at a specific wavelength. In principle these can be used to measure absorption even if the absorption takes place in a region other than visible, say, uv or ir. Most of the spectrophotometers cover the range 200-800 nm, i.e., the uv and visible regions. Many commercial models are available. The main parts of a spectrophotometer are an appropriate source of light (hydrogen discharge lamp for uv and tungsten lamp for visible), a prism to monochromatise light cells and a sensitive vacuum photocell detector.

### **Criteria for Satisfactory colorimetric Estimations :**

In principle, any substance that is coloured or any substance that gives a colour reaction with a reagent can be estimated colorimetrically. However, certain characteristics for the coloured system are required for reliable estimation.

**1. Stability of colour :** When a reagent has to be added to the desired constituent to produce a colour, the colour, the colour should be stable for sufficient time to permit accurate measurement. The colour may fade because of air oxidation, photochemical decomposition, effects of acidity, temperature of other conditions.

**2. Intense Colour :** This is desirable for detecting small amounts and for making accurate measurements with low concentrations.

**3. Solubility of the coloured product :** Reactions yielding a colloidal system or suspension are not desirable since a turbid solution absorbs as well as scatters light.

**4. Specificity :** The colour produced should be specific only for the desired constituent. Very few reagents are specific for a particular substance. Generally, reagents give colours for a small group of related substances. If other constituents interfere with the colour reaction, they must be removed or prevented from functioning through appropriate treatment like use of other complex-forming agents, altering of oxidation states or control of pH.

**5. Validity of Beer's Law :** For visual colorimeters, it is essential that Beer's law is strictly valid for the system, i.e., the intensity of the colour is proportional to the concentration. However, when a photoelectric colorimeter or a spectrophotometer is used for the colorimetric estimation, this is not an essential requirement. In cases where deviation is noted from Beer's law, a calibration curve connecting optical density (or transmittance) and concentration may be constructed.

**6. Sensitivity of Human Eyes :** Human eye has a maximum sensitivity in the spectral region ranging from 475 to 675 nm. If the absorption is in this region, visual comparisons would be fairly accurate.

**Advantages of colorimetric Analysis :**

1. The operations involved in the estimation are simple, especially when a photoelectric colorimeter is available.
2. This method is not time consuming. Therefore, it is ideally suited for routine work.
3. Determination of minute quantities of substances is possible.
4. The instruments / apparatus required are inexpensive.

**Fluorimetry :**

**1. General Discussion :** Fluorescence is caused by the absorption of radiant energy and the re-emission of some of this energy in the form of visible light. The light emitted is almost always of higher wavelength than that absorbed. In true fluorescence the absorption and emission takes place in a short but measurable time – of the order of  $10^{-12}$  -  $10^{-9}$  second. If the light is emitted with a time delay ( $>10^{-8}$  second) the phenomenon is known as phosphorescence; this time delay may range from a fraction of a second to several weeks, so that the difference between the two phenomena may be regarded as one of degree only. Both fluorescence and phosphorescence are designated by the term photoluminescence; the later is therefore the general term applied to the process of absorption and re-emission of light energy.

Relationship between intensity of fluorescence and concentration. The Beer-Lambert law applies to the intensity of radiation transmitted by a substance or solution; since fluorescent radiation is that emitted by a substance, the law cannot be applied directly. The following relationship has been developed :

$$F = K (I_0 - I) \quad \dots \quad (1)$$

Where  $I_0$  = intensity of incident radiant energy;

$I$  = intensity of transmitted radiant energy;

$F$  = intensity of fluorescent radiant energy; and

$K$  = a proportionality constant.

$F$  is assumed proportional to the intensity of the radiant energy absorbed ( $I_0 - I$ ).

Applying the Beer-Lambert law.

$$I = I_0 \cdot 10^{-dc} \quad \dots \quad (2)$$

$$\text{and } I_0 - I = I_0 (1 - 10^{-dc}) \quad \dots \quad (3)$$

$$\text{we have } F = KI_0 (1 - 10^{-dc}) \quad \dots \quad (4)$$

Writing  $KI_0 = F_0 \dots (5)$

$F = F_0 - F_0 \cdot 10^{-dc} \dots (6)$

or  $\log \frac{F_0}{F_0 - F} = dc \dots (7)$

In these equations, K is the fraction of the incident radiation that is absorbed (this is determined by such factors as the dimensions of the light beam, the area of the solution irradiated, the transmission band of the filter before the photocell, and the spectral response of the photocell),  $\epsilon$  is the molar absorption coefficient and is dependent upon the substance, l is the thickness of the solution in the cell, and c is the molar concentration of the fluorescent substance.

When  $\epsilon cl$  becomes small and approaches a value of 0.01 or less, equation (4) reduces to : \*

$F = 2.303 Kl_0 \cdot \epsilon \cdot cl \dots (8)$

or  $F = K'C \dots (9)$

i.e., the fluorescent intensity is practically proportional to the concentration of the fluorescent substance provided  $cl \leq 0.01 \epsilon$  K' is an over all constant for one particular substance in a given instrument. In practice, equation (8) holds up to a few parts per million : at higher concentrations the fluorescence-concentration curve will bend towards the concentration axis.

Factors, such as dissociation, association, or salvation, which would vitiate the Beer-Laembert law, would be expected to have a similar effect in fluorescence. Any material that causes the intensity of fluorescence to be less than the expected value given by equation (8) is known as a quencher, and the effect is termed quenching; it is normally caused by the presence of foreign ions or molecules. Fluorescence is affected by the pH of the solution, by the nature of the solvent, the concentration of the reagent which is added in the determination of inorganic ions, and, in some cases by temperature. The time taken to reach the maximum intensity of fluorescence varies considerably with the reaction.

### Some Applications of Fluorimetry :

Fluorimetry is generally used if there is no colorimetric method sufficiently sensitive or selective for the substance to be determined. In inorganic chemistry the most frequent applications are for the determination of metal ions as fluorescent organic complexes, although uranium compounds fluoresce with a brilliant yellow colour. Uranium may be determined by measuring the fluorescence of a bead produced by fusing the substance with a mixture of sodium carbonate and sodium fluoride. Many of the complexes of oxine fluoresce strongly: aluminium, zinc, magnesium, and gallium are sometimes determined at low concentrations by this method, Aluminium forms fluorescent complexes with the dyestuff Eriochrome Blue

Black RC (Pontachrome Blue Black R), while beryllium forms a fluorescent complex with quinizarin.

Important applications are to the determination of quinine and the vitamins riboflavin (vitamin B<sub>2</sub>) and thiamine (Vitamin B<sub>1</sub>). Riboflavin fluoresces in aqueous solution; thiamine must first be oxidized with alkaline hexacyanoferrate (III) solution to thiochrome, which gives a blue fluorescence in butanol solution.

The intensity and colour of the fluorescence of many substances depend upon the pH of the solution; indeed, some substances are so sensitive to pH that they can be used as pH indicators. These are termed fluorescent or luminescent indicators. Those substances which fluoresce in ultraviolet light and change in colour or have their fluorescence quenched with change in pH can be used as fluorescent indicators in acid - base titrations. The merit of such indicators is that they can be employed in the titration of coloured (and sometimes of intensely coloured) solutions in which the colour changes of the usual indicators would be masked. Titrations are best performed in a silica flask. Examples of fluorescent indicators are given in Table 4.1

Table - 4.1 Some Fluorescent Indicators

Name of Indicator	Approx pH range	Colour change
Acridine	5.2 - 6.6	Green to violet - blue
Chromotropic acid	3.0 - 4.5	Colourless to blue
2-Hydroxycinnamic acid	7.2 - 9.0	Colourless to green
3, 6-Dihydroxyphthalimide	0.0 - 2.5	Colourless to yellowish - green
	6.0 - 8.0	yellowish-green to green
Erosin	3.0 - 4.0	Colourless to green
Erythrosin-B	2.5 - 4.0	Colourless to green
Fluorescein	4.0 - 6.0	Colourless to green
4-Methyl-aesculetin	4.0 - 6.2	Colourless to green
	9.0 - 10.0	Blue to light green
2-Naphthoquinoline	4.4 - 6.3	Blue to colourless
Quinine sulphate	3.0 - 5.0	Blue to violet
	9.5 - 10.0	Violet to Colourless
Quininic acid	4.0 - 5.0	Yellow to blue
Umbelliferone	6.5 - 8.0	Faint blue to bright blue

#### Flame - Photometry

Consider the simplified energy level diagram shown in Fig. 4.6. Where E<sub>0</sub> represents the ground state in which the electron of a given atom are at their lowest energy level and E<sub>1</sub>, E<sub>2</sub>, E<sub>3</sub>, etc. represent higher or excited energy levels.

Transitions between two quantized energy levels, say from E<sub>0</sub> to E<sub>1</sub>, correspond to the absorption of radiant energy, and the amount of energy absorbed ( $\Delta E$ ) is determined by Bohr's equation.

$$\Delta E = E_1 - E_0 = h\nu = hc/\lambda$$

Where  $c$  is the velocity of light,  $h$  is Planck's constant, and  $\nu$  is the frequency and  $\lambda$  the wavelength of the radiation absorbed. Clearly, the transition from  $E_1$  to  $E_0$  corresponds to the emission of radiation of frequency  $\nu$ .

Since an atom of a given element gives rise to a definite, characteristic line spectrum, it follows that there are different excitation states associated with different elements. The consequent emission spectra involve not only transitions from excited states to the ground state, e.g.,  $E_3$  to  $E_0$ ,  $E_2$  to  $E_0$ , but also transitions such as  $E_3$  to  $E_2$ ,  $E_3$  to  $E_1$  etc. Thus it follows that the emission spectrum of a radiation by already excited states to occur e.g.,  $E_1$  to  $E_2$ ,  $E_2$  to  $E_3$ , etc., but in practice the ratio of excited to ground state atoms is extremely small, and thus the absorption spectrum of a given element is usually only associated with transitions from the ground state to higher energy states and is consequently much simpler in character than the emission spectrum.

The relationship between the ground state and excited state populations is given by the Boltzmann equation.

$$N_1/N_0 = (g_1/g_0)e^{-DE/kT}$$

where  $N_1$  = number of atoms in the excited state,

$N_0$  = number of ground state atoms,

$g_1/g_0$  = ratio of statistical weights for ground and excited states,

$DE$  = energy of excitation =  $h\nu$ ,

$k$  = Boltzmann constant,

$T$  = the temperature of Kelvin

It can be seen from this equation that the ratio  $N_1/N_0$  is dependent upon both the excitation energy  $\Delta E$  and the temperature  $T$ . An increase in temperature and a decrease in  $\Delta E$  (i.e. when dealing with transitions which occur at longer wavelength) will both result in a higher value for the ratio  $N_1/N_0$ .

Calculation shows that only a small fraction of the atoms are excited, even under the most favourable conditions, i.e. when the temperatures is high and the excitation energy low. This is illustrated by the data Table, 4.2 for some typical resonance lines.

Table - 4.2 Variation of atomic excitation with wavelength and with temperature

Element	Wavelength (nm)	$N_1/N_0$	
		2000 K	4000 K
Na	589.0	$9.86 \times 10^{-6}$	$4.44 \times 10^{-3}$
Ca	422.7	$1.21 \times 10^{-7}$	$6.03 \times 10^{-4}$
Zn	213.9	$7.31 \times 10^{-15}$	$1.48 \times 10^{-7}$

Since as already explained the absorption spectra of most elements are simple in character as compared with the emission spectra, it follows that atomic absorption spectroscopy is less prone to inter-element interferences than is flame emission spectroscopy. Further, in view of the high proportion of ground state to excited atoms, it would appear that atomic absorption spectroscopy should also be more sensitive than flame emission spectroscopy. However, in this respect the wavelength of the resonance line is a critical factor, and elements whose resonance lines are associated with relatively low energy values are more sensitive as far as flame emission spectroscopy is concerned than those whose resonance lines are associated with higher energy values. Thus sodium with an emission line of wavelength 589.0 nm shows great sensitivity in flame emission spectroscopy, whereas zinc (emission line wavelength 213.9 nm) is relatively insensitive.

The integrated absorption is given by the expression

$$Kd\nu = fN_0(\pi e^2 / mc)$$

Where K is the absorption coefficient at frequency  $\nu$ ,

e is the electronic charge,

m the mass of an electron,

c the velocity of light,

f the oscillator strength of the absorbing line (this is inversely proportional to the lifetime of the excited state).

$N_0$  is the number of metal atoms per  $\text{cm}^3$  capable of absorbing the radiation.

In this expression the only variable is  $N_0$  and it is this which governs the extent of absorption. Thus it follows that the integrated absorption coefficient is directly proportional to the concentration of the absorbing species.

It would appear that measurement of the integrated absorption coefficient should furnish an ideal method of quantitative analysis. In practice, however, the absolute measurement of the absorption coefficients of atomic spectral lines is extremely difficult. The natural line width of an atomic spectral line is about  $10^{-5}$  nm., but owing to the influence of Doppler and pressure effects, the line is broadened to about 0.002 nm at flame temperatures of 2000 - 3000 K. To measure the absorption coefficient of a line thus broadened would require a spectrometer with a resolving power of 500 000. This difficulty was overcome by Walsh, who used a source of sharp emission lines with a much smaller half width than the absorption line, and the radiation frequency of which is centred on the absorption frequency. In this way, the absorption coefficient at the centre of the line,  $K_{\text{max}}$ , may be measured. If the profile of the absorption line is assumed to be due only to Doppler broadening, then there is a relationship between  $K_{\text{max}}$  and  $N_0$ . Thus the only requirement of the spectrometer is that

it shall be capable of isolating the required resonance line from all other lines emitted by the source.

It should be noted that in atomic absorption spectroscopy, as with molecular absorption, the absorbance  $A$  is given by the logarithmic ratio of the intensity of the incident light signal  $I_0$  to that of the transmitted light  $I_t$ , i.e.,

$$A = \log I_0/I_t = KLN_0$$

where  $N_0$  is the concentration of atoms in the flame (number of atoms per  $\text{cm}^3$ );

$L$  is the path length through the flame (cm),

$K$  is a constant related to the absorption coefficient.

For small values of the absorbance, this is a linear function.

With flame emission spectroscopy, the detector response  $E$  is given by the expression.

$$E = k\alpha c,$$

Where  $k$  is related to a variety of factors including the efficiency of atomization and of self absorption.

$\alpha$  is the efficiency of atomic excitation,

$c$  is the concentration of the solution.

It follows that any electrical method of increasing  $E$ , as for example, improved amplification, will make the technique more sensitive.

The basic equation for atomic fluorescence is given by

$$F = QI_0kcs$$

Where  $Q$  is the quantum efficiency of the atomic fluorescence process,

$I_0$  is the intensity of the incident radiation,

$k$  is the constant which is governed by the efficiency of the atomization process,

$c$  is the concentration of the element concerned in the test solution.

It follows that the more powerful the radiation source, the greater will be the sensitivity of the technique.

To summarise, in both atomic absorption spectroscopy and in atomic fluorescence spectroscopy, the factors which favour production of gaseous atoms in the ground state determine the success of the techniques. In flame emission spectroscopy, there is an additional requirement, namely, the production of excited atoms in the vapour state. It should be noted that the conversion of the original solid  $MX$  into gaseous metal atoms ( $M_{\text{gas}}$ ) will be governed by a variety of factors including the rate of vapourization, flame composition and flame temperature, and further, if  $MX$  is replaced by a new solid,  $MyA$  and the formation of  $M$ , may proceed in a different manner, and with more efficiency than that observed with  $MX$ .

## Flame Emission Spectrometry and Atomic Absorption Spectrometry :

In flame emission spectrometry, the sample solution is nebulized (converted into a fine aerosol) and introduced into the flame where it is desolvated, vaporized, and atomized, all in rapid succession. Subsequently, atoms and molecules are raised to excited states via thermal collisions with the constituents of the partially burned flame gases. Upon their return to a lower or ground electronic state, the excited atoms and molecules emit radiation characteristic of the sample components. The emitted radiation passes through a monochromator that isolated the specific wavelength for the desired analysis. A photodetector measures the radiant power of the selected radiation, which is then amplified and sent to a read-out device, meter, recorder, or microcomputer system.

The radiant power of the spectral emission line that appears at frequency,  $\gamma$ ,  $L_\gamma$ , is determined by the number of atoms that simultaneously undergo the spectral transition associated with the emission line. It is given by the expression

$$P_\gamma = \frac{V \cdot A_t \cdot h \cdot \nu \cdot N_0 \cdot g_u \cdot e^{-E/kT}}{B(T)}$$

where  $V$  is the flame volume (aperture ratio) viewed by the detector,  $A_t$  is the number of transitions each excited atom undergoes per second,  $N_0$  is the number of free analyte atoms present in the electronic ground state per unit volume (which is proportional to the concentration of analyte in the sample solution nebulized),  $g_u$  is the statistical weight of the excited atomic state,  $k$  is the Boltzmann constant,  $T$  is the absolute temperature,  $B(T)$  is the partition function of the atom over all states, and  $E$  is the energy of the excited state. The above equation indicates that the higher the flame temperature, the greater the number of atoms in the excited state. The ratio of excited atoms to ground-state atoms under conditions of thermal equilibrium is given in Table for selected emission lines for some commonly determined elements.

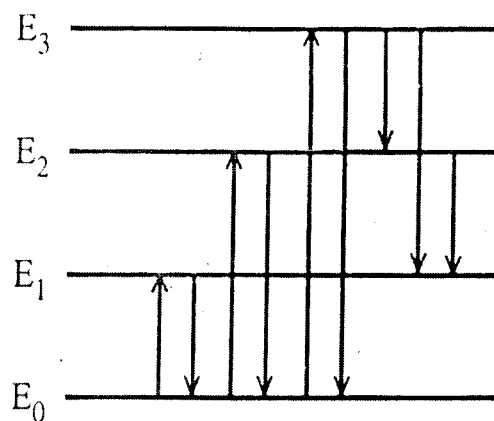


Fig. 4.6

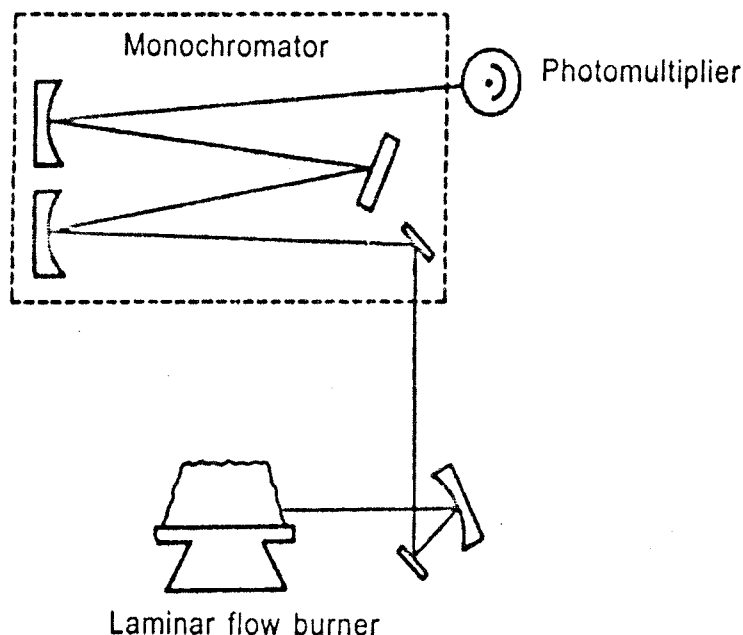
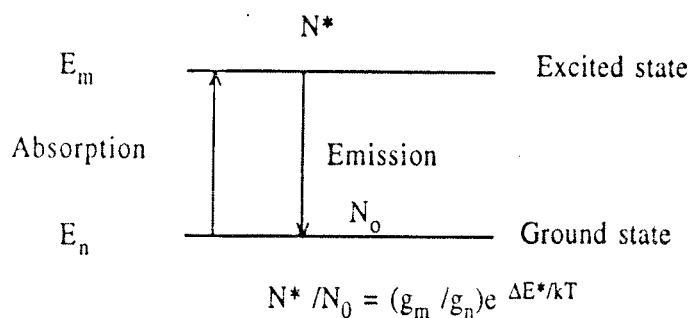


Fig. 4.7 Schematic arrangement of a flame emission spectrophotometer

Table 4.3 VALUES OF  $N^*/N_0$  FOR VARIOUS RESONANCE LINES :



Resonance line	Gm/gnΔE(in eV)	N* / no			
		2000 K	3000K		
Cs	8521	2	1.45	$4.44 \times 10^{-4}$	$7.24 \times 10^{-3}$
Na	5890	2	2.10	$9.86 \times 10^{-6}$	$5.88 \times 10^{-4}$
Ca	4227	3	2.93	$1.21 \times 10^{-7}$	$3.69 \times 10^{-5}$
Fe	3720		3.33	$2.29 \times 10^{-9}$	$1.31 \times 10^{-6}$
Cu	3248	2	3.82	$4.82 \times 10^{-10}$	$6.65 \times 10^{-7}$
Mg	2852	3	4.35	$3.35 \times 10^{-11}$	$1.50 \times 10^{-7}$
Zn	2139	3	5.80	$7.45 \times 10^{-15}$	$5.50 \times 10^{-10}$

A grating spectrometer, equipped with a laminar flow burner and a good detection-readout system, services equally well for FES and flame AAS because both require the measurement of the intensity of selected wavelengths of radiation that emerge from the flame. The wavelengths usually fall into the visible or ultraviolet region and the resulting photons are

detected by photomultiplier tubes. FES requires a monochromator capable of providing a bandpass of 0.05 nm or less in the first order. Slits should be adjustable to allow for greater radiant power for situations where high resolution is not required. Spectrometers of 0.33 – 0.5 m focal length with adjustable slits meet these requirements. The instrument should have sufficient resolution to minimize the flame background emission and to separate atomic emission lines from nearby lines and molecular fine structure. In contrast, emission band spectra from molecular species show up more clearly with instruments of low dispersion. The ability to scan a portion of a spectrum is often a desirable instrumental feature. Proper positioning of the flame to ensure sampling of the optimum flame zone is important. The best entrance optics design just fills the monochromator optics with a solid angle of radiation. At a high aperture ratio, the limit of detection is restricted, not by the shot noise of the photodetector, but by the instability of the flame and the flicker noise of emission from the matrix.

Background correction in FES can be accomplished with a dual-channel instrument. One channel is turned to the emission line of the analyte and the other is set to a nearby wavelength where analyte emission is not observed, but where background emission from the flame or continuum is measured. The analytical signal is the difference in the intensities from the two wavelengths. The Zeeman method of correction can also be applied to FES measurements.

#### **Atomic Absorption Spectrometry :**

The absorption of radiation by atoms in the sun's atmosphere was first observed in 1814. However, it was only in 1953 that an Australian physicist, Alan Walsh, demonstrated that atomic absorption could be used as a quantitative analytical tool in the chemical laboratory. Today AAS is one of the most widely used methods in analytical chemistry.

The AAS phenomenon can be divided into two major processes : (1) the production of free atoms from the sample and (2) the absorption of radiation from an external source by these atoms. The conversion of analytes in solution to free atoms in the flame was discussed earlier in this chapter.

The absorption of radiation by free atoms (those analyte atoms removed from their chemical environment but not ionized) in the flame involves a transition of these atoms from the highly populated ground state to an excited electronic state. Although other electronic transitions are possible, the atomic absorption spectrum of an element consists of a series of resonance lines, all originating with the ground electronic state and terminating in various excited states. Usually the transition between the ground state and the first excited state, known as the first resonance line, is the line with the strongest absorptivity. The absorptivity for a given element decreases as the energy difference between the ground state and the excited states increases. All other factors being equal, if any analysis requires high sensitivity, the first resonance line of the analyte is used.

The wavelength of the first resonance line for all metals and many metalloids is longer than 200 nm, short wavelength limit for operation in the conventional ultraviolet region. The first resonance line for most nonmetals falls into the vacuum ultraviolet region below 185 nm and, therefore, cannot be measured with conventional spectrometers. Thus AAS

instrumentation finds wide application for the analysis of metals and metalloids. The optical systems of AAS instruments can be modified to detect resonance lines of nonmetals (<200nm), but these modifications and a significant expense to the instrument and are not commonly used.

For AAS to function as a quantitative method, the width of the line emitted by the narrow-line source must be smaller than the width of the absorption line of the analyte in the flame. The shape of the spectral line emitted by the source is a critical parameter in AAS. The flame gases are considered as a sample cell that contains free, unexcited analyte atoms capable of absorbing radiation at the wavelength of the resonance line emitted by the external source. Unabsorbed radiation passes through a monochromator that isolates the resonance line and then into a photodetector that measures the power of the transmitted radiation. Absorption is determined by the difference in radiant power of the resonance line in the presence and absence of analyte atoms in the flame. Instrumentation for AAS is shown in Fig. 4.8

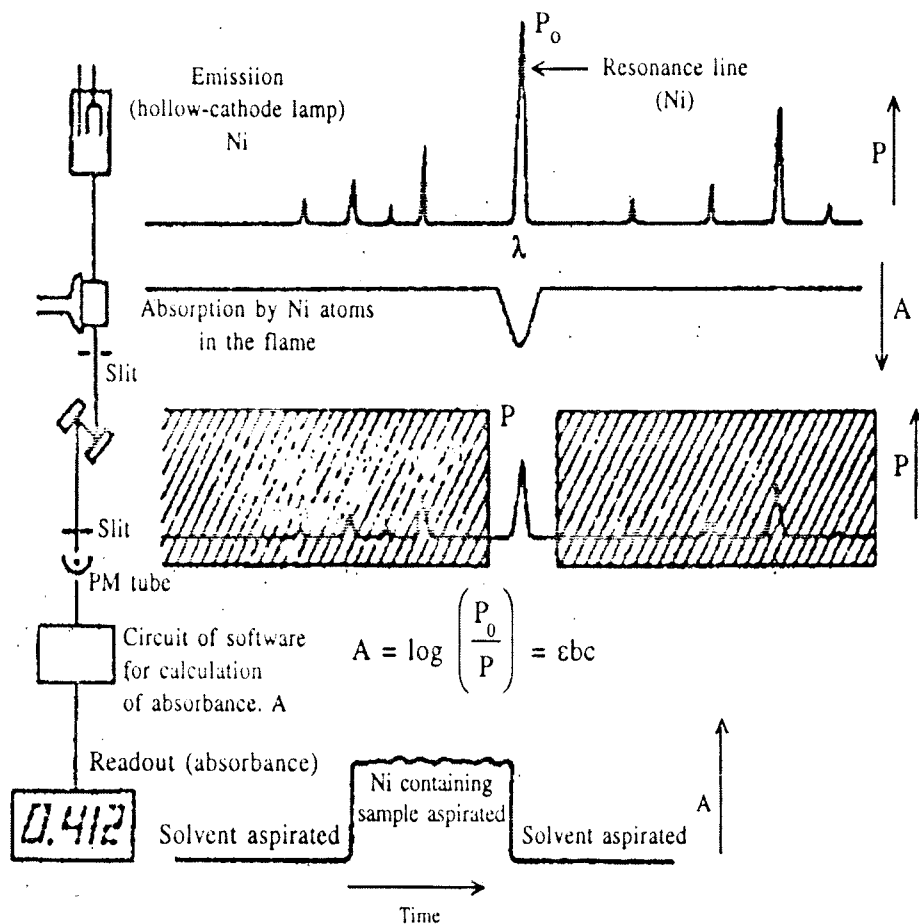


Fig. 4.8 Atomic absorption measurements and results

Transitions from the ground state to the first excited state occur when the frequency of incident radiation from the source is exactly equal to the frequency of the first resonance line of the free analyte atoms. Part of the energy of the incident radiation,  $P_0$ , is absorbed. The transmitted power,  $P$ , may be written

$$P = P_0 e^{-(k_1 \nu \cdot b)}$$

where  $k_1$ , is the absorption coefficient of the analyte element and  $b$  is the average thickness of the absorbing medium – that is, the horizontal path length of the radiation through the flame. Around the center of the resonance line there is a finite band of wavelengths caused by absorption line broadening within the flame and also broadening associated with the emission source. The two principal causes of line broadening associated with the emission source. The two principal causes of line broadening are Doppler and Lorentz, or pressure broadening. Lorentz, or pressure broadening. Lorentz broadening is caused by collisions of the absorbing atoms with other molecules or atoms present in all flames. These collisions cause the analyte atoms to have a small range of energies centered on the resonance frequency, resulting in a broadening of the resonance line.

For the above equation to be valid, the bandwidth of the incident radiation from the source absorbed by the analyte atoms must be narrower than the absorption line of the analyte. This means that the line width of the primary radiation source must be less than 0.001 nm, the usual width of resonance lines found in the absorption spectra of free atoms. This requirement on the width of resonance lines emitted from the source arises because all but the most expensive monochromators have bandpasses greater than 0.01 nm, the usual width of resonance lines found in the absorption spectra of free atoms. This requirement on the width of resonance lines emitted from the source arises because all but the most expensive monochromators have bandpasses greater than 0.01 nm. Walsh demonstrated that a hollow cathode made of the same element as the analyte emits lines that are narrower than the corresponding atomic absorption line width of the analyte atoms in the flame. This is the basis for current commercial AAS instrumentation.

## **Applications**

### **Flame Emissions Spectroscopy**

Most applications of both FES and flame AAS have been the determination of trace metals, especially in liquid samples. It should be remembered that FES offers a simple, inexpensive, and sensitive method for detecting common metals, including that alkali and alkaline earths, as well as several transition metals such as Fe, Mn, Cu, and Mn. FES has been extended to include a number of nonmetals: H, B, C, N, P, As, O, S, Se, Te, halogens, and noble gases. FES detectors for P and S are commercially available for use in gas chromatography.

FES has found wide application in agricultural and environmental analysis, industrial analysis of ferrous metals and alloys as well as glasses and ceramic materials, and clinical analyses of body fluids. FES can be easily automated to handle a large number of samples. Array detectors interfaced to a microcomputer system permit simultaneous analyses of several elements in a single sample.

### **Atomic Absorption Spectroscopy :**

AAS has been used for trace metal analyses of geological, biological, metallurgical, glass, cement, engine oil, marine sediment, pharmaceutical, and atmospheric sample. As in FES, liquid sample usually present few problems in pretreatment. Thus, most solid samples are first dissolved and converted to solutions to facilitate analysis. Gas sample are generally pretreated by scrubbing out the analyte and analyzing the scrubbing solution or adsorbing the analytes on a solid surface and then leaching them into solution with appropriate reagents. Direct sampling of solids may be accomplished using an electrothermal furnace.

The chemistry involved in the pretreatment of samples is a vital component of both FES and AAS determinations. In trace analysis, the analyst must be alert to possible sources of sample contamination such as storage containers, impurities in pretreatment reagents and solvents, and incomplete removal of prior samples from the nebulizer system. Careful attention must be given to minimizing contamination from room dust and contact with an analyst's skin or clothing and laboratory; glassware.

The detection limits and sensitivities provide a means of comparing the quantitative characteristics of atomic spectroscopic methods for a given element.

### **ATOMIC FLUORESCENCE SPECTROMETRY :**

The basic principle of atomic fluorescence spectroscopy (AFS) is the same as that of molecular fluorescence. Free analyte atoms formed in a flame absorb radiation from an external source, rise to excited electronic states, and then return to the ground state by fluorescence. AFS offers the same advantages over AAS for trace analysis that molecular fluorescence has over ordinary absorption spectroscopy: the radiation from fluorescence is measured (in principle) against a zero background, whereas ordinary absorption measurements involve the ratio of two signals.

In AFS the exciting source is placed at right angles to the flame and the optical axis of the spectrometer. Some of the incident radiation from the source is absorbed by the free atoms of the test element. Immediately after this absorption, energy is released as atomic fluorescence at a characteristic wavelength upon the return of the excited atoms to the ground state.

The best burner system for AFS is probably a combination of acetylene / nitrous oxide and hydrogen / oxygen / argon using a rectangular flame with a premixed laminar flow burner. The flame should have a low background and a low quenching cross section, in addition to being efficient in producing a large freeatom population. Although the influence of flame background on detection limits in AFS is most severe with an unmodulated source and dc

detection, the presence of intense flame background is a problem even in systems that use modulation. Even though the unmodulated flame background is not amplified directly with ac modulation. Its presence results in noise at the output of the amplifier. The intensity of the fluorescence is linearly proportional to the exciting radiation flux. When there is no analyte, only background radiation from the flame is detected. This difference between AFS and AAS is significant near the analyte detection limit and makes AFS the method of choice for trace analysis for selected metals. AFS exhibits its greatest sensitivity for elements that have high excitation energies.

#### **Nephelometry and Turbidimetry :**

Small amounts of some insoluble compounds may be prepared in a state of aggregation such that moderately stable suspensions are obtained. The optical properties of each suspension will vary with the concentration of the dispersed phase. When light is passed through the suspension, part of the incident radiant energy is dissipated by absorption, reflection, and refraction, while the remainder is transmitted. Measurement of the intensity of the transmitted light as a function of the concentration of the dispersed phase is the basis of turbidimetric analysis. When the suspension is viewed at right angles to the direction of the incident light the system appears opalescent due to the reflection of light from the particles of the suspension (Tyndall effect). The light is reflected irregularly and diffusely, and consequently the term scattered light is used to account for this opalescence or cloudiness. The measurement of the intensity of the scattered light (at right angles to the direction of the incident light) as a function of the concentration of the dispersed phase is the basis of nephelometric analysis (Gr. Nephelē = a cloud). Nephelometric analysis is most sensitive for very dilute suspensions (> 100 mg per litre). Techniques for turbidimetric analysis and nephelometric analysis resemble those of filter photometry and fluorimetry, respectively.

The construction of calibration curves is recommended in nephelometric and turbidimetric determinations, since the relationship between the optical properties of the suspension and the concentration of the dispersed phase is, at best, semi-empirical. If the cloudiness or turbidity is to be reproducible, the utmost care must be taken in its preparation. The precipitate must be very fine, so as not to settle rapidly. The intensity of the scattered light depends upon the number and the size of the particles in suspension and, provided that the average size of particles is fairly reproducible, analytical applications are possible.

The following conditions should be carefully controlled in order to produce suspensions of reasonably uniform character:

1. The concentrations of the two ions which combine to produce the precipitate as well as the ratio of the concentrations in the solutions which are mixed.

2. The manner, the order and the rate mixing.
3. The amounts of other salts and substances present, especially protective colloids (gelatin, gum Arabic, dextrin, etc.)
4. The temperature.

#### **Instruments for Nephelometry and Turbidimetry :**

Visual and photoelectric colorimeters may be used as turbidimeters : a blue filter usually results in greater sensitivity. A calibration curve must be constructed using several standard solutions, since the light transmitted by a turbid solution does not generally obey the Beer-Lambert law precisely.

'Visual' nephelometers (comparator type) have been superseded by the Photoelectric type. It is possible to adapt a good Duboscq colorimeter for nephelometric work. Since the instrument is to measure scattered light, the light path must be so arranged that the light enters the side of the cups are therefore replaced by clear glass tubes with opaque bottoms; the glass plungers are accurately fitted with opaque sleeves. The light, which enters at right angles to the cups, must be regulated so that equal illumination is obtained on both sides. A standard suspension is placed in one cup, and the unknown solution is treated in an identical manner and placed in the other cup. The dividing line between the two fields in the eyepiece must be thin and sharp, and seem to disappear when the fields are matched. Most fluorimeters may be adapted for use in nephelometry.

#### **Thermal Analysis**

##### **General Discussion :**

Thermal methods of analysis may be defined as those technique in which changes in physical and / or chemical properties of a substance are measured as a function of temperature. Methods that involve changes in weight or changes in energy come within this definition.

The thermal analytical techniques discussed in this chapter are :

Thermogravimetry (TG), a technique in which a change in the weight of a substance is recorded as a function of temperature or time.

Differential Thermal Analysis (DTA), which is a method for recording the difference in temperature between a substance and an inert reference material as a function of temperature or time.

Differential Scanning Calorimetry (DSC), a method whereby the energy necessary to establish a zero temperature difference between a substance and a reference material is recorded as a function of temperature or time.

## Thermogravimetry (TG) :

The basic instrumental requirement for thermogravimetry is a precision balance with a furnace programmed for a linear rise of temperature with time. The results may be presented as, (i) a thermogravimetric (TG) curve, in which the weight change is recorded as a function of temperature or time, or (ii) as a derivative thermogravimetric (DTG) curve where the first derivative of the TG curve is plotted with respect to either temperature or time.

A typical thermogravimetric curve, for copper sulphate pentahydrate  $\text{CuSO}_4 \cdot 5\text{H}_2\text{O}$ .

The following features of the TG curve should be noted :

- the horizontal portions (plateaus) indicate the regions where there is no weight change;
- the curved portions are indicative of weight losses;
- since the TG curve is quantitative, calculations on compound stoichiometry can be made at any given temperature.

Fig. 4.9, shows, sulphate pentahydrate has four distinct regions of decomposition :

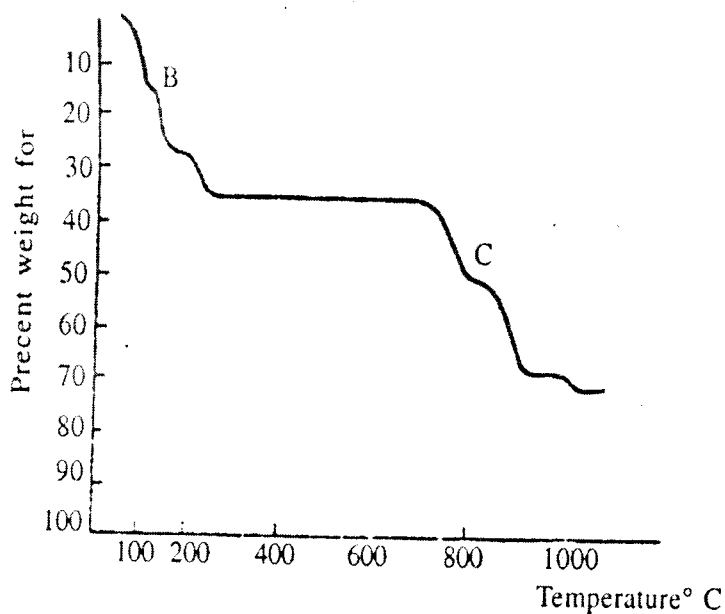
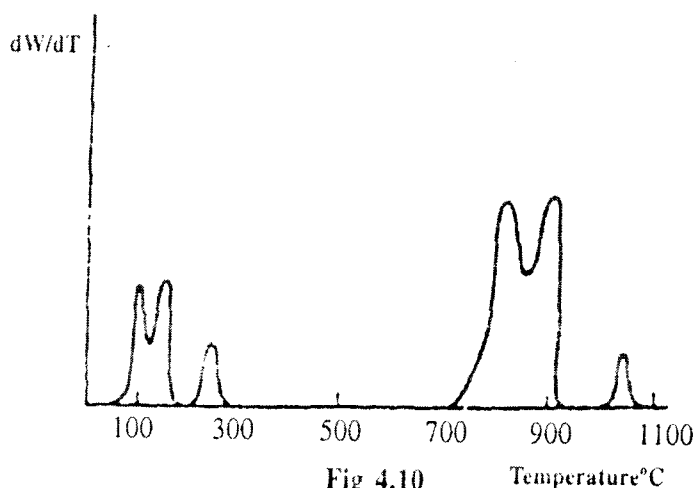


Fig. 4.9

	Approximate temperature region
$\text{CuSO}_4 \cdot 5\text{H}_2\text{O} \rightarrow \text{CuSO}_4 \cdot \text{H}_2\text{O}$	90 - 150° C
$\text{CuSO}_4 \cdot \text{H}_2\text{O} \rightarrow \text{CuSO}_4$	200 - 275° C
$\text{CuSO}_4 \rightarrow \text{CuO} + \text{SO}_2 + \frac{1}{2} \text{O}_2$	700 - 900° C
$2\text{CuO} \rightarrow \text{Cu}_2\text{O} + \frac{1}{2} \text{O}_2$	1000 - 1100° C

The precise temperature regions for each of the reactions are dependent upon the experimental conditions. Although in Fig. XXIII, 1 the ordinate is shown as the percentage weight loss, the scale on this axis may take other forms :

1. as a true weight scale;
2. as a percentage of the total weight;
3. in terms of molecular weight units.



An additional feature of the TG curve should now be examined, namely the two regions B and C where there are changes in the slope of the weight loss curve. If the rate of change of weight with time  $dW/dt$  is plotted against temperature, a derivative thermogravimetric (DTG) curve is obtained. In the DTG curve when there is no weight loss then  $dW/dt = 0$ . The peak on the derivative curve corresponds to a maximum slope on the TG curve. When  $dW/dt$  is a minimum but not zero there is an inflection, i.e., a change of slope on the TG curve. Inflections B and C on Fig. 4.9 1 may imply the formation of intermediate compounds. In fact the inflection at B arises from the formation of the trihydrate  $\text{CuSO}_4 \cdot 3\text{H}_2\text{O}$ , and that at point C is reported by Duval to be due to formation of a golden yellow basic sulphate of composition  $2\text{CuO} \cdot \text{SO}_3$ . Derivative thermogravimetry is useful for many complicated determinations and any change in the rate of weight loss may be readily identified as a trough indicating consecutive reactions; hence weight changes occurring at close temperatures may be ascertained.

#### **Experimental factors :**

In the previous section it was stated that the precise temperature regions for each reaction of the thermal decomposition of copper sulphate pentahydrate is dependent upon experimental conditions. When a variety of commercial thermobalances became available in the early 1960s it was soon realized that a wide range of factors could influence the results obtained. Reviews of these factors have been made by Simons and Newkirk and by Coats and Redfer as a basis for establishing criteria necessary to obtain meaningful and reproducible results. In addition, several sources of error can arise in thermogravimetry which may lead to both inaccurate temperatures and weight change values. This may necessitate the

construction of a correction curve. It must be stressed that with some modern instruments the need for corrections is minimized.

### Correction curve

When an empty crucible is heated from ambient temperature to, say,  $1000^{\circ}\text{C}$  there is an apparent gain in weight. This weight gain is governed by the heating rate employed and by the crucible weight and volume. A typical correction curve is shown in Fig. 4.11. In this experiment a platinum crucible of 1 g weight showed an apparent gain of 1.5 mg when heated at  $4^{\circ}\text{C min}^{-1}$  from ambient temperature to  $1000^{\circ}\text{C}$ . Although the error produced is 0.15 per cent of the crucible weight, a 100 mg sample contained in this crucible would suffer an apparent weight change of 1.5 per cent. This apparent weight change is due to a variety of factors including the air buoyancy and convection currents within the furnace. A correction curve must be constructed giving the apparent weight change in order to calculate the actual change occurring in a sample.

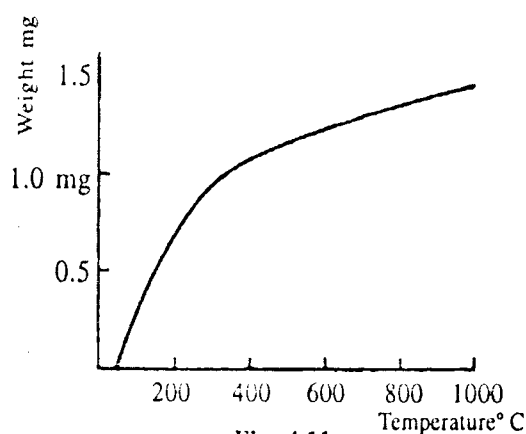


Fig. 4.11

The factors which may affect the results can be classified into the two main groups of instrumental effects and the characteristics of the sample:

#### Instrumental Factors :

(a) *Heating Rate* : When a substance is heated at a fast heating rate, the temperature of decomposition will be higher than that obtained at a slower rate of heating. The effect is shown for a single – step reaction in Fig. 4.12. The curve AB represents the decomposition curve at a slow heating rate, whereas the curve CD is that due to the faster heating rate.

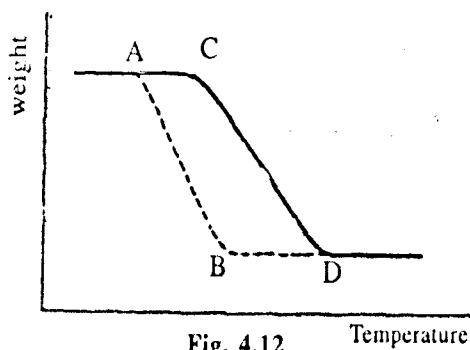


Fig. 4.12

If  $T_A$  and  $T_C$  are the decomposition temperatures at the start of the reaction and the final temperatures on completion of the decomposition are  $T_S$  and  $T_D$ ; the following features can be noted :

$$T_A < T_C$$

$$T_B < T_D$$

$$T_B - T_A < T_D - T_C$$

The heating rate has only a small effect when a fast reversible reaction is considered. The points of inflection B and C obtained on the thermogravimetric curve for copper sulphate pentahydrate may be resolved into a plateau if a slower heating rate is used. Hence the detection of intermediate compounds by thermogravimetry is very dependent upon the heating rate employed.

**(b) Furnace atmosphere :** The nature of the surrounding atmosphere can have profound effect upon the temperature of a decomposition stage. For example, the decomposition of calcium carbonate occurs at a much higher temperature if carbon dioxide rather than nitrogen is employed as the surrounding atmosphere. Normally the function of the atmosphere is to remove the gaseous products evolved during thermogravimetry, in order to ensure that the nature of the surrounding gas remains as constant as possible throughout the experiment. This condition is achieved in many modern thermobalances by heating the test sample in vacuo.

1) Static air (air from the surroundings flows through the furnace)

2) 'dynamic air', where compressed air from a cylinder is passed through the furnace at a measured flow rate :

3) nitrogen gas (oxygen free) which provides an inert environment.

Atmospheres that take part in the reaction - for example, humidified air - have been used in the study of the decomposition of such compounds as hydrated metal salts.

Since thermogravimetry is a dynamic technique, convection currents arising in a furnace will cause a continuous change in the gas atmosphere. The exact nature of this change further depends upon the furnace characteristics so that widely differing thermogravimetric data may be obtained from different designs of thermobalance.

**(c) Crucible geometry :** The geometry of the crucible can alter the slope of the thermogravimetric curve. Generally, a flat, plate-shaped crucible is preferred to a 'high form' cone shape because the diffusion of any evolved gases is easier with the former type.

**Sample characteristics :** The weight, particle size and the mode of preparation (the pre-history) of a sample all govern the thermogravimetric results. A large sample can often create a deviation from linearity in the temperature rise. This is particularly true when a fast exothermic

reaction is studied; for example, the evolution of carbon monoxide during the decomposition of calcium oxalate to calcium carbonate. A large volume of sample in a crucible can impede the diffusion of evolved gases through the bulk of the solid large crystals especially those of certain metallic nitrates which may undergo decrepitation ('spitting' or 'spattering') when heated. Other samples may swell, or foam and even bubble. In practice a small sample weight with as small a particle size as practicable is desirable for thermogravimetry.

Diverse thermogravimetric results can be obtained from samples with different pre-histories; for example; TG and DTG curves showed that magnesium hydroxide prepared by precipitation methods has a different temperature of decomposition from that for the naturally occurring material. It follows that the source and / or the method of formation of the sample should be ascertained.

#### **Applications of Thermogravimetry :**

Some of the applications of thermogravimetry are of particular importance to the analyst. These are :

1. The determination of the purity and thermal stability of both primary and secondary standards.
2. The investigation of correct drying temperatures and the suitability of various weighing forms for gravimetric analysis.
3. Direct application to analytical problems (automatic thermogravimetric analysis)
4. The determination of the composition of complex mixtures.

Thermogravimetry is a valuable technique for the assessment of the purity of materials. Analytical reagents, especially those used in titrimetric analysis as primary standards, e.g, sodium carbonate, sodium tetraborate, and potassium hydrogenphthalate, have been examined. Many primary standards absorb appreciable amounts of water when exposed to moist atmospheres. TG data can show the extent of this absorption and hence the most suitable drying temperature for a given reagent may be determined.

#### **Differential Thermal Analysis and Differential Scanning Calorimetry :**

In differential thermal analysis (DTA) both the test sample and an inert reference material (usually  $\alpha$ -alumina) undergo a controlled heating or cooling programme which is usually linear with respect to time. There is a zero temperature difference between the sample and the reference material when the former does not undergo any chemical or physical change. If, however, any reaction takes place, then a temperature difference  $\Delta T$  will occur between the sample and the reference material. Thus in an endothermic change, e.g., when the samples melts or is

dehydrated, the sample temperature is lower than that of the reference material. This condition is only transitory because on completion of the reaction the sample will again show zero temperature difference compared with the reference.

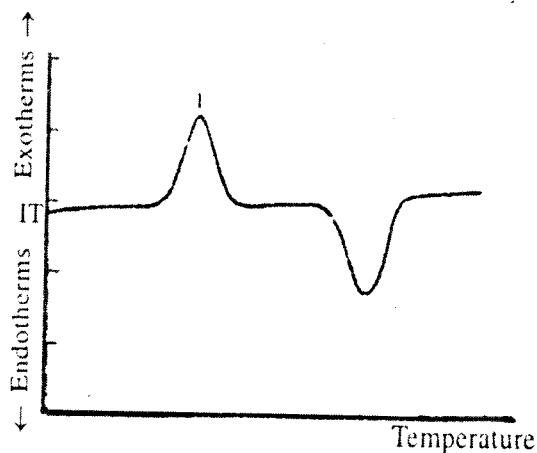


Fig. 4.13

In DTA a plot is made  $\Delta T$  against temperature or time, if the heating or cooling programme is linear with respect to time. An idealized DTA curve is shown in Fig. 4.13, in which (1) is an exothermic peak and (2) is an endothermic peak. Both the shape the size of the peaks can give a large amount of information about the nature of the test sample. Thus sharp endothermic peaks often signify changes in crystallinity or fusion processes, whereas broad endotherms arise from dehydration reactions. Physical changes usually result in endothermic curves whilst chemical reactions, particularly those of an oxidative nature, are predominantly exothermic.

Differential scanning calorimetry (DSC) measures the differential energy required to keep both the sample and reference chemicals at the same temperature. Thus when an endothermic transition occurs, the energy absorbed by the sample is compensated by an increased energy input to the sample in order to maintain a zero temperature difference. Because this energy input is precisely equivalent in magnitude to the energy absorbed in the transition direct calorimetric measurement of the energy of the transition is obtained from this balancing energy. The DSC curve is recorded with the chart abscissa indicating the transition temperature and peak area measures the total energy transfer to or from the sample.

#### Applications of DTA and DSC :

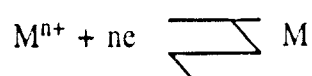
DTA and DSC both be used in conjunction with TG for certain analytical applications, e.g., the determination of moisture content or the analysis of solid mixtures.

Early applications of DTA were in the qualitative analysis of complex materials. Thus DTA provided a rapid method for the 'finger printing' of minerals, clays and polymeric materials. Indeed, an extremely wide range of materials may be studied by DTA and DSC. The areas of study include thermal stability and decompositions, fusion, phase changes, and purity determinations. A recent important application has been in the measurement of the degree of conversion of high alumina cement.

It must be stressed that all the thermal methods outlined in this chapter are frequently used in conjunction with other techniques. Thus the analysis of evolved gases during a TG, DTA or DSC experiment may be performed by gas chromatography or mass spectrometry, X-ray crystallography may be used to study the structure of reaction intermediates isolated as a result of thermal studies.

### Electrochemical Cell and Electrode Potentials :

When a metal is immersed in a solution containing its own ions, say, zinc sulphate solution, a potential difference is established between the metal and the solution. The potential difference  $E$  for an electrode reaction.



Is given by the expression :

$$E = E^0 + \frac{RT}{nF} \ln a_M \dots (1)$$

Where  $R$  is the gas constant,  $T$  is the absolute temperature,  $F$  the Faraday constant,  $n$  the valency of the ions,  $a_M$  the activity of the ions in the solution, and  $E^0$  is a constant dependent upon the metal. Equation (1) can be simplified by introducing the known values of  $R$  and  $F$ , and converting natural logarithms to base 10 by multiplying by 2.3026; it then becomes:

$$E = E^0 + \frac{0.00019837}{n} \log a_M$$

For a temperature of 25° C ( $T = 298K$ )

$$E = E^0 + \frac{0.0591}{n} \log a_M \dots (2)$$

For most purposes in quantitative analysis, it is sufficiently accurate to replace  $\log a_M$  by  $\log c_M$  the ion concentration (in moles per  $dm^3$ ):

$$E = E^0 + \frac{0.0591}{n} \log c_M \dots (3)$$

The latter is a form of the Nernst equation.

If in equation (2),  $a_M^{**}$  is put equal to unity,  $E$  is equal  $E^\circ$ .  $E^\circ$  is called the standard electrode potential of the metal.

In order to determine the potential difference between an electrode and a solution, it is necessary to have another electrode and solution accurately known potential difference. The two electrodes can then be combined to form a voltaic cell, the e.m.f of which can be directly measured. The e.m.f of the cell is the arithmetical sum or difference of the electrode potentials (depending upon the sign of these two potentials); the value of the unknown potential can then be calculated. The primary reference electrode is the normal or standard hydrogen electrode.

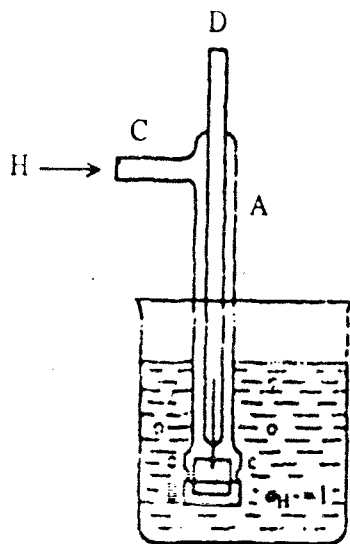
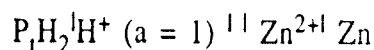


Fig 4.14

This consists of a piece of platinum foil, coated electrolytically with platinum black, and immersed in a solution of hydrochloric acid containing hydrogen ions at unit activity. (This corresponds to 1.8 M-hydrochloric acid at 25° C). Hydrogen gas at a pressure of one atmosphere is passed over the platinum foil through the side tube C and escapes through the small holes B in the surrounding glass tube A. Because of the periodic formation of bubbles, the level of the liquid inside the tube fluctuates, and a part of the foil is alternately exposed to the solution and to hydrogen. The lower end of the foil is continuously immersed in the solution to avoid interruption of the electric current. Connection between the platinum foil and an external circuit is made with mercury in D. The platinum black has the remarkable property of absorbing large quantities of hydrogen, and it permits the change from the gaseous to the ionic form and the reverse process to occur without hindrance; it therefore behaves as though it were composed entirely of hydrogen, that is, as a hydrogen electrode. Under fixed conditions, viz., hydrogen gas at atmospheric pressure and unit activity of hydrogen ions in the solution in contact with the electrode, the hydrogen electrode possesses a definite potential. By convention, the potential of the standard hydrogen electrode is equal to zero at all temperatures. Upon connecting the

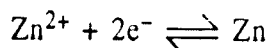
standard hydrogen electrode with a metal electrode (a metal in contact with a solution of its ions unit activity) by means of a salt, (say, potassium chloride) bridge the standard electrode potential may be determined, the cell is usually written as



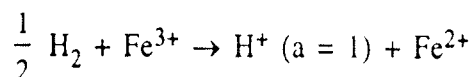
or the e.m.f of the half-cell  $\text{Zn}^{2+} | \text{Zn}$ , The cell reaction is :



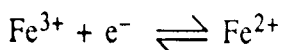
and the half-cell reaction is written as :



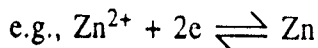
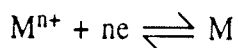
The electrode potential of the  $\text{Fe}^{3+}, \text{Fe}^{2+} | \text{Pt}$  electrode is the e.m.f of the cell: or the e.m.f of the half - cell  $\text{Fe}^{3+}, \text{Fe}^{2+} | \text{Pt}$ . The cell reaction is



and the half-cell reaction is written :



The convention is adopted of writing all half-cell reactions as reductions :



$$E^\circ = -0.76 \text{ volt}$$

when the activity of the ion  $\text{M}^{n+}$  is equal to unity (approximately true for a 1 M solution), the electrode potential  $E$  is equal to the standard potential  $E^\circ$ . Some important standard electrode potentials referred to the standard hydrogen electrode at 25°C (in aqueous solution) are collected in

Table. 4.4 Standard Electrode Potentials at 25° C

Electrode reaction	$E^\ominus$ (volts)	Electrode reaction	$E^\ominus$ (volts)
$\text{Li}^+ + e = \text{Li}$	-3.045	$\text{Ti}^+ + e = \text{Ti}$	-0.336
$\text{K}^+ + e = \text{K}$	-2.925	$\text{Co}^{2+} + 2e = \text{Co}$	-0.277
$\text{Ba}^{2+} + 2e = \text{Ba}$	-2.90	$\text{Ni}^{2+} + 2e = \text{Ni}$	-0.25
$\text{Sr}^{2+} + 2e = \text{Sr}$	-2.89	$\text{Sn}^{2+} + 2e = \text{Sn}$	-0.136
$\text{Ca}^{2+} + 2e = \text{Ca}$	-2.87	$\text{Pb}^{2+} + 2e = \text{Pb}$	-0.126
$\text{Na}^+ + e = \text{Na}$	-2.714	$2\text{H}^+ + 2e = \text{H}_2$	0.000

$\text{Mg}^{2+} + 2e = \text{Mg}$	-2.37	$\text{Cu}^{2+} + 2e = \text{Cu}$	+0.337
$\text{Al}^{3+} + 3e = \text{Al}$	-1.66	$\text{Hg}^{2+} + 2e = \text{Hg}$	+0.789
$\text{Mn}^{2+} + 2e = \text{Mn}$	-0.763	$\text{Ag}^+ + e = \text{Ag}$	+0.799
$\text{Zn}^{2+} + 2e = \text{Zn}$	-0.763	$\text{Pd}^{2+} + 2e = \text{Pd}$	+0.987
$\text{Fe}^{2+} + 2e = \text{Fe}$	-0.440	$\text{Pt}^{2+} + 2e = \text{Pt}$	+1.2
$\text{Cd}^{2+} + 2e = \text{Cd}$	-0.403	$\text{Au}^{3+} + 3e = \text{Au}$	+1.50

It may be noted that the standard hydrogen electrode is rather difficult to manipulate. In practice, electrode potentials on the hydrogen scale are usually determined indirectly by measuring the e.m.f of a cell formed from the electrode in question and a convenient reference electrode whose potential with respect to the hydrogen electrode is accurately known. The reference electrodes generally used are the calomel electrode and the silver-silver chloride electrode.

When metals are arranged in the order of their standard electrode potentials, the so-called electrochemical series of the metals is obtained. The greater the negative value of the potential, the greater is the tendency of the metal to pass into the ionic state. A metal will normally displace any other metal below it in the series from solutions.

## 12. Controlled Electrode Potential

Electro-separation is electrolysis in which a quantitative reaction or, at the very least, an appreciable amount of electro-oxidation or electroreduction takes place at an electrode. Bulk (or exhaustive) electrolytic methods are characterized by a large ratio of electrode area to solution volume and by mass-transfer conditions as effective as possible. Although bulk electro-separations are generally characterized by large currents and time scales of experiments of minutes or longer, the basic principles governing electrode reactions described in the previous chapters still apply.

### Completeness of an Electrode Process :

Since the potential of the working electrode is the basic variable that controls the degree of completion of an electrolytic process in most cases, controlled-potential techniques are usually the most desirable for bulk electrolysis. The extent of completion of a bulk electrolytic process can often be predicted for reversible reactions from the applied electrode potential and the Nernst equation. For the deposition of a solid, when more than a monolayer of solid is deposited on an inert electrode (such as platinum), the activity of the solid is constant and equal to unity at the completion of the electrolysis. The Nernst equation yields.

$$E = E^\circ + \frac{RT}{nF} \ln [C_i(1-x)] \quad \dots \quad (1)$$

Where  $C_i$  is the initial concentration of the oxidized form and  $x$  is the fraction of the oxidized form reduced at the electrode potential  $E$ .

For example, for 99.9% completeness of reduction of an oxidant to the metallic state, the potential of the working electrode at 25° C should be

$$E = E^\circ + \frac{0.0592}{n} \log [C_i(1-0.999)] \quad \dots \quad (2)$$

Or  $178 / n$  mV more negative than  $E^\circ$ . The current through the system steadily decreases as the deposition proceeds. However, the maximum permissible current is used at all times so that the electrolysis proceeds at the maximum rate.

Any over potential terms is added to Equation (2) and takes the sign of the electrode. The potential range for a successful separation can best be found by determining the current-potential curve on a microelectrode under the same condition (concentration, supporting electrolyte, temperature) considered for the separation.

#### **Controlled Potential Techniques :**

The fundamental requirements of coulometric analysis are that only one overall reaction of known stoichiometry may take place and that it proceed with 100% current efficiency. There may be no side reactions of different stoichiometry. The method is particularly useful and accurate in the range from milligram quantities down to microgram quantities and, therefore, in trace analysis. In practice, sensitivity is limited only by problems of sample handling and end point detection.

Coulometric methods eliminate the need for burets and balances, and the preparation, storage and standardization of standard solutions. Procedures can be automated readily and are especially adaptable to remote operation and control. In a sense the electron becomes the primary standard. Coulometric methods produce reagents in solution that would otherwise be difficult to use, volatile reactants such as chlorine, bromine, or iodine, or unstable reactants such as titanium (III), chromium (II), copper (I), or silver (II).

#### **General Principles :**

In controlled-potential coulometry the total number of coulombs consumed in an electrolysis is used to determine the amount of substance electrolyzed. A three-electrode potentiostat maintains a constant electrode potential by continuously monitoring the potential of the working electrode as compared with a reference electrode. The current is adjusted continuously to maintain the desired potential.

Consider the case when one or more of the ions present can undergo reduction or oxidation within the potential frame extending from the reduction of hydrogen ions to the region where water is oxidized to oxygen. Controlling the potential of the working electrode allows for selectivity of the redox reaction. The mini-potential frame for a particular redox reaction is represented by the Nernst equation<sup>4</sup>. To lower the oxidant to 0.001% of its initial concentration, or  $10^{-6} C_i$ , requires a potential change of  $E^\circ - 0.355/n$ . In the reverse situation, a potential change of  $E^\circ + 0.355/n$  is needed to convert the reduced form to the oxidized state. A second redox system whose mini-potential frame overlaps this system would constitute an interference.

To conduct controlled - potential coulometry, current - potential diagrams must be available for the oxidation / reduction systems to be determined and also for any other system that can react at the working electrode. Current - potential diagrams are obtained by plotting current against the cathode-reference electrode potential (rather than the cathode-anode potential, which would include the large and variable  $iR$  drop in the cell). The necessary data can be obtained by setting the potentiostat to one cathode-reference potential after another in sequence, allowing only enough time at each setting for the current indicator to balance. Alternatively, the reduction (or oxidation) is performed in the usual manner except that periodically throughout the electrolysis the potentials is adjusted to a value that stops the current flow. The net charge transferred up to this point and the electrode potential are noted, and the electrolysis is then continued. Curves plotted from a series of points, called coulograms, establish the optimum electrode potentials because they relate the extent of reaction with electrode potentials under actual titration conditions and with actual electrode material.

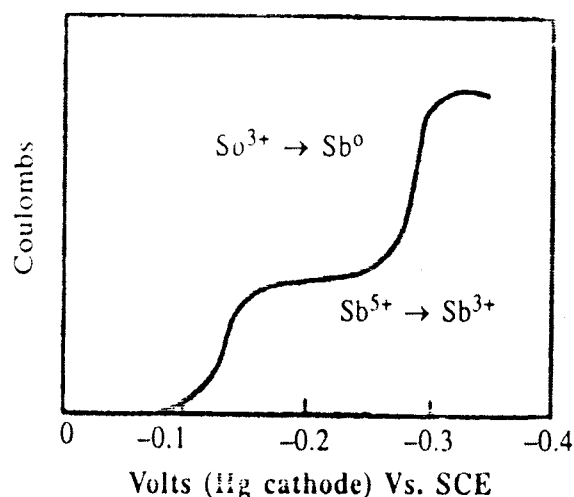


Fig. 4.15 Electrolytic reduction of antimony (V) by a two-step process in 6M HCl plus 0.4M tartaric acid. (after L.B. Dunlap and W.D. Shults, Anal. Chem., 34, 499 (1962). Courtesy of American Chemical Society]

## **Voltammetric Techniques :**

Voltammetry represents a wide range of electrochemical techniques. These techniques can be used to study the solution composition through current-potential relationships in an electrochemical cell and with the current-time response of a microelectrode at a controlled potential. The development of polarography (the name applied to be voltammetry when a deopping mercury microelectrode is used), commencing with the work of Heyrovsky in 1922 (and for which he received the Nobel Prize in 1959), marked a significant advance in electrochemical methodology. The existence of polarized electrodes was recognized and utilized in a practical way.

The original dc voltammetric technique suffered from a number of difficulties that made it less than ideal for routine analytical purposes and made the results obtained somewhat difficult to interpret. With the advent of low-cost, fast, stable, operational amplifiers in the early 1960s, some problems were overcome. Investigations of new approaches, such as potential step methods, potential sweep voltammetry, phase-sensitive alternating current voltammetry, hydrodynamic methods, and stripping voltammetry, demonstrated the utility and desirability of the new voltammetric methods.

The advantage of voltammetry quickly demonstrates that it is a potent analytical tool. The foremost advantage is sensitivity. Voltammetry ranks among the most sensitive analytical techniques available; it is routinely used for the determination of electroactive substances in the sub-parts per million range. Analysis times of seconds are possible. The simultaneous determination of several analytes by the single scan is often possible with a voltammetric procedure. Voltammetric techniques have a unique capability to distinguish between oxidation states that may affect a substance's reactivity and toxicology. The theory of voltammetry is well developed, and reasonable estimates of unknown parameters can be made.

In analytical applications the composition of a sample can be investigated using various potential step methods, possibly by ac voltammetry in any of several forms and perhaps anodic and cathodic stripping voltammetry.

### **Cyclic Potential sweep Voltammetry :**

Cyclic voltammetry (also called linear sweep voltammetry) consists of cycling the potential of a stationary electrode immersed in a quiescent solution and measuring the resulting current. The excitation signal is a linear potential scan with a triangular waveform. Symmetrical triangular scan rates range from a few millivolts per second to hundreds of volts per second. This triangular potential excitation signal sweeps the potential of the working electrode back and forth between two designated values called the switching potentials. The triangle returns at the same speed and permits the display of a complete voltammogram with cathodic (reduction)

and anodic (oxidation) waveforms one above the other, as shown in Fig. 4.16. The current at the stationary working electrode is measured under diffusion-controlled, mass-transfer conditions. Although the potential scan is frequently terminated at the end of the first cycle, it can be continued for any number of cycles. Both the scan rate and the switching potentials are easily varied. Typically, the scan rate is from 20 V / sec to 100 V / sec at macroscopic electrodes, but it can be as high as  $10^6$  V / sec at ultramicroelectrodes.

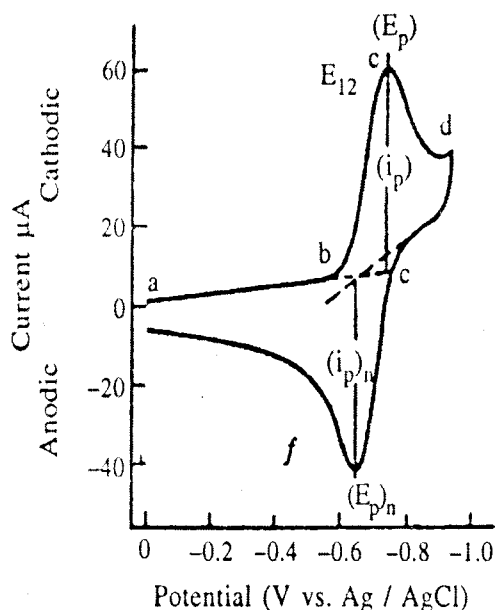


Fig. 4.16 Schematic cyclic voltammogram. Scan initiated at 0.0 V versus Ag / AgCl and in negative direction at 20 mV/ sec. Scan reversed at -0.9V.

In the example (figure 4.16), the initial potential (0.0 V) applied at point a is chosen to avoid any electrolysis of electroactive species in the sample when the experiment is initiated. Then the potential is scanned in the negative direction. When the potential becomes sufficiently negative (-0.6 V) to cause a reduction of an electroactive species at the electrode surface, cathodic current (indicated at b) begins to flow. The cathodic current increases rapidly until the surface concentration of oxidant at the electrode surface approaches zero, as signaled by the current, now diffusion controlled, peaking at point c. The current then decays with  $t^{-1/2}$  according to the Cottrell equation as the solution surrounding the electrode is depleted of oxidant due to its electrochemical conversion to the reduced state. The final rise at point d is caused by the discharge of the supporting electrolyte. At the switching potential (-0.9 V) the potential is switched to scan in the positive direction. However, the potential is still sufficiently negative to continue the reduction of the oxidant and so a cathodic current continues

for a brief period. Finally the electrode potential becomes sufficiently positive to bring about oxidation of the reductant that had been accumulating adjacent to the electrode surface. At this point an anodic current begins to flow and to counteract the cathodic current. The anodic current increases rapidly until the surface concentration of the accumulated reductant approaches zero, at which point the anodic current peaks (point f). The anodic current then decays as the forward scan. In the course of the cathodic variation in potential, the reduced form of the reactant is produced in the vicinity of the electrode, while the oxidized form is depleted. Given sufficient time, the reduced form would diffuse into the bulk of the solution, but the potential is taken back to the initial value at a rate such that some of the reduced form is still present at the electrode surface and undergoes a process of oxidation back to the form of the couple initially present in the solution.

The important parameters of a cyclic voltammogram are the magnitudes of the anodic peak current ( $i_p$ )<sub>a</sub>, the cathodic peak current, ( $i_p$ )<sub>c</sub>, the anodic peak potential ( $E_p$ )<sub>a</sub>, the cathodic peak potential, ( $E_p$ )<sub>c</sub>, and the half-peak potential, ( $E_{p/2}$ )<sub>c</sub>. Note that ( $E_{p/2}$ )<sub>c</sub>, at which the current is half the peak value, differs from the half-wave potential,  $E_{1/2}$ . The peak current (in amperes) for the oxidant (assuming the initial scan is cathodic) is

$$i_p = n^{3/2} F^{3/2} (\pi v D_{ox} / RT)^{1/2} A C_{ox} \chi(\sigma t)$$

where  $\chi(\sigma t)$  is a tabulated function whose value is 0.446 for a simple, diffusion controlled electron transfer reaction,  $R$  is in  $J K^{-1} mol^{-1}$ , and  $T$  is Kelvin. At 25° C this reduces to

$$i_p = (2.69 \times 10^5) n^{3/2} A D_{ox}^{1/2} v^{1/2} C_{ox} \dots (2)$$

for  $A$  in  $cm^2$ ,  $D$  in  $cm^2/sec$ ,  $C$  in  $mol / cm^3$ , and  $v$  in  $V/sec$

To measure accurately peak currents, it is essential to establish the correct baseline. This is not always easy, particularly for more complicated systems. Because the peak may be somewhat broad, so that the peak potential may be difficult to determine, it is sometimes more convenient to report the potential at half the peak height ( $E_{p/2}$ )<sub>c</sub>.

For a reversible wave,  $E_p$  is independent of the scan rate, and  $i_p$ , as well as any other point on the wave, is proportional to  $v^{1/2}$ . A convenient normalized current function is  $i_p / v^{1/2} C$ , which depends on  $n^{3/2}$  and  $D^{1/2}$ . For a simple diffusion controlled reaction, this current function is a constant independent of the scan rate. This constant can be used to estimate  $n$  for an electrode reaction if a value of  $D$  can be estimated (or the reverse if  $n$  is known).

The number of electrons transferred in the electrode for a reversible couple can be determined from the separation between the peak potentials.

$$(E_p)_a - (E_p)_c = \frac{0.057}{n}$$

which is valid when the switching potential is at least  $100/n$  mV past the cathodic peak potential. The formal potential for a reversible couple is centered between the peak potentials. Electrochemical quasi-reversibility is characterized by a separation of peak potentials greater than indicated by Equation, and irreversibility by the disappearance of a reverse peak.

On the reverse scan, the position of the peak depends on the switching potential. As this potential becomes more negative, the position of the anodic peak becomes constant at  $28.5/n$  mV anodic of the half-way potential. When the switching potential is more negative than  $100/n$  mV of the reduction peak, the separation of the two peaks is  $57/n$  mV and independent of the scan rate. This is a commonly used criterion of reversibility. Reversibility can also be ascertained by plotting  $(i_p)_c$  or  $(i_p)_a$  versus the square root of the scan velocity. The plots should be linear with intercepts at the origin. Care must be taken to eliminate any background currents.

### **Stripping Voltammetry :**

Stripping voltammetry, also called stripping chronoamperometry, has the lowest detection limit of any commonly used electroanalytical technique. Basically, electrochemical stripping analysis is a two-step operation. During the first step, analyte is electrolytically deposited onto or into the surface of an electrode typically consisting of a thin film or a drop of mercury or, in some cases, a solid electrode by controlled potential electrolysis. This is followed by a reverse electrolysis, or stripping, step, in which the deposited analyte is removed from the electrode. Each electrochemical species strips at a characteristic potential.

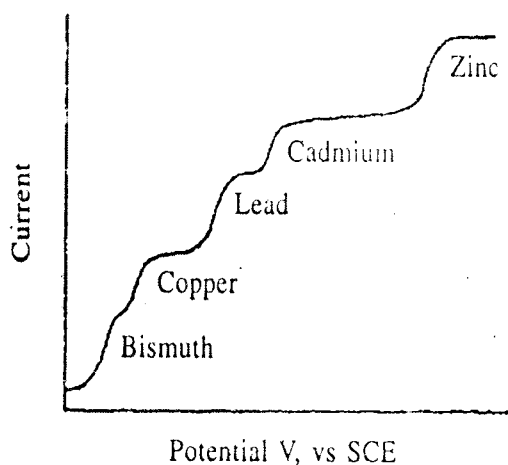
The preconcentration or electrodeposition step provides the means for substantially improving the detection limit for the analytical (stripping) step. Since the volume of the mercury electrode or the solid electrode surface is considerably less than the volume of the sample solution in the electrochemical cell, the resulting amalgam or deposit of metal atoms into or onto the electrode may be more concentrated than the original test solution by a factor of up to 1 million.

### **Anodic Stripping voltammetry :**

Anodic stripping voltammetry (ASV) is used primarily to determine the concentration of trace metals that can be preconcentrated at an electrode by reduction. The method is especially effective for metals that dissolve or a thin-film mercury amalgams. Either a hanging

mercury drop electrode or a thin-film mercury electrode can be used. Very electropositive metal ions, such as mercury (II), gold (III), silver, and platinum (IV), are deposited on solid electrodes such as glassy carbon. The geometry of diffusion is critical within or on the electrode surface. A thick planar electrode, such as a mercury pool, is not useful.

In the first step, a deposition potential is chosen that is more negative than the half-wave potential of the metal or metals to be determined. Regions in which particular metal ions are reduced at a mercury electrode are determined from the current-potential curves discussed in previous sections. A suitable potential would lie on the diffusion current plateau of a dc polarogram or a normal pulse voltammogram. For example, copper (II) can be selectively reduced in the potential range 0 to 0.25 V (vs.SCE) whereas copper (II) bismuth, lead, cadmium, and zinc could be reduced simultaneously at a potential of  $-1.3$  V. Similarly copper and bismuth could be selectively deposited at  $-0.4$  V. The solution is generally stirred during deposition to maximize analyte - electrode contact.



Potential V, vs SCE

Fig. 4.17 (a)

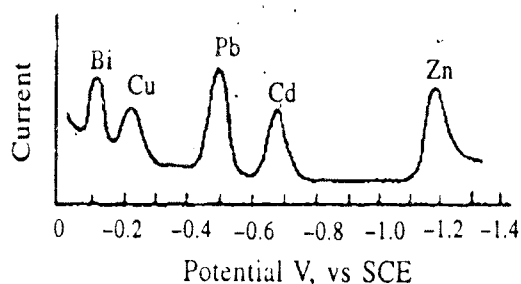


Fig. 4.17 (b)

- (a) Voltammogram of a solution that contains bismuth, copper (II), lead, cadmium and zinc ions. (b) Anodic stripping voltammogram using differential pulse detection of the same solution

If more sensitivity is required, the deposition time is simply increased. This increases the degree of preconcentration, making more deposited analyte available at the electrode during the stripping step. However, the deposition step is seldom carried to completion. Usually, only a fraction of the metal ions needs to be deposited, just a sufficient amount to produce a measurable current during the stripping step. However, it is important that the same fraction of metal ion be removed during each experiment. This the temperature

and stirring of the sample solutions must be kept as constant and reproducible as possible, and the deposition time must be carefully controlled for samples and standards alike.

Following the deposition step, there is a short rest period of 30 – 60 sec. The deposition potential is still applied to the working electrode, but stirring is halted. This allows convection currents from the stirring to decrease to a negligible level and also gives time for any amalgam to stabilize. If desired, at this time the electrolyte may be changed to one better suited for the stripping process.

In the final stripping step, there is no stirring of the solution. The potential is scanned in the positive direction (typically linear potential sweep voltammetry, differential pulse voltammetry, or square-wave voltammetry). At characteristic potentials the deposited metal atoms are stripped from the electrode back into the solution by oxidation to the ionic form. The potentials of the stripping peaks identify the respective metals, since, ideally, the different metals strip back into solution in reverse sequence to their reduction potentials. The area under the resulting current peaks is proportional to the concentrations of the respective analyte species.

Prior to each anodic stripping experiment, the supporting electrolyte must be conditioned or purified. In the conditioning step, a potential of 0.0 V versus SCE (usually just negative of the oxidation potential of mercury) is applied to the electrode for a controlled time (60 - 120 sec) to clean the electrode by removing contaminants from the mercury drop or material not removed during the prior stripping step. If a thin-film electrode is being formed in situ, the conditioning potential may be set positive of the oxidation potential of mercury to provide a clean electrode surface for the deposition step. The solution is stirred during the conditioning step. Purging the solution with purified nitrogen gas for 2 - 10 min eliminates interference from oxygen.

Standard samples and a blank are carried through identical electrodeposition and stripping steps. Often the method of standard addition is used for evaluation. The limit of detection is nearly always governed by the magnitude of the blank value and not by instrumental sensitivity.

Differential pulse anodic stripping has two advantages. First, it discriminates against the capacitive component of the stripping signal. Only a portion of the metal atoms oxidized as a result of the potential step that ends an anodic pulse has a chance to diffuse away from the electrode surface before the potential step that begins the next pulse returns the potential to a value at which the metal is redeposited. Consequently, metal atoms make multiple contributions to the analytical signal and render the detection limit of differential pulse anodic stripping voltammetry lower than that of linear potential sweep anodic stripping voltammetry.

The second advantage is that linear sweep methods have continuous interference from charging current as long as the potential is scanned.

Anodic stripping voltammetry can be complicated by intermetallic formation, particularly with a thin-film mercury electrode. This occurs when metal such as zinc and copper are in high concentrations. When such intermetallics are present, the stripping peaks for the constituent metals may be shifted, severely depressed, or absent completely. The formation of intermetallics is less likely to be a problem with a hanging mercury drop electrode because the large electrode volume diminishes the maximum achievable preconcentration. Intermetallic compound formation can render the results of standard addition evaluation incorrect.

#### **Cathodic Stripping Voltammetry :**

The procedure for cathodic stripping voltammetry follows the same steps as outlined for anodic stripping voltammetry. It involves preconcentration by oxidation with subsequent stripping via a negative potential scan. Cathodic stripping voltammetry is used to determine those materials that form insoluble mercury salts on the electrode surface. At a relatively positive potential, mercury (I) ions are produced at the mercury electrode surface during an anodic preelectrolysis. Materials that precipitate with mercury (I) ions form an insoluble film on the surface of materials that precipitate with mercury (I) ions form an insoluble film on the surface of the mercury electrode. After a rest period, a cathodic scan causes the reduction of the salt to mercury and the original anion, giving a cathodic current peak.

Silver can be used as the electrode for the determination of anions that form insoluble silver salts. Materials that can be determined by cathodic stripping voltammetry include arsenate, chloride, bromide, iodide, chromate, tungstate, molybdate, vanadate, sulfate, oxalate, succinate, selenide, sulfide, mercaptans, thiocyanate, and thio compounds. Lead has been determined by cathodically stripping a film of  $PbO_2$  deposited on a  $SnO_2$  electrode.

#### **Amperometric Titrations :**

When the potential applied across two electrodes is maintained at some constant value, the current may be measured and plotted against the volume of the titrant-hence, the name amperometric titration. The current is measured either on the limiting current plateau or somewhere within the diffusion current region of a current-potential curve.

#### **Working Electrode-Reference Electrode :**

The potential of the indicator electrode is maintained at a constant value with respect to a reference electrode so that a limiting current, which is proportional to the concentration of one or more of the reactants or products of the titration, is measured. A titration curve is obtained by plotting the limiting current as a function of the volume of titrant added. The shape of the titration curve can be predicted from hydrodynamic voltammograms of the solution

obtained at various stages of the titration. As an example, consider the titration of reducible substance (lead ions) with a nonreducible titrant (sulfate ions). A voltammogram of a solution containing lead ions is represented by curve A in Fig. 4.18. If the applied potential is held at any value on the diffusion-current plateau, the current is represented by  $i_0$ , the titrant exhibits on diffusion current at the applied voltage. Successive increments of titrant remove lead ions to form a precipitate of lead sulfate. As the concentration of lead ions decreases, the diffusion current decreases successively to  $i_1$ ,  $i_2$ ,  $i_3$  and finally  $i_r$ , the residual current characteristic of the supporting electrolyte.

The intersection of the extrapolated branches of the titration curve gives the end point. Only three or four experimental points need to be accumulated to establish each branch of the curve. Amperometric titration curves are linear, as opposed to logarithmic, and thus do not rely on data in the vicinity of the end point. This is in marked contrast to the difficulty in establishing the end point in a logarithmic titration curve (as in potentiometry).

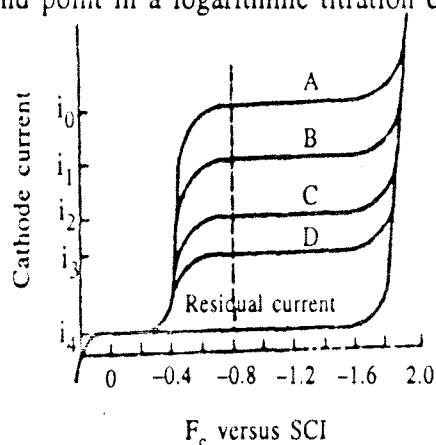


Fig. 4.18 Successive current potential curves of lead ion made after increments of sulfate ion were added.

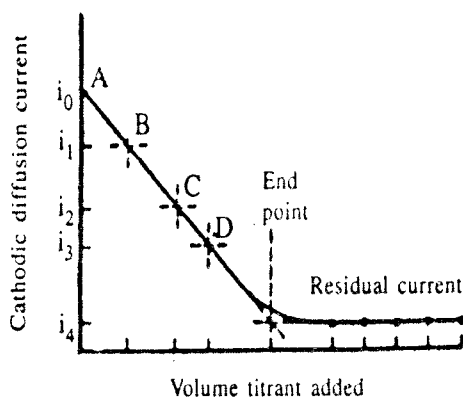


Fig. 4.19 Amperometric titration curve for the reaction of lead ions with sulfate ions. See figure 23.17 for corresponding current-potential curves. Performed at  $-0.8\text{V}$  vs. SCE.

When both titrant and sample ions give diffusion currents at the chosen voltage, the current will decrease up to the end point and then increase again to give a V-shaped titration curve. If the sample is not electroactive but the titrant is, a horizontal line is obtained that rises after the end point. When possible, the reversed L-shaped curve is preferred.

Automation is easy. The titrator can be programmed to shut off when a specified current level is reached. Titrant is run into a blank until the specified current is reached, sample is added, and the titrant is again added until the specified current level is attained.

Strictly, a correction for dilution is necessary to attain a linear relationship between current and volume of titrant, but by working with a reagent that is tenfold more concentrated than the solution being titrated, the correction becomes negligible. Incompleteness of the reaction in the vicinity of the end point usually does not detract from the results provided the reaction equilibrium is attained quickly. Points can be selected between 0% and 50% and between 150% and 200% of the end-point volume for the construction of the two branches of the titration curve. In these regions the common ion effect represses dissociation of complexes and solubility of precipitates.

#### Two-working Electrodes :

In a modification of the usual amperometric titration system, the current that results from a small fixed potential impressed between two working electrodes is measured. One electrode functions as an anode and the other as a cathode. The shape of the amperometric titration curve strongly depends on the reversibility of the electrode reactions of the titrant and titrate systems.

When the titrant (sample) involves reversible electrode reactions, a small amount of electrolysis takes place, but no net change in solution composition occurs because the amount of the oxidized form reduced at the cathode is compensated by that formed by oxidation of the reduced form at the anode. If the titrant electrode reactions are irreversible, the titration curve has the shape shown in Fig. 4.20. After the equivalence point, the current is zero or close to zero. The method was introduced years ago under the name "dead-stop end point".

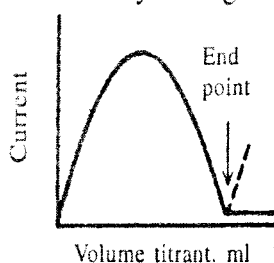


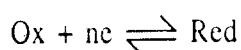
Fig.4.20: Two electrode amperometric titration when titrant electrode reactions are irreversible and with a constant potential difference impressed between two platinum indicator electrodes, The dashed line represents the curve after the end point when titrant electrode reactions are reversible.

When the titrant and its reaction product form a reversible oxidation / reduction system, the current is zero or close to zero only at the end point. Past the equivalence point, the current increases due to the increasing amount of unused electroactive titrant being added to the system.

### Chronopotentiometry :

If an unstirred ground solution containing a small amount of a depolarizer is electrolysed at constant current using a cell provided with a working electrode, a counter electrode, and a reference electrode and the potential of the working electrode is plotted against time. Then the resultant curve is similar to a conventional polarogram. The curve is referred to as a chronopotentiogram and its shape can be explained as follows.

The potential of a cathode at which a reversible reduction reaction is involved.



is given by

$$E = E^\ominus + \frac{RT}{nF} \ln(\text{Ox})/(\text{Red})$$

As soon as a small amount of reductant has been produced, the ratio (Ox)/(Red) only changes relatively slowly, and hence the potential of the electrode changes only gradually with respect to time. As electrolysis proceeds, however, the concentration of the oxidant adjacent to the electrode decreases, and although it is to a certain extent replenished by diffusion, if the magnitude of the electrolysis current is high enough, a situation is reached in which the concentration of the oxidant in the electrode layer is virtually reduced to zero. The conditions for a fixed electrode potential no longer apply, and the potential changes rapidly to a value at which a new electrode reaction is possible. The time from the commencement of electrolysis to the rapid change in potential is termed the transition time,  $\tau$ , and it was shown by Sand that this is related to the concentration of the electro-active species by the expression.

$$\tau^{1/2} = \frac{n^{1/2} n F A D^{1/2} C_0}{2I}$$

Where  $n$  = number of electrons involved in the reduction reaction.

$A$  = surface area of electrode

$D$  = diffusion coefficient of the electro-active species involved

$C_0$  = initial concentration of the depolarizer,

$I$  = the constant electrolysis current.

The variation of electrode potential with time can be expressed by the equation.

Where  $E^\ominus$  is a constant, the standard electrode potential of the metal.  $E$  can be measured by combining the electrode with a reference electrode (commonly a saturated calomel electrode), and measuring the e.m.f. of the resultant cell. It follows that knowing the potential  $E_r$  of the reference electrode, we can deduce the value of the electrode potential  $E$ , and provided the standard electrode potential  $E^\ominus$  of the given metal is known, we can then proceed to calculate the metal ion activity  $a_M^{n+}$  in the solution. For a dilute solution the measured ionic activity will be virtually the same as the ionic concentration, and for stronger solutions, given the value of the activity coefficient, we can convert the measured ionic activity into the corresponding concentration.

This procedure of using a single measurement of electrode potential to determine the concentration of an ionic species in solution is referred to as direct potentiometry. The electrode whose potential is dependent upon the concentration of the ion to be determined is termed the indicator electrode, and when, as in the case above, the ion to be determined is directly involved in the electrode reaction, we are said to be dealing with an electrode of the first kind.

It is also possible in appropriate cases to measure by direct potentiometry the concentration of an ion which is not directly concerned in the electrode reaction. This involves the use of an electrode of the second kind, an example of which is the silver-silver chloride electrode which is formed by coating a silver wire with silver chloride; this electrode can be used to measure the concentration of chloride ions in solution.

The silver wire can be regarded as a silver electrode with a potential given by the Nernst equation as

$$E = E^\ominus_{Ag^+} + (RT/nF) \ln a_{Ag^+}$$

The silver involved are derived from the silver chloride, and by the solubility product principle, the activity of these ions will be governed by the chloride ion activity.

$$a_{Ag} = K_{s(AgCl)}/a_{Cl}$$

Hence the electrode potential can be expressed as

$$E = E^\ominus_{Ag^+} + (RT/nF) \ln K_s - (RT/nF) \ln a_{Cl}$$

and is clearly governed by the activity of the chloride ions, so that the value of the latter can be deduced from the measured electrode potential.

In the Nernst equation the term  $RT/nF$  involves known constants, and introducing the factor for converting natural logarithms to logarithms to base 10, the term has a value at a temperature of 25° C of 0.0591V when  $n$  is equal to 1. Hence, for a univalent metal, a tenfold

change in ionic activity will alter the electrode potential by about 60 millivolts, whilst if the metal is bivalent, a similar change in activity will alter the electrode potential by approximately 30 millivolts, and the ionic concentration by direct potentiometry, the electrode potential must be capable of measurement to within 0.26 mV for the univalent metal, and to within 0.13 mV for the bivalent metal.

An element of uncertainty is introduced into the e.m.f measurement by the liquid junction potential which is established at the interface between the two solutions, one pertaining to the reference electrode and the other to the indicator electrode. This liquid junction potential can be largely eliminated however if one solution contains a high concentration of potassium chloride or of ammonium nitrate; electrolytes in which the ionic conductivities of the cation and the anion have very similar values.

One way of overcoming the liquid junction potential problem is to replace the reference electrode by an electrode composed of a solution containing the same cation as in the solution under test, but at a known concentration, together with a rod of the same metal as that used in the indicator electrode : in other words we set up a concentration cell. The activity of the metal ion in the solution under test is given by

$$E_{\text{cell}} = (RT / nF) \ln \frac{(\text{activity})_{\text{known}}}{(\text{activity})_{\text{unknown}}}$$

As a further refinement of this procedure, provided that we start with a solution containing a known ionic concentration which is greater than that in the solution under measurement, then by a process of accurate dilution of the standard solution, we can adjust its concentration to be the same as that in the solution under test. This process will be accompanied by a gradual fall in the e.m.f of the concentration cell, and when the two solutions have the same concentration the cell e.m.f will be zero; this procedure is termed null point potentiometry.

In view of the problems referred to above in connection with direct potentiometry, much attention has been directed to the procedure of potentiometric titration as an analytical method. As the name implies, it is a titration procedure in which potentiometric measurements are carried out in order to fix the end point. In this procedure we are concerned with changes in electrode potential rather than in an accurate value for the electrode potential with a given solution, and under these circumstances the effect of the liquid junction potential may be ignored. In such a titration, the change in cell e.m.f occurs most rapidly in the neighbourhood of the end point, and as will be explained later, various methods can be used to ascertain the

point at which the rate of potential change is at maximum; this is the end point of the titration.

#### **Ion - sensitive electrodes :**

Pungor developed an iodide-ion-sensitive electrode by incorporating finely dispersed silver iodide into a silicone rubber monomer and then carrying out polymerization. A circular portion of the resultant silver iodide-impregnated polymer was used to seat the lower end of a glass tube which was then partly filled with potassium iodide solution (0.1 M), and then a silver wire was inserted to dip into a potassium iodide solution. When the membrane end of the assembly is inserted into a solution containing iodide ions, we have a situation exactly similar to that encountered with glass membrane electrodes. The silver iodide particles in the membrane set up an exchange equilibrium with the solutions on either side of the membrane. Inside the electrode, the iodide ion concentration is fixed and a stable situation results. Outside the electrode, the iodide ion concentration is fixed and a stable situation results. Outside the electrode, the position of equilibrium will be governed by the iodide ion concentration of the external solution, and a potential will therefore be established across the membrane and this potential will vary according to the iodide ion concentration of the test solution.

The original Pungor or heterogeneous membrane type of electrode has been extended to give electrodes capable of measuring the concentration of  $\text{Cl}^-$ ,  $\text{Br}^-$ ,  $\text{CN}^-$ ,  $\text{S}^{2-}$ , and many other anions, and electrodes suitable for measuring the concentration of  $\text{Cl}^-$ ,  $\text{Br}^-$ ,  $\text{I}^-$  can be obtained by using a membrane cast from the appropriate pure silver halide; that is to say, the inert matrix is dispensed with, and we are dealing with a solid state electrode. A particularly useful application of this last technique is the single crystal lanthanum fluoride electrode developed by Orion Research Inc, which can be used to measure the concentration of fluoride ions in solution.

#### **Liquid Membrane Electrodes :**

Another type of selective ion electrode is based upon the use of liquid ion exchange materials, usually consisting of an ion exchange material dissolved in an organic solvent which is not miscible with water to any great extent and thus obviating undue mixing of the electrode material with the solution to be analysed. Two different types of electrode are used : (a) those in which the liquid exchanger contains the ion to which the electrode is responsive, and (b) those in which the liquid exchanger is electrically neutral and does not contain any ions.

Important electrodes of the first type are (i) the calcium-responsive electrode based upon the calcium salt of didecyl hydrogen phosphate dissolved in di-n-octylphenylphosphonate, and (ii) the anion-responsive electrodes based upon the methyl tri-octanoyl-ammonium cation: these are suitable, inter alia, for the determination of  $\text{ClO}_4^-$ ,  $\text{SO}_4^{2-}$ , and many organic anions. An example of the second kind of electrode is the Philips potassium electrode in which the

ion exchange material is an antibiotic (valinomycin) dissolved in diphenylether. Valinomycin forms an association complex with alkali metal ions with the important feature that the selectivity coefficient  $K^+$  as compared with  $Na^+$  is about 4000, and for  $K^+$  as compared with  $H^+$  is about 18000, so that the electrode can be used to determine potassium in the presence of large amounts of sodium, and in relatively strongly acid solutions.

In these liquid membrane electrodes, the solution of the ion exchange material is placed in a tube closed by a porous diaphragm at its lower end, and the internal silver-silver chloride electrode in potassium (or sodium) chloride solution is placed in a narrow tube which is mounted inside the wider one.

In a recent development it has been shown that if the active components of a liquid membrane electrode (exchange medium plus solvent) are added to a solution of polyvinyl chloride in tetrahydrofuran, and the resulting mixture allowed to stand for some days for the tetrahydrofuran to evaporate, then a solid residue is left, from which a circle may be cut and cemented to the end of a PVC tube. This arrangement then functions as a heterogeneous membrane type of electrode, responding to the same ion(s) as the original liquid membrane electrode.

#### Commercially Available Ion-Sensitive Electrodes :

At present, a number of ion selective electrodes are available from laboratory supply houses and new ones are frequently being added : whilst not intended to be an exhaustive list Table XIV, 2 serves to indicate the range of determinations for which electrodes are now available.

A range of gas-sensing electrodes are also available which can be used to determine soluble gases such as hydrogen chloride, ammonia, sulphur dioxide, and carbon dioxide. In these electrodes the gas stream is passed through a tube containing a semi-permeable membrane separating it from a solution of carefully selected pH. The soluble gas will pass through the membrane, dissolve in the solution and thus affect the pH. The actual measuring electrode is a pH-responsive glass electrode, and the measured change in pH can be related to the concentration of the gas under investigation.

As already explained, some care must be exercised in using an ion-sensitive electrode to ensure that interferences do not arise from other ions, and it is of course also necessary to ensure that the ion which is to be measured has not undergone complex formation with any of the reagents which have been added to the solution; conversely, it may be possible to reduce the interference due to a given ion by adding a reagent which will complex the interfering ion.

**Table 4.5 : A selection of commercially available ion sensitive electrodes :**

Type of membrane	Ion	Lower Limit of detection (mol dm <sup>-3</sup> )
Glass	H <sup>+</sup>	10 <sup>-14</sup>
	Na <sup>+</sup>	10 <sup>-6</sup>
	K <sup>+</sup>	10 <sup>-6</sup>
Liquid	K <sup>+</sup>	10 <sup>-6</sup>
	Ca <sup>2+</sup>	10 <sup>-5</sup>
	NO <sub>3</sub> <sup>-</sup>	10 <sup>-5</sup>
	ClO <sub>4</sub> <sup>-</sup>	10 <sup>-5</sup>
Solid	Ag <sup>+</sup>	10 <sup>-17</sup>
	Pb <sup>2+</sup>	10 <sup>-7</sup>
	Cd <sup>2+</sup>	10 <sup>-7</sup>
	Cu <sup>2+</sup>	10 <sup>-8</sup>
	F <sup>-</sup>	10 <sup>-6</sup>
	Cl <sup>-</sup>	5 × 10 <sup>-5</sup>
	Br <sup>-</sup>	5 × 10 <sup>-6</sup>
	I <sup>-</sup>	5 × 10 <sup>-8</sup>
	CN <sup>-</sup>	10 <sup>-6</sup>
	SCN <sup>-</sup>	10 <sup>-5</sup>
	S <sup>2-</sup>	10 <sup>-17</sup>

As an example, if it is required to measure the fluoride ion concentration of a solution with a fluoride-responsive electrode, it is important to ascertain whether the solution contains any aluminium which causes formation of the ion  $\text{AlF}_6^{3-}$ ; the fluoride ion which is thus bound will not affect the fluoride ion electrode. If the solution does contain aluminium, it is treated with a complexing agent (e.g., cyclohexane - diamine - tetra - acetic acid) which complexes the aluminium and releases the fluoride ion from the  $\text{AlF}_6^{3-}$  ion.

#### **Column Chromatography :**

Chromatography is based on the general principles of phase distribution. The method involves the selective removal of the components of one phase from that phase when it flows past a second stationary phase. The stationary (fixed) phase is generally a column or strip through which flows the moving phase. The removal of a component by the fixed phase is essentially an equilibrium process. Separation of two or more components is possible when the equilibrium constants for the distribution of these components between the two phases vary. Expressed simply, the molecules of a substance which interact strongly with the fixed phase

will move only slowly through the column whereas substances which do not interact strongly are carried through more rapidly. This results in the migration of components into separate regions referred to as the bands of the fixed phase.

Chromatography was invented by the Russian botanist Mikhail Tswett who employed this technique to separate plant pigments like chlorophylls and xanthophylls using a column of calcium carbonate. Since the separated components appeared as coloured bands on the column, the name chromatography was given by the inventor of this technique (chroma = colour). As of now, chromatography encompasses a diverse group of separation methods that make possible separation, purification and identification of closely related components of a mixture. The only common factor of all these separation methods is that these employ a stationary phase and a mobile phase.

There are three types of chromatographic methods depending on the nature of the fixed phase.

**1. Adsorption Chromatography :** A solid which is insoluble in the solvents chosen may be used as the fixed phase. The mode of interaction between the components of the mixture and the fixed phase is adsorption. Hence the method is called adsorption chromatography. The adsorption could be caused by electrostatic attraction, complexation, hydrogen-bonding, van der Waals forces, etc.

**2. Partition Chromatography :** The fixed phase may be a solid on which a liquid is very firmly adsorbed so as to form a stationary phase. Distribution of components of a mixture could occur between the adsorbed liquid and the flowing liquid (mobile phase) because of differences in solubility. The adsorbed liquid should be immiscible with the flowing liquid. The technique is referred to as partition chromatography.

In paper chromatography, a paper strip is used as the 'column' through which flows the mixture in an organic solvent. Since a layer of adsorbed water carried by the paper acts as the fixed phase, this method is regarded as a kind of partition chromatography.

**3. Ion-Exchange Chromatography :** This involves an exchange of ions of like sign between a solution and an essentially insoluble solid in contact with the solution. The mobile phase could be a liquid (which can percolate through the fixed phase by forces of gravity or capillary forces) or a gas which can be forced through the fixed phase by pressure.

#### **Column Chromatography :**

The technique is a type of solid liquid adsorption chromatography. The fixed phase is a solid and the mobile phase a liquid. The basis of separation is selective adsorption of the components presents in the liquid phase on the solid.

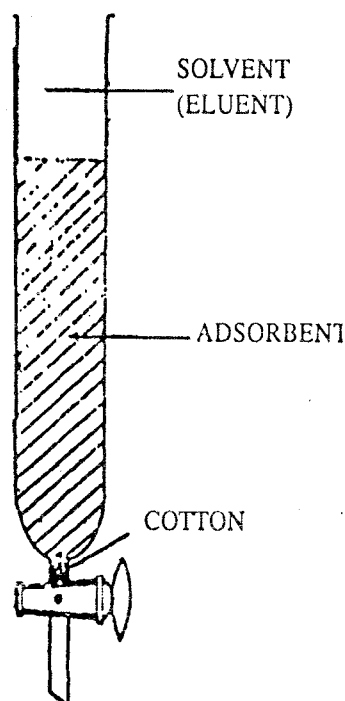


Fig. 4.21

A column such as the one shown in Fig. 4.21 is used. According to scale of the experiment, columns from a few mm to several cm in diameter are used. A long, thin column assures best separation in many difficult cases but large quantities of readily separable substances can be separated more rapidly using a wide column. The column is packed with an active solid such as alumina or silica gel. Apart from these two substances, charcoal, magnesia, calcium carbonate, starch, sucrose, talc and fluorisil (fluorinated silicon polymer) are also used as solid adsorbents. For a good separation, the solid adsorbent should be of uniform particle size and of high specific area, a property which can contribute to rapid equilibrium of the solute between the two phases.

The column has to be filled with adsorbent very carefully, because irregularities such as air gaps may lead to : (i) mixing of separated zones and (ii) channels through which the solution can flow unchanged. The adsorbent is usually made into a slurry with a solvent such as petroleum ether, poured into the column and allowed to settle. During the packing, continual tapping of the column with a pencil or glass rod may help form an evenly packed column. After packing the column with the adsorbent a small liquid sample is poured on the top. The sample gets adsorbed at the top of the column. An eluting solvent is then allowed to flow through the column. This solvent carries with it the components of the mixture. Because of the selective adsorption capacity of the solid phase the components move down the column at different rates. The progressive separation of the components into bands is shown in Fig. 4.22

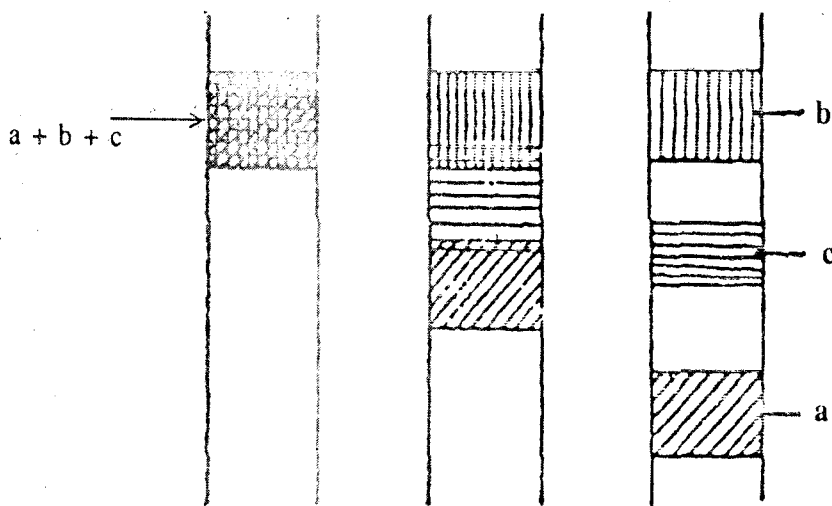


Fig. 4.22 Separation of components into bands.

The separated components may be recovered from the column in two ways :

(i) The solvent can be sent through the column until the bands are eluted from the bottom of the column and collected in different containers. Removal of the solvent by a suitable method gives the pure components of the mixture.

(ii) If the solid can be extracted from the column in one piece, the portion of the solid containing different bands may be cut out separately and extracted with appropriate solvents. This method is more difficult than the first.

**Note :** The bands may be directly observed only with coloured materials. In dealing with colourless materials the chromatographic experiment is followed by collecting a series of fractions of eluent of constant volume, say, 10 ml. The solvent is then evaporated to check whether any solute is present. The different components may be distributed among several containers. Even though the method is tedious, this is generally adopted. With a few colourless materials the separation can be attempted with coloured derivatives; for example, mixed aldehydes and ketones could be converted into dinitrophenylhydrazones and then separated. Colourless samples may sometimes be made visible on the column by fluorescence excited by an ultraviolet source.

The success of a chromatographic separation not only depends on the proper choice of a column material but also on the proper selection of solvent(s). The solvent also may be adsorbed on the solid. Thus, there is a competition between solvent molecules and the component molecules for the active centres on the solid. If the solvent is more polar and hence more strongly adsorbed than the components of the mixture, the latter would remain almost entirely in the mobile phase and little separation would occur. Therefore, the eluting solvent must be less polar than the components of the mixture. Besides, the components must be soluble in the solvent; otherwise, the components remain permanently adsorbed on the solid. The eluting powers of solvents increase in the order.

The best solvent for a particular mixture is chosen only by trial and error. A mixture of two solvents is sometimes found to be more useful than individual solvents.

**Note :** For a demonstration in a class, separation of syn- and anti-azobenzene may be attempted. A 50 ml burette may be used to prepare a column of alumina (about 15 g). Petroleum ether may be used as the solvent.

#### **Applications of Column Adsorption Chromatography :**

1) This technique is used to remove small amounts of impurities whose structures differ widely from that of the major component. A column material through which the major component passes readily but the impurities get adsorbed can be selected. Many solvents for spectroscopy are purified this way; for example, commercial samples of aliphatic hydrocarbons are freed from aromatic hydrocarbons by a single passage through silica gel column.

2) The homogeneity of a coloured compound can be tested easily.

3) The most useful application is separation of structurally similar compounds.

4) Using column adsorption, chromatography, even gases can be separated. In this technique, referred to as Gas Adsorption Chromatography, a 'carrier' gas such as nitrogen replaces the solvent. The method is normally applied to the separation of mixtures of gases or low boiling hydrocarbons.

#### **Thin layer chromatography :**

Thin-layer chromatography, abbreviated as tlc, involves the same principles as those of column chromatography. It is a form of solid liquid adsorption chromatography. The tlc, separation takes place on a layer of finely divided solid that is fixed on a flat surface.

**Preparation of tlc Plates.** The same solid adsorbents used for column chromatography are employed for tlc. Silica and alumina are widely used. A thin layer plate is prepared by spreading an aqueous slurry of the finely ground solid on the clean surface of a glass or rigid plastic. A small amount of a binder (for example, plaster of Paris, calcium sulphate or starch) is incorporated into the slurry to increase adhesion of the solid particles to the glass and to one another. The plate is then heated in an oven for about 30 minutes, and cooled inside the oven itself. Care is taken to avoid exposing the surface to the atmosphere. Otherwise, the plate adsorbs water in a few minutes and the solid merely becomes a support for water.

**Plate Development :** A drop of the solution of the mixture to be separated is placed near one edge of the plate and its position is marked with a pencil. The plate is then placed in a container (developing chamber) with enough solvent to come to a level just below the original sample spot. The chamber is kept closed with a flat glass plate. The solvent migrates

up the plate carrying with it the components of the mixture at different rates. After the solvent has reached almost the top edge of the plate, the latter is removed and dried.

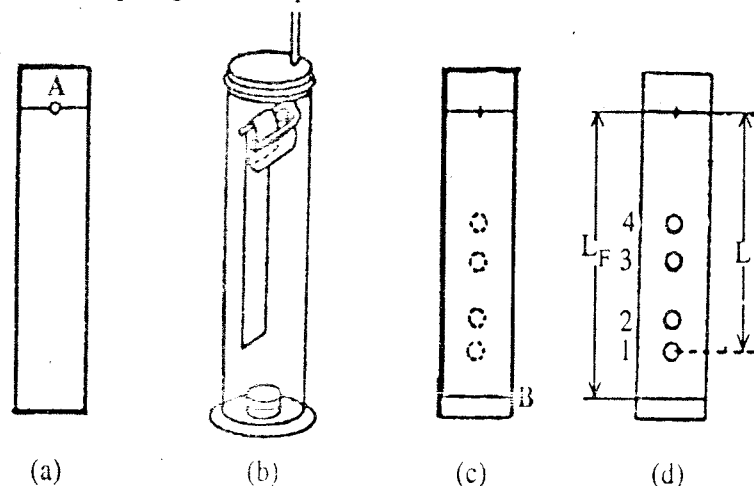


Fig. 4.23

A number of methods are available for locating the spots of colourless materials. Irradiation of the plate with ultraviolet light will permit location of spots of compounds that exhibit fluorescence. There are some detecting agents, which when sprayed on the chromatograms, make the spots readily visible for example, sulphuric acid and potassium permanganate solution. Iodine is another good detecting agent. In this case the plate is kept in a vessel saturated with iodine vapour. Iodine is absorbed by many organic compounds and consequently brown spots appear on the chromatogram.

Under a given set of conditions (adsorbent, solvent, layer thickness) the rate of movement of a compound with respect to the rate of movement of the solvent front is a property characteristic of the compound. This property, represented by the symbol  $R_f$  (Retention Front) is obtained by dividing the distance traveled by the substance by the distance traveled by the solvent front from the original spot.

**Note :** For a demonstration experiment, the teacher may attempt the separation of green leaf pigments. A few green leaves may be crushed with a few milliliters of a 2 : 1 mixture of petroleum ether and ethanol with a pestle. The extract is washed with water and the aqueous layer rejected. The petroleum ether solution can be used for spotting the plate. Using a mixture of benzene and acetone (7:3) as a developing solvent, as many as eight coloured spots would be observed.

#### Applications :

1. Since the technique is easy and can be done rapidly, it is ideal for routine analysis of mixture composition. A great advantage of the method is that only a very small quantity of the sample (approximately  $10^{-9}$ g) is required.

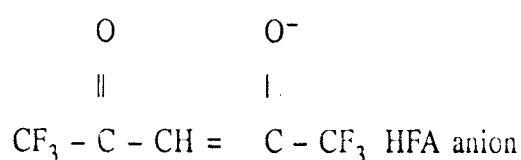
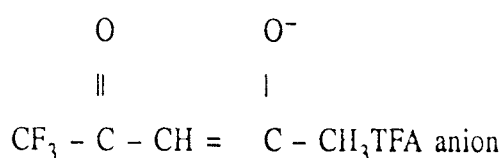
2. Tlc may be used to find out the best eluting agent for column chromatography.

3. A semiquantitative estimate of the amount of a component present can be obtained by a comparison of the area of a spot with that of a standard.

4. TLC of Inorganic Ions. The individual ions can be readily identified by the common detection reactions of a chromatogram. This pre-separation of ions into groups by classical methods is desirable. For example, using a silica gel thin-layer plate with a mixture of n-butane and 1.5 N hydrochloric acid as solvent, the ions of copper group can be separated and identified. The sequence of ion movement is  $Hg > Bi > Cd > Pb > Cu$ . The plate is inserted into a tank filled with hydrogen sulphide gas. The ions are identified by the appropriate coloured spots.

#### Gas Liquid Chromatography :

Although inorganic compounds are generally not so volatile as are organic compounds, gas chromatography has been applied in the study of certain inorganic compounds which possess the requisite properties. If gas chromatography is to be used for metal separation and quantitative analysis, the types of compounds which can be used are limited to those that can be readily formed in virtually quantitative and easily reproducible yield. This feature, together with the requirements of sufficient volatility and thermal stability necessary for successful gas chromatography, make neutral metal chelates the most favourable compounds for use in metal analysis.  $\beta$ -Diketone ligands, e.g., acetylacetone and the fluorinated derivatives, trifluoroacetylacetone (TFA) and hexafluoroacetylacetone (HFA) form stable, volatile chelates with aluminium, beryllium, chromium (III) and a number of other metal ions; it is thus possible to chromatograph a wide range of metals as their  $\beta$ -diketone chelates.



The number of reported applications to analytical determinations at the trace level appear to be few, probably the best known being the determination of beryllium in various samples. The method generally involves the formation of the volatile beryllium trifluoroacetylacetonate chelate, its solvent extraction into benzene with subsequent separation and analysis by gas chromatograph.

## Gas Liquid Chromatography (GLC or GLPC)

In GLC the mixture to be separated is vaporized and sent through a column by a flowing inert gas such as hydrogen or helium. The inert gas is called the carrier gas. The gaseous mixture is the mobile phase. The column is packed with a solid on the surface of which is adsorbed a liquid of very low volatility. This liquid serves as the fixed phase. The components of the mixture move through the column at different rates due to selective phase distribution between the two phases and thus get separated.

In general, low boiling and highly volatile components move through the column faster than low volatile components because, to a rough approximation, the higher the vapour pressure of a gas, the lower is its solubility in a liquid. Apart from volatility, polar interactions significantly affect the solubility of a solute in a solvent.

Numerous instruments for GLC are available commercially. The basic components of a gas-liquid chromatograph are shown schematically in Fig. 4.24

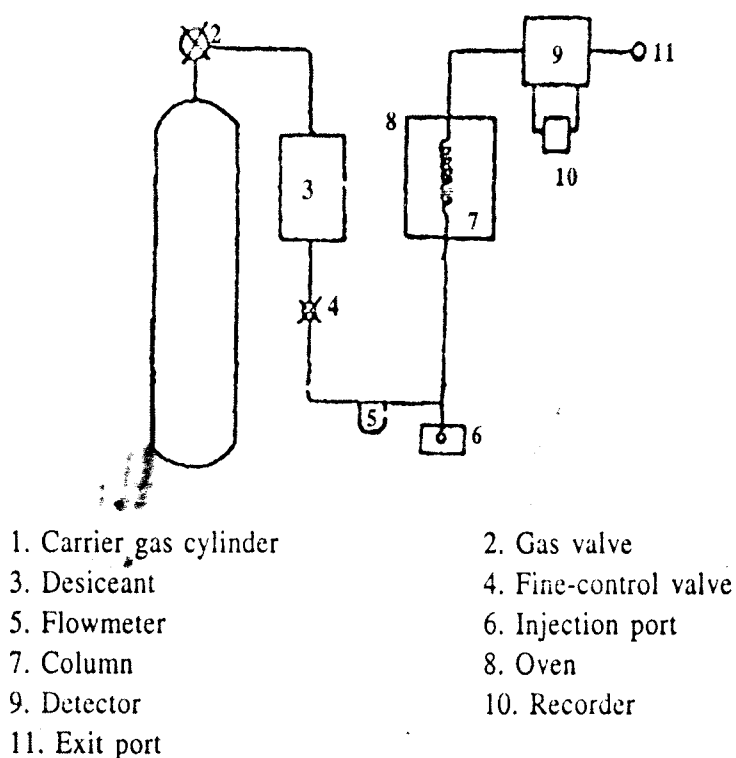
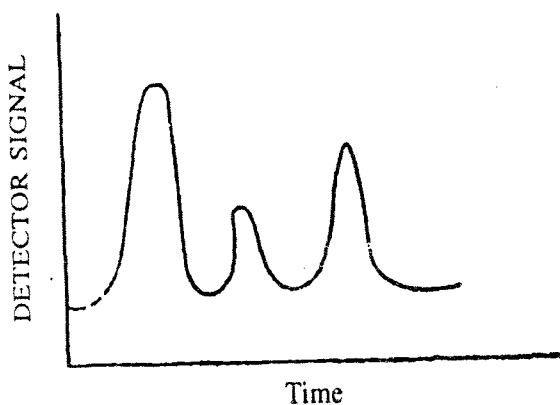


Fig. 4.24 Schematic diagram of a gas chromatograph

The column is kept in an oven whose temperature is controlled by a thermostat and heating elements. The sample is introduced into the flow system at the injection part. This unit is individually heated to facilitate vaporization of the sample. As the vaporized sample is swept

into the column by the carrier gas, its components separate into individual bands in the carrier gas and pass into the detector.

A relatively simple detection system consists of an instrument called katharometer which measures changes in the thermal conductivity of the gas stream. The instrument consists of an electrically heated wire which forms one arm of a wheatstone bridge. The wire assumes a steady temperature and resistance when the pure carrier gas flows over it. As the separated components reach the wire, its temperature increases as a result of a decrease in thermal conductivity of its surroundings. The consequent change in resistance is measured by the bridge. The change in resistance is proportional to the concentration of the component. The bridge is coupled to a pen recorder and chromatogram consists of a plot concentration of the component in the carrier gas versus time. A typical chromatogram is shown in Fig. 4.25



**Fig.4.25 A typical chromatogram**

Note : The thermal conductivities of hydrogen and helium are roughly six to ten times than those of most organic compounds. The presence of even traces of other materials causes a relatively large decrease in thermal conductivity. That is why these two gases are preferred to nitrogen and carbon dioxide, whose thermal conductivity values are in the same range as those of most organic substances.

The choice of the stationary liquid phase depends on the types of compounds to be separated. The best choice would be that liquid giving rise to significant differences in partition coefficients of the components to be separated. Squalene, polyethylene glycol, diethylene glycol adipate, diethylene glycol succinate and butanediol succinate are some of the substances commonly used as stationary phases. The liquid is coated on the solid support by dissolving the liquid in a low boiling solvent and mixing the solid with this solution. Evaporation of the solvent leaves the solid granules evenly coated.

**Detection Systems :** The solute concentration in a carrier gas at any instant is only a few parts per thousand. The detector system that is used, therefore, should be sensitive enough to respond to such low through the detector is usually one second or less. The detector,

therefore should be capable of exhibiting its full response within this period. More than a dozen different types of detectors are used. The most widely used of these are the thermal conductivity detector, the flame ionization detector and the electron capture detector. The first of these has already been described.

**Flame-Ionisation Detector :** Many organic compounds, when pyrolysed at the temperature of a hydrogen / air flame, produce species. These ions can be collected and the resulting ion-current measured. An electrometer must be employed for measurement of current since the latter would be very small because of the high resistance of flame. The hydrogen-flame detector is a very popular and sensitive detector. A schematic diagram of flame-ionisation detector is shown in Fig. 4.26

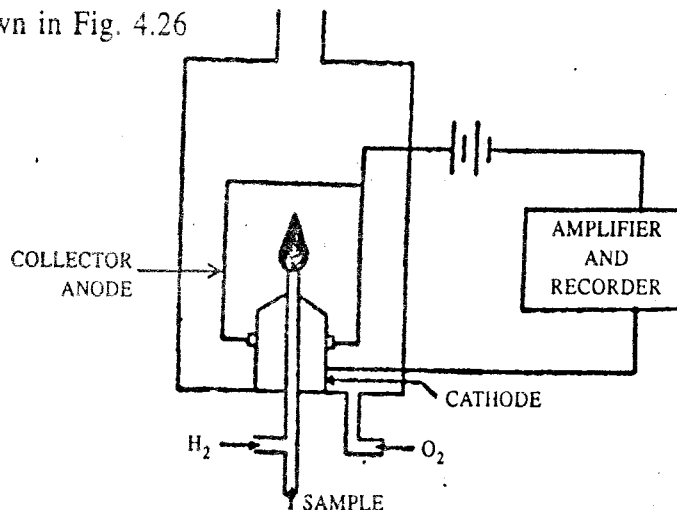


Fig. 4.26 Flame - ionisation detector

The hydrogen - flame detector is more expensive than the thermal conductivity detector but is much more sensitive than the latter.

**Electron-capture Detector :** This functions in the same way as a proportional counter for measurement of X-radiation. The effluent from the column is allowed to pass over a  $\beta$ -emitter such as nickel-63. An electron from the emitter causes ionization of the carrier gas and production of an innumerable number of electrons. A constant standing current results from this ionization process in the absence of organic molecules. However, in the presence of organic molecules that tend to capture electrons, a decrease in the current is expected and this is what is measured.

The electron-capture detector is very sensitive towards a few functional groups such as halogens, peroxides, quinines and nitro groups but insensitive to compounds such as alcohols, hydrocarbon and amines.

### Applications

1) GLC is used for separation of mixtures and identification of the components from a quantity called retention time. The time taken by a given component to pass from the injection part to the detector is known as its retention time. For any given column and a set of conditions (flow rate and temperature) the retention time is a characteristic property of the compound and therefore may be used to identify the latter.

2. GLC provides a convenient method of quantitative analysis of small amount of mixtures: provided all the components are known. The area under the peak in a chromatogram is proportional to the concentration of the component responsible for that peak.

3. GLC can be used for purification of a compound as an alternative to distillation. As the vapour of the compound comes from the exit part, it is collected and condensed.

### High Performance Liquid Chromatography (HPLC)

In the conventional column chromatography, flow rates of the eluting solvent are of the order of a few drops per minute. Separations using column chromatography are, therefore, time consuming. Attempts to speed up the classical procedure by application of vacuum or by pumping decrease the efficiency of separation. The column efficiency increases greatly on decreasing the particle size of the solid adsorbent. In 1960, a powerful technique, taking advantage of this observation, was developed. Particles with diameter as small as  $10 \mu\text{m}$  are used as packings in the column. Generally, finely divided silica gel is used for packing the columns. Occasionally alumina and Celite are also employed. To have appreciable flow rates (approximately  $3 \text{ ml / min}$ ) high pressure of the order of  $1000 - 6000 \text{ psi}$  is employed. The technique is known as High Performance Liquid Chromatography.

Although the currently available commercial equipment is rather expensive, HPLC has already shown itself to have wide application in organic chemistry. The development of inorganic application is likely, e.g., in the field of ion exchange chromatography where pellicular resins, that is, resins produced as thin coatings on the surface of spherical glass beads ( $20 - 50 \text{ micrometres}$  diameter), are now available commercially under the trade name 'Zipax'. The beads have a porous surface about  $2 \text{ micrometres}$  thick which serves to bond the resin coating.

The application of high performance ion exchange chromatography for the separation of inorganic compounds is illustrated by the separation of transplutonium elements; the method is based on sequential elution of the cations from a cation exchange column with an anionic complexing agent. Exposure of separation is achieved in a much shorter time, and radiation induced damage to the resin is minimized.

### Solvent Extraction :

Extraction with solvents is used as a method for separation of dissolved substances from solutions. It can also be used for the separation of one constituent from a solid mixture as well as for the removal of undesired soluble impurities from mixtures.

Extraction with a second solvent is an application of the Nernst distribution law which states that at constant temperature a solute distributes itself between two immiscible solvents only in a particular ratio. When a substance distributes itself between two solvents without the complications of dissociation or association, it is possible to calculate the weight of the substance which can be removed by a series of extractions. If  $\gamma_1 \text{ ml}$  of a solution contains  $W_g$  of a substance and if the substance is repeatedly extracted with  $\gamma_2 \text{ ml}$  of another solvent, the weight of the substance  $W_n$  remaining in the first solvent after  $n$  extractions is given by

$$W_n = W \left( \frac{K\gamma_1}{K\gamma_1 + \gamma_2} \right)^n$$

Where  $K$  is the distribution coefficient. The equation predicts that for a given volume of solvent the extraction process is more efficient with several extractions with aliquot parts than a single extraction with all the available solvent. Larger the value of  $K$ , more efficient is the extraction.

Consider now a solution of two compounds in a solvent. For effective separation of these two compounds by extraction with a second solvent, the distribution coefficient of one should be significantly greater than 1.0 whereas the distribution coefficient of the other should be significantly smaller than 1.0. If this condition is met, one compound will be mainly distributed in one solvent and the other in the other solvent. Physical separation of the two liquids results in a partial separation of the two compounds.

The common solvents used for extraction in the laboratory are diethyl ether, benzene, petroleum ether, chloroform and carbon tetra chloride. A good solvent for extraction should satisfy two important conditions, viz, : (i) the substance extracted should be highly soluble in the solvent, (ii) after the extraction the solvent should be easily separable from the solute. For the extraction of organic substances generally, diethyl ether is used because organic substances are generally soluble in ether and ether has got a low boiling point making its removal after the extraction very easy. Ether is highly flammable and hence should be handled with care. Di isopropyl ether is better than diethyl ether in this respect but it is not very commonly used because of its very high cost.

The extraction with a second solvent may be carried out in the laboratory with a separating funnel. The separating funnel is provided with a ground glass stopper and a stop-cock. The funnel is usually mounted in a ring on a stand. When an aqueous solution is shaken with ether in a separating funnel and allowed to settle, two sharply defined layers are formed. The two layers can be separated by opening the stop-cock and allowing the lower aqueous layer to drain slowly into a beaker.

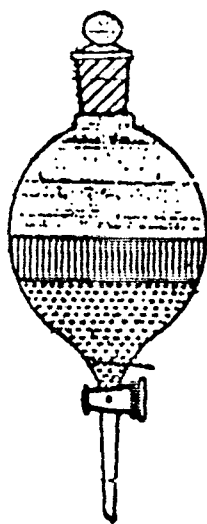


Fig 4.27 Separating funnel

When metal ions are converted into chelate compounds by treatment with suitable organic reagents, the resulting complexes are soluble in organic solvents and can thus be extracted from the aqueous solution. Many ion-association complexes containing bulky ions which are largely organic in character (e.g. the tetraphenylarsonium ion  $(C_6H_5)_4As^+$ ) are soluble in organic solvents and can thus be utilized to extract appropriate metal ions from aqueous solutions and can thus be utilized to extract appropriate metal ions from aqueous solution. Such treatment may be used to isolate the ion which is to be determined, or alternatively, to remove interfering substances.

### **Ion Exchange Chromatography :**

Ion-exchange is a process involving exchange of ions of like sign between a solution and a solid in contact with the solution. The ion-exchange properties of clays and zeolites have long been realized. But several synthetic materials which act as ion-exchangers have been made since 1935, Today, ion-exchange resins are the most widely used packings in column chromatography. Ion-exchange chromatography is a special name given to column chromatography when the stationary phase is an ion-exchange resin.

Synthetic ion-exchange resins are high molecular weight polymeric materials containing a large number of ionic functional groups per molecule. Cation exchangers contain sulphonic acid groups ( $RSO_3^-H^+$ ) or carboxylic acid groups. Anion - exchange resins contain amines attached to the polymer molecule  $RN(CH_3)_3 OH$ .

Ion-exchange chromatography found its first major application in the separation of rare earths. A column was packed with an acid resin and treated first with hydrochloric acid to make sure that all exchange points were occupied by hydrogen ions. A mixture of rare earths as their chlorides was sent down the column. This resulted in the displacement of hydrogen ions by rare earth cations. The rare earth ions could then be eluted one after another. Since elution with water was very slow, a solution of citric acid was used as eluting solvent. The cations moved at different rates depending on the stability of the corresponding complex with citric acid.

There are two distinct advantages in ion-exchange chromatography :

1. Since the capacity of the resins for exchange is quite high, it is easy to handle as much as 0.1 g at a time.

2. The recovery of ions from the column is virtually complete which is an important factor in dealing with expensive materials and in quantitative works.

Ion exchange materials are insoluble substances containing ions which are capable of replacement by ions from a solution containing electrolytes. The phosphate ion is an interference encountered in many analyses involving the determination of metals; in other than acidic solutions the phosphates of most metals are precipitated. If, however, the solution is passed through a column of an anion exchange resin in the chloride form, then phosphate ions are replaced by chloride ions. Equally, the determination of phosphates is difficult in the presence of a variety of metallic ions, but if the solution is passed through a column of a cation exchange resin in the protonated form, then the interfering cations are replaced by hydrogen ions.

## UNIT - V

### ORGANOMETALLIC CHEMISTRY

#### Introduction :

Organometallic chemistry is the chemistry of compounds containing metal-carbon bonds. Main-group metals and transition metals, as well as lanthanides and actinides, form bonds to C.

Organometallic chemistry has undergone a renaissance in the last 40 years. However, Zeise prepared the first organometallic compound in 1827, and Frankland developed chemistry of alkyl zinc compounds in the mid-and late nineteenth century. Much interest centers on organometallic chemistry because of its importance in catalysis. Transformations in organic molecules on laboratory and industrial scales often involve catalysis, providing a low-energy reaction pathway for their combination with other bonded species, and release the weakly bonded products. For example, Reppe found over 40 years ago that  $\text{Ni}(\text{CN})_2$  catalyzes tetramerization of acetylene to cyclooctatetraene, which presumably involves assembling the reactants by coordination to Ni :

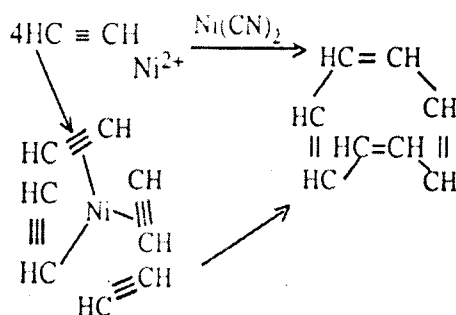


Fig. 5.1

Synthetic, spectroscopic, and kinetic techniques have been used to probe processes that occur with reactants in the same phase (homogeneously). Investigation of the fundamental chemistry of organometallic complexes has uncovered a tremendous number of intriguing reactions and modes of ligand attachment. The results have been applied to improving product yield and selectivity of catalyzed reactions. A variety of novel and synthetically useful stoichiometric reactions also have been developed.

#### Effective Atomic Number (EAN) Rule :

The most satisfactory formula of carbon monoxide is  $:\text{C}:::\text{O}:$

From the structure of carbon monoxide, it is probable that the lone pair of electrons on the carbon atom can be used by forming a dative bond with certain metals ( $\text{M} \leftarrow \text{C} \equiv \text{O}$ ). Thus, ( $\text{M} \leftarrow \text{C} \equiv \text{O}$ ) types of bonds were assumed to be present in metal carbonyls.

Table 5 : 1

Carbonyls	Atomic number of the metal	Number of electron contributed by CO groups	E.A.N	Succeeding inert gas
Cr(CO) <sub>6</sub>	24	12	36	Kr(36)
Fe(CO) <sub>5</sub>	26	10	36	Kr(36)
Ni(CO) <sub>4</sub>	28	8	36	Kr(36)
Mo(CO) <sub>6</sub>	42	12	54	Xe(54)
Ru(CO) <sub>5</sub>	44	10	54	Xe(54)
W(CO) <sub>6</sub>	74	12	86	Rn(86)
O <sub>5</sub> (CO) <sub>5</sub>	76	10	86	Rn(86)

In the formation of  $M \leftarrow C \equiv O$  bonds, the electrons are supplied solely by the molecules of carbon monoxide and the metal atom is thus said to have zero-valency. The number of molecules of carbon monoxide which can unite with one atom of the metal is apparently controlled by the tendency of the metal atom to acquire the effective atomic number of the next inert gas. This is given for the stable monomeric carbonyl :

$$E.A.N. = m + 2y = G$$

where  $m$  is the atomic number of the metal  $M$  and  $y$  is the number of carbon monoxide molecules is one molecule of the carbonyl  $M(CO)_y$  and  $G$  is the atomic number of the next inert gas.

On the basis of EAN rule it can be explained why Ni atom fails to form a hexacarbonyl,  $Ni(CO)_6$ . Non-formation of  $Ni(CO)_6$  would be equal to  $28 + 2 \times 6 = 40$  which is not the atomic number of any of the noble gases.

Mononuclear carbonyls having the metallic atom with odd atomic number :  $V(CO)_6$  and hypothetical carbonyls viz.  $Mn(CO)_5$  and  $Co(CO)_4$  are the examples of such carbonyls. These carbonyls do not obey EAN rule as shown below :

$$\begin{array}{rcl}
 V = 23e^- & Mn = 25e^- & Co = 27e^- \\
 6CO = 12e^- & 5CO = 10e^- & 4CO = 8e^- \\
 \hline
 V(CO)_6 = 35e^- & Mn(CO)_5 = 35e^- & Co(CO)_4 = 35e^- \\
 \hline
 \end{array}$$

The metals with odd atomic numbers cannot form mononuclear carbonyls because they cannot acquire an inert gas electronic configuration by combination with CO molecules. Therefore, such metals form poly-nuclear carbonyls. For example, the simplest carbonyl formed by Mn(25) and Co(27) are  $Mn_2(CO)_{10}$  and  $Co_2(CO)_8$ , respectively.

Evidence for the structure of polynuclear carbonyls is not complete.

### Polynuclear carbonyls :

Sidgwick and Bailey have shown that the formulae of polynuclear carbonyl can be fitted to an extension of the same rule. For the carbonyl  $M_x(CO)_y$  the general relation is

$$G - \frac{xm + 2y}{x} = x - 1$$

Where G = The atomic number of the next inert gas,

m = The atomic number of metal atoms and

y = The number of CO molecules in one molecule of the carbonyl.

As regards polynuclear carbonyls such as  $Mn_2(CO)_{10}$ ,  $Co_2(CO)_8$ ,  $Fe_2(CO)_9$ ,  $Fe_3(CO)_{12}$  etc. obey the E.A.N. rule, their E.A.N. per atom of metal is 36. For example. E.A.N. of  $Mn_2(CO)_{10}$  may be calculated as :

$$\text{Electrons from 2Mn atom} = 25 \times 2 = 50$$

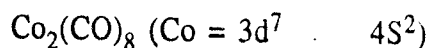
$$\text{Electron from 10CO molecules} = 10 \times 2 = 20$$

$$\text{Electrons from one Mn - Mn} = 1 \times 2 = 2$$

$$\text{Total} = 72$$

$$\text{E.A.N for one Mn atom} = 72/2 = 36$$

The formation of binuclear carbonyls having metal atoms with odd atomic number can also be explained on the basis of 18 - electron rule as shown below for  $Co_2(CO)_8$  and  $Mn_2(CO)_{10}$  carbonyls having metal atoms with odd atomic number can also be explained on the basis of 18-electron rule as shown below for  $Co_2(CO)_8$  and  $Mn_2(CO)_{10}$  carbonyls :

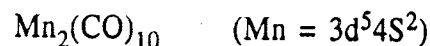


$$2Co = 2 \times 9e^- = 18e^-$$

$$8 CO = 2 \times 8e^- = 16e^-$$

$$\text{Co - Co bond} = 1 \times 2e^- = 2e^-$$

$$Co_2(CO)_8 = 36e^-$$



$$2Mn = 2 \times 7e^- = 14e^-$$

$$10CO = 10 \times 2e^- = 20e^-$$

$$Mn - Mn bond = 2e^-$$

$$Mn_2(CO)_{10} = 36e^-$$

$\therefore$  Electrons on one Co atoms =  $18e^-$   $\therefore$  Electrons on one Mn atom =  $18e^-$

Here it may be noted that although Fe has an even atomic number (=26), the formation of its binuclear carbonyl,  $Fe_2(CO)_9$  can also be accounted for by the 18 - electron rule as shown below :

$$2Fe \quad (Fe = 3d^6 \quad 4s^2) = 2 \times 8e^- = 16e^-$$

$$9CO = 9 \times 2e^- = 18e^-$$

$$Fe - Fe bond = 1 \times 2e^- = 2e^-$$

---


$$Fe_2(CO)_9 = 36e^-$$


---

$\therefore$  Electrons on the Fe atom =  $36^- / 2 = 18^-_e$

**Objection :**

From the X-ray or electron diffraction method, it is well established that the bonds are intermediate between the  $M-C\equiv O$  and  $M=C=O$  states, i.e., there is some double bond character in  $M-CO$ .

Thus, the above older views cannot explain the double bond character in  $M-CO$ .

This had been explained by both molecular orbital as well as valence bond method.

**The 18-Electron Rules :**

The first carbonyls discovered were  $Ni(CO)_4$ ,  $Fe(CO)_5$  and  $Co_2(CO)_8$ . Their formula, as well as the formulas of carbonyls discovered later, were suggestive to Sidgwick of a stable 18-electron (pseudo-noble-gas) valence shell configuration around the metal, comparable to the stable octet for the lighter elements suggested by Lewis. A very large number of metal carbonyls-including many anionic and cationic species, nitrosyl, hydrogen, and halogen-substituted metal carbonyls, and small metal cluster carbonyls-conform to the 18-e rule. This rule can also be formulated in terms of the total number of electrons around the metal-in which case this number is usually found to be 36, 54, or 86 corresponding to the atomic numbers of the noble gases Kr, Xe and Rn. The metals are then said to have the effective atomic number of the noble gases, or to obey the EAN rule. Because the pseudo-noble-gas valence shells of Kr, Xe and Rn contain 18 e's, it is simpler just to count valence shell electrons.

Counting rules help to predict and understand the stoichiometry and structures of the binary metal carbonyls. In counting the electrons around a single metal atom, follow these simple (but arbitrary) rules.

1. Count two electrons for each CO.
2. Count one electron for each metal-metal bond.
3. Find the number of electrons that formally belong to the metal atom alone by (a) adding up the charges on the ligands and changing the sign, (b) finding the metal oxidation number by adding this number to the total charge on the complex, and (c) subtracting oxidation number from the valence electron count of the neutral metal.
4. Add together the counts from steps 1 – 3.

**Example :** 1) Count electrons in  $Mo(CO)_6$  (its Oh structure is shown in fig. 5.2)

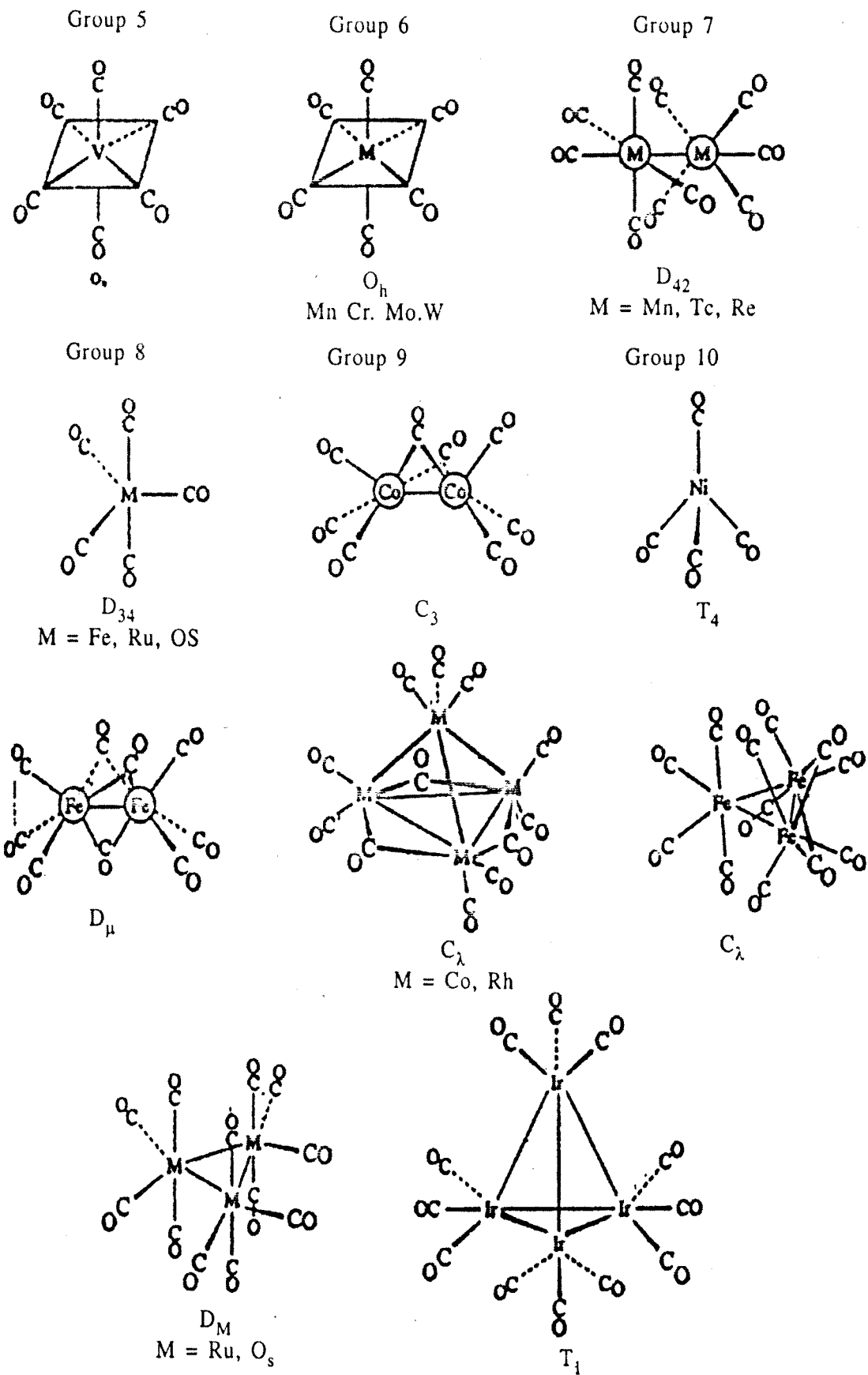
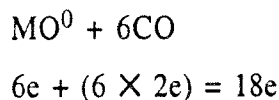


Fig. 5.2. Solid-state structures of some neutral binary metal carbonyls

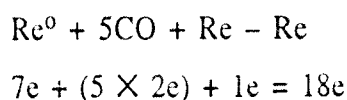
**Solution :** In neutral binary carbonyls, the metal oxidation number is always 0.



The counting rules merely book keep electrons; they provide no information about the actual density distribution

**Example :** 2 Count electrons around each Re in  $\text{Re}_2(\text{CO})_{10}$  (the  $D_{4d}$  structure is shown in Fig. 2

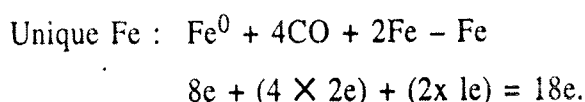
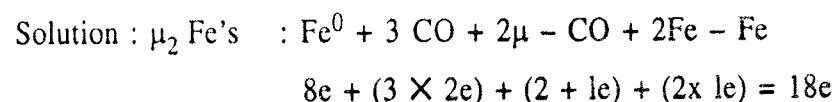
**Solution :** We consider a single Re atom :



The molecular structure of  $\text{Fe}_3(\text{CO})_{12}$  (Fig. 5.2) reveals a new-feature – CO's that bridge two metals. In line formulae, doubly bridging carbonyls are written as  $\mu\text{-CO}$  or  $\mu_2\text{-CO}$  to emphasize that two metals are bridged. Hence, a formula for triirondodecacarbonyl that conveys structural information is  $\text{Fe}_3(\mu_2\text{-CO})_2(\text{CO})_{10}^2$ .

Each bridging CO is considered to be  $sp^2$  - hybridized and to contribute one hybrid orbital and one electron to each metal.

**Example :** 3 Count electrons around each Fe in  $\text{Fe}_3(\text{CO})_{12}$ .



we could predict via the EAN rule the presence of  $\mu_2\text{-CO}$ s. Without any structural information we still calculate the number of e's/Fe as  $[(3 \times 8e)] + (12 + 2e) + (3 \times 2e) / 3\text{Fe} = 54e/3\text{Fe} = 18e/\text{Fe}$ . The number of e's per M is the total number around all metal atoms divided by the number of metal atoms which share them. Both  $\text{Ru}_3(\text{CO})_{12}$  and  $\text{Os}_3(\text{CO})_{12}$  adopt structures containing only terminal (nonbridging) carbonyls. Presumably, this occurs because distances between large metal atoms are too great for effective bridge-bond formation. Similar considerations apply to  $\text{M}_4(\text{CO})_{12}$  (M=Co, Rh, Ir), where Co and Rh give a  $C_{3v}$  structure whereas Ir forms a  $T_d$  one (Fig. 2).

Different structures consistent with the 18-e rule can occur in different environments. For example,  $\text{Co}_2(\text{CO})_8$  has a solid-state structure with two  $\mu_2^-$  Co's. In solution, however,

no fewer than three isomers exist: the bridged form, a form containing all terminal CO's, and a third form of unknown structure. The structures M – M and M – M are equivalent in electron count, and bridge terminal tautomerism occurs frequently.

CO is also known to bridge metals through both C and O. An example of this relatively uncommon coordination mode is  $(PPh_3)_4 W(CO)_4$  ( $CO \rightarrow AlBr_3$ ).

Some known exceptions to the 18-e rule among binary carbonyls are  $V(CO)_6$  (17<sub>e</sub>) and  $Rh_6(CO)_{16}$ .

Conformity of transition-metal carbonyls to the 18-e rule is a result of the fact that the nine  $nd$ ,  $(n + 1)s$ , and  $(n + 1)p$  orbitals are all valence orbitals in the transition series, and that all their bonding capacity is used when the 18-e configuration is reached.

### Carbonyl Complexes :

#### 1. CO - The most Important $\pi$ Acid Ligand

CO provides a paradigm for bonding of  $\pi$ -acid ligands to metals. The valence-bond (VB) structure of CO shows two nonbonding electron pairs :



The molecular orbital (MO) energy diagram of CO shows that the electron pair in the MO localized on C is more loosely bound and is the one available for electron donation to a metal. Fig. shows the bonding resulting from overlap of the filled C  $\sigma$  orbital and an empty metal  $\sigma$  orbital. CO also has a pair of empty, mutually perpendicular  $\pi^*$  orbitals that overlap with filled metal orbitals of  $\pi$  symmetry and help to drain excess negative charge from the metal onto the ligands. Because ligands containing empty  $\pi^*$  orbitals accept electrons, they are Lewis acids and are called  $\pi$  acids. Metal-to-ligand electron donation is referred to as **back-bonding**.

Energetically, the most important bonding component is  $\sigma L \rightarrow M$  donation. Back-bonding (the  $\pi$  component) assumes greater relative importance when the metal has many electrons to dissipate; thus, low oxidation states are stabilized by  $\pi$ -acid ligands.

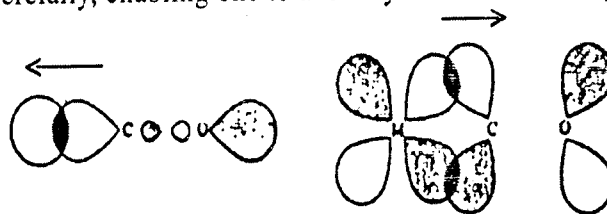
$\sigma$ - and  $\pi$ -bonding reinforce each other : The greater the electron donation from a filled ligand  $\sigma$  orbital, the greater the partial positive charge on the ligand and the more stable the  $\pi^*$  orbitals become, making them better acceptors. This mutual reinforcement is called synergism. The importance of synergic bonding is indicated by the fact that CO forms a very large number of complexes with transition metals in low oxidation states, even though it is an extremely poor Lewis base toward metals in low oxidation states, even though it is an extremely poor Lewis base toward other species. (The description of back-bonding given here is the MO equivalent of the VB formulation)

Other  $\pi$ -acid ligands, such as  $CN^-$ , also exhibit synergism. Organic ligands that also act as two-electron  $\sigma$ -donors and have empty  $\pi^*$  orbitals include isocyanides ( $:CNR$ ) and

carbenes (:C(X)(Y)). Still other ligands are capable of back-bonding but do not contain C, including NO<sup>+</sup> (isoelectronic with CO), phosphines R<sub>3</sub>P, arsines R<sub>3</sub>AS, stibines R<sub>3</sub>Sb bipyridine (bipy), and 1, 10 - phenanthroline (phen). Both CNR and NO<sup>+</sup> have two mutually perpendicular π\* orbitals, like CO. For bipy and phen, only one delocalized π\* orbital perpendicular to the molecular plane is properly oriented for back bonding. For Group 15 ligands just one empty d orbital, and for carbenes a single empty C 2p<sub>z</sub> of π symmetry, can back-bond. Accordingly, complexes containing these ligands are treated with organometals, even though, strictly speaking, not all of them are organic.

### Binary Carbonyls Complexes :

Binary carbonyls are the simplest class of π-acid complexes. Table 5.2 lists neutral carbonyls, which often are used as reactants in the preparation of other compounds. Most are available commercially, enabling one to avoid syntheses involving high pressures of CO.



(a) ligand-to-metal- σ bonding (b) Metal to ligand π\* bonding (one of a mutually perpendicular set show)

Fig. 5.3 Orbital overlap in M - CO bonding. Arrows show direction of electron flow.

Table 5.2 Binary Metal Carbonyls.

Ti(CO) <sub>6</sub> Green : dec. 40-50 K	V(CO) <sub>6</sub> Blue-green; Oh; dec. 60-70° C; air-stable	Cr(CO) <sub>6</sub> Colorless; oh; mp 150-152° C (in vacuo); air-stable	Mn <sub>2</sub> (CO) <sub>10</sub> Golden-yellow; D <sub>4d</sub> ; mp 154-155° C heat/air- sensitive	Fe(CO) <sub>5</sub> Light yellow, D <sub>3h</sub> ; mp -20° C bp 103° C	Co <sub>2</sub> (CO) <sub>8</sub> Dark orange D <sub>3d</sub> (sol'n) ; Dec. 51-52° C; air - sensitive	Ni(CO) <sub>4</sub> Colorless; T <sub>d</sub> ; mp-17° C; bp 42° C; dec to Ni+CO 180° C
		Mo(CO) <sub>6</sub> Colorless; oh;mp 146° C (in vacuo); air-stable	Tc <sub>2</sub> (CO) <sub>10</sub> Colorless;4 <sub>4d</sub>	Ru(CO) <sub>5</sub> Colorless; D <sub>3h</sub> (sol'n);mp -22° C difficult to purify	Rh <sub>2</sub> (CO) <sub>8</sub> Stable only at low T and high CO pressure	
		W(CO) <sub>6</sub> Colorless; oh;mp 166° C (in vacuo) ; air-stable	Re <sub>2</sub> (CO) <sub>10</sub> Colourless; D <sub>4d</sub> ; Dec. 170° C; Air-stable	Os(CO) <sub>5</sub> Colorless; D <sub>3h</sub> (sol'n) ;	Ir <sub>2</sub> (CO) <sub>8</sub> Stable only at low T and high pressure	

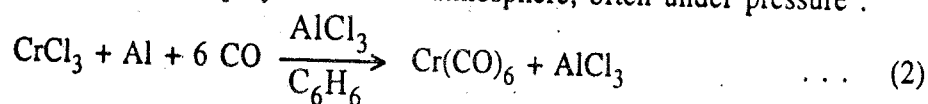
$\text{Fe}_2(\text{CO})_9$	
Yellow-orange	
100° C; more	
reactive than	
$\text{Fe}(\text{CO})_5$	
$\text{Ru}_2(\text{CO})_9$	
$\text{Os}_2(\text{CO})_9$	
$\text{Fe}_3(\text{CO})_{12}$	$\text{Co}_4(\text{CO})_{12}$
Green-black;	Black- $\text{C}_{3v}$ ;
$\text{C}_{2v}$ (Solid);	dec. 60° C;
Dec. 140° C;	air sensitive
Air-sensitive	
$\text{Ru}_3(\text{CO})_{12}$	$\text{Rh}_4(\text{CO})_{12}$
Orange; $\text{D}_{3h}$	Red; $\text{C}_{3v}$ ;
Dec. 155° C;	dec. 150° C
air-stable	air-stable
$\text{Os}_3(\text{CO})_{12}$	$\text{Ir}_4(\text{CO})_{12}$
Yellow; $\text{D}_{3h}$ ;	Yellow; $\text{T}_d$
mp 224° C;	dec. 230° C
air-stable	air-stable

### Synthesis of Carbonyls :

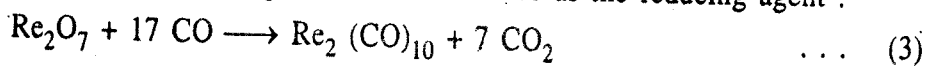
Simple transition - metal carbonyls are made in two ways : direct reaction of a metal with CO, and reductive carbonylation in which a metal salt reacts with CO in the presence of a reducing agent (which also be CO).

Only Fe and Ni react directly with CO under mild conditions to give  $\text{Fe}(\text{CO})_5$  and  $\text{Ni}(\text{CO})_4$ , both of which are very toxic because they decompose thermally to release very toxic CO. The extreme ease of thermal decomposition for  $\text{Ni}(\text{CO})_4$  is the basis of the Mond process for Ni purification. Impure Ni reacts with CO at 100° C to give gaseous  $\text{Ni}(\text{CO})_4$  which is separated easily and decomposed back to Ni and CO (which can be recycled) by heating.

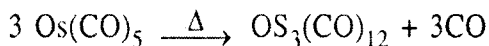
Particularly common is synthesis from a metal halide; a reducing agent that is also a halide acceptor is employed in a CO atmosphere, often under pressure :



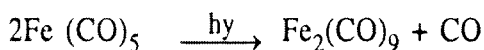
When halide is not present, CO can serve as the reducing agent :



Higher nuclearity carbonyls (those containing more metals) result from thermolysis of lower ones. Metal-CO bond cleavage products unsaturated fragments which combine. In some cases, such as OS (CO)<sub>5</sub> the lower carbonyl is unstable even at ambient temperatures:



Photochemical bond cleavage also occurs, as in the synthesis of diiron nonacarbonyl:



### Reactions of Carbonyls

The number of carbonyls and the number and variety of their reactions is so enormous that only a few types of reaction can be mentioned. For Mo(CO)<sub>6</sub> and Fe(CO)<sub>5</sub>, Fig. 5.4 gives a suggestion of the extensive chemistry which any individual carbonyl typically has.

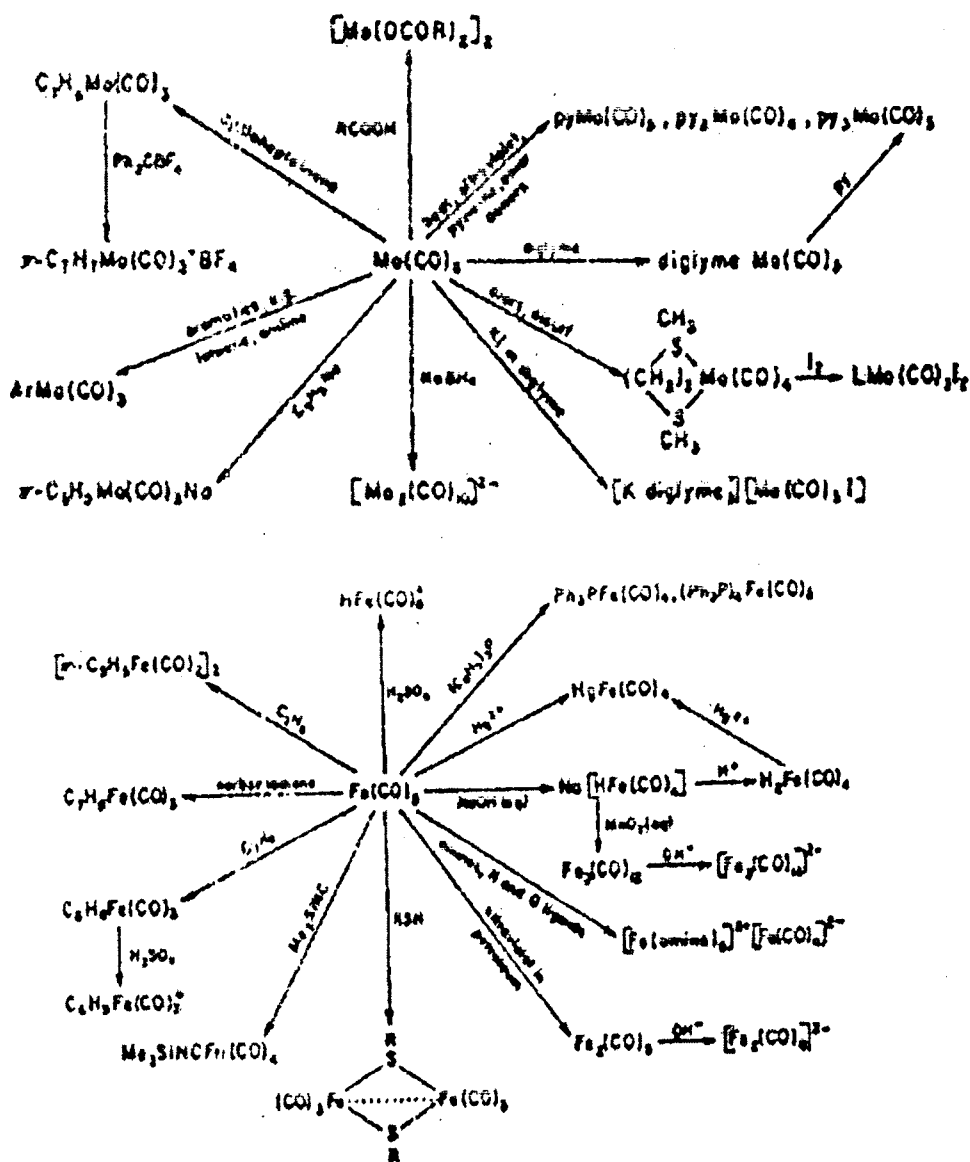


Fig. 5.4 Some reactions of molybdenum and iron carbonyls

The most important general reactions of carbonyls are those which CO groups are displaced by other ligands. These may be individual donor molecules, with varying degrees of back-acceptor ability themselves, e.g.,  $PX_3$ ,  $PR_3$ ,  $P(OR)_3$ ,  $SR_2$ ,  $OR_2$ ,  $RNC$ , etc., or unsaturated organic molecules such as  $C_6H_6$  or cycloheptatriene.

Another important general reaction is that with bases ( $OH^-$ ,  $H^-$ ,  $NH_2^-$ ) leading to the carbonylate anions. Although many of the substitution reactions with other  $\pi$ -acid ligands proceed thermally (temperature up to  $200^\circ$  in some cases being required for the less reactive carbonyls) it is sometimes more convenient to obtain a particular product by photochemical methods; in some cases, substitution proceeds readily only under irradiation. For example the thermal reactions of  $Fe(CO)_5$  and triphenylphosphine or triphenylarsine (L) give mixtures, whereas, photochemically,  $Fe(CO)_4L$  and  $Fe(CO)_3L_2$  can be obtained quite simply. Manganese carbonyl and  $\pi-C_5H_5Mn(CO)_3$  are usually quite resistant to substitution reactions, but the former under irradiation gives  $[Mn(CO)_4PR_3]_2$ . In the very rapid photochemical production of acetylene and olefin complexes from  $Mo(CO)_6$  and  $W(CO)_6$  it is believed that  $M(CO)_5$  radicals are the initiating species; even in absence of other ligands, bright yellow solutions are produced when Cr, Mo and W hexacarbonyls are irradiated in various solvents. Metal carbonyls in presence of organic halogen compounds such as  $CCl_4$  have been found to act as initiators for the free radical polymerization of methyl methacrylate and other monomers.

Kinetic and mechanistic studies of metal carbonyl reactions have been limited mainly to CO exchange processes. In general these reactions seem to take place by an  $S_N1$  mechanism, although some specific exceptions are known. In a general way, the rates of exchange and reactivity in general can be correlated with the degree of M-C  $\pi$  bonding, as would be expected for processes controlled by a dissociative step. For example, the rates of CO exchange for the manganese carbonyl halides,  $XMn(CO)_5$  ( $X = Cl, Br, I$ ), show two main features. (1) In each case four CO's exchange more rapidly than the fifth. This can be attributed to the fact that the CO which is trans to X has a greater degree of M-C  $\pi$  bonding, because the X's are poorer back-acceptors than CO. (2) The overall rates of exchange decrease in the order  $Cl > Br > I$ . This is the order of decreasing electronegativity of X which means that it is also the order of decreasing partial positive charge on the metal and hence the order of increasing M-C  $\pi$  bonding.

### Infra-red Spectra of Carbonyls

Because of the relative ease of observing and interpreting the CO stretching frequencies of metal carbonyls and their derivatives, the observation of these frequencies has become by

far the single most potent physical aid in the study of metal carbonyl chemistry. While Raman data are sometimes obtained, and are equally useful, nearly all data, except for certain simple molecules, have been obtained from infrared spectra.

One general way in which infrared data can be used, namely, to infer and correlate changes in M-C bonding, has already been described. In addition to many purely empirical, though important uses, which as following the course of reactions, or teting for impurities, there is a second important general application of vibrational data, namely, the inference of molecular structure. This can be done in two ways, one depending on the frequency range in which the bands are found, the other depending on the number and, to some extent, the relative intensities of the observed bands. However, since several factors influence the frequencies of CO stretching, interpretation must be done with caution, and usually with the help of collateral data.

It is especially important to note that CO stretching frequencies show appreciable solvent shifts; the use of nonpolar solvents such as hexane is hence desirable.

Because doubly bridging CO groups are similar to organic keto groups (having essentially double CO bonds) their stretching frequencies are to be expected at substantially lower values than those of terminal carbonyl groups in the same or similar molecules, namely  $1700\text{-}1850\text{ cm}^{-1}$ . The appearance of bands in this region can therefore be taken as indicative of the presence of ketonic bridges, provided it is known that terminal CO frequencies have not been lowered into this range by the presence of many non  $\pi$  accepting ligands or negative charge of the metal, as discussed earlier. As examples, the spectra of  $\text{Fe}_2(\text{CO})_9$  and  $\text{Os}_3(\text{CO})_{12}$  are shown in Fig. 5.5 The latter, which contains no.

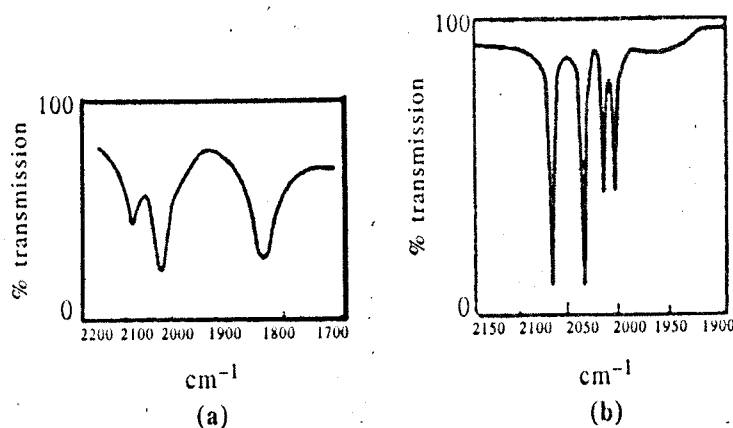


Fig. 5.5. The infrared spectra in the CO stretching region of (a) solid  $\text{Fe}_2(\text{CO})_9$  and (b)  $\text{Os}_3(\text{C})_{12}$  in solution. Note the greater sharpness of the solution spectra. The most desirable spectra are those obtained in nonpolar solvents or in the gas phase bridging groups has four CO bands, all in the terminal CO range, whereas  $\text{Fe}_2(\text{CO})_9$  has not only two bands

in the terminal CO range, but also one in the bridging range ( $-1830\text{ cm}^{-1}$  in the solid). Since there is no reason to expect a terminal frequency as low as this, the inference can be drawn that one or more ketonic bridges are present. This, of course, is true.

Inferring structures from the number of CO bands observed in the infrared spectrum is a common and useful practice, though a certain amount of judgement and experience are necessary in order to consistently avoid errors. The procedure consists in first determining from the mathematical and physical requirements of symmetry how many CO stretching bands ought to appear in the infrared spectrum for each of several possible structures. The experimental observations are then compared with the predictions and those structures for which the predictions disagree with observation are considered to be eliminated. In favourable cases there will be only one possible structure which remains. In carrying out this procedure, due regard must be given to the possibilities of bands being weak or superposed, and of course, the correct model must be among those considered. The reliability of the procedure can usually be increased if the behaviour of approximate force constants and the relative intensities of the bands are also considered.

To illustrate the procedure, consider the cis and trans isomers of an  $\text{ML}_2(\text{CO})_4$  molecule. Fig. 5.6 shows the approximate forms of the CO stretching vibrations and also indicates which ones are expected to absorb infrared radiation, when only the symmetry of the  $\text{M}(\text{CO})_4$  portion of the molecule is considered. When  $\text{L} = (\text{C}_2\text{H}_5)_3\text{P}$ , the two isomeric compounds can be isolated. One has four infrared bands ( $2016, 1915, 1900, 1890\text{ cm}^{-1}$ ) and is thus the cis isomer, while the other shows only one strong band ( $1890\text{ cm}^{-1}$ ) and is thus the trans isomer.

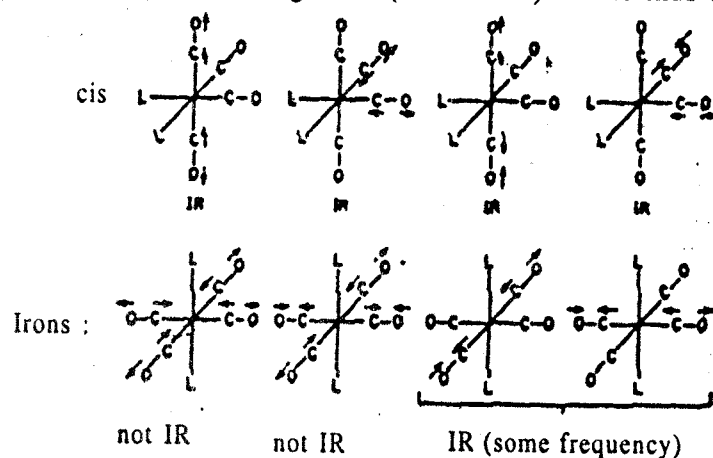


Fig. 5.6 Schematic indication of the forms of the CO stretching vibrations of cis and trans  $\text{ML}_2(\text{CO})_4$  molecules. For the cis isomer, all four are distinct and can absorb infrared radiation. For the trans isomer, two are equivalent and have the same frequency, forming a degenerate vibration; only this one this one can absorb infrared radiation.

It may also be noted that since no major interaction is to be expected between the CO stretching motions in two  $M(\text{CO})_4$  groups if they are connected only through the two heavy metal atoms,  $\text{Os}_3(\text{CO})_{12}$  should have the 4-band spectrum of a cis- $\text{ML}_2(\text{CO})_4$  molecule, and as seen in Fig. 5.6 it does.

The arrangement of CO groups in  $\text{Co}_4(\text{CO})_{12}$  (Fig. 5.7) was determined from the infrared spectrum and this provides an excellent example of both the utility of the procedure and its skilful use.

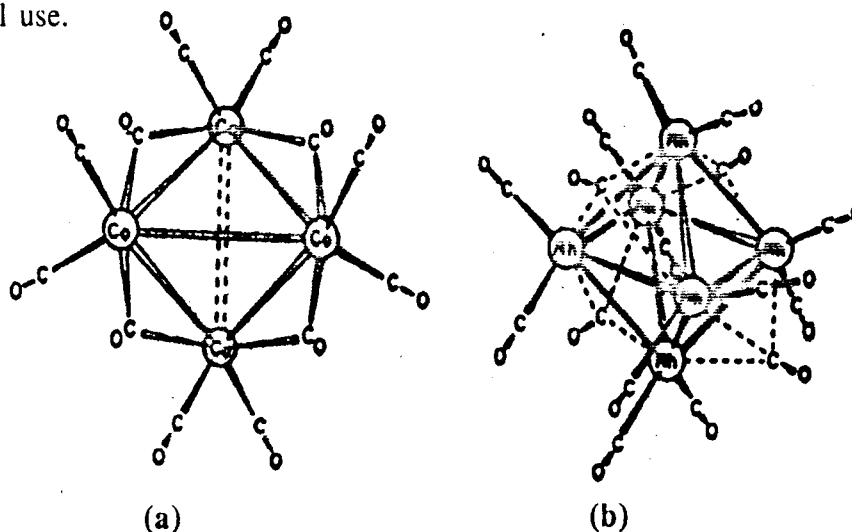


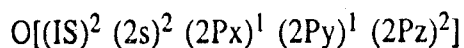
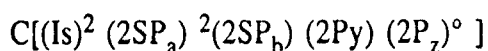
Fig. 5.7 (a) The  $D_{2d}$  structure proposed for  $\text{Co}_4(\text{CO})_{12}$  ion solution on the basis of its infrared spectrum. (b) The structure (symmetry  $T_d$ ) of  $\text{Rh}_6(\text{CO})_{16}$  determined entirely by X-rays crystallography.

Finally we may note the very simple case in which there are two CO (or NO) groups present in an octahedral type molecule. If the groups are trans there will be only one CO band in the infrared (see, for example, trans- $[\text{Cr}(\text{CO})_2(\text{diphos})_2]$ , due to the antisymmetrically coupled stretching of the two groups, whereas when they are cis (as in cis- $M(\text{NO}_2)_2L_4$  complexes) both, the symmetric and the antisymmetric combinations cause infrared absorption and two strong bands are observed.

#### Molecular - Orbital Approach :

This can be understood by considering the following facts :

(a) Carbon undergoes  $sp$  hybridization involving  $2s$  and  $2p_x$  orbitals, forming two hybrid orbitals, which are designated as  $SP_a$  and  $SP_b$ . These orbitals are oriented through  $180^\circ$ . Now we can write the configuration of C and O atoms as follows :



According to the molecular orbital theory, carbon and oxygen atoms undergo overlapping to form bonds in CO as follows :

- (i)  $2SP_b$  hybrid orbital of carbon and  $2P_x$  of oxygen overlap to form a localized  $\sigma$  bond.
- (ii)  $2P_y$  of carbon and  $2P_y$  of oxygen overlap to form a  $\pi$ -bond
- (iii)  $2p_z$  of carbon and  $2P_z$  of oxygen overlap to form another  $\pi$ -bond

The distribution of electrons of carbon and oxygen (of the second quantum shell) in the various molecular orbitals formed is as follows :

- (i) There will be 2 electrons in  $\sigma$ -bonding orbital.
- (ii) There will be 2 electrons in the  $\pi$ -bonding orbital which is formed by the combination of  $2p_y$  atomic orbitals of carbon and oxygen.
- (iii) There will be 2 electrons in the  $\pi$  - bonding orbital, formed by the combination of  $2p_z$  orbitals of oxygen and carbon.
- (iv) There will be 2 non-bonding electrons in the  $2SP_a$  hybrid orbital of carbon.
- (v) There will be 2 non-bonding electrons in the  $2s$  atomic orbital of oxygen.
- (vi) There will be no electron in the antibonding molecular orbitals, formed as a result of  $\sigma$  and  $\pi$  overlappings.

As the total number of bonding electrons is six and that of antibonding electrons nil, bond order of the molecule is three. Hence, the number of bonds between carbon and oxygen atoms in CO molecule is 3, one  $\sigma$  and two  $\pi$ .

The lone pair of electrons on carbon could be expected to form a strong dative bond ( $\sigma$ ) due to the electron density remaining close to the nucleus of the carbon atom. As metal atom-carbon monoxide bonds are readily formed in metal carbonyls, it is expected that there is some additional bonding mechanism in the formation of metal-carbon monoxide bonds in the metal carbonyls. The accepted view is that the weak M-C  $\sigma$  is formed along with M-C  $\pi$  bond.

The above situation can be understood in the following way :

- (i) Firstly, there is a dative overlapping of filled carbon  $\sigma$  orbital i.e. hybrid orbital with an empty metal  $\sigma$  orbital ( $M \leftarrow CO$ ).

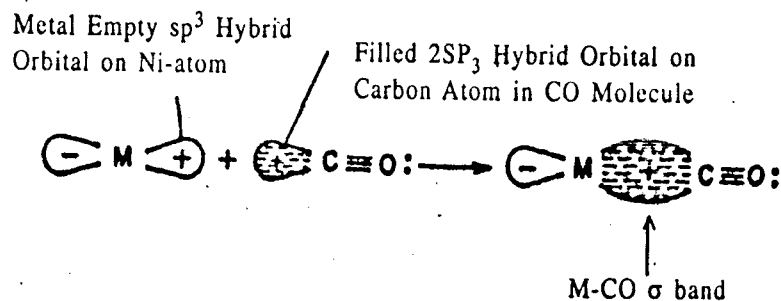
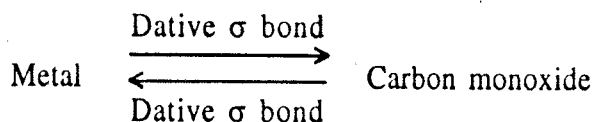


Fig. 5.8 a The formation of a  $\sigma$  bond using a shared pair of electron on C atom i.e. ( $M \leftarrow CO$ ) :

(ii) Secondly, there is a dative overlapping of a filled d-orbitals of metal with empty antibonding p orbital of the carbon atom ( $M^{\pi} \rightarrow CO$ ), resulting in the formation of a dative  $\pi$  bonds (Fig. 23.2)



Shaded portions in Figs (5.8 a and 5.8 b) indicate the filled orbitals whereas empty portions indicate vacant orbitals i.e., having no electrons.

As there is a drift of metal electrons into carbon monoxide ( $M^{\pi} \rightarrow CO$ ), orbitals will tend to make the CO as a whole negative and at the same time there is the drift of electrons from CO to the metal ( $M^{\sigma} \rightarrow CO$ ) to make the CO positive, thus enhancing the acceptor strength of the  $\pi$  orbitals. Thus, in a way the formation of  $\sigma$  bond strengthens the  $\pi$  bond formation and vice versa.

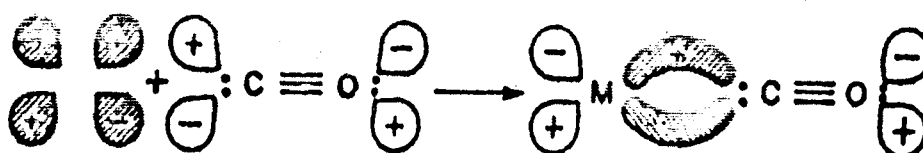
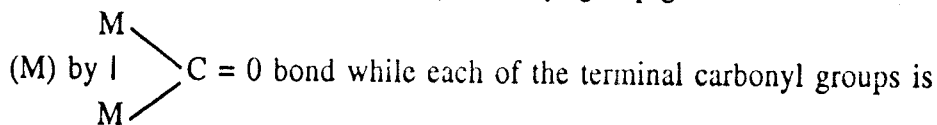


Fig 5.8b  $M \rightarrow CO$   $d\pi - p\pi$  back bonding

The strongest support for this type of bonding mechanism comes from IR spectra. A major consequence of back donation of electrons into  $\pi$  orbitals of CO molecule is that the carbon-oxygen bond order in them, which is three in the free uncomplexed CO molecules, is reduced. This reduction in bond order on complexation reduces the force constant enabling the bond to be stretched with less energy. A decrease in the C-O stretch frequency value is thus predicted. It is observed that C-O stretch frequency in the uncomplexed CO molecules is  $2155 \text{ cm}^{-1}$  while in a complexed molecule, it has been observed to be in the neighbourhood of  $2000 \text{ cm}^{-1}$ . This observation, hence, supports the mechanism proposed.

**Dinuclear Carbonyls :** (a)  $Mn_2(CO)_{10}$ ,  $Tc_2(CO)_{10}$  and  $Re_2(CO)_{10}$  carbonyls. In all these carbonyls each M atom gets directly linked with the other M atom by a  $\sigma$  bond (M-M  $\sigma$ -bond) and five terminal ported by the diamagnetic nature of these carbonyls. These carbonyls are not having bridging carbonyl groups ( $< C = O$ ) in between M atoms. As the coordination number of each M atom in these carbonyls are paired and hence these carbonyls are diamagnetic. The structure of  $Mn_2(CO)_{10}$  has been explained in detail elsewhere.

(b)  $\text{Co}_2(\text{CO})_8$ ,  $\text{Fe}_2(\text{CO})_9$  and  $\text{Os}_2(\text{CO})_9$  carbonyls : These carbonyls have both types of carbonyl groups which are bridging carbonyl groups ( $>\text{C}=\text{O}$ ) and terminal carbonyl groups ( $-\text{C}\equiv\text{O}$ ). Bridging carbonyl groups exist between two metal atoms. The number of bridging carbonyl groups present in  $\text{Co}_2(\text{CO})_8$  (only in one isomeric form),  $\text{Fe}_2(\text{CO})_9$  and  $\text{Os}_2(\text{CO})_9$  has been 2, 3 and 1 respectively while the number of terminal carbonyl groups is 6, 6 and 8 respectively. Each of the bridging carbonyl group gets attached with the metal.



attached with the metal atom by  $\text{O}\equiv\text{C}\rightarrow\text{M}$  coordinate bond. All these carbonyls have M-M bond. The presence of M-M bond confirms the diamagnetic nature of these carbonyls.

**Trinuclear carbonyls :** Here an attempt is made to consider the structure of  $\text{Fe}_3(\text{CO})_{12}$ ,  $\text{Ru}_3(\text{CO})_{12}$  and  $\text{Os}_3(\text{CO})_{12}$  carbonyls. The trinuclear carbonyls viz  $\text{Os}_3(\text{CO})_{12}$  and  $\text{Ru}_3(\text{CO})_{12}$  possess similar structures whereas  $\text{Fe}_3(\text{CO})_{12}$  has a different structure.  $\text{Os}_3(\text{CO})_{12}$  and  $\text{Ru}_3(\text{CO})_{12}$  contain three metal (M) atoms. Each of these gets linked with the remaining two M atoms. Thus there are three M-M bonds in each of these carbonyls. All the three M-M bonds are situated in an equilateral triangle. Each M atom gets attached with four terminal CO groups which make an approximately octahedral configuration around each M atom. These molecules do not have any bridging CO groups.

Evidence for the structure of the polynuclear carbonyls is still incomplete. In most of the polynuclear complexes the coordination centres are joined through ligand (CO) bridges but such crystal structure determinations have been carried out that have shown that direct metal bonds are an important features of the polynuclear carbonyls

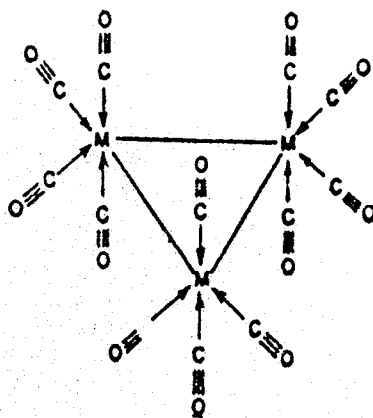


Fig. 5.9 Structure of  $\text{M}_3(\text{CO})_{12}$  type carbonyls (M=Os, Ru)

**Structure of some carbonyls :**

(i) The vapour density of nickel carbonyl and the freezing points of its solution in benzene indicate the molecular formula to be  $\text{Ni}(\text{CO})_4$ .

(ii) Electron diffraction studies made on this compound in the vapour state and X-ray diffraction studies made on this compound in the solid state have shown that  $\text{Ni}(\text{CO})_4$  molecule has tetrahedral shape with Ni-C-O linear units (fig. 5.10). the Ni-C bond length in this molecule is 1.50 Å which is shorter by 0.32 Å in comparison to Ni-C single bond length (=1.82 Å) found in carbonyls. The C-O bond length in this carbonyl has been found to be equal to 1.15 Å which is longer than the C-O bond length in CO molecule (=1.128 Å) (iii) Raman spectral studies have revealed that the oxygen atom is triply bonded to the carbon atom in the CO group. Thus the nickel atom in the nickel carbonyl must be tetrahedrally hybridized. (Fig. 5.10)

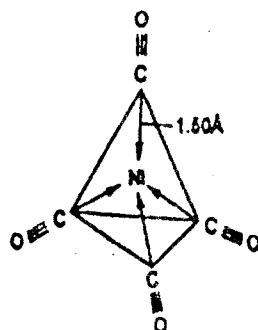
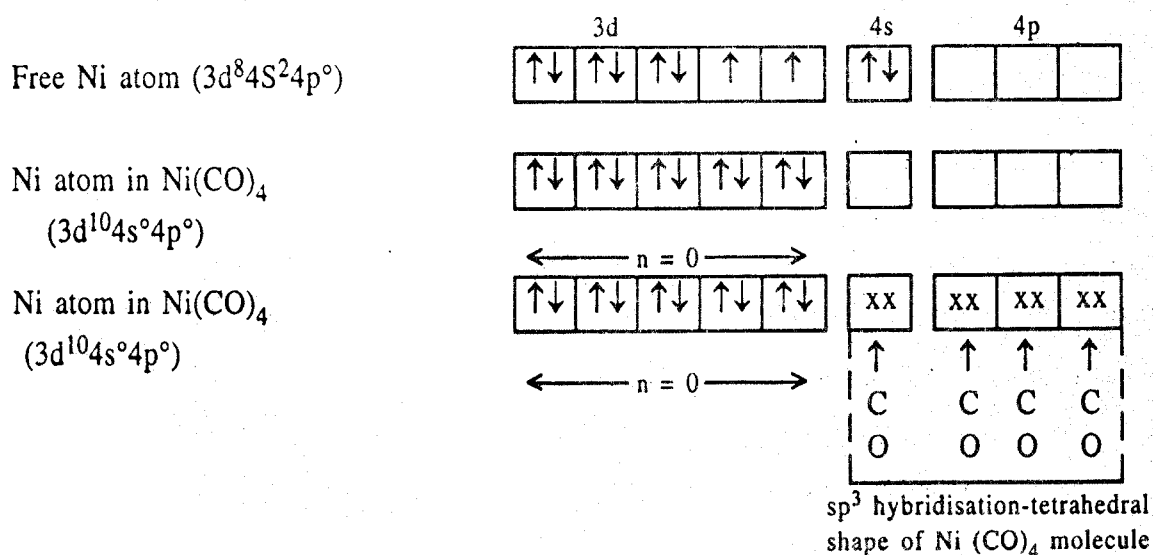


Fig. 5.10 Tetrahedral structure of  $\text{Ni}(\text{CO})_4$  molecule

Tetrahedral shape of  $\text{Ni}(\text{CO})_4$  arises due to  $sp^3$  hybridisation of Ni-atom. As  $\text{Ni}(\text{CO})_4$  molecule is diamagnetic, all the ten electrons present in the valence shell of Ni-atom ( $\text{Ni}=3d^84s^2$ ) are paired in 3d orbitals. Thus the valence-shell configuration of Ni-atom in  $\text{Ni}(\text{CO})_4$  molecule becomes  $3d_{10}4s^0$ . CO  $\rightarrow$  Ni - bond is caused by the overlap between the empty  $sp^3$  hybrid orbital on Ni-atom and doubly-filled  $sp$  hybrid orbital on C atom in CO molecules. (Fig. 23.5)

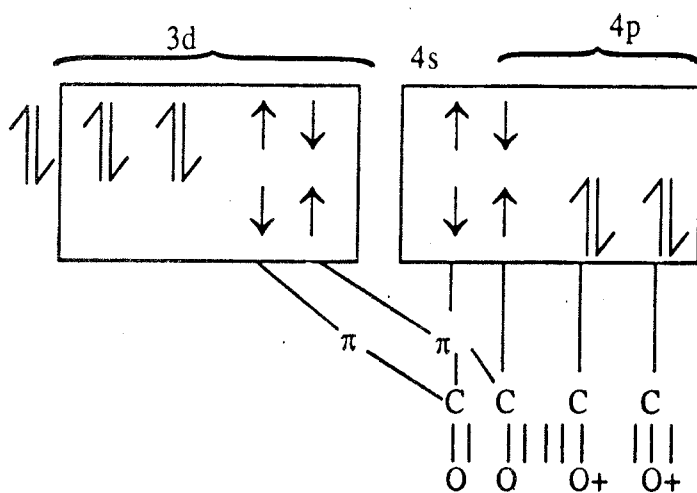


$sp^3$  hybridisation of Ni atom in tetrahedral  $\text{Ni}(\text{CO})_4$  xx indicate the electron pair donated by CO molecules. These electrons are in opposite spin.

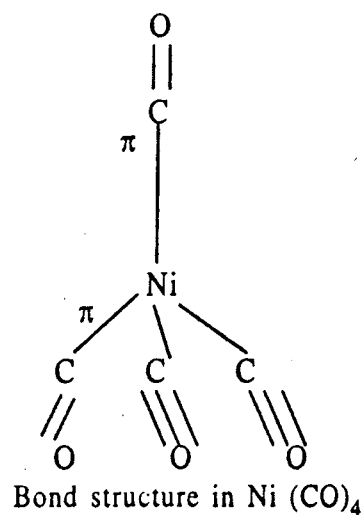
Because of the formation of four  $OC \rightarrow M$  bonds, a large negative charge gets accumulated on the central Ni atom. This is most unlikely. In such a situation, Pauling suggested that the double bonding occurs with the back donation of d-electron from Ni atom to CO ligands to such an extent that electroneutrality principle is obeyed. According to this principle the electron pair is not shared equally between Ni and C-atoms of CO ligands but gets attracted more strongly by C-atom which prevents the accumulation of negative charge on Ni-atom and is in keeping with the greater electronegativity of C-atom compared to Ni atom ( $C = 2.5$ ,  $Ni = 1.8$ )

Recent Orbital Diagram : It is now assumed that nickel atom has the following configuration.  $Ni_{28} = 1s^2 2s^2 2p^6 3s^2 3p^6 3d^8 4s^1 4p^1$ .

On the basis of this electronic configuration, the orbital diagram of  $Ni(CO)_4$  is shown in Fig. 5.11 and the bond structure is shown in Fig. 5.11



sp<sup>3</sup> Hybridisation  
Orbital diagram of  $Ni(CO)_4$   
Fig. 5.11 A



Bond structure in  $Ni(CO)_4$   
Fig. 5.11 B

## 2. Structure of $Fe(CO)_5$

(i) The various evidence are : The vapour density and the freezing points of benzene solution of iron pentacarbonyl show that studies of this compound have shown that  $Fe(CO)_5$  molecule has trigonal bipyramidal shape (Fig. 5.12). Electron diffraction study of  $Fe(CO)_5$  in the vapour state has shown that  $Fe-C$  axial bond and  $Fe-C$  basal bond lengths are equal to 1.797 Å and 1.842 Å respectively while X-ray study has shown that these bond lengths are almost the same. Trigonal bipyramidal shape of  $Fe(CO)_5$  results from  $dsp^3$  hybridisation of Fe-atom. (see Fig. 5.12)

(iii) The molecule is diamagnetic and the distance of  $Fe-C$  is 1.84 Å.

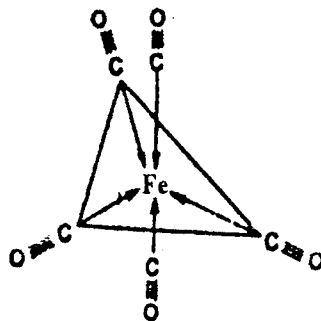
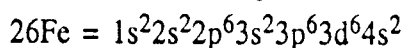


Fig. 5.12 Trigonal bipyramidal structure of  $\text{Fe}(\text{CO})_5$

Old Orbital Diagram.

The electronic configuration of iron atom is



This may revert to the energetically similar  $3d^6$  outer arrangement permitting  $dsp^3$  hybridisation. Thus, five empty orbitals are available which can accept five carbon monoxide groups, giving rise to a trigonal bipyramid structure. However, this can not be supported by the experimental studies.

In this molecule Fe is in zero oxidation state and since  $\text{Fe}(\text{CO})_5$  is diamagnetic, all the eight electrons in the valence-shell of Fe atom ( $\text{Fe} = 3d^6, 4s^2$ ) get paired in 3d orbitals. Thus the valence-shell configuration of Fe-atom in  $\text{Fe}(\text{CO})_5$  becomes  $3d^8, 4s^0$ ,  $\text{CO} \rightarrow \text{Fe}$   $\sigma$ -bond results by the overlap between empty  $dsp^3$  hybrid orbital on Fe-atom and doubly-filled sp hybrid orbital on C-atom in CO molecule.

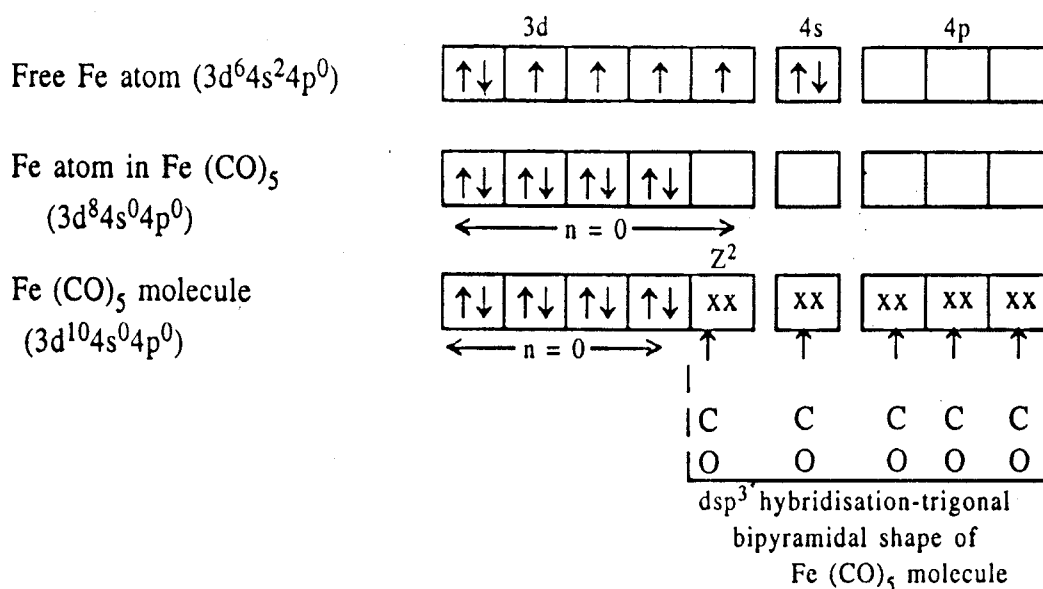


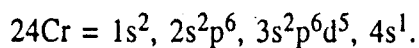
Fig 5.13  $dsp^3$  hybridisation of Fe atom in trigonal bipyramidal  $\text{Fe}(\text{CO})_5$  molecule

### 3. Structure of Cr (CO)<sub>6</sub>

From the molecular formula Cr(CO)<sub>6</sub>, it follows that it should possess an octahedral configuration which has been confirmed by the results of electron diffraction studies. The internuclear lengths are :

Cr - C	Cr - O	C - O
1.92	3.08	1.16A

The electronic configuration of chromium is given below :



According to old concept it was believed that when chromium forms Cr(CO)<sub>6</sub> one electron of 4s orbital comes in 3d orbitals and 3d orbitals have six electrons. Since CO is a strong ligand hence six electrons of 3d orbitals paired up. In this way two 3d orbitals, one 4s orbital and three 4p orbitals become empty which are hybridized to form six d<sup>2</sup>sp<sup>3</sup> hybrid orbitals. Now six molecules of CO donate a lone pair of electrons to six vacant hybrid orbitals to form six Cr → CO σ bonds as shown Fig. 5.14. Therefore Cr(CO)<sub>6</sub> molecule is diamagnetic in nature and octahedral in geometry.

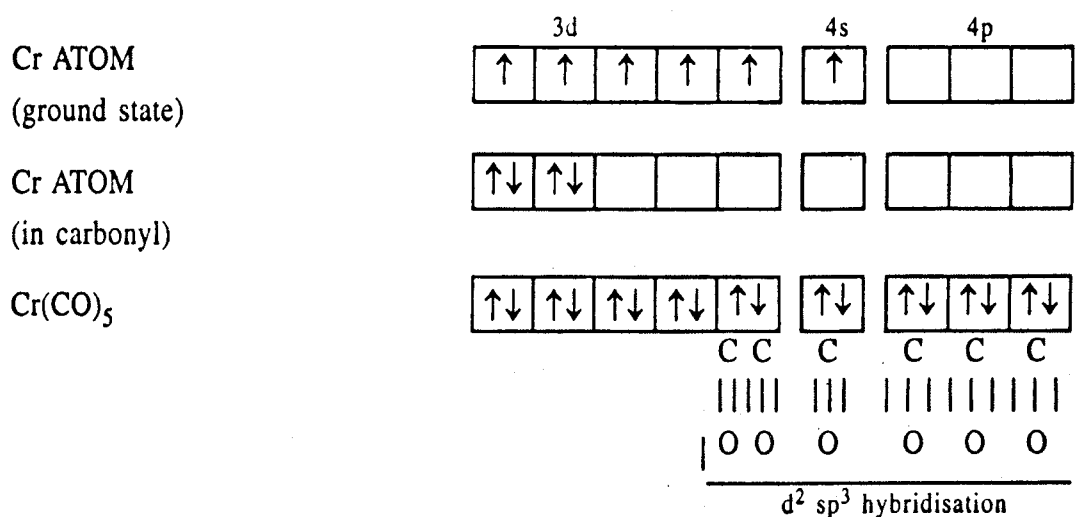


Fig. 5.14

Various inter nuclear bond lengths of these carbonyls are given in Table 5.13

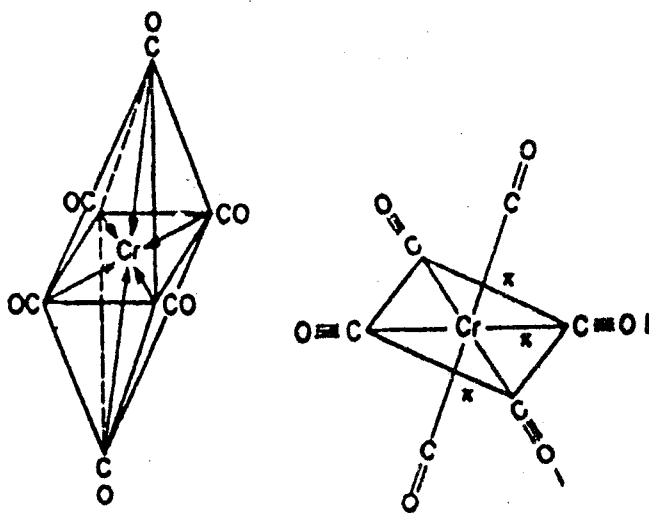
Table 5.13

## INTERNUCLEAR BOND LENGTHS

Metal	M-C(Å)	M-O(Å)	C-O(Å)
Cr	1.916	3.98	1.171
Mo	2.063	3.23	1.145
W	2.06	3.19	1.148

The bond structure of  $\text{Cr}(\text{CO})_6$  reveals two kinds of bonds between Cr and CO. These are.

- (i) Simple covalent bonds  $\text{Cr}-\text{C} \equiv \text{O}$  shown by I
- (ii) Double bonds  $\text{Cr} \pi \text{Cr} = \text{O}$  shown by II

Fig. 5.15 Structure of  $\text{Cr}(\text{CO})_6$ 

In the resultant resonance structure all Cr-C bonds are identical

4. Structures of  $\text{Mo}(\text{CO})_6$ ,  $\text{W}(\text{CO})_6$  and  $\text{V}(\text{CO})_6$ : Like  $\text{Cr}(\text{CO})_6$  these also possess octahedral structures.

#### 5. Structure of $\text{Re}_2(\text{CO})_{10}$

The molecular weight of rhenium carbonyl in solution indicates the dimeric formula  $\text{Re}_2(\text{CO})_{10}$ . The infra-red absorption spectrum shows that there are no bonds in the neighbourhood of  $1800 \text{ cm}^{-1}$ : this is taken to indicate that there are no bridging carbonyl groups in the molecule. X-ray diffraction analysis shows that the molecule of rhenium carbonyl contains two directly linked metal atoms. The distance Re-Re is 3.02 Å; the covalent bond length would be about 2.7 Å. Each rhenium atom has octahedral coordination. Of the six

bonds, five go to carbonyl groups and one to the other metal atom. The two octahedral groups in the molecule are turned through  $45^\circ$  with respect to one another.

## 6. Structure of Polynuclear Carbonyls

Evidence for the structure of the polynuclear carbonyls are still incomplete. The diamagnetism of polynuclear carbonyls is accounted for on the assumption that metal-metal bonds are formed. For instance, crystallographic studies of iron enneacarbonyl  $\text{Fe}_2(\text{CO})_9$  have shown that the two iron atoms are joined by three ketonic bridges ( $>\text{C}=\text{O}$ ): the other six CO groups are joined in three each to iron atom by coordinate bonds (Fig. 23.16). Metal-metal bonding is also evident in  $\text{Mn}_2(\text{CO})_{10}$  and  $\text{Re}_2(\text{CO})_{10}$  although ketonic groups are absent here.

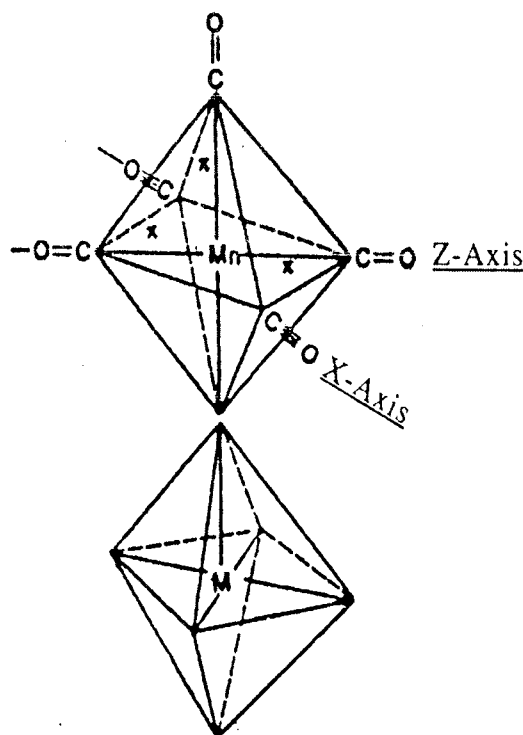
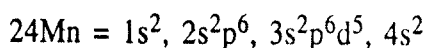


Fig. 5.16 Bond structure of  $\text{Re}_2(\text{CO})_{10}$

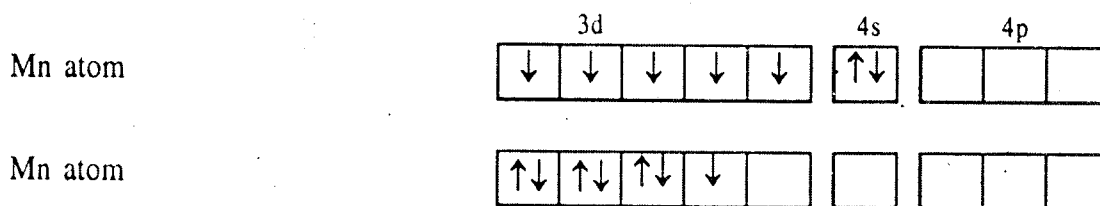
### Structure of $\text{Mn}_2(\text{CO})_{10}$

The electronic configuration of manganese is given below :



Thus there are five unpaired 3d - electrons and one paired 4s-electrons. When CO molecules approach Mn atoms these electrons get paired and only one unpaired electron remains in 3d - orbitals. Now Mn atom gets hybridized and forms six  $d^2sp^3$  hybrid orbitals. Out of six hybrid orbitals only one hybrid orbital is having one electron. Now five CO molecules donate lone pair of electrons to five vacant hybrid orbitals to form five  $\text{Mn} \leftarrow \text{CO}$   $\sigma$  bonds. Now both  $\text{Mn}(\text{CO})_5$  groups are having one unpaired electron each of which overlaps

to form Mn-Mn bond. In this way this molecule becomes diamagnetic with octahedral geometry (5CO and M) and the two octahedra get rotated through  $45^\circ$  from the eclipsed position. The Mn-Mn bond length is  $2.92 \text{ \AA}$  are attributed to the large negative formal charge and to repulsion between the CO groups.



The structures of  $\text{Re}_2(\text{CO})_{10}$  and  $\text{Tc}_2(\text{CO})_{10}$  are similar to  $\text{Mn}_2(\text{CO})_{10}$ , the metal-metal bond length in Re and Tc carbonyls are  $3.02 \text{ \AA}$  respectively.

But according to new concept the structure of  $\text{Mn}_2(\text{CO})_6$  may be explained as below:

It excited state one electron of 4s orbital is shifted to 4p orbitals, hence there are seven unpaired electrons. Now Mn exhibits  $d^2sp^3$  hybridization.

The diagram clearly reveals that three CO groups from  $\text{Mn}^\pi - \text{C}=\text{O}$  and two CO groups form  $\text{Mn}-\text{C}\equiv\text{O}$  type of bonding. One electron of each  $d^2sp^3$  hybrid orbital overlaps to form metal-metal bond. Hence the structure of  $\text{Mn}_2(\text{CO})_{10}$  may be represented in Fig. 5.17

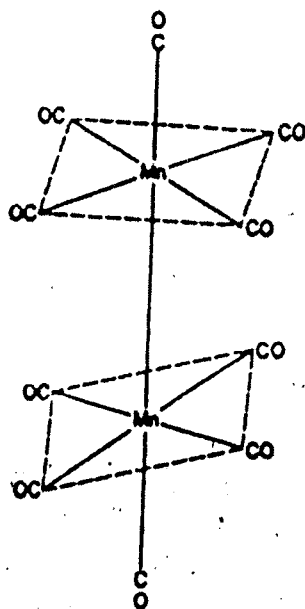


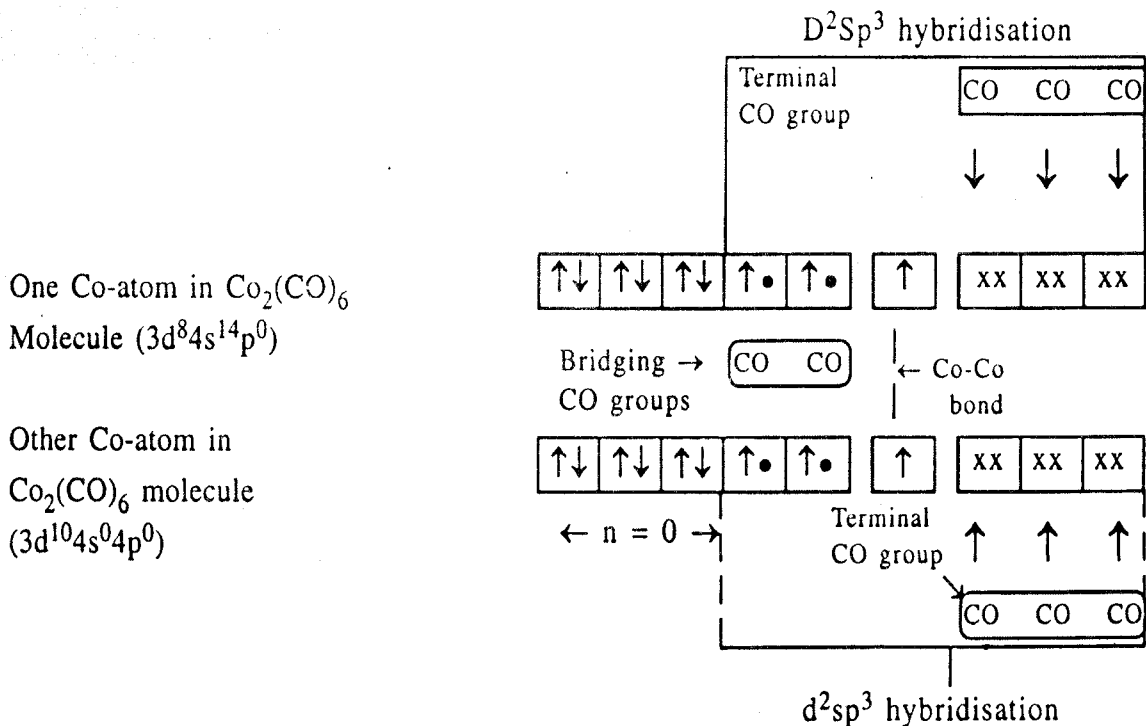
**Fig. 5.17** Orbital diagram of  $\text{Mn}_2(\text{CO})_{10}$

$\text{Te}_2(\text{CO})_{10}$  and  $\text{Re}_2(\text{CO})_{10}$  also have the  $\text{Mn}_2(\text{CO})_{10}$  structure.

Infrared spectra reveals that there is no bridging carbonyl groups in the molecule X-ray diffraction analysis shown that there is metal bonding in the molecule.

## Structure of $\text{Co}_2(\text{CO})_8$

Infra-red study of the solution of this compound reveals that the solution, this compound exists in two isomeric forms. One of these forms is having a bridged structure while the other form is having a non-bridged structure. The bridged structure is having two bridging carbonyl groups, six terminal carbonyl groups and one Co-Co bond. Each of the two Co-atoms gets directly linked with the other Co-atom by a Co-Co bond, with two bridging Carbonyl groups and with three terminal carbonyl groups. Co-Co bond distance in this structure is 2.52 Å. In this structure the coordination number of each Co-atom is six and hence both Co-atoms are  $d^2sp^3$  hybridised as shown in Fig. 23.19. Three  $d^2sp^3$  hybrid orbitals on each Co-atom (which are vacant) accept a lone pair of electrons donated by the C-atom of the three terminal carbonyl groups and form three  $\text{CO} \leftarrow \text{CO}$  Co-ordinate bonds. Such six bonds get formed. One  $d^2sp^3$  hybrid orbital on one Co-atom (singly - filled) overlaps with the  $d^2sp^3$  hybrid orbital on the other Co - atom (singly filled) and forms and (Co - Co bond. Two  $d^2sp^3$  hybrid orbital on each Co-atom (singly-filled) overlap with the appropriate orbital (singly-filled) on C-atom of the two bridging carbonyl groups and form Co-Co bonds. Thus it is seen that all the electrons in  $\text{Co}_2(\text{CO})_8$  become paired and hence the molecule is having diamagnetic character. Note that the valence-shell configuration of each Co-atom in  $\text{Co}_2(\text{CO})_8$  is  $3d^84s^1$  and not  $3d^7, 4s^2$ ,  $d^2sp^3$  hybridisation of Co-atom in  $\text{Co}_2(\text{CO})_8$  molecule. XX represents the electron pair donated by carbon atom of terminal carbonyl groups while the dot (•) represents an electron of carbon atom of bridging carbonyl groups.  $\uparrow\downarrow$  represents the electron pair on Co-atom.



The non bridged structure is having the Co-Co bond and eight terminal carbonyl groups. Each of the two Co-atom gets directly linked with the other Co-atom by a Co-Co bond and with four terminal carbonyl groups. The presence of Co-Co bond in both the forms is also supported by the diamagnetic character of  $\text{Co}_2(\text{CO})_8$  molecule. The two isomeric forms are having little difference in their energies and exist in equilibrium with each other in a given solution.

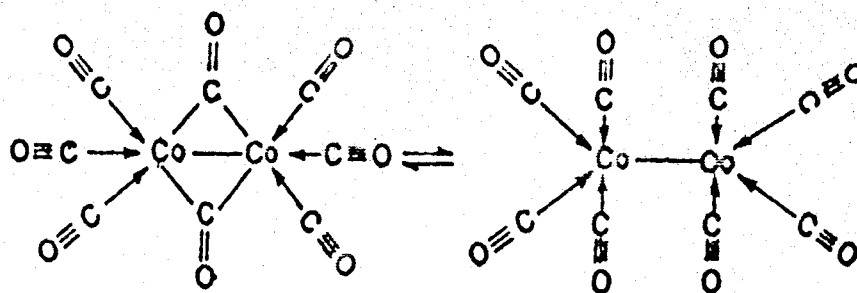


Fig. 5.18 Bridged structure

Non-Bridged structure

Two isomeric of  $\text{Co}_2(\text{CO})_8$  existing in equilibrium with each other in a given solution. One form has bridged structure while the other form has a non-bridged structure.

At very low temperature the bridged structure predominates and as the temperature is raised, the non-bridged structure appears.

X-ray study of the crystal of  $\text{Co}_2(\text{CO})_8$  has shown that the molecule in the solid state has bridged structure which is similar to that of one of the isomeric forms of this molecule in solution. On the basis of electron diffraction study various bond lengths are :  $\text{Co-Co} = 2.42 \text{ \AA}$ ,  $\text{Co-C (bridging)} = 1.92 \text{ \AA}$ ,  $\text{C-O (bridging)} = 1.21 \text{ \AA}$ ,  $\text{Co-C (terminal)} = 0.80 \text{ \AA}$  and  $\text{C - O (terminal)} = 1.17 \text{ \AA}$ .

### Structure of $\text{Fe}_2(\text{CO})_9$

Infra-red and X-ray crystal studies made on  $\text{Fe}_2(\text{CO})_9$  molecule have shown that in this molecule each Fe atom is directly linked with the other Fe-atom by a  $\delta$ -bond (Fe-Fe  $\delta$ -bond), to three bridging carbonyl groups ( $>\text{C}=\text{O}$ ) by a  $\delta$ -bond (Fe-C  $\sigma$ -bond) and to three terminal carbonyl groups ( $-\text{C}\equiv\text{O}$ ) by a co-ordinate bond (Fe  $\leftarrow$  C co-ordinate bond). The presence of Fe-Fe bond is also supported by the diamagnetic character of  $\text{Fe}_2(\text{CO})_9$  molecule. Fe-Fe bond distance has been found to be equal to  $2.46 \text{ \AA}$ . The terminal C-O bond distances are smaller than the bridging C-O bond distance. From the structure given in Fig. 5.19 it may be seen that the coordination number of each Fe atom is not equal to 6 but equal to 7.

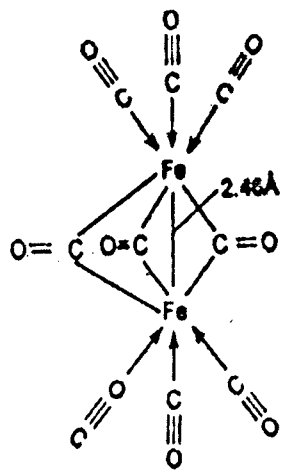


Fig. 5.19 Structure of  $\text{Fe}_2(\text{CO})_9$  molecule  
Structure of  $\text{Fe}_3(\text{CO})_{12}$

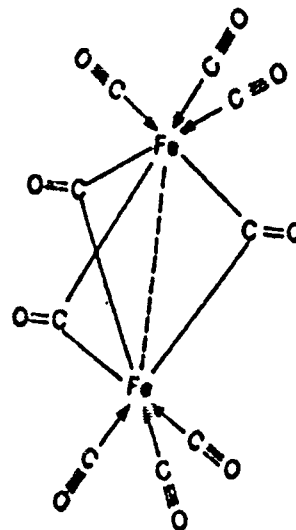


Fig. 5.20 Orbital diagram of  $\text{Fe}_2(\text{CO})_9$

According to old concept, each iron atom gets hybridized trigonal bipyramidally ( $d^2sp^3$ ). The three trigonal bipyramids get arranged in such a manner so that the carbonyl groups (the bridging carbonyl groups) at two of the equatorial apices of each bipyramid and held in common by two bipyramids  $d_{xz}$  and  $d_{yz}$  orbitals are available to form Fe-Fe bonds.

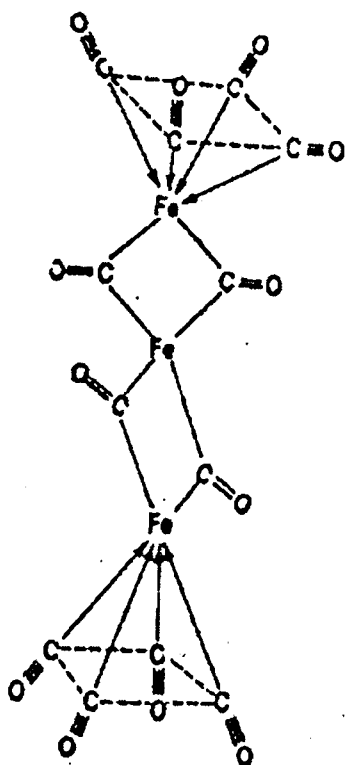


Fig. 5.21 Bond structure of  $\text{Fe}_3(\text{CO})_{12}$

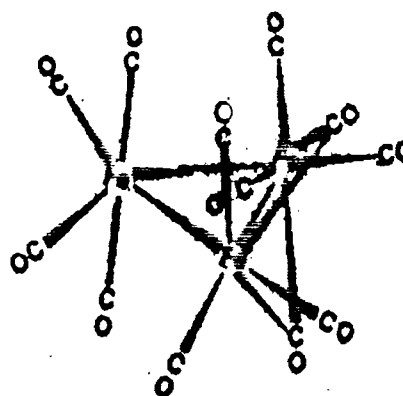


Fig. 5.22 Structure of  $\text{Fe}_3(\text{CO})_{12}$

Now it is accepted that  $\text{Fe}_3(\text{CO})_{12}$  molecule in solid state gets formed by the replacement of one of the bridging CO group in  $\text{Fe}_2(\text{CO})_9$  by the unit  $\text{Fe}(\text{CO})_4$ , the third Fe atom being equidistant from the other two. The three Fe atoms get situated at the corner of an isosceles triangle and the twelve CO arranged at the vertices of an icosahedron. Two Fe-Fe bond lengths are 2.698 Å and one Fe-Fe bond length is 2.56 Å.

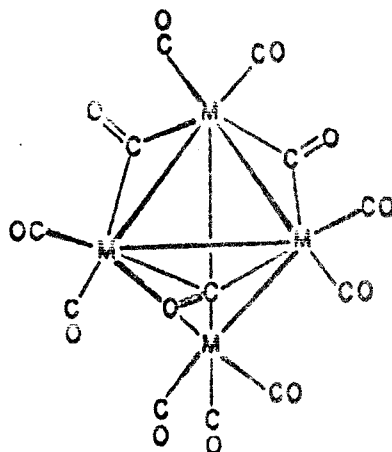


Fig 5.23 Structure of  $\text{Co}_4(\text{CO})_{12}$

### Substituted Carbonyls, Other $\pi$ -Acid Complexes, and Carbonylate Anions

CO replacement by another 2-e donor ligand or by electron addition produces 18-e species. Thus, replacing CO by  $\text{Br}^-$  in  $\text{Mo}(\text{CO})_6$ . Likewise, replacing Mo by isoelectronic  $\text{Mn}^+$  leads to  $[\text{Mn}(\text{CO})_6]^+$ . The anions  $[\text{Co}(\text{CO})_4]^-$  and  $[\text{Fe}(\text{CO})_4]^{2-}$  also are known 18-e species. Table gives electron counts for selected ligands.

### Phosphine - Containing Complexes :

Neutral Lewis bases such as  $\text{PR}_3$  (phosphines),  $\text{P}(\text{OR})_3$  (Phosphates), and  $\text{CNR}$  (isocyanides) often replace CO's.  $\text{P}^{\text{III}}$  ligands have a P lone pair for  $\sigma$ -donation, filled  $\pi$  symmetry (which could be the P d orbitals or antibonding P-C or P-O orbitals). The donor and acceptor ability of these ligands is influenced by the identity of R. The  $\sigma$ -donation ability is expected to parallel the  $pK_a$ 's of  $\text{HPR}_3^+$ , and  $\pi$  acidity is promoted by electron withdrawing groups such as F, Cl, and OR on P.

Table 5.4 – Electron counts for some ligands :

Ligand	Number of valence electrons contribute
$\text{H}^-$ , $\text{F}^-$ , $\text{Cl}^-$ , $\text{Br}^-$ , $\text{I}^-$ , $\text{CN}^-$ , $\text{NCS}^-$ , $\text{CO}$ , $\text{CNR}$ , $\text{NO}^+$ , $\text{NO}^-$ , $\text{PR}_3$ , $\text{P}(\text{OR})_3$ , $\text{AsR}_3$ , $\text{NR}_3$ , $\text{SbR}_3$ , $\text{SR}_2$ ,	2
$\text{R}^-$ , $\text{C}^-$ ( $\text{OR}$ ), $\text{Ar}^-$ ( $\text{Ar}$ = aromatic), $:\text{C}(\text{X})(\text{Y})$ , $\text{CR}^+$	3
$\text{NO}$	3
$\text{C}(\text{X})(\text{Y})^{2-}$	4
$\text{CR}^{3-}$	6

One can sort out whether a ligand is acting as a  $\sigma$  donor only or also as a  $\pi$  acid by drawing a graph. In brief, a plot of  $-\Delta H^\circ$  (or some other measured property) versus  $pK_a$  is made for a particular reaction. Some points lie on a straight line, and these are considered to belong to the class of  $\sigma$ -donor ligands. Those which lie above the line (more - negative than - expected  $\Delta H^\circ$ ) are considered to exhibit enhanced stability due to  $\pi$  acidity. Those lying below the line (less-negative-than-expected  $\Delta H^\circ$ ) belong to the class of  $\sigma$  and  $\pi$  donors. Three classes of ligands were distinguished : Class I,  $\sigma$  donor and  $\pi$  donor ; class II,  $\sigma$  donor only; Class III,  $\sigma$  donor and  $\pi$  acceptor. Class membership changes somewhat with the metal, but, in general, trialkyl phosphones are class I whereas phosphates and  $P(CH_2CH_2CN)_3$  are class III. Based on these results and IR and NMR studies, the generally accepted order of  $\pi$  acidity for  $P^{III}$  ligands is

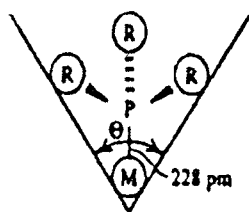
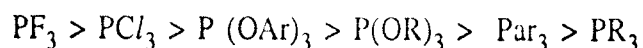


Fig 5.24 Tolman cone angle for  $PR_3$

Although it is difficult to disentangle steric and electronic factors, the approach has helped to sort them out. If we take those points that fall above the line and plot their "extra" enthalpy contribution ( $\Delta H_\pi$ ), measured by their deviations from the line, against an electrochemical parameter measuring  $\pi$  acidity, any negative deviation from the expected straight line is attributed to a steric effect which again is measured by the distance from the line. No deviations are seen, suggesting that steric effects are unimportant in the reaction examined. Cone angles of  $140-160^\circ$  are usually required for significant steric effects.

#### Nitrosyl Complexes :

No contains one more electron than CO (in an N-O  $\pi^*$  orbital) and thus acts as a three electron donor. In electron-counting terms,  $3CO = 2NO$ . Thus,  $Fe(NO)_2(CO)_2$  is isoelectronic with  $Fe(CO)_5$ , and  $Cr(NO)_4$  and  $V(CO)_5NO$  are isoelectronic with  $Cr(CO)_6$ . Three VB structures can be written for nitrosyl complexes.

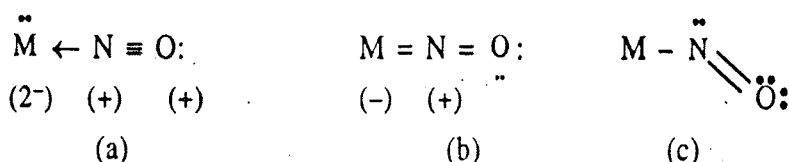


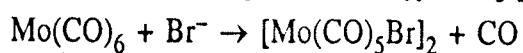
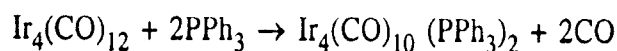
Fig. 5.25

Structure (a) implies that NO places its  $\pi^*$  electron in a singly occupied metal  $\pi$  orbital giving a nonbonding pair on M and donates two electrons in a  $\sigma$  bond. This is the so called  $\text{NO}^+$  coordination mode. The formal charges in (a) are larger than the ones in the analogous isocyanide structure. In structure (b), the nonbonding pair is back-donated into the  $\pi^*$  orbital of NO, thereby lowering the NO bond order. In (c), an electron pair is localized on the N in an  $sp^2$  orbital, leading to a bent structure. In a formal sense, one lone-pair electron must have come from the metal, giving the so-called  $\text{NO}^-$  coordination mode. Nitrosyl complexes are known with both linear and bent NO. Transition metals late in the series with relatively many electrons tend to adopt the bent more. For example, treating  $d^8$   $(\text{IrCl})(\text{CO})(\text{PPh}_3)_2$  with  $\text{NO}^+ \text{PF}_6^-$  gives square – pyramidal  $[\text{IrCl}(\text{CO})(\text{PPh}_3)_2 \text{NO}]^+$  with bent apical NO. This could be considered a compound to  $\text{Ir}^{III}$  in which two electrons from  $\text{Ir}^I$  have converted  $\text{NO}^+$  to  $\text{NO}^-$  with bent geometry. On the other hand, isoelectronic  $[\text{RuC}(\text{PPh}_3)_2(\text{NO}_2)]^+$  has a linear equatorial and a bent apical NO. Like wise,  $[\text{Co}(\text{diars})_2(\text{NO})]^{2+}$  (diars =  $o\text{-(Me}_2\text{As)}_2\text{C}_6\text{H}_4$ ) has a trigonal bipyramidal structure with a linear equatorial NO. When an additional electron pair is introduced into the Co-ordination sphere, the  $[\text{Co}(\text{NCS})(\text{diars})_2(\text{NO})]^+$  is octahedral with bent NO. In contrast complexes of the electron-poor early transition metals, such as  $[\text{Cr}(\text{CN})_5\text{NO}]^{3-}$ , display linear NO. The energetic factors involved in bending are correlated with other factors, so that it is not always possible to predict which mode of coordination will be observed.

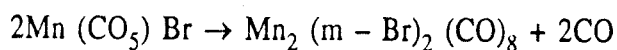
#### Routes to Substitution :

Three preparative routes are common for substituted carbonyls :

- 1) Direct replacement
- 2) Oxidation by halogens
- 3) Reactions between metal halides and CO



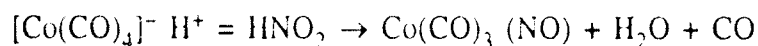
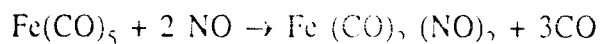
some monomers form bridged dimers on thermally induced CO loss :



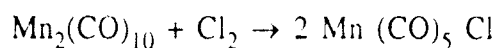
Photochemical activation sometimes can aid in breaking the M-CO bond, but many reactions are carried out thermally. Except when the substituting ligands are very good  $\pi$  acids, substitution usually stops after two or three carbonyls have been replaced, because the remaining CO's become saturated in their ability to withdraw electron density from the metal. With good  $\pi$  acids, however, all CO's can be replaced, giving compounds such as  $\text{Ni}(\text{PF}_3)_4$ ,  $\text{Cr}(\text{CNPh})_6$ , and so on. For reasons that are not well understood,  $\text{Pt}(\text{CO})_4$  is unstable, but

Pt(PPh<sub>3</sub>)<sub>4</sub> can be prepared. The relatively large cone angle (145°) for PPh<sub>3</sub> promotes ligand dissociation in solution to Pt(PPh<sub>3</sub>)<sub>3</sub> and even Pt(PPh<sub>3</sub>)<sub>2</sub>.

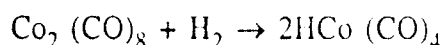
Direct displacement with NO is a route to nitrosyl complexes as is treatment with acidified nitrites :



Carbonyl halides result from halogen oxidation of carbonyls :

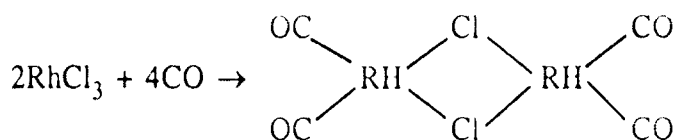


A formally related reaction is

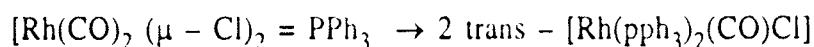


It seems strange to think of an "oxidation" H<sub>2</sub>! However, it is an arbitrary convention to obtain oxidation states of transition metals in complexes by "removing" ligands in closed-shell configuration. (The exception to this is μ<sub>2</sub> 2e-donor ligands such as CO and (CNR). Thus, M-H compounds are treated as containing H<sup>-</sup>. In fact, the chemical behaviour of HCo(CO)<sub>4</sub><sup>-</sup> containing Co<sup>-1</sup>.

Typical of reactions between metal halides and CO is



Note that a noncarbonyl ligand bridges in the product, as in most carbonyl halides including Cu<sub>2</sub>(CO)<sub>2</sub>(μ-Cl)<sub>2</sub>(H<sub>2</sub>O)<sub>2</sub>. Bridged species can be claved by Lewis bases; for example



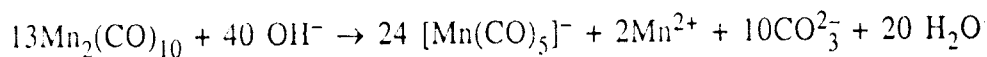
Although metal carbonyls undergo many different kinds of reactions, substitutions are among the most important. In later sections we shall encounter examples in which carbonyls are substituted by organic groups.

### Carbonylate Anions :

We know of a very large number of carbonyl anions but very few cations. This is reasonable in view of the π acidity of CO, which stabilizes low oxidation states.

Carbonylate anions often are made in situ and used for reaction without isolation. Three common preparations are :

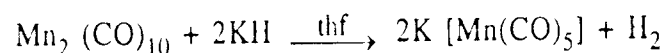
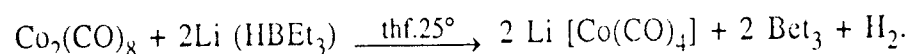
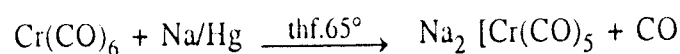
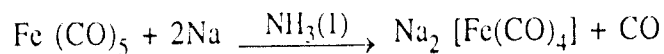
### 1. Base-induced redox reactions. Examples include :



The above equations amount to base-induced disproportionation which, although convenient, involves conversion of part of the metal to a cationic product.

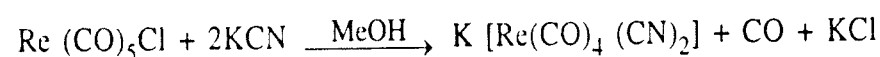
### 2. Reaction of metal carbonyls with reducing agents :

Alkali metal amalgams, hydride reagents, and Na / K alloy in basic solvents, including liquid ammonia, have been used. Examples include :

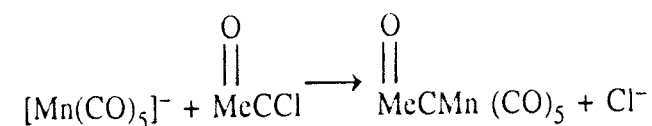
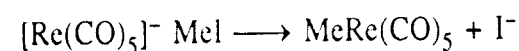


### 3. Carbonyl Substitution by Anions :

Substitutions such as the following lead to carbonylate anions

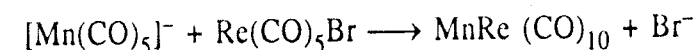


Two especially important reactions of carbonylate anions are those with alkyl or acylhalides to give organic derivatives and protonation to afford metal hydrides.

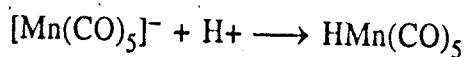


When carbonylate anions displace halide from carbonyl halides, heteronuclear carbonyls result.

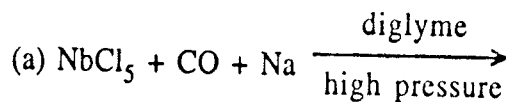
An example is



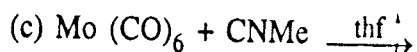
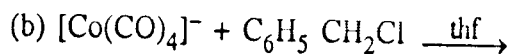
The above reactions are analogous to  $S_N2$  displacements on organic halides. Protonation of carbonylate anions is a route to hydride complexes :



Example : What will be the products(s) of mixing the following reactants ?



(Diglyme is an ether  $(\text{CH}_3 \text{OCH}_2 \text{CH}_2)_2\text{O}$ )



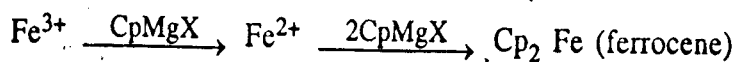
**Solution :** (a) Because CO is one of the reactants, a carbonyl is a likely product. Nb is in the +V oxidation state, and carbonyls are stable for low oxidation states. However, Na is a reducing agent. We need to know the stable carbonyl(s) of Nb. Because Nb is in the same group as V, it is a reasonable guess that  $\text{Nb}(\text{CO})_6$  could be formed because the analogous carbonyl is known for V. However, this is a 17-e compound. Thus, like  $\text{V}(\text{CO})_6$ , it should be easily reduced to  $[\text{Nb}(\text{CO})_6]^-$  by Na. Thus, we predict that  $\text{Na}[\text{Nb}(\text{CO})_6]$  and NaCl will be formed.

(b)  $[\text{Co}(\text{CO})_4]^-$  is a carbonylate anion and a nucleophile. It displaces  $\text{Cl}^-$  from the alkyl halide to give  $\text{C}_6\text{H}_5\text{CH}_2\text{Co}(\text{CO})_4$ .

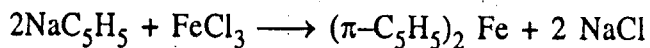
(c) CNMe is a two-electron donor ligand isoelectronic with CO. Depending on the stoichiometric proportions, it will displace one or more CO's, giving  $\text{Mo}(\text{CO})_{6-n}(\text{CNMe})_n$  ( $n=1-3$ ) and CO.

### Metalloenes : Ferrocene

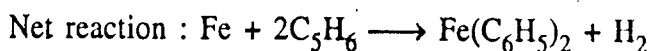
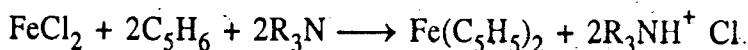
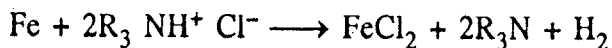
When scientists tried to prepare fulvalene by oxidation of cyclopentadienyl Grignard reagent, a stable orange compound was isolated which was characterized and named ferrocene.



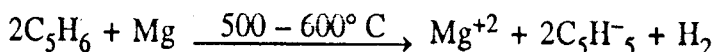
The cyclopentadienide salts of alkalimetals react with ferric chloride in THF, DMF, ethylene glycol, dimethylether or similar solvent giving  $\text{Cp}_2\text{Fe}$ .



Use of amines facilitates the removal of acidic hydrogen of cyclopentadiene and allows formation of ferrocene at lower temperatures.



Magnesium cyclopentadienide is directly prepared



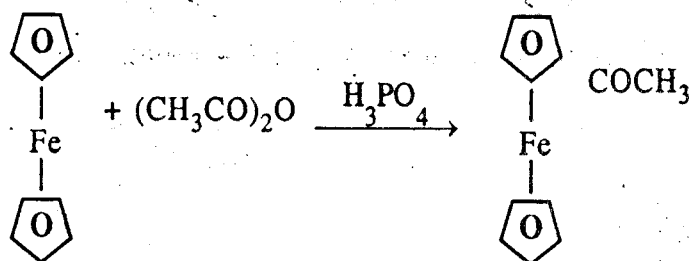
This is a white solid, stable indefinitely under dry nitrogen and may be used as a source of cyclopentadienide ions.

### Reactions :

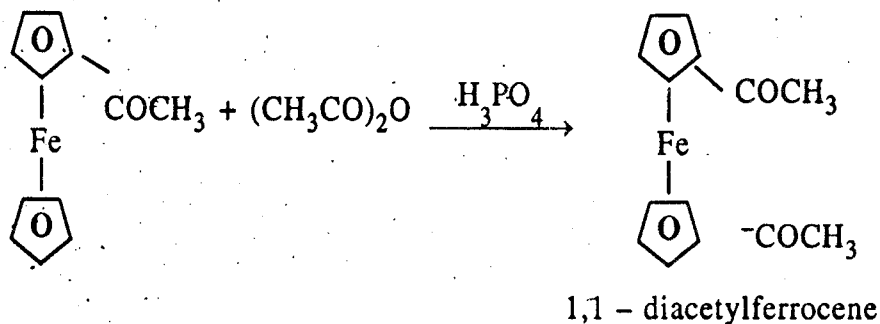
The cyclopentadienyl rings in ferrocene are aromatic and undergo many of the same reactions as benzene. The metallocene, are in general more reactive toward electrophilic reagents than benzene indicating that electrons are more readily available.

### Acetylation :

Acetylation of ferrocene by acetic anhydride impresence of  $\text{H}_3\text{PO}_4$  as catalysis gives 1-acetylferrocene.

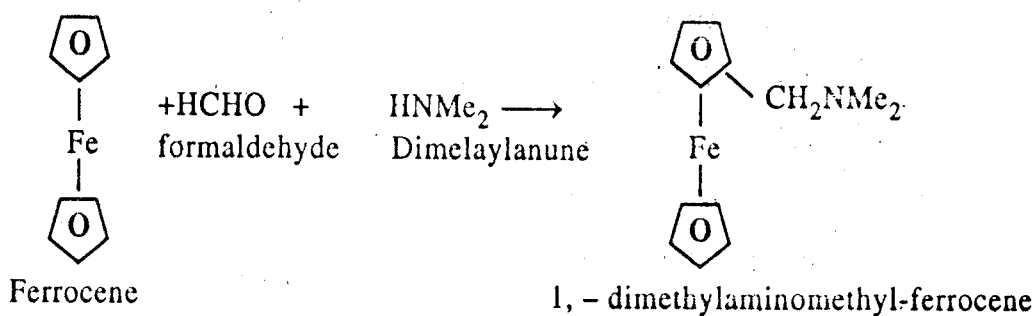


Acetylation of ferrocene deactivates the molecule. In order to obtain the diacetyl compound conditions similar to the usual acetylation of aromatic rings are required.



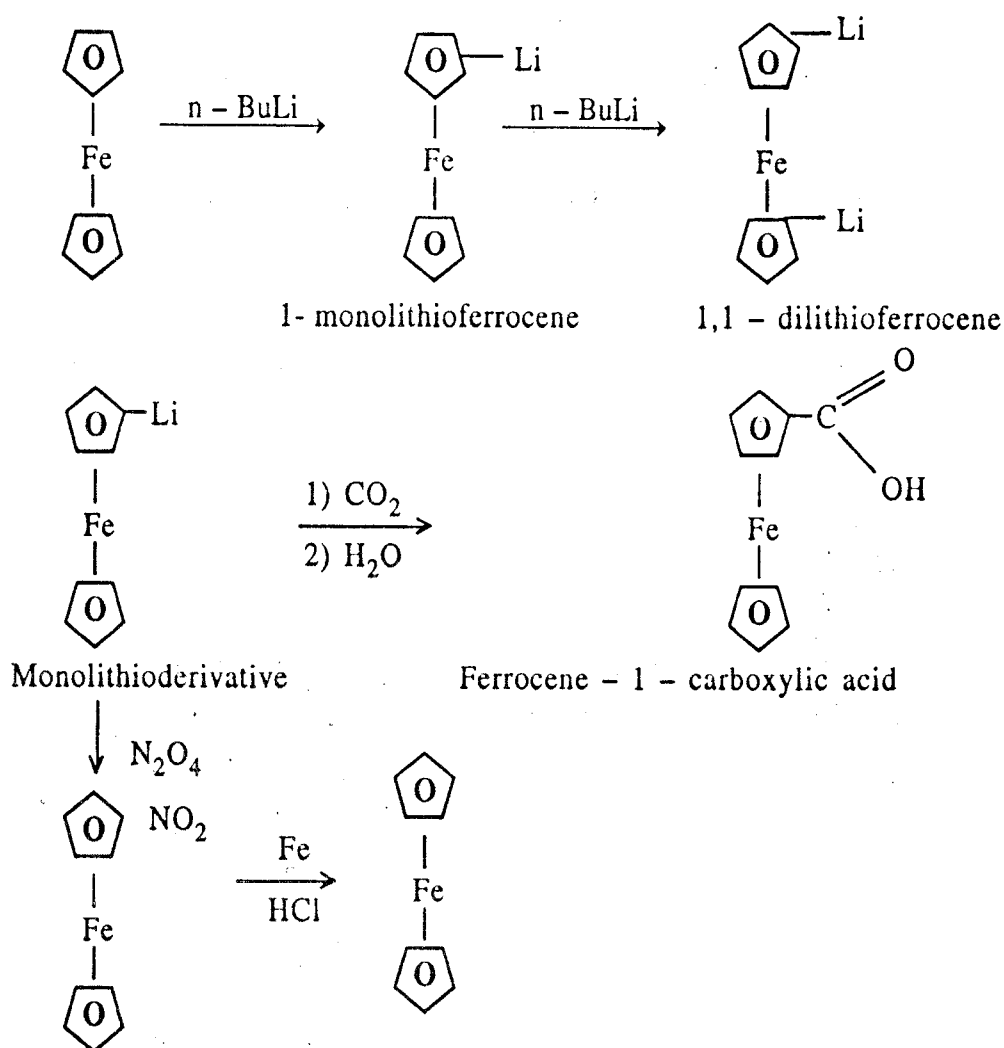
### Mannich reaction :

Ferrocene condenses with formaldehyde and amines (Mannich reaction)



### Metalation Reaction :

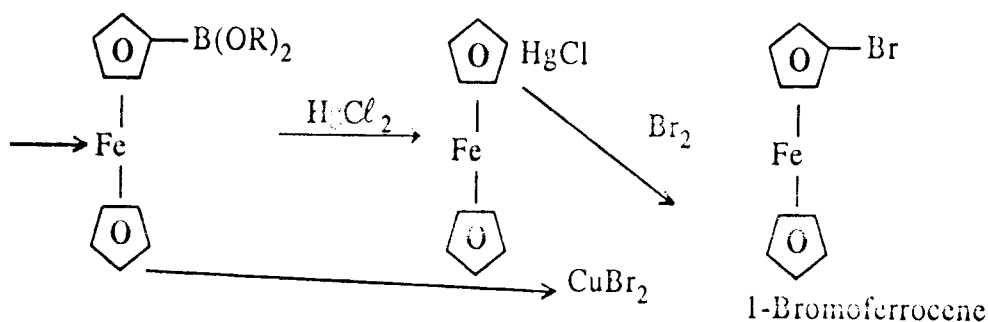
Many derivatives of ferrocene can be obtained by following the reaction which is typical of aromatic systems. Just as phenyllithium can be obtained from benzene, analogous ferrocene compounds can be prepared.



(i) B (OR) 3

1 - aminoferrocene

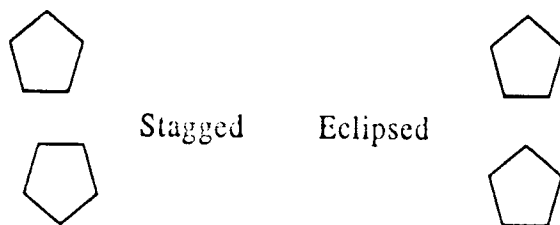
(ii) O



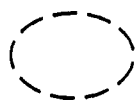
### Structure :

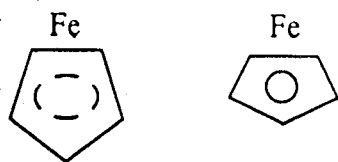
The crystalline bis -  $\pi$  - cyclopentadienyls of the elements  $(\pi-C_5H_5)_2M$  where  $M=V, Cr, Fe, Co, Ni$  are isomorphous. X-ray and other methods should that these molecules are sandwich structures.

In ferrocene, the solid phase structure is found to be staggered configuration but the gas phase ferrocene has eclipsed configuration. All the C-C distance in the ring are  $1.40 \pm 0.02 \text{ \AA}$ , almost same as in the case of benzene, The rings are planar. The inner ring distance is  $3.2 \text{ \AA}$  and iron Carbon distance is  $2.04 \text{ \AA}$ . The compound is diamagnetic.



The bonding is best studied by LCAO - MO approximation. Each  $C_5H_5$  ring taken on a regular pentagon has five  $\pi$  - molecular orbitals. There is a single orbital at lowest energy strongly bonding (a) that consists of an unbroken (i.e) nodeless doughnut of electron density above and below the plane of the ring. At slightly higher energy there is a doubly degenerate set of orbitals each of which has one nodal plane containing the principal axis and which are weakly bonding ( $C_1$ ). This is followed by another doubly degenerate set with two nodal planes and yet higher energy which are markedly antibonding ( $e_2$ ). The pairs of rings taken together then has ten  $\pi$ -orbitals and  $D_{5d}$  symmetry is assumed so that there is a centre of symmetry in the  $(\pi-C_5H_5)_2M$  molecule. There will be a centrosymmetric (g) and antisymmetric (u) contribution. Of the 18 electrons to be accommodated five  $\pi$  -electron come from  $C_5H_5$  ring and eight valence shell electrons from iron.

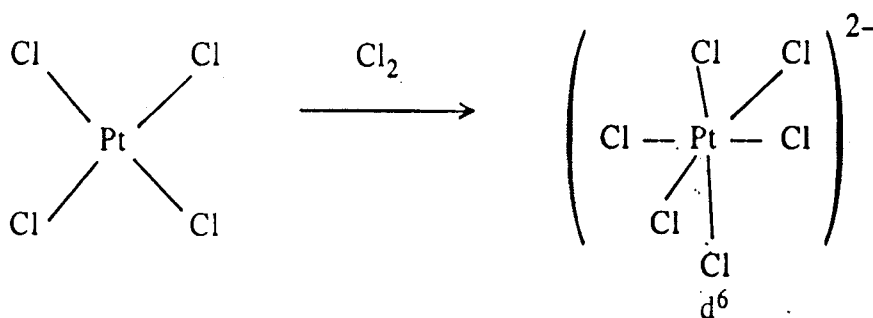




Hence the 18 electrons can just fill the bonding and non-bonding MO's giving a closed shell configuration. Thus the molecular orbital allows us to rationalize the magnetic properties of metallocenes. Thus  $\text{Cp}_2\text{Fe}$  is diamagnetic whereas  $\text{Cp}_2\text{Co}$  and  $\text{Cp}_2\text{Ni}$  have magnetic moment of 1.73 and 2.83 B.M., respectively.

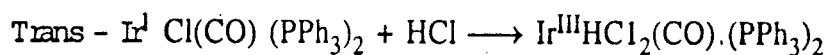
#### Oxidative addition and reductive elimination processes :

A coordinately unsaturated complex in homogenous catalysis may remain stable by its ability to have stable complexes with different coordination number. The complex may remain stable and relatively free from unwanted reaction until the appropriate species appears and then expand its coordination shell to receive it. If there is a formal loss of electron accompanying this change in coordination, the reaction is classified as an oxidative addition.



The reverse reaction in which the oxidation number decreases while there is a formal gain in electrons is termed reductive elimination.

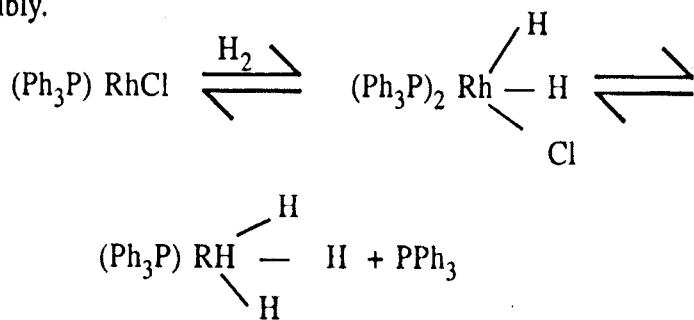
The best choices for oxidative addition are 4 and 5 coordinated  $d^{10}$  and  $d^8$  species notably  $\text{Fe}^0$ ,  $\text{Ru}^0$ ,  $\text{Os}^0$ ,  $\text{Rh}^I$ ,  $\text{Ir}^I$ ,  $\text{Ni}^0$ ,  $\text{Pd}^0$ ,  $\text{Pt}^0$  and  $\text{Pd}^{II}$  and  $\text{Pt}^{II}$ . Thus iridium square planar complex undergoes reaction such as



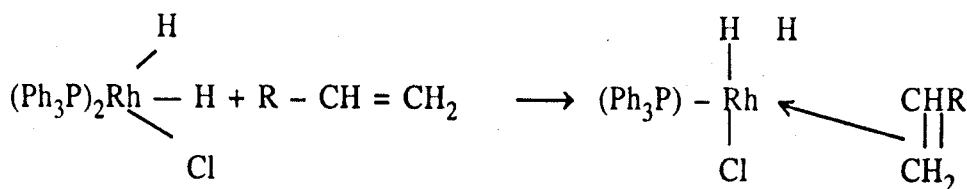
It will be noted that in addition of molecules such as  $\text{H}_2$ ,  $\text{HCl}$  or  $\text{Cl}_2$  two new bonds to the metal are made and the  $\text{H}-\text{H}$ ,  $\text{H}-\text{Cl}$ ,  $\text{Cl}-\text{Cl}$  bonds are broken. However, molecules that contain multiple bonds may be added oxidatively without cleavage to form new complexes which have 3-membered rings. Vaska's complex is a well known example.

There may be situation where the most stable coordination number in the oxidized state is exceeded so that expulsion of a ligand may occur.

The (triphenylphosphine) chlororhodium known as Wilkinson's catalyst can act as homogen to form metal hydride from which one molecule of triphenylphosphine dissociates reversibly.

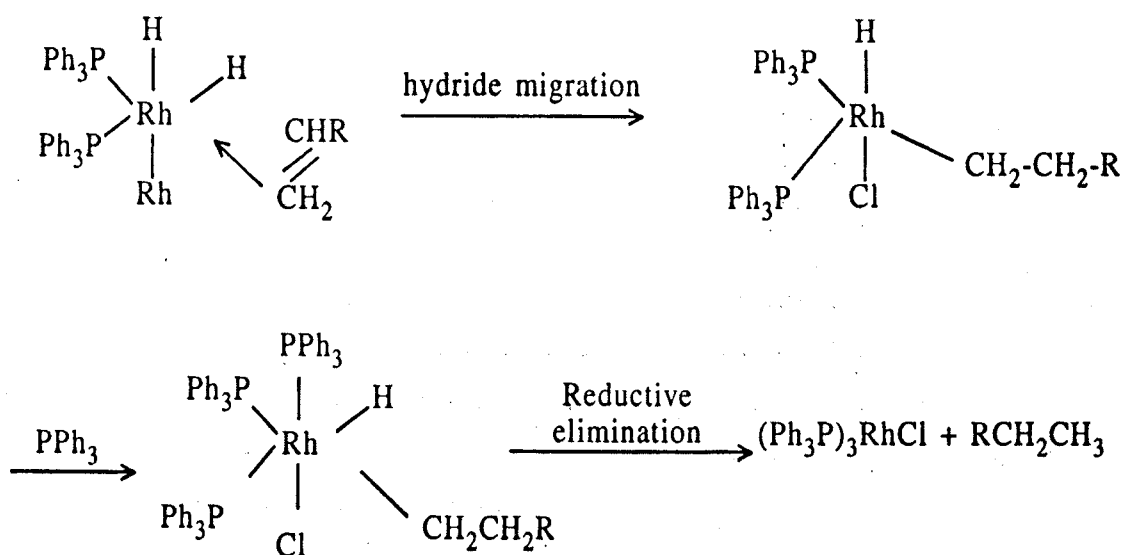


In the presence of a suitable alkene substrate in which the alkene competes with triphenylphosphine for coordination to the rhodium atom.



### Reductive Elimination :

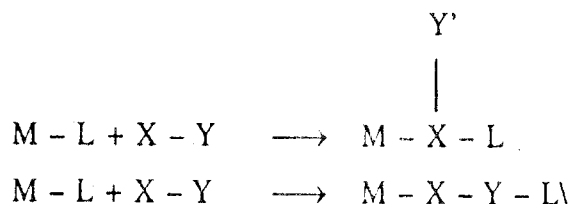
When an unsaturated complex undergoes decrease in coordination number and simultaneously gains electrons, the process is called reductive elimination. Intramolecular hydride ion transfer from rhodium to carbon then gives an alkyl rhodium complex still having the hydrogen atom attached to rhodium atom. An alkane is formed by a reductive elimination process with the generation of the catalyst.



Wilkinson catalyst catalyses the hydrogenation of non-conjugated alkenes and alkynes at room-temperature and atmospheric pressure whereas the conjugated alkenes and dienes which form intermediate chelates require higher pressure (10 atm) for reduction.

### Insertion and Elimination Reaction :

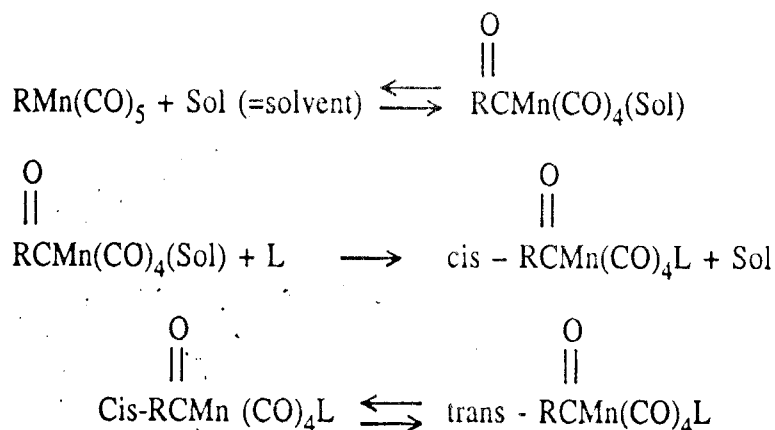
A large class of reactions involves insertion of small molecules X-Y into metal-ligand bonds, especially M-C and M-H bonds.



The term "insertion" describes only the result of the reaction; it has no mechanistic significance. Many insertion reactions are reversible, and the reverse reaction is called extrusion or elimination. It shows a representative sampling of insertion reactions involving transition metals. We will discuss only insertions of CO, SO<sub>2</sub>, and olefins.

### CO Insertion

A good deal of what is known about CO "insertion" (or carbonylation) comes from studies on RMn(CO)<sub>5</sub> as a model, CH<sub>3</sub>Mn(CO)<sub>5</sub> reacts with <sup>14</sup>CO to give OCH<sub>3</sub>CMn(CO)<sub>4</sub> (<sup>14</sup>CO); that is, the inserted CO is one previously coordinated to the metal not the labelled one added to the complex. This suggests that other Lewis bases L can also bring about insertion. The generally accepted mechanism is



An acyl intermediate is formed with solvent occupying one coordination position (if the solvent is basic enough). Increasing the size of solvent molecules when the basicity is similar hinders formation of the solvated acyl and slows down carbonylation. The Lewis base L enters to give the cis complex, which then equilibrates with the trans isomer. Both basicity

and size of L influence its ability to capture the intermediate before it reverts back to the alkyl. Alkyl complexes of Mo, Fe, CO, Rh, and Ir behave similarly.

The labeling experiment depicted in that the Mn alkyl group moves during the carbonylation because the product distribution observed is just that predicted by the "alkyl migration" model. Electron withdrawing R groups migrate more slowly than electron-donating ones, presumably because of the greater strength of the Mn-R bond which must be seriously weakened in the transition state. For example,  $\text{CF}_3\text{Mn}(\text{CO})_5$  does not insert even under 333 and of CO and temperatures up to  $200^\circ\text{C}$  even though  $\text{CH}_3\text{Mn}(\text{CO})_5$  inserts at 1 atm at room temperature. Configuration is retained at the alkyl. Stereochemistry at the metal can be quite variable. Reaction of optically active  $\text{CpFe}^*(\text{CO})(\text{PR}_3)\text{R}$  with CO leads to inversion or retention, depending on the solvent.

Many acyl complexes may be decarbonylated either thermally or photochemically. As required by the principle of microscope reversibility, a terminal CO is lost followed by migration of R to fill the vacant coordination position. For example

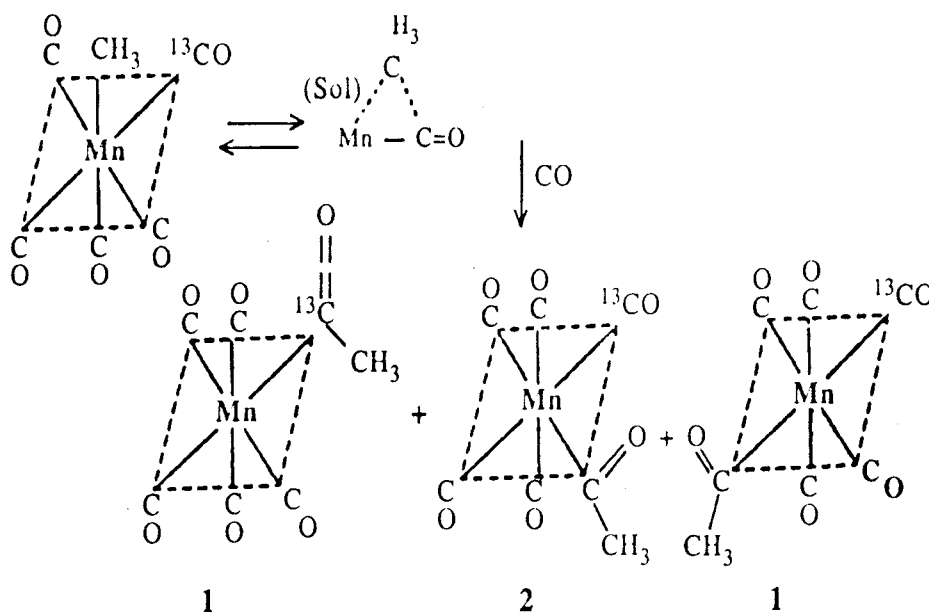


Fig 5.26 Stereochemical course of carbonylation

### $\text{SO}_2$ Insertion :

In contrast to CO,  $\text{SO}_2$  inserts directly into M-C bonds, often producing

an S-sulfinate. For example,  $\text{CpFe}(\text{CO})_2\text{CH}_3$  gives  $\text{CpFe}(\text{CO})_2\text{S}(\text{O})_2\text{CH}_3$  when refluxed in  $\text{SO}_2$  (1).



Kinetic studies have shown that  $\text{SO}_2$  behaves as a Lewis acid attacking the alkyl ligand rather than the metal so that more electron-donating alkyls react faster. As indicated in the figure, backside attack leads to inversion of configuration at C. Also in contrast to CO, extrusion of  $\text{SO}_2$  occurs much less readily and its insertion is seldom reversible.

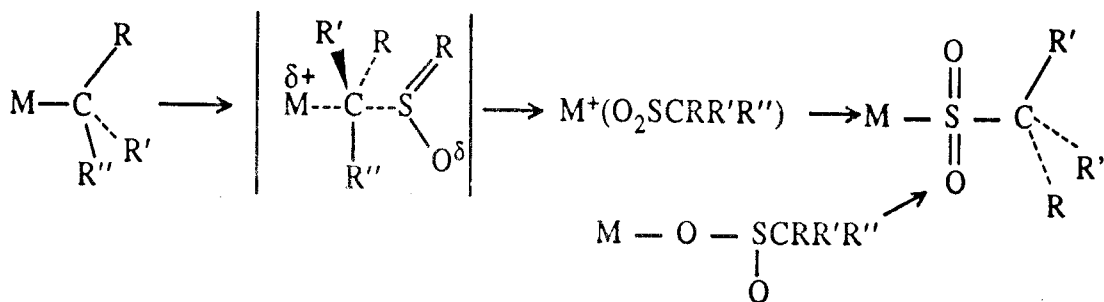


Fig. 5.27 Mechanism of  $\text{SO}_2$  insertion

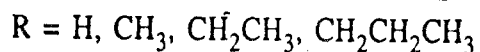
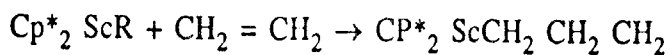
### Olefin Insertion

Olefins can insert into M-C and M-H bonds. When the metal has sufficient d electrons for back-bonding, the olefin is often coordinated before insertion. This may require ligand dissociation to vacate a coordination position. For example,

Insertion converts a hydrido- or alkyl-olefin complex into an alkyl complex by addition of H or C to the  $\beta$ -carbon of the olefin. Note that the metal oxidation state does not change. In contrast to CO, olefins often undergo multiple insertions providing a mechanism for their polymerization.

The reverse of olefin insertion into a M-H bond is the  $\beta$ -elimination reaction of metal alkyl complexes, which can occur only if a vacant orbital and a vacant coordination position are available and  $\beta$ -H is present. If these conditions are fulfilled, a facile route exists for the decomposition of metal alkyl complexes. The initial product is a hydride / olefin complex which may then go on to dissociate the olefin.

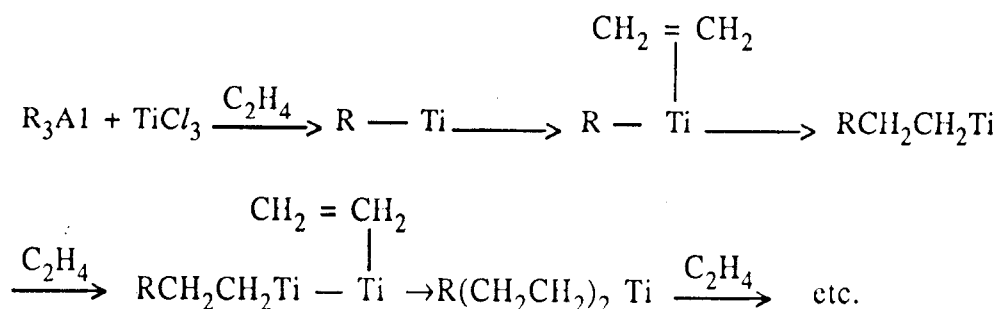
Fundamental features of olefin insertion were brought out in an investigation of some Sc complexes ( $\text{Cp}^* = \eta^5 - \text{Me}_5\text{C}_5$ ).



$\text{Cp}^*_2 \text{ScR}$  are coordinatively unsaturated  $d^0$ , 14-e compounds stabilized by bulky electron-donating  $\text{Cp}^*$  ligands. They represent ideal models for studying insertion and  $\beta$ -elimination because no complications arise from the need to dissociate other ligands to provide vacant coordination sites nor from the kinetics of olefin coordination because this does not happen for  $d^0$  complexes which are incapable of back donation.

The rates of  $\beta$  - H elimination from a series of substituted complexes  $Cp^*_2 ScCH_2CH_2C_6H_4p-X$  showed that the rate decreased with the electron withdrawing power of X, indicating development of positive charge on the  $\beta$ -carbon in the transition state.

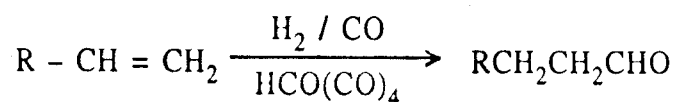
Ethylene polymerization catalyzed heterogeneously the  $Ti^{III}$  salts and Al alkyls (Ziegler - Natta catalysts) surely involves insertion.  $R_3Al$  could alkylate the surface of a  $TiCl_3$  crystal. Coordination of ethylene to a vacant Ti site may be followed by insertion, coordination of another ethylene, and so on :



In spite of the reactivity of M-H bonds toward olefin insertion, only two examples of Co insertion to give an isolable  $MCH$  formyl complex have yet been found - namely, with  $HRh$  (octaethylprophyrin) and  $Cp_2 ThH(OR)$ . This likely results from the greater M-H than M-C bond strength which makes the reactions thermodynamically unfavourable.

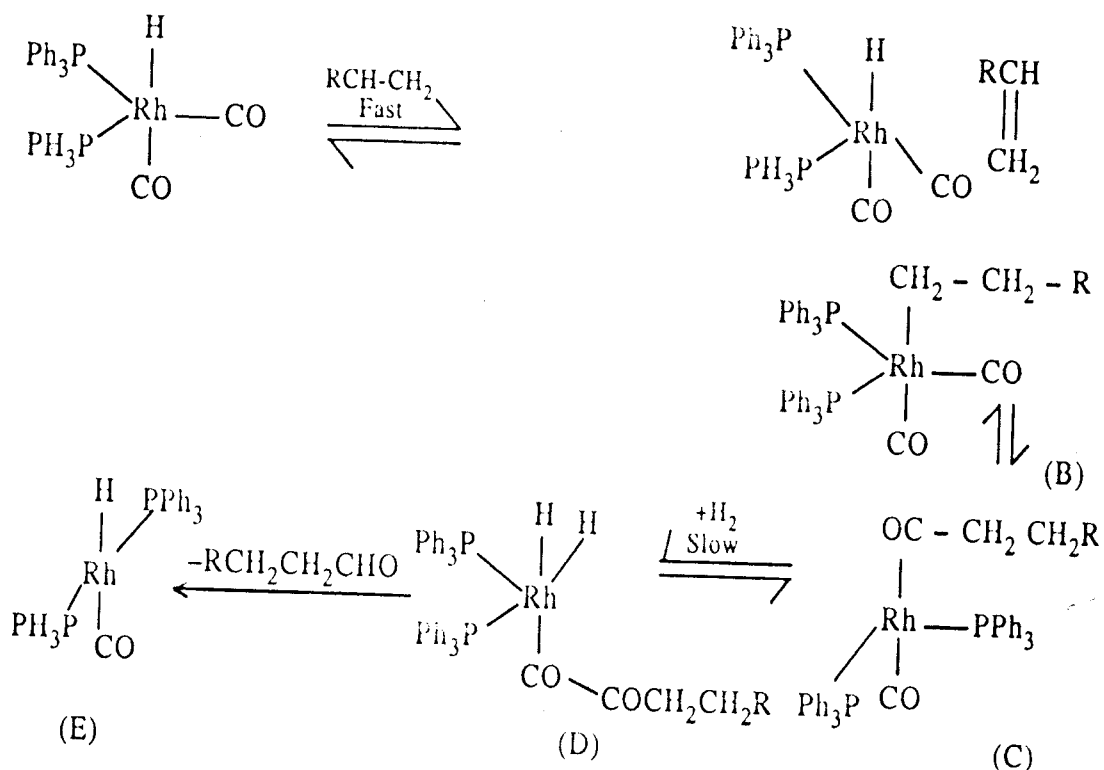
#### Homogeneous catalysis - Hydroformylation Reactions :

One of the most important catalytic reaction studied using transition metal complexes is migratory insertion reaction or the hydroformylation reaction in which a group Y is inserted into an X-Z bond. This is best exemplified by the industrially important 'OXO' or hydroformylation reaction which involves the addition of  $H_2$  and CO across the olefinic double bond catalysed by tetracarbonyl hydridocobalt.



The product is an aldehyde having one more carbon atom than the initial alkene.

Recent studies have shown that rhodium catalysts are more effective than cobalt ones, allowing the reaction to proceed at lower temperatures and pressures ( $25^\circ C$  with 1 atm. Pressure). The most active complex is  $RhH(CO)(PPh)_3$  which, with CO, rapidly gives the actual catalyst.  $RhH(CO)_2(PPh)_2$ .



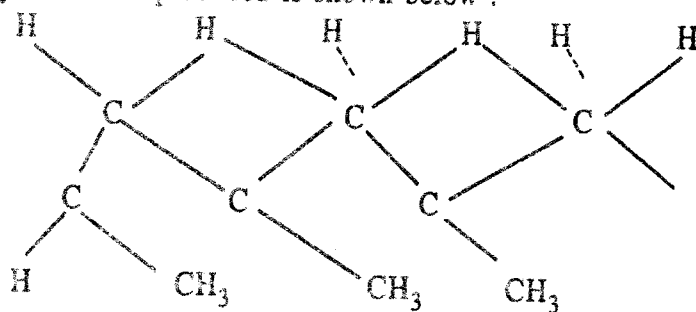
The initial step is the associative attack of the alkene on the species  $\text{RhH}(\text{CO})_2(\text{PPh}_3)_2$ , (A), followed by the intramolecular hydride ion transfer which leads to the alkyl complex (B). The latter then undergoes CO insertion to form the acyl derivative (C) which subsequently undergoes oxidative addition of molecule of hydrogen to give the dihydridoacyl complex (D). The last of these steps which is involving change of oxidation state of the metal is probably rate - determining. The final steps are another H transfer to the carbon atom of the acyl group in (D) followed by the loss of aldehyde and regeneration of the 4-coordinate species (E).

Insertion of CO into methanol using sodium catalyst to produce acetic acid has been employed on an industrial scale.

### Ziegler - Natta Catalysts

Alkenes can be converted into a high molecular weight linear polymers by heating the gas under high pressure. Polymers with molecular weights ranging from 150 to several millions were prepared by using metal catalysts. Organometallic catalysts are useful in catalyzing polymerization at low temperatures and ordinary pressures Ziegler in Germany and Natta in Italy developed the techniques. The Ziegler - Natta catalyst is heterogenous in nature and is prepared by heating  $\text{TiCl}_4$  with  $\text{AlEt}_3$  to form a fibrous form of  $\text{TiCl}_3$  which is partially alkylated. Stereochemically oriented polymers are produced on the Ziegler - Natta catalyst surface.

Polypropylene chain produced is shown below :



The titanium does not have a filled coordination sphere and acts as Lewis acid accepting propylene as another ligand. After promotion of an electron from Titanium - alkyl bond to molecular orbital of the complex a four - centre transition state is provided which enables an alkyl group to coordinated propylene. A further molecule of propylene is then bound to the vacant site and the process is repeated.

An important extension of Ziegler - Natta polymerization is the styrene, butadiene and a third component like dicyclopentadiene or 1, 4 - hexadiene to give synthetic rubber. Then vanadyl halides rather than titanium halides are used.

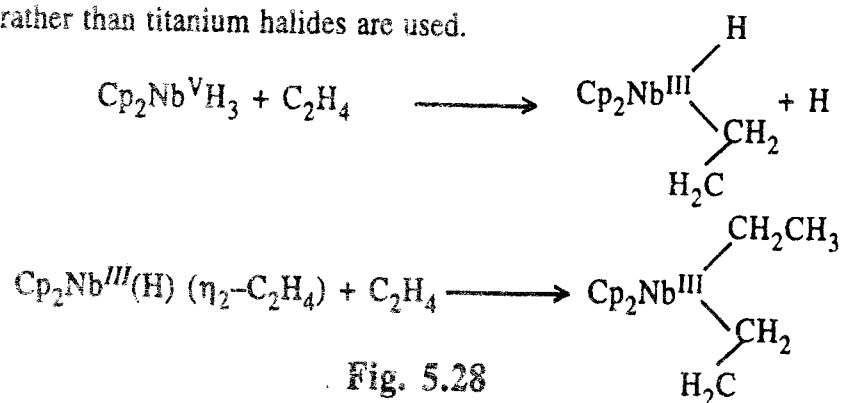


Fig. 5.28

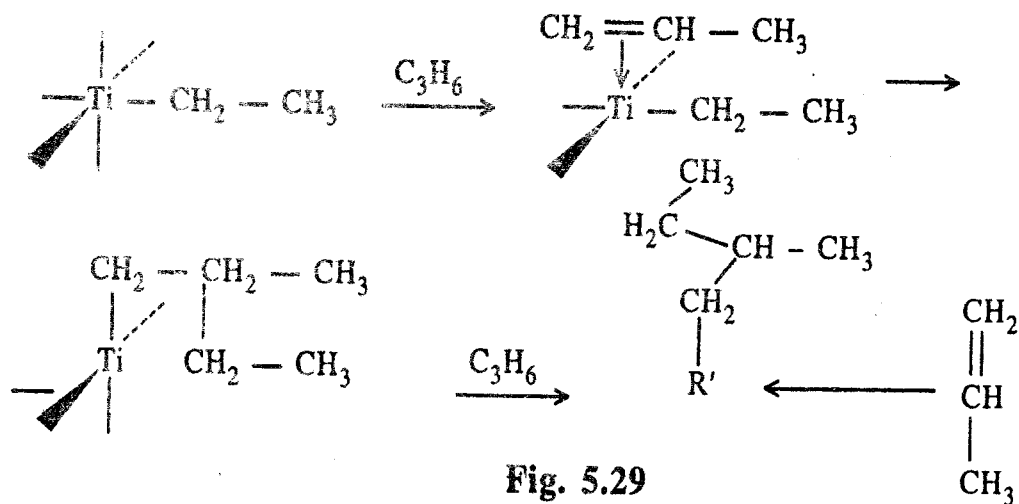


Fig. 5.29

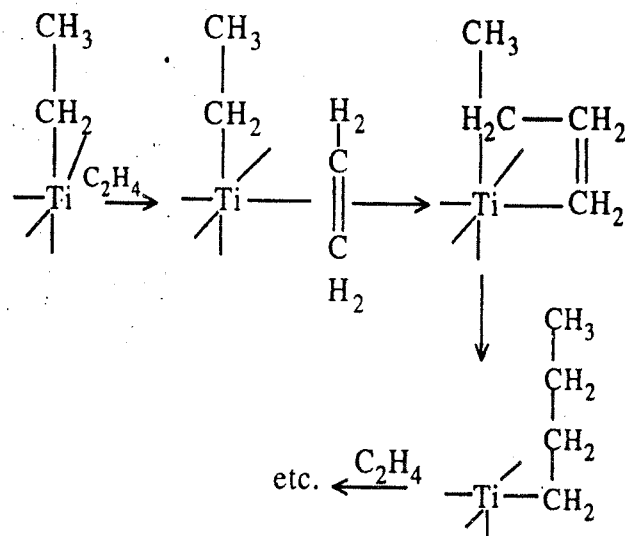


Fig. 5.30

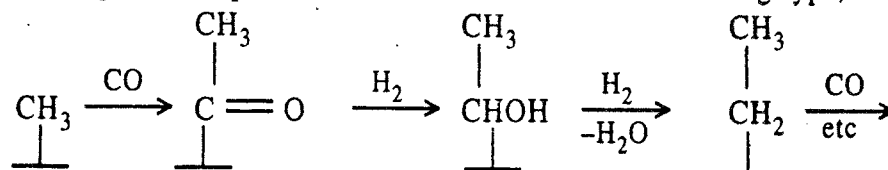
### Fischer - Tropsch Synthesis

In this process, hydrocarbons are synthesized by passing a mixture of hydrogen and carbon monoxide over certain transition - metal surfaces.



A previously widely accepted mechanism for this reaction involves the generation of a methyl group on the surface, followed by a series of steps in which, in effect, methylene groups are successively inserted between the metal and the alkyl group, thus building up a linear alkyl group. The alkyl group is severed from the metal in a hydrogenation step, thus releasing a product hydrocarbon molecule. The methyl group is presumably formed by the reaction of adsorbed hydrogen atoms formed by the surface dissociation of H<sub>2</sub> with adsorbed CO in a sequence such as the following :

The alkyl-chain growth steps in this mechanism are of the following type,



and the hydrocarbon production step is presumably as follows :

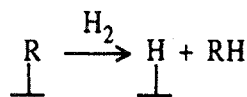
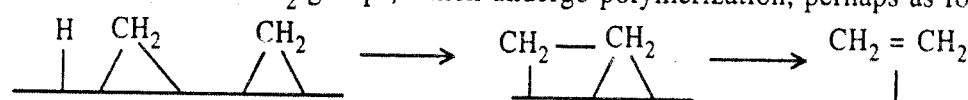


Fig. 5.31

This mechanism derived some credibility from the fact that the various proposed steps have known analogs in homogeneous organometallic reactions.

However, both X-ray and ultraviolet photoelectron spectroscopy have shown that carbon monoxide is dissociated to surface carbide and oxide atoms on some metal surfaces. For example, consider the oxygen 1s spectra of CO on tungsten. The data indicate that CO is

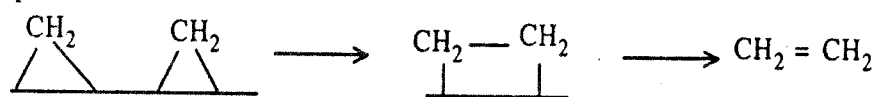
adsorbed molecularly at 100 K. but that, on warming the oxygen atoms become directly bonded to the metal surface and acquire a more negative charge than they have in the undissociated CO groups. The relative ease with which various metal surfaces break the C-O bond of carbon monoxide can be related to the stability of the corresponding metal carbides. Thus tungsten and molybdenum dissociate CO below 170 K, whereas metals with thermally unstable carbides, such as iron and nickel, dissociate CO between 300 and 420 K, and adsorption on the platinum metals (most of which do not form carbides) is mainly nondissociative. In this basis it has been proposed that CO dissociation is involved in Fischer - Tropsch synthesis. It is proposed that adsorbed hydrogen atoms convert the oxygen to water, which is desorbed, and convert the carbon atoms to CH or CH<sub>2</sub> groups, which undergo polymerization, perhaps as follows.



However, when a mixture of hydrogen and diazomethane is passed over.

This mechanism provides an explanation of the relative activities of metals in Fischer-Tropsch synthesis. On iron, the CO is expected to be completely dissociated at synthesis temperature. The concentration of CH<sub>2</sub> groups is therefore high and, in agreement with observation, formation of higher hydrocarbons is facilitated. On nickel, CO dissociation is more difficult. Thus the concentration of CH<sub>2</sub> is expected to be lower, and in agreement with observation, hydrogenation, with formation of methane, predominates. On tungsten and molybdenum, which are poor Fischer - Tropsch catalysts, the carbide species are probably too stable to be easily hydrogenated.

It has been observed that diazomethane, CH<sub>2</sub>N<sub>2</sub>, reacts on metal surfaces to give mainly ethylene, together with nitrogen. Presumably the ethylene forms by the simple dimerization of CH<sub>2</sub> groups :



However, when a mixture of hydrogen and diazomethane is passed over Co, Fe, and Ru, a linear hydrocarbon mixture, similar to that produced in the Fischer - Tropsch synthesis, is obtained. These data give strong support to a mechanism involving the dissociation of CO and the formation of adsorbed CH<sub>2</sub> groups. It is interesting that this mechanism is essentially the same as that proposed by Fischer and Tropsch in 1926.

The oil crisis of the 1970s has caused chemists to seek chemical raw materials from sources other than petroleum. The Fischer - Tropsch process could compete with petroleum if (1) the process selectively were improved (i.e. if high relative yields of particular hydrocarbons, rather than a broad spectrum of hydrocarbons, could be obtained), (2) crude oil were to become even scarcer, and (3) coal were to become relatively inexpensive. Considerable effort is being expanded to improve the efficiency and selectivity of the process.

\*\*\*\*\*

## Question Pattern

Marks : 100

**SECTION - A (5×5=25 Marks)**

Answer any FIVE out of EIGHT.

**SECTION - B (5×15=75 Marks)**

Answer any FIVE out of EIGHT.